AN ABSTRACT OF THE THESIS OF

Mary-Lynn Dickson for the degree of Doctor of Philosophy in Oceanography presented on April 15, 1994.

Title: Nitrogen Dynamics in a Coastal Upwelling Regime

Redacted for Privacy

Abstract approved: _____
Patricia A. Wheeler

The purpose of this study was to understand the seasonal nitrogen dynamics under a variety of oceanographic conditions in a coastal upwelling regime. Ambient biomass and nutrient concentrations, as well as production and regeneration rates, were measured during two upwelling seasons and one winter. Nitrate assimilation accounted for 55% of the nitrogen utilized, compared to 35% for ammonium and 10% for urea. High nitrate uptake rates occurred in the upper 8 m of the water column after water had been upwelled from depth into the euphotic zone. Observed temporal changes in particulate nitrogen–specific nitrate uptake rates reflected variations in phytoplankton biomass rather than changes in phytoplankton–specific activity. The highest ammonium uptake rates were routinely measured at 12 m. Uptake rates were highest during upwelling–induced phytoplankton blooms and decreased with the demise of the blooms. The lowest ammonium uptake rates coincided with active upwelling events and the winter. During periods of relaxed upwelling, water with concentrations of ammonium between 2 and 4 μM were found centered around 20 m. Indirect evidence suggests that macrozooplankton grazing may have been responsible.

Estimates of annual rates of primary production indicate that these

waters were more productive than previously thought. Total nitrogenous production at this site was 257 g N m^{-2} y^{-1}. Of the total primary production, 137 g N m^{-2} y^{-1} was attributed to new production, compared to 119 g N m^{-2} y^{-1} from regenerated nitrogen sources. Ammonium assimilation accounted for 92 g N m^{-2} y^{-1}, whereas urea comprised 27 g N m^{-2} y^{-1} of the regenerated production.

Ammonium uptake and regeneration rates measured over 12 to 18 h long time course experiments remained essentially constant. However, as the length of the incubations increased the amount of usable data decreased dramatically due to key assumptions of the ^{15}N method being violated. Mass balance calculations indicated that 22 to 51% of the ammonium removed from the dissolved pool was not recovered in the particulate fraction. In addition, the amount of label that could not be accounted for appeared to be a more serious problem at 0 and 8 m (47%) than 25 m (22%).

Daily uptake and regeneration rates were fastest in the upper 12 m of the water column and decreased with depth. At 0, 12, and 20 m uptake rates either balanced or exceeded regeneration rates, whereas at 8 and 25 m net regeneration took place. Ammonium uptake rates were highest during the two upwelling seasons (11 to 17 mmol N m^{-2} d^{-1}) and lowest during the winter (3 mmol N m^{-2} d^{-1}), whereas regeneration rates did not differ seasonally (11 to 20 mmol N m^{-2} d^{-1}). Ammonium regeneration by the microbial community was able to supply all of the ammonium requirements of the phytoplankton (i.e. >100%) and provided 27% of the assimilated nitrogen.

Nitrogen Dynamics in a Coastal Upwelling Regime

by

Mary–Lynn Dickson

A THESIS

submitted to

Oregon State University

in partial fulfillment of
the requirements for the
degree of

Doctor of Philosophy

Completed April 15, 1994

Commencement June 1994

APPROVED:

Redacted for Privacy

Professor of Oceanic and Atmospheric Sciences in charge of major

Redacted for Privacy

Dean of College of Oceanic and Atmospheric Sciences

Redacted for Privacy

Dean of Graduate School

Date thesis is presented April 15, 1994

Typed by researcher for Mary-Lynn Dickson

For my parents, Jack and Charlotte Dickson

ACKNOWLEDGEMENTS

First and foremost, I would like to thank my supervisor, Patricia Wheeler, for the opportunity to undertake this study. Without her guidance, patience, and advice, this body of work would not have been nearly as complete. Comments and suggestions by Pat and the rest of my committee, Tim Cowles, Fred Prahl, Steve Giovannoni, and Dave Myrold are greatly appreciated.

I would like to thank the numerous students who assisted in the sampling program carried out off the Oregon coast from 1989 to 1991. Without their efforts, this work could never have come to fruition. In particular, I am indebted to Lynne Fessenden and Susanne Neuer. Their friendship made the long hours at the coast bearable and many stimulating discussions with them aided me in interpreting the results. The chlorophyll *a* data are provided courtesy of Lynne and Susanne.

Finally, I thank the many people in the College of Atmospheric and Oceanic Sciences, Oregon State University and the Graduate School of Oceanography, University of Rhode Island who made each day an enjoyable one. Their friendship, support and encouragement will not be forgotten.

This work was supported by a NASA Graduate Student Fellowship in Global Change Research.

TABLE OF CONTENTS

LIST OF FIGURES

LIST OF TABLES

NITROGEN DYNAMICS IN A COASTAL UPWELLING REGIME

CHAPTER 1

INTRODUCTION

The Physical Setting

The coastal waters off Oregon offer a dynamic and complex hydrographic setting in which to conduct oceanographic research. Understanding the physical oceanography of this region, and to a lesser extent the biological oceanography, has been an area of active investigation. Physical oceanographic results have been summarized in the context of the biology by Peterson et al. (1979), Small and Menzies (1981) and more recently in a series of papers on the coastal oceanography of Washington and Oregon edited by Landry and Hickey (1989). What follows is a brief description of the upwelling cycle and hydrography of the Oregon coast and the biological response to upwelling.

Wind–driven coastal upwelling is the result of larger scale atmospheric and oceanic processes. This seasonal phenomena occurs in both the northern and southern hemispheres along the western side of continents (Fig. 1.1). In the northern hemisphere the best known coastal upwelling systems are along the west coast North America, principally off Oregon and northern California, and off northwest Africa. In the southern hemisphere, Peru and the Benguela upwelling system off southern Africa are the two most studied regions to date. In all these places the same physical principles resulting

in a wind–driven coastal upwelling regime apply, although the remainder of this discussion will concentrate on our knowledge of the upwelling dynamics along the west coast of United States of America.

The presence of a stationary mid–ocean atmospheric high pressure system in the Gulf of Alaska sets up a circulation pattern in which strong northerly and northwesterly winds move down the west coast of North America in the spring and summer (Fig. 1.2a). Because the coast is on the cyclonic side of the wind, there is net Ekman transport of the top few meters of water offshore. The removal of surface water is in turn balanced by the upwelling of cold, nutrient–rich water close to the coast (Fig. 1.2b).

Off Oregon, wind–driven coastal upwelling is the dominant oceanographic process from May through October (Bakun et al. 1974). However, upwelling here is intermittent and episodic in nature, in contrast to the continuous upwelling off Peru and northwest Africa. As many as 4 to 5 major upwelling events can take place each year, in addition to many smaller events (Huyer 1976). The duration and strength of the winds determine the degree of upwelling. Generally, the time required for the upwelling circulation to respond to the wind at 45°N off Oregon is about 17 h (Barber and Smith 1981). If the wind blows continuously for at least as long as the inertial period, the surface Ekman layer is transported offshore at a velocity of several kilometers per day. Off Oregon the Ekman layer is relatively thin due to the weak wind stress (Lentz 1992). Estimates of the thickness of this layer during

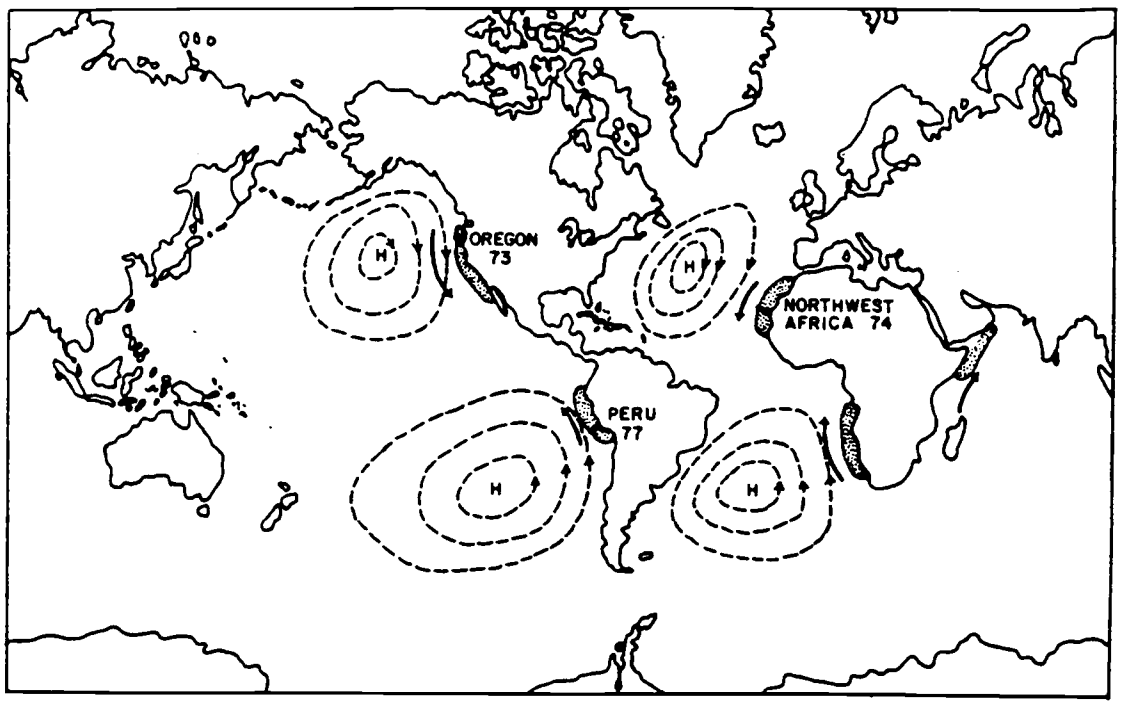

Figure 1.1. Major coastal upwelling regions of the world and sea–level atmospheric pressure systems (anticyclones) that influence them. The dashed circles represent mean idealised positions of isobars during the season of maximum upwelling in a given region. Major areas of upwelling are shown by stippled areas. Arrows indicate the location of the (a) California current off the USA, (b) Peru current off Peru, (c) Canary current off northwest Africa, (d) Benguela current off southwest Africa, and (e) the Somali current in the Indian Ocean east of Africa. From Barber and Smith (1981).

Figure 1.2. (a) Atmospheric circulation pattern in the northern hemisphere during the spring and summer months that result in wind–driven coastal upwelling along the western side of the North American continent. Strong northerly and northwesterly winds move down the west coast and result in the surface layer of the water column being moved offshore. (b) Cross–section of the upwelling circulation off Oregon. Once the surface or Ekman layer moves offshore, water from 100 to 200 meters replaces it. From Neshyba (1987).

A

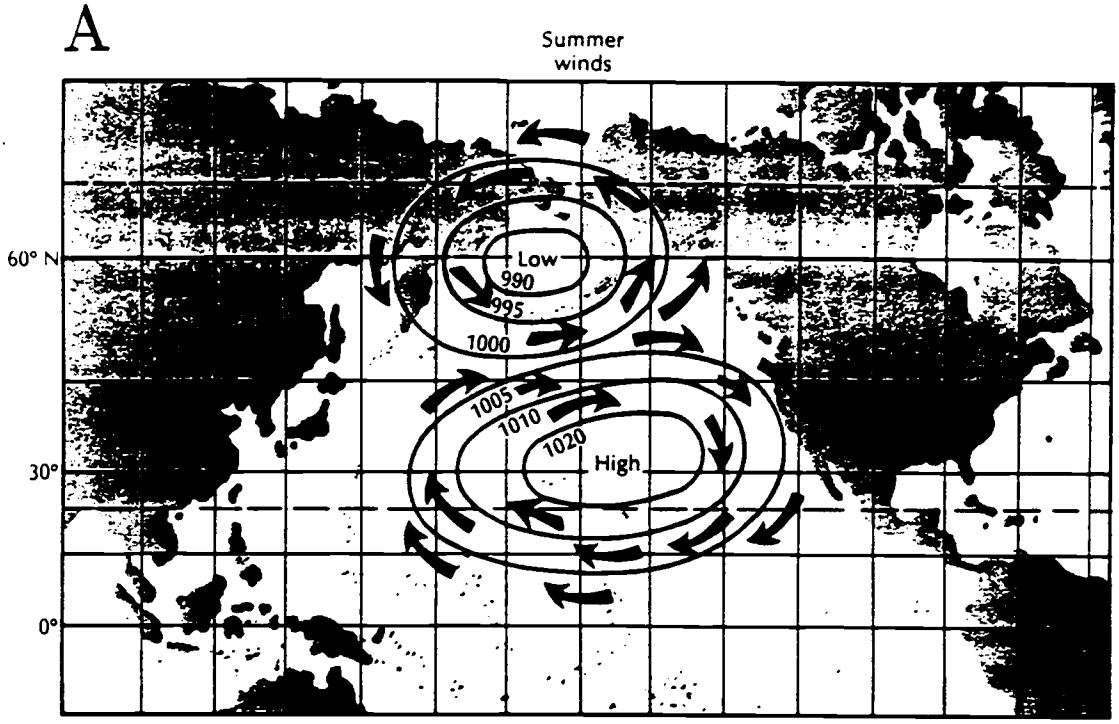
Summer winds
60° N
30°
0°
Low
990
995
1000
1005
1010
1020
High

B

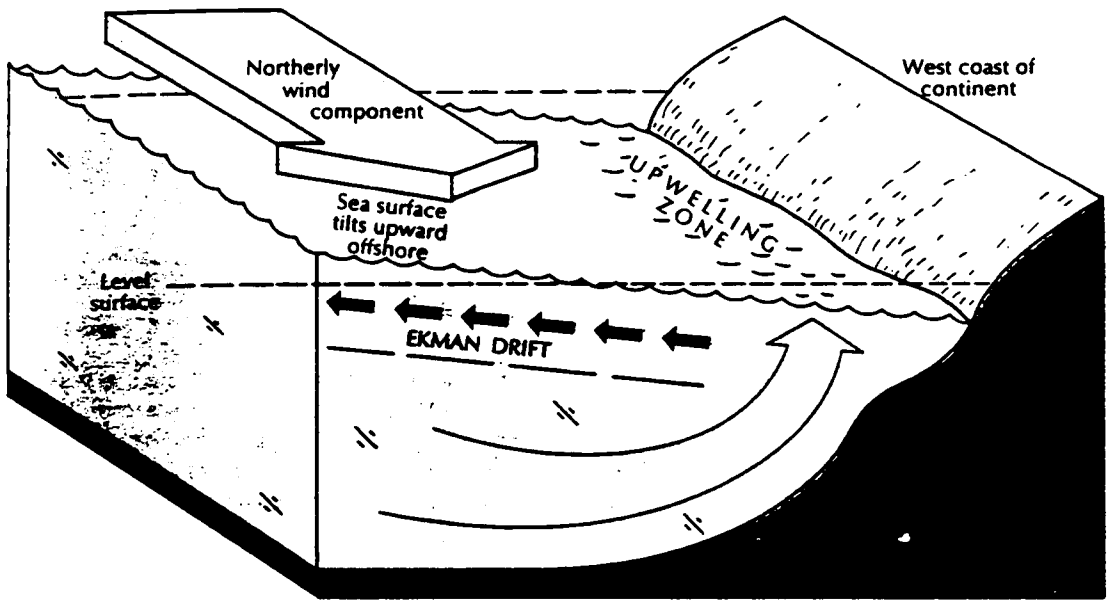
Northerly wind component
West coast of continent
Sea surface tilts upward offshore
UPWELLING ZONE
Level surface
EKMAN DRIFT

the upwelling season vary from <5 m (Peterson et al. 1979) to ~2 m (Lentz 1992). The source water which replaces the surface layer, typically comes from 20 to 35 km offshore and from depths between 100 and 200 m (Huyer 1976). This deep water is characterized by nitrate concentrations between 15 and 25 μM (Small and Menzies 1981). The position of the permanent pycnocline (σ_t=25.5–26.0), an indicator of the maximum vertical density gradient inshore (Small and Menzies 1981), defines the degree of upwelling (Fig. 1.3). When strong winds set up an upwelling circulation, the pycnocline intersects the sea surface between 5 and 10 km from shore. This region of pronounced temperature and salinity gradients marks the position of the upwelling front. During the upwelling season it is not uncommon for the wind direction and/or speed to change. If the winds weaken, the pycnocline will not intersect the sea surface. Under those conditions weak upwelling can occur. Conversely, if the winds reverse direction (i.e. come from the south,) upwelling will cease and downwelling can result (Fig. 1.4). The latter situation is commonly referred to as upwelling relaxation.

The upwelling regime off Oregon has a strong two–layered flow. In addition to the offshore movement of surface water, there is also a compensating onshore component of flow occurring at mid–depth over the Oregon shelf. This onshore flow is thought to be important for carrying regenerated nutrients back into the more biologically productive waters of the upwelling

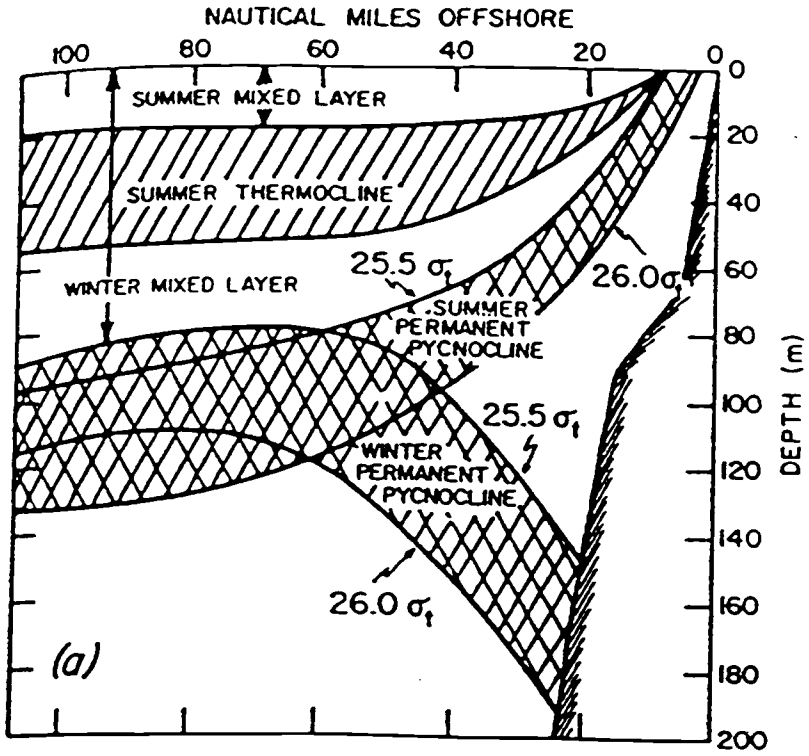

Figure 1.3. Cross–section of the water column off Oregon showing the hydrography and position of the 25.5 and 26.0 isopycnals during the summer and winter. From Small and Menzies (1981).

Figure 1.4. Diagram illustrating the occurrence of a downwelling circulation when the winds reverse direction and come from the south, instead of the north. Although such a situation typically happens during the winter months due to the circulation pattern of the atmosphere, it can also occur for brief periods during the spring and summer months. From Neshyba (1987).

A

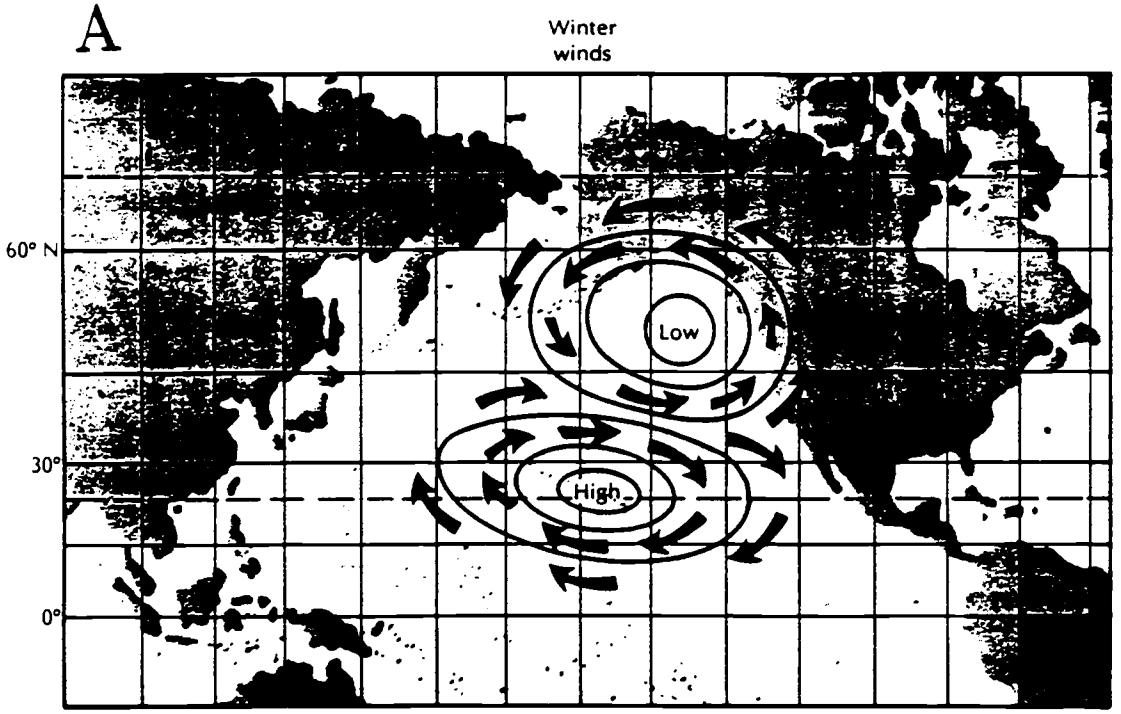
Winter
winds
60° N
30°
0°
Low
High

B

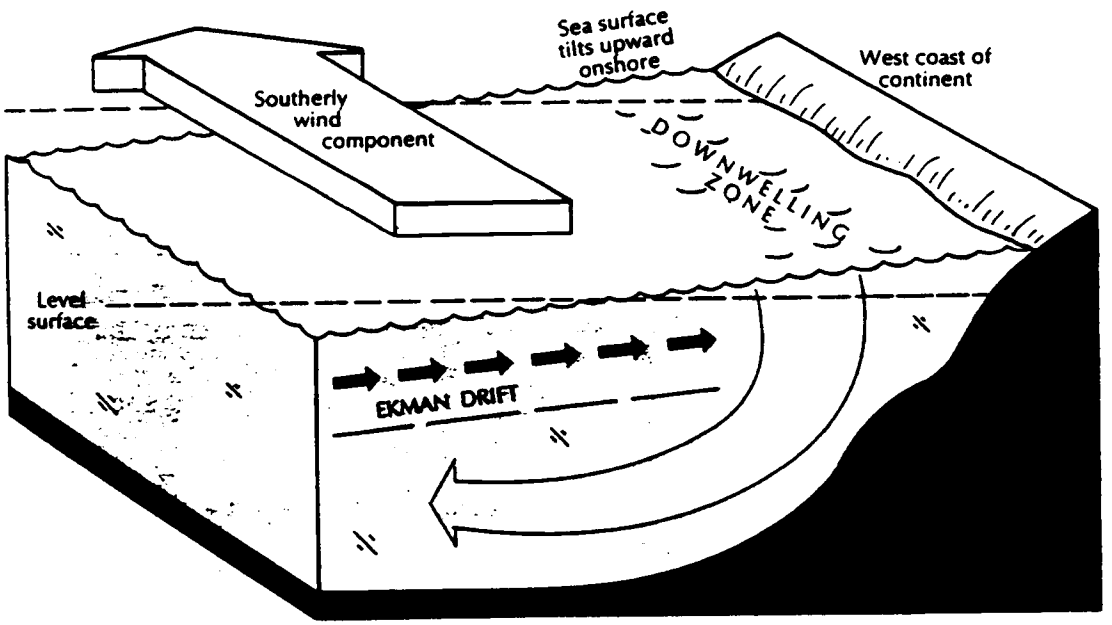
Sea surface
tilts upward
onshore
West coast of
continent
Southerly
wind
component
DOWNWELLING
ZONE
Level
surface
EKMAN DRIFT

front (Barber and Smith 1981). Originally, it was thought that the cross–shelf circulation could be explained by a one–cell model (Huyer 1976). In this model, water from depth upwells next to the coast, mixes with the surface water and then moves offshore (Fig. 1.5a). Subsequent analysis of physical and biological field data and modelling efforts suggest that some variation of a two–cell circulation model is more appropriate (Halpern 1976, Wroblewski 1976, Peterson et al. 1979). In the two–cell model (Fig. 1.5b), newly upwelled water moves offshore and sinks along the isopycnals of the permanent pycnocline while still on the landward side of the front. A second cell is positioned on the seaward side of the front and above the first cell. Here upwelled water just mixes with the surface water and is transported offshore.

In addition to the complex circulation patterns induced by upwelling, the Oregon coast also receives significant outflow from the Columbia River and many smaller coastal rivers. In the winter when surface currents are northward and toward the coast, the effluent from the Columbia River is restricted to the Washington coast and does not affect Oregon coastal waters (Huyer 1977). Winter runoff from smaller coastal rivers reduces salinities, especially inshore. Generally during the upwelling season the Columbia River plume is pushed southward by the prevailing winds and away from the coast due to the transport of the surface layer offshore (Fig. 1.6). During periods of relaxed upwelling warm, low salinity water is able to move closer inshore.

Figure 1.5. (a) One–cell model of the cross–shelf circulation in an upwelling regime proposed by Huyer (1976). In this model, upwelled water mixes with the surface water and then moves offshore. (b) Diagram of the two–cell model of upwelling circulation of Wroblewski (1977). In this scenario, newly upwelled water moves offshore and sinks along isopycnals of the permanent pycnocline while still on the landward side of the upwelling front. A second cell is located on the seaward side of the front where upwelled water mixes with surface water and is transported offshore. From Peterson et al. (1979).

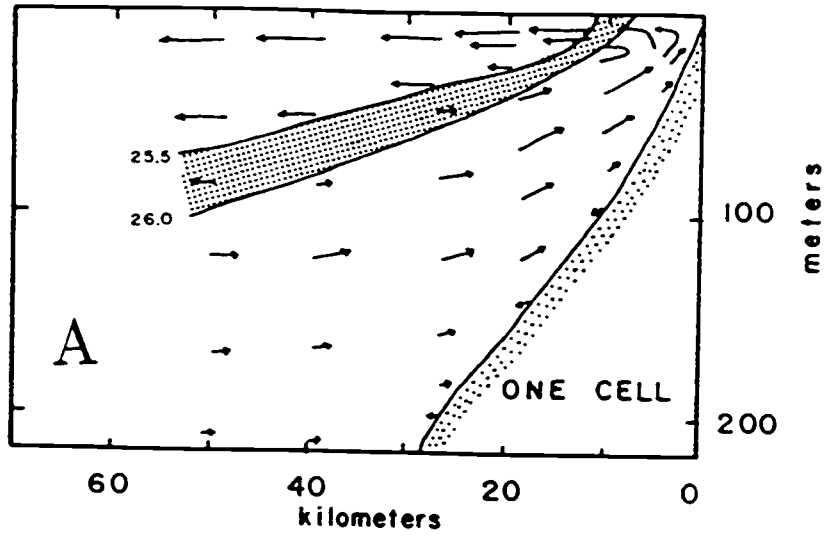
25.5
26.0
A
ONE CELL
100
200
meters
60
40
20
0
kilometers

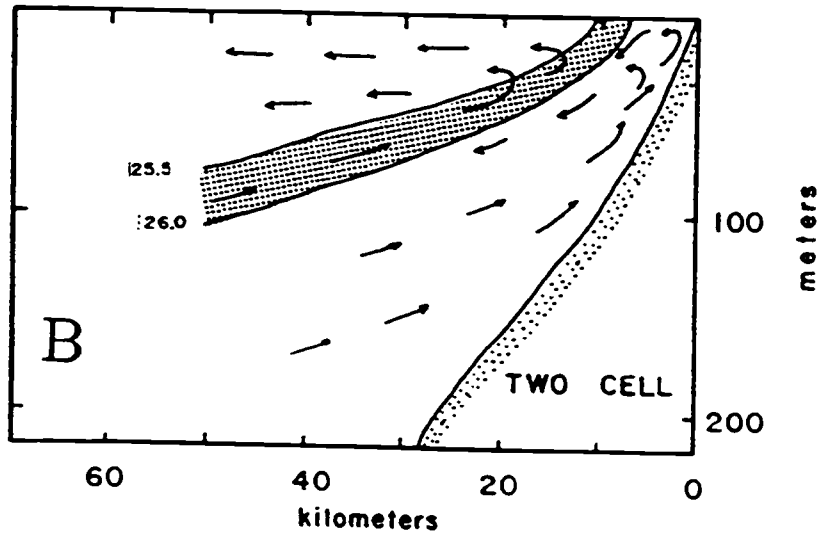
25.5
26.0
B
TWO CELL
100
200
meters
60
40
20
0
kilometers

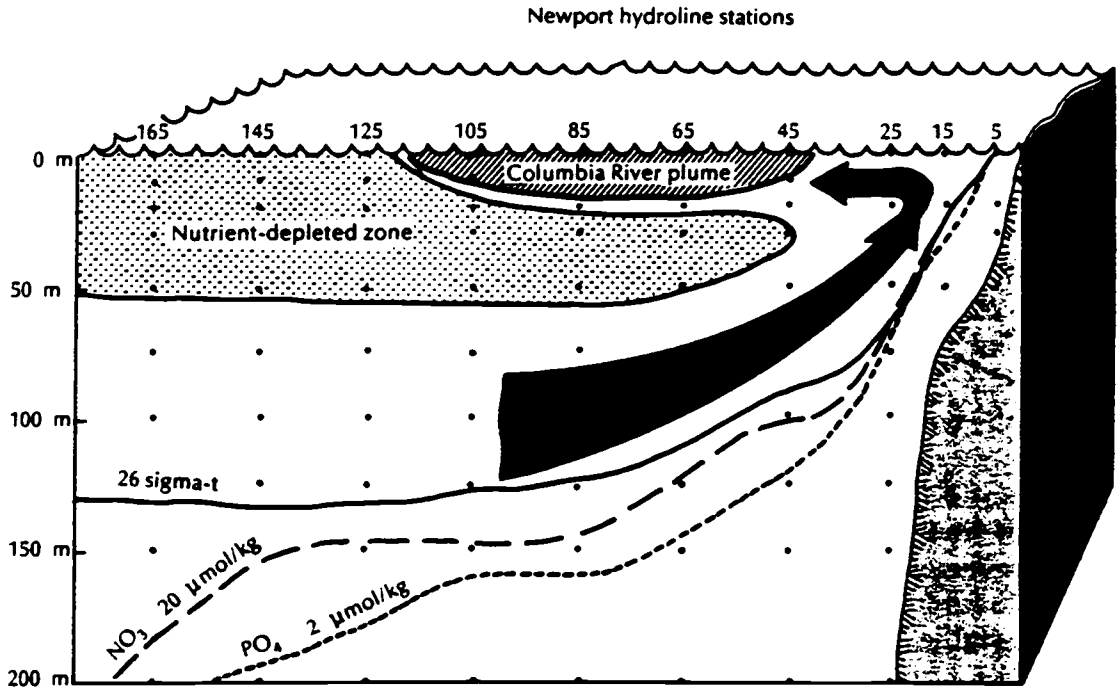

Figure 1.6. Position of the Columbia River plume in relation to other features during upwelling. From Neshyba (1987).

The Biological Response to Upwelling

Wind–driven coastal upwelling regimes are amongst the most biologically productive regions in the ocean (Ryther 1969) (Table 1.1). In addition to supporting high levels of primary production, these areas are responsible for almost half of the world's fish catch even though they only represent 0.1% of the ocean's area. Originally it was believed that most of the primary production was transferred to higher trophic levels, such as fish, due to the small number of trophic links between the top and bottom of the food chain and the high transfer efficiencies between them. Since then we have come to realize that upwelling systems are not simply characterized by a linear foodchain (i.e. phytoplankton $\rightarrow$ copepods $\rightarrow$ fish), but also possess extremely complex trophic relationships in the form of the "microbial loop" (Azam et al. 1983, Neuer 1992). As well, the pioneering work of Dugdale and Goering (1967) and Eppley and Peterson (1979) have suggested that the source of assimilated nitrogen (i.e. new versus regenerated nitrogen – see the next section on using ^{15}N isotopes to measure primary production) has important ramifications for determining the amount of material that can be transferred to higher trophic levels in any ecosystem. Now it is generally recognized that the functioning of ecosystems is closely intertwined with its structure and vice versa. For instance, not only can the species composition of the autotrophs or level of primary production affect the grazer assemblage

and grazing rates, there can also be a compensating affect of the grazers on the primary producers via the availability of nutrients (e.g. Walsh 1976, Harrison 1990).

The most complete picture of the nitrogen dynamics during the development of a phytoplankton plume has come from the coupling of a numerical model of upwelling circulation with a model of primary production (Wroblewski 1977). High concentrations of nitrate introduced into the euphotic zone by upwelling are assimilated by the phytoplankton. Initially phytoplankton utilization of the nitrate is low due to the low autotrophic biomass and its short residence time in the euphotic zone. As the phytoplankton are advected offshore, stabilization of the water by surface warming occurs and results in a nutrient–rich, well lit environment. Such conditions are conducive to massive accumulations of plant biomass and extremely high levels of primary production. Subsequent relaxation of the wind reduces the rate of upwelling and eventually leads to the depletion of nitrate in the surface layers and lower primary production rates. The cessation of upwelling ultimately results in the decay of the phytoplankton bloom.

The extent of an upwelling event determines the amount of nitrate available to the phytoplankton. The subsequent aging and circulation patterns of the upwelled water also affect the distribution of biomass and productivity along the coast. Upwelling-favorable winds produce alongshore

Table 1.1. Estimates of mean annual primary production and fish production in three ocean provinces. From Ryther (1969).

Table 2. Division of the ocean into provinces according to their level of primary organic production.

Province	Percentage of ocean	Area (km^2)	Mean productivity (grams of carbon/m^2/yr)	Total productivity (10^9 tons of carbon/yr)
Open ocean	90	326×10^6	50	16.3
Coastal zone*	9.9	36×10^6	100	3.6
Upwelling areas	0.1	3.6×10^5	300	0.1
Total				20.0

* Includes offshore areas of high productivity.

Table 3. Estimated fish production in the three ocean provinces defined in Table 2.

Province	Primary production [tons (organic carbon)]	Trophic levels	Efficiency (%)	Fish production [tons (fresh wt.)]
Oceanic	16.3×10^9	5	10	16×10^8
Coastal	3.6×10^9	3	15	12×10^7
Upwelling	0.1×10^9	1½	20	12×10^7
Total				24×10^7

gradients in phytoplankton biomass and production parallel to the Oregon coast (Fig. 1.7). Small and Menzies (1981) noted, for example, that strong upwelling conditions early in the upwelling season resulted in a single band of high phytoplankton biomass and production that ran parallel to the bottom contours. Later in the season, when a two–cell circulation pattern had been established, similar wind conditions caused two bands of biomass. Weak upwelling conditions produced biomass bands further inshore that were twice as productive as when strong upwelling conditions prevailed.

Off central Oregon the highest phytoplankton and zooplankton biomass (Fig. 1.8a) and the maximum carbon uptake rates and assimilation ratios (Fig. 1.8b) are usually found in the upper 20 m of the upwelling front (Peterson et al. 1979, Small and Menzies 1981). Nitrate concentrations are usually higher than the half–saturation concentration for nitrate uptake by phytoplankton (K_s=1.26 μM – see Chapter 2). As a result, phytoplankton growth in the surface layers appears to be nitrogen sufficient and is independent of nitrate concentrations most of the time (Curl and Small 1965, Barber and Smith 1981). Below the surface layer, light is probably the single most important environmental variable affecting primary production and especially rates of new production (MacIsaac and Dugdale 1972).

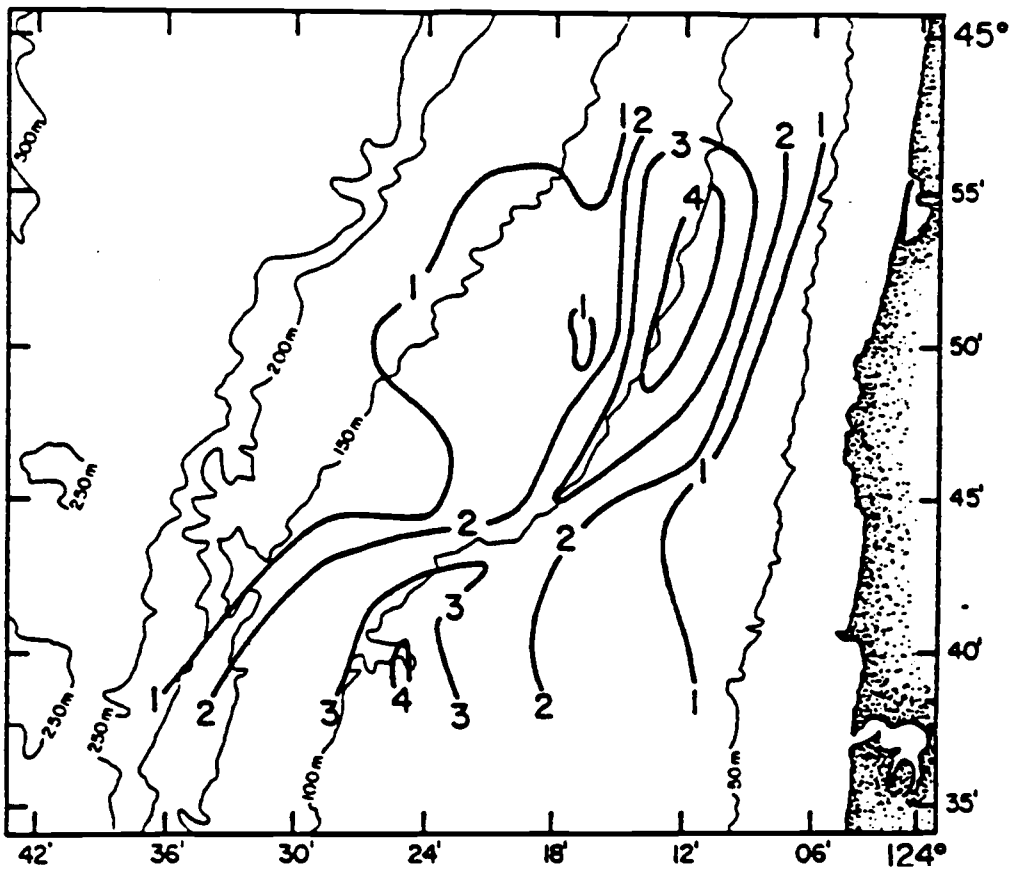

Figure 1.7. A surface map of chlorophyll *a* concentrations (μg liter^{-1}) during the upwelling season off Oregon. The upwelling circulation results in alongshore gradients in chlorophyll *a* running parallel to the coast and bottom bathymetry. From Small and Menzies (1981).

Figure 1.8. Profiles of (a) ten parameters along a transect off central Oregon under strong upwelling conditions. From Small and Menzies (1981). (b) *Pseudocalanus* sp. abundance (number of animals per m^{-3}) along the Newport hydrographic line. From Peterson et al. (1979).

A

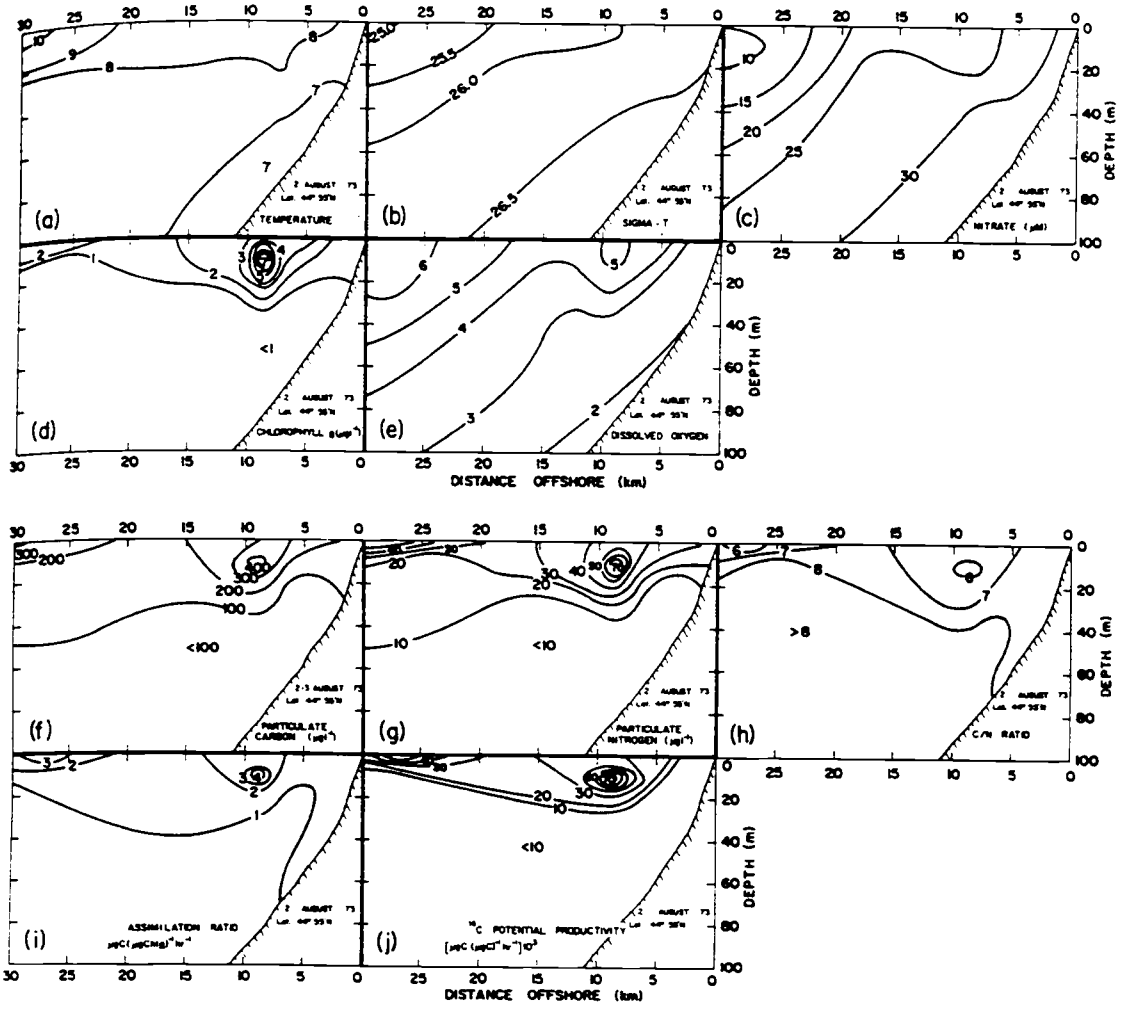
(a)
TEMPERATURE
(b)
SIGMA - T
(c)
NITRATE (µM)
(d)
CHLOROPHYLL a (µg l⁻¹)
(e)
DISSOLVED OXYGEN
DEPTH (m)
DISTANCE OFFSHORE (km)
(f)
PARTICULATE CARBON (µg l⁻¹)
(g)
PARTICULATE NITROGEN (µg l⁻¹)
(h)
C/N RATIO
(i)
ASSIMILATION RATIO
(j)
¹⁴C POTENTIAL PRODUCTIVITY

B

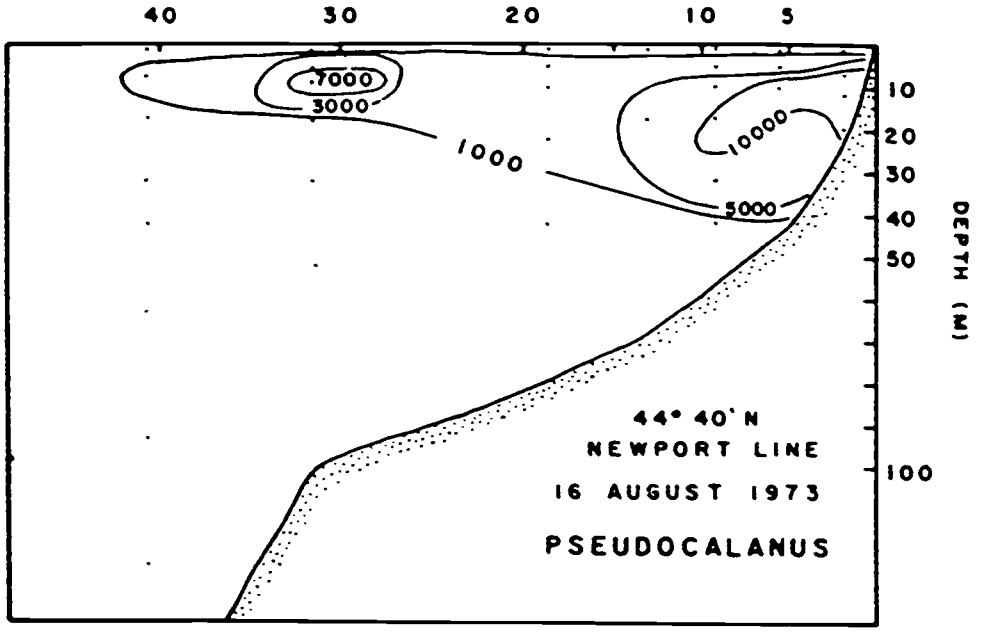
40
30
20
10
5
7000
3000
1000
10000
5000
10
20
30
40
50
100
DEPTH (M)
44° 40' N
NEWPORT LINE
16 AUGUST 1973
PSEUDOCALANUS

The Utility of ^{15}N Isotopes in Measuring Primary Production

Primary production measurements (i.e. the rate at which phytoplankton synthesize organic material from the utilization of inorganic/organic nutrients) in the ocean began in earnest during the 1950's when Steeman Nielsen (1952) introduced the application of $H_2{}^{14}CO_3$, a radioisotope, to the problem. The use of nitrogen isotopes for rate measurements took longer to develop, probably due in part to the relative unavailability of an analogous radioactive isotope. ^{13}N is a radioactive isotope of nitrogen, however with a half–life of 10 minutes it has not been used extensively and is especially problematic to apply to field studies. More than a decade passed before the use of nitrogenous compounds labelled with ^{15}N (a stable isotope) became available to biological oceanographers. The development of nitrogen isotopic techniques meant that more precise rate measurements could be made than analytical chemical oceanographic methods had provided. The availability of this isotope also meant that specific nitrogenous compounds could be labelled and various transformational pathways traced.

The theoretical framework for tracer methodology originally came from a treatise on the subject by Sheppard (1962). The initial use of ^{15}N in field studies was pioneered by Dugdale (1967) and Dugdale and Goering (1967). They introduced the concept that primary production consisted of two components, based on the source of the nitrogenous nutrients. New

production was defined as the amount of primary production dependent on the input of new sources of nitrogen, such as nitrate, from below the euphotic zone or from outside the euphotic zone (i.e. atmospheric or terrestrial inputs). Conversely, regenerated production is based on nutrients such as ammonium and urea that are generated within the euphotic zone either as by–products of grazing by micro– and macrozooplankton or due to the remineralization of organic matter by bacteria.

The ideas of Dugdale and Goering (1967) were subsequently refined and expanded by Eppley and Peterson (1979). They realized that under steady state conditions new production should be equivalent to the export flux of material out of the euphotic zone. In addition, Eppley and Peterson (1979) defined a non–dimensional variable, the f–ratio, as the ratio of new to total production and similarly, [1−(f–ratio)] as a qualitative measure of nutrient regeneration. Their analysis showed that the amount of nutrient recycling varied regionally with the total primary production rate. Ecosystems in which most of the assimilated nitrogen was in the form of ammonium or urea had lower total primary production rates than systems mainly dependent on nitrate (e.g. oligotrophic central gyres versus coastal upwelling regimes).

Methods

Methological aspects of using ^{15}N isotopes in marine studies have been addressed by Harrison (1983), and more recently by Glibert and Capone (1993). Reviews of the protocols for ^{15}N sample analysis by emission and mass spectrometry can be found in Fiedler and Proksch (1975), Preston (1993) and Mulvaney (1993). A brief summary of ^{15}N experimental design, the equations used to calculate uptake and regeneration rates and the assumptions of these methods follow.

The measurement of ^{15}N uptake rates involves using a labelled form of a nitrogenous substrate; either a dissolved inorganic (e.g. nitrate, ammonium) or organic (e.g. urea) form of nitrogen. Seawater is confined in a bottle, preferably made of polycarbonate to minimize potential contamination effects by trace metals, and spiked with the appropriate label. In order not to perturb the system, the amount of added label is $\sim$10% of the ambient concentration of the nitrogenous substrate. The sample is then incubated, usually at ambient light and temperature levels, either for several minutes if transport rates across the cell wall are desired or several hours for the measurement of ^{15}N incorporation into amino acids and proteins. Incubations are terminated by the filtration of the seawater and collection of particulate nitrogen on the filters. The filters are then frozen and subsequently dried before being processed and analyzed for ^{15}N incorporation

into particulate matter. Filters are ground with a copper catalyst (i.e. CuO) and placed in Pyrex tubes with CaO (to absorb gaseous impurities, such as H_2O and CO_2). Sample tubes are then evacuated on a vacuum line, sealed and heated for 24 h in a 550°C oven. As a result of this modified Dumas combustion, the particulate nitrogen is converted to N_2 gas.

Isotopic analysis of N_2 gas is made using either an emission or mass spectrometer. Mass spectrometry has the advantage of better analytical precision and much lower detection limits for labelled nitrogen than is possible with emission spectrometry. However, emission spectrometers are not as expensive to purchase, run or maintain and sample sizes can be significantly smaller. For instance, mass spectrometers require a minimum sample of 30 μg N, whereas emission spectrometers can measure samples containing only 0.2 to 10 μg N. Both emission and mass spectrometers are used to measure the ratio of $^{15}N/^{14}N$ from which the isotopic abundance, expressed as atom% ^{15}N, is calculated. Mass spectrometry measures a ratio of the intensities of the currents produced by two or more ion beams, $^{14}N_2$, $^{14}N^{15}N$, $^{15}N_2$. Emission spectrometry involves measuring differences in the relative intensities of electromagnetic radiation emitted in the ultra–violet region of the spectrum when the various species of N_2 gas (i.e. $^{14}N_2$, $^{14}N^{15}N$, and $^{15}N_2$) are excited by an external energy source. Because these dinitrogen atoms have small differences in their mass, there are slight differences in their outer orbital energy levels and in the wavelengths of their emission lines.

Calculations: Uptake Rates

Once the abundance of mass 28 ($^{14}N_2$), 29 ($^{14}N^{15}N$) and 30 ($^{15}N_2$) in a sample is determined, its atom% ^{15}N can be calculated by:

$$\text{atom\% } ^{15}\text{N} = \frac{(\text{mass } 30) + 1/2(\text{mass } 29)}{(\text{mass } 30) + (\text{mass } 29) + (\text{mass } 28)} \quad (1)$$

In emission and mass spectrometry it is possible to calculate the $\%^{15}N$ abundance from the mass 28 and 29 dinitrogen molecules;

$$\text{atom\% } ^{15}\text{N} = \frac{100}{(2R + 1)} \quad (2)$$

where, R = [(mass 28)/(mass 29) x sensitivity setting]. The atom% excess for a sample is then determined by subtracting the natural isotopic abundance of ^{15}N (i.e. 0.365%) from the atom% ^{15}N calculated in equation (2).

The specific uptake rate, V, has units of $(\text{time})^{-1}$ and is given by;

$$V = \frac{\text{atom\% excess}}{(\text{atom\% enrichment x incubation time})} \quad (3)$$

Where the atom% enrichment of the substrate is determined from;

$$\text{atom\% enrichment} = \left[\frac{^{15}\text{N conc. added}}{(^{15}\text{N conc. added} + \text{ambient conc.})}\right] \times 100 \quad (4)$$

The absolute uptake rate, ρ, with units of [(mass of nitrogen taken up) $(\text{volume})^{-1}$ $(\text{time})^{-1}$] is calculated by multiplying the specific uptake rate by the particulate nitrogen concentration (PN), such that;

$$\rho = V \times PN \quad (5)$$

As well, uptake rates can also be normalized by the chlorophyll *a* concentration to give a biomass specific uptake rate, V^{Chl}, having units of [(mass of nitrogen taken up) (mass of Chl *a*)$^{-1}$ (time)$^{-1}$]. This is calculated by dividing ρ by the chlorophyll *a* concentration, where;

$$V^{Chl} = \frac{\rho}{Chl} \tag{6}$$

The ^{15}N experimental approach assumes:

• *There is no change with time in the isotopic enrichment of the substrate.* The next section of this chapter will deal with how ammonium uptake rates are corrected for changes in enrichment due to the regeneration of ammonium.

• *No significant substrate depletion occurs during the incubation.* This problem arises when ambient nitrogen concentrations are low and can lead to an underestimation of the uptake rate. It tends to be more of a concern for studies carried out in oligotrophic waters rather than coastal ones.

• *There is no significant change in the particulate nitrogen concentration over the course of the experiment.* This potential error can be detected by taking particulate nitrogen samples at the beginning and end of the incubation and can be minimized by keeping incubation times short.

In addition to the assumptions listed above, Harrison (1983) has reviewed those that are implicit in tracer studies. The characteristics of the behaviour of an "ideal" tracer is based on the work of Atkins (1969) who identified them as;

- *"The tracer undergoes the same metabolic transformations as the unlabelled substrate, i.e., "isotope effects" are negligible (or quantifiable)."*
- *"The tracer does not disturb the steady state existing in the system as a whole, i.e., there are no significant perturbations to compartments or their transformations."*
- *"The tracer is initially not in equilibrium with the system studied and its changes over time are quantifiable and reflect transfers (or transformations) of the traced substance."*
- *"There is no exchange of the isotope between the labelled substance and other substances in the system."*

Harrison (1983) has pointed out that studies utilizing ^{15}N isotopes rarely violate the first and last assumptions. The second assumption may be violated if true trace additions (i.e. $\sim$10% of ambient substrate concentrations) cannot be achieved, while long incubation times may lead to the violation the third assumption.

Calculations: Regeneration Rates

Uptake rates measured for regenerated nitrogen sources, such as ammonium and urea, have to be corrected for isotope dilution. In the case of ammonium, the atom% enrichment of the ^{15}N changes over time due to the excretion of $^{14}NH_4^+$ by zooplankton and/or bacteria, which dilutes

the label. Ammonium uptake and regeneration rates are calculated using the linear differential equation model of Blackburn and Caperon (Blackburn 1979, Caperon et al. 1979) from measured changes in the ammonium concentration and atom% enrichment of ^{15}N in the dissolved ammonium pool. This model assumes that changes in the ammonium concentration and enrichment are linear with time. Two equations are solved simultaneously and can be written:

$$P_t = P_0 + (d - \rho)t \tag{7}$$

and

$$\ln(R_t) = \ln(R_0) - [d/(d - \rho)] \times [\ln(P_t/P_0)] \tag{8}$$

where P is the substrate concentration at the beginning (0) and end (t) of the incubation, d is the regeneration rate, ρ is the absolute uptake rate, t is the incubation time, and R is the atom% excess of ^{15}N in the ammonium pool at the beginning (0) and end (t) of the incubation. The slopes of these two equations allow one to calculate d and ρ.

A difficulty in using the above equations to calculate regeneration rates occurs when no change can be measured in the ambient ammonium concentration over time. When such a case arises, it is still possible to estimate a regeneration rate by correcting the ammonium uptake rate using an average atom% enrichment for the incubation period (Glibert et al.

1982b). This method assumes there is an exponential decrease in the enrichment over time. The average atom% enrichment is calculated by;

$$\bar{R} = (R_0/k_t) \times (1 - e^{-kt}) \tag{9}$$

where R is the atom% enrichment at the beginning (0) and end (t) of the incubation, and k is the first order rate constant for the time dependent change in R (i.e. k=-($\ln[R_t/R_0]$)/Δt). Therefore, the regeneration rate is the product of k and the mean ammonium concentration.

Objectives of this Study

The purpose of this study was to understand the relationship between seasonal nitrogen dynamics in the Oregon upwelling zone and varying hydrographic conditions. Ambient concentrations of biomass and nutrients and production rates using ^{15}N isotopes were used to address this goal. A site located along the Newport hydrographic line, which has a fairly extensive biological (e.g. Peterson et al. 1979, Small and Menzies 1981, Curl and Small 1965) and physical oceanographic (e.g. Huyer 1976 and 1977, Halpern 1976) database, was selected and sampled repeatedly over two upwelling seasons and one winter (Fig. 1.9). Although the Oregon system may be one of the best known examples of a wind–driven coastal upwelling regime, relatively little is known about the nitrogen dynamics here compared to other

upwelling ecosystems, such as Peru and the Benguela system off southern Africa. Results of previous nitrogen work on the Oregon and Washington shelf have been presented by Kokkinakis (1987), Kokkinakis and Wheeler (1987 and 1988), and Dortch and Postel (1989), although none of these entailed a seasonal study.

This thesis consists of five chapters, three of which present the results and significance of research carried out on the utilization and regeneration of various nitrogen sources in an upwelling environment. This chapter introduced the physical principles that result in a seasonal upwelling circulation off the west coast of North America and the biological response to the physical forcing. The ^{15}N method, its assumptions, limitations and the objectives of this project have been outlined. The second chapter entitled "Nitrate uptake rates: A comparison of PN–specific, absolute and Chl *a*–specific rates" compares three measures of nitrate uptake rates. The purpose of making such a comparison was to evaluate whether temporal changes in uptake rates in other coastal upwelling regimes were due to the phytoplankton physiologically adapting to the upwelling environment or merely reflected changes in the phytoplankton biomass over time. Surprisingly, such a comparison had not been made prior to this study. The third and longest chapter of the thesis is entitled "Nitrogen dynamics". Its goal was to identify patterns in the nutrient fields, biomass concentrations and parameters, and utilization rates of nitrate, ammonium and urea as a

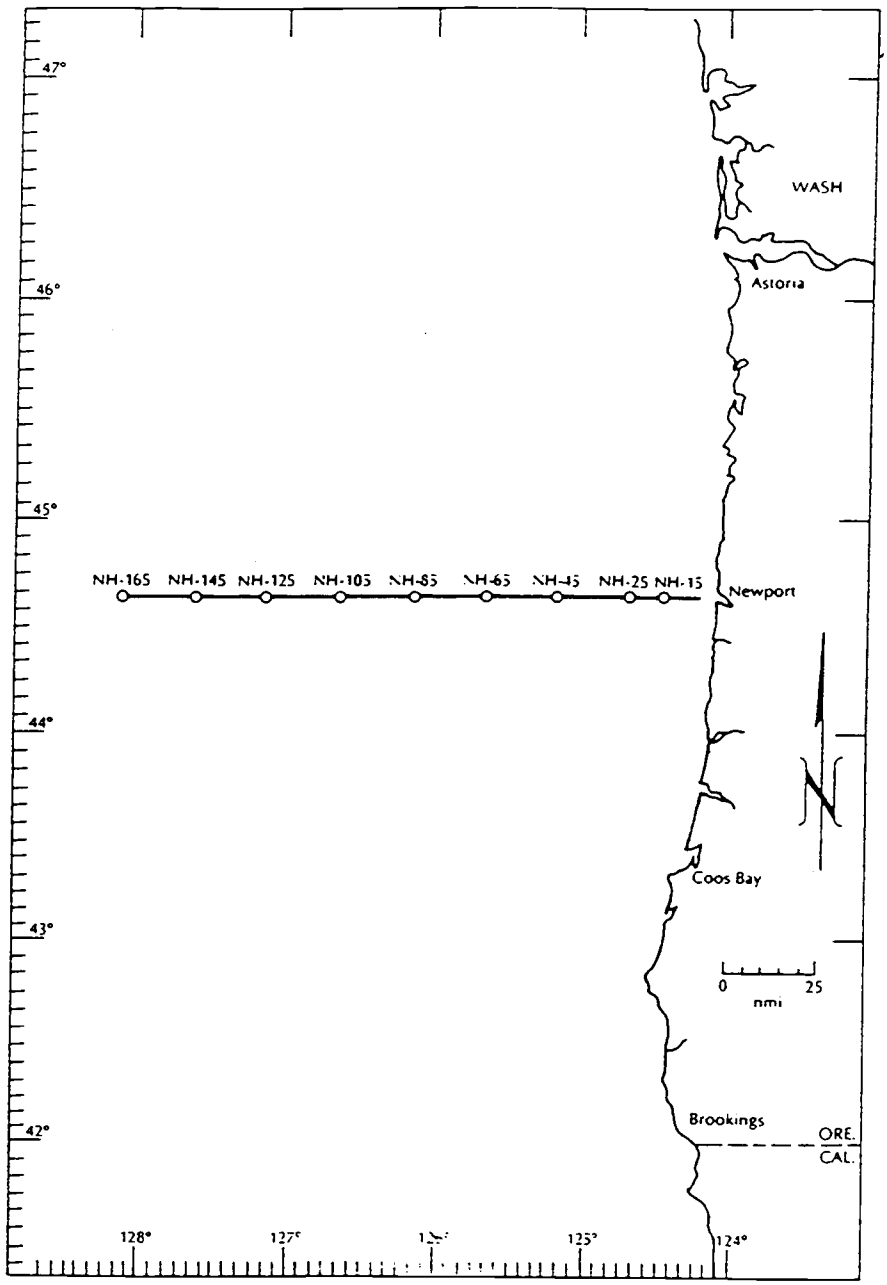

Figure 1.9. Location of the Newport hydrographic (NH) line off central Oregon. Our sampling site, 5 nautical miles from Newport (NH–5), is not shown. From Neshyba (1987).

function of changing hydrographic conditions during the upwelling season and between seasons (i.e. the upwelling season versus the winter). In addition, it was possible to estimate annual production rates for each of the nitrogen sources and compare the total amount of nitrogen used to primary production measurements made at the same time with ^{14}C. Chapter four ("Ammonium uptake and regeneration rates") explores the relationship between ammonium uptake and regeneration rates. Of particular interest were the time scales over which the two processes were coupled and the importance of ammonium regeneration in fulfilling phytoplankton nutritional requirements. Finally, chapter five summarizes the results of this study and the important questions that might be addressed in future studies of this ecosystem.

CHAPTER 2

NITRATE UPTAKE RATES: A COMPARISON OF PN–SPECIFIC, ABSOLUTE, AND CHL *a*–SPECIFIC RATES

Abstract

PN–specific, absolute and Chl *a*–specific nitrate uptake rates were measured during two upwelling seasons and one winter off Oregon. Although PN–specific and absolute uptake rates showed no dependence on the nitrate concentration, Michaelis–Menten kinetics were found to apply when the uptake rates were normalized to Chl *a*. Phytoplankton–specific nitrate uptake rates were saturated when nitrate concentrations were greater than 5 μM. Uptake rates decreased in response to either low nitrate concentrations or when extremely high phytoplankton biomass caused shading. PN– and Chl *a*–specific uptake rates were similar when Chl *a* concentrations were $\geq$4 μg liter^{-1} and phytoplankton nitrogen comprised most of the PN pool. When Chl *a* was <4 μg liter^{-1}, however, phytoplankton accounted for only 20–30% of the PN, and phytoplankton–specific uptake was five–fold greater than PN–specific uptake rates. These results suggest that observed temporal changes in PN–specific nitrate uptake rates reflect variations in phytoplankton biomass rather than changes in phytoplankton–specific activity. A comparison of Chl *a*–specific nitrate uptake rates from a variety of coastal upwelling ecosystems showed these rates to be high and almost identical. As well, a comparison of Chl *a*–specific nitrogen uptake rates between coastal and HNLC (i.e. high nitrate, low chlorophyll) waters

indicated that the major difference between these ecosystems was the form of nitrogen utilized and *not the rate* at which it was assimilated.

Introduction

In coastal upwelling regimes the distribution of biomass and primary production are strongly influenced by the combined effects of physical and biological processes. Small and Menzies (1981) recognized that phytoplankton biomass and primary production patterns were related to the strength of an upwelling event and the subsequent aging of the upwelled water. Later, MacIssac et al. (1985) suggested that temporal changes observed in nitrate uptake rates were due to physiological adjustments of the phytoplankton to their environment. They described a productivity cycle consisting of four zones of physiological condition along the axis of an upwelling plume. Similar results obtained during a series of drifter experiments and shipboard incubations led to the "conveyor–belt" (Wilkerson and Dugdale 1987) or "Shift–Up" hypothesis (Zimmerman et al. 1987, Dugdale and Wilkerson 1991).

An important tenet of this hypothesis is the existence of a lag period prior to the development of maximum uptake rates, presumably a time during which phytoplankton adapt to increased irradiance. Whether phytoplankton in fact adjust their metabolism in response to the upwelling cycle has recently been addressed in a modeling study by Garside (1991). Results of this model showed that changes in the particulate organic nitrogen (PN)–specific nitrate uptake rates could be explained by changes in the concentration of phytoplankton nitrogen relative to total particulate organic nitrogen concentration. A metabolic shift did not have to be invoked to explain temporal changes in uptake rates. As well, a series of ^{14}C experiments done in the equatorial Pacific concluded that upwelling and vertical mixing

did not affect the photosynthetic performance of phytoplankton (Cullen et al. 1992). No evidence was found to indicate that phytoplankton were poorly adapted to the upwelling environment. Previous field studies have not specifically examined the correlation between variations in phytoplankton biomass and changes in PN–specific nitrate uptake rates.

Estimates of primary production obtained by incubating seawater with $H^{14}CO_3$ are routinely normalized to the Chl *a* concentration and referred to as the assimilation number (Curl and Small 1965). By taking the phytoplankton biomass into account, photosynthesis under saturating light conditions can be compared over different spatial and temporal scales (Harrison and Platt 1980). In contrast, nitrogen–specific uptake rate measurements are usually normalized to the PN concentration. The PN trapped on filters includes detritus, bacteria, microzooplankton and mesozooplankton, in addition to phytoplankton (Dugdale and Goering 1967, Dugdale and Wilkerson 1991). There are many occasions when phytoplankton only make up a small percentage of the planktonic biomass. When this occurs, PN–specific uptake rates can significantly underestimate true phytoplankton–specific activity (Dugdale and Goering 1967). Only under bloom conditions, when Chl *a* concentrations and the percentage of phytoplankton nitrogen in the PN pool are high, would one expect PN–specific uptake rates to closely approximate phytoplankton–specific uptake rates. Thus, it is essential to account for variations in phytoplankton biomass for valid comparisons of changes or differences in nitrogen uptake rates. This is especially imperative in coastal upwelling regions where biomass and nutrient concentrations undergo large fluctuations.

In an effort to expand our knowledge of the environmental factors regulating nitrate utilization in coastal upwelling systems, a series of nitrate uptake experiments were undertaken at a site off Oregon. This location was sampled repeatedly over two upwelling seasons and one winter. We use the results from our studies of the nitrogen dynamics in these waters to examine the relative roles that nitrate availability and phytoplankton biomass play in determining nitrate uptake rates. We will show the utility of normalizing nitrate uptake rates to the Chl *a* concentration to estimate phytoplankton–specific uptake rates and in comparing nitrate use by phytoplankton from various coastal upwelling and oceanic regimes.

Materials and Methods

Sample Collection

A site located 8 km off the Oregon coast (44° 40'N, 124° 40'W) was sampled from July 1990 until August 1991. During the upwelling season (May through October) sampling was carried out every two weeks when possible. Winter sampling was conducted on a monthly basis when weather permitted (days 347 and 387; Table 2.1). Water was collected between 0800 and 0900 hrs from 6 depths (0, 8, 12, 20, 25, 40 m) with 5 liter Niskin bottles. It was immediately placed in acid–washed polypropylene carboys and transported to shore in containers filled with surface seawater to keep the samples at ambient temperature. Once on shore, the water was mixed by gently inverting the carboys a number of times before samples were drawn. Conductivity, temperature and pressure data were collected with an Ocean Sensors 100 CTD. All experimental work was carried out at the Hatfield Marine Science Center, Oregon State University, Newport, OR.

^{15}N Additions

Trace amounts (~10% of the ambient NO_3^- concentration) of $Na^{15}NO_3$ (98.9 atom%, MSD Isotopes) or 0.1 μM (final concentration) of $(^{15}NH_4)_2SO_4$ (99.0 atom%, MSD Isotopes) were added to the collected water in 1 liter Nalgene polycarbonate bottles. Once spiked with label, the bottles were placed in an environmental chamber simulating ambient seawater

Table 2.1. Sampling days, wind conditions for upwelling as determined by Neuer (1992), surface nitrate and Chl *a* concentrations, and designated upwelling status.

Day*	Date	Wind Condition	$[NO_3^-]$ (μM)	Chl *a* (μg liter^{-1})	Upwelling Status
191	July 10, 1990	Favorable	21	1	Upwelling
205	July 24, 1990	Favorable	5	38	Bloom
219	August 7, 1990	Favorable	14	11	Bloom
233	August 21, 1990	Unfavorable	<1	2	Post–bloom
248	September 5, 1990	Unfavorable	<1	4	Post–bloom
284	October 11, 1990	Unfavorable	2	16	Bloom
347	December 13, 1990	–	6	0.5	Winter
387	January 22, 1991	–	9	3	Winter
501	May 16, 1991	Favorable	<1	9	Post–bloom
541	June 25, 1991	Unfavorable	<1	8	Post–bloom
555	July 9, 1991	Favorable	25	4	Upwelling
569	July 23, 1991	Unfavorable	6	57	Bloom
597	August 20, 1991	Favorable	<1	32	Bloom

*January 1, 1990 was day 1

temperatures (~8–10°C) and saturating light conditions (~500 μEinst m^{-2} s^{-1}). Bottles from the lower 5 depths were placed in bags made of neutral density screening to simulate light levels of 50, 30, 15, 5 and 1% of saturated irradiance. Incubations lasted from 4 to 6 h. At the end of the incubation

period, samples were filtered under low vacuum pressure (<180 mm of Hg) onto combusted 47 mm Whatman GF/F filters. The filters were frozen and then dried at 60°C for 24 h. Dried filters were prepared for emission spectrometry following the micro–Dumas dry combustion method of LaRoche (1983), and analyzed for ^{15}N incorporation into particulate matter with a Jasco N–150 emission spectrometer (Fiedler and Proksch 1975). Ammonium uptake rates were corrected for isotope dilution using the methods described in Wheeler et al. (1989). The equations of Dugdale and Goering (1967) were used to calculate PN–specific (V) and absolute (ρ) uptake rates. In this paper we will denote PN–specific nitrate uptake rates as $V_{NO_3}^{PN}$ (units: h^{-1}), absolute nitrate uptake rates as ρ_{NO_3} (units: nmol $liter^{-1}$ h^{-1}), Chl *a*–specific nitrate uptake rates as $V_{NO_3}^{Chl}$ (units: nmol μg^{-1} h^{-1}) and Chl *a*–specific nitrogen uptake rates (i.e. nitrate plus ammonium uptake) as V_{Sum}^{Chl} (units: nmol μg^{-1} h^{-1}).

Biomass and Nutrient Concentrations

Initial and final seawater samples were taken from the uptake experiments and stored frozen until analyzed for $[NO_2^- + NO_3^-]$ and $[NO_2^-]$ using a Technicon II AutoAnalyzer and the protocols of Whitledge et al. (1986). Samples were not filtered prior to storage and analysis. Ammonium

concentrations were measured manually in triplicate within 1 h of collection using the phenolhypochlorite method (Solórzano 1969).

The chlorophyll *a* concentration was determined for each depth by filtering duplicate 100 ml aliquots of seawater onto combusted 25 mm Whatman GF/F filters. Filters were extracted in 90% acetone at 4°C in the dark for 24 h and measured using a Turner Designs 10 fluorometer (Strickland and Parsons 1972). The fluorometer was calibrated with a primary standard of pure Chl *a* (i.e. *Anacystis nidulans*) and with daily working standards of coproporphyrin I, purchased from Sigma Chemical Co.. The instrument was zeroed with extracted filter blanks and 90% acetone blanks (Venrick 1987).

Particulate organic nitrogen (PN) concentrations were determined by filtering 500–1000 ml of seawater onto a combusted 25 mm Whatman GF/F filter, freezing the filter and then drying it at 60°C for 24 h. A persulfate digestion converted the PN to NO_3^- (Grasshoff et al. 1983), which was then measured with a Technicon II AutoAnalyzer (Whitledge et al. 1986).

The percentage of phytoplankton nitrogen in the PN pool was estimated for each sampling from regressions of PN and Chl *a* concentrations. The intercept of the regression (i.e. the PN concentration when Chl *a* was 0 μg liter^{-1}) was taken as the amount of non–phytoplankton nitrogen and subtracted from the total PN concentration to estimate the concentration of phytoplankton nitrogen. For these regressions, the mean r^2=0.80 $\pm$ 0.07 ($\pm$ SE, n=10). On three occasions (days 233, 248 and 569) we could not estimate

non–phytoplankton nitrogen using the regression method due to negative intercepts. For these cases, a Chl *a*:cell N value of 2.25 μg Chl *a* μmol N^{-1}, based on culture studies of diatoms (Chan 1980, Darley 1980), was assumed. For all the data, except day 347, the average inverse of the slope obtained from our regression analyses was 2.19 $\pm$ 0.45 μg Chl *a* μmol N^{-1}.

Criteria Used to Characterize the Upwelling State

Neuer (1992) used the mean weekly wind data collected at Newport, OR to calculate the Bakun upwelling index (Bakun et al. 1974) for the physical characterization of the upwelling conditions during this sampling. Upwelling–favorable winds were present during six of the 11 sample days during the upwelling season (Table 2.1). However, the Bakun index is a broadscale, slow responding parameter for the assessment of upwelling status (Small and Menzies 1981). Consequently, we used the surface nitrate and Chl *a* concentrations for a more accurate biological characterization of the upwelling status (Table 2.1). High nitrate and low Chl *a* on days 191 and 555 indicated active upwelling conditions. Moderate nitrate and high Chl *a* indicated the occurrence of phytoplankton blooms on days 205, 219, 284, and 569. On day 597, high Chl *a* and low nitrate suggests that a phytoplankton bloom had recently depleted surface nitrate. The remaining four days during

the upwelling period were characterized by very low nitrate (<1 μM) and low Chl *a* concentrations and these days are designated as post–bloom conditions.

Results

Physical Structure of the Water Column

Contours of temperature, salinity, and density (σ_t) are shown in Fig. 2.1a–c. The transport of cold water (8.5°C) from depth to the euphotic zone and its subsequent warming, was evident during both upwelling seasons (Fig. 2.1a). Particularly strong warming of the water down to 16 m was observed on day 233, marking a relaxation event. Increased stratification of the upper 8 m began prior to the end of the upwelling season and remained that way throughout the winter due to the presence of low salinity water (Fig. 2.1b). Off the central Oregon coast, salinities of $\leq$32.5 psu characterize water originating in the Columbia River (Atlas et al. 1977), however during the winter months the effluent from the Columbia River is restricted to the Washington coast. During the winter the sources of this freshwater are the many small rivers along the Oregon coast (Huyer 1977). At times, temperature and salinity separately controlled the density structure of the upper water column. For example, warming dominated when the winds were unfavorable for upwelling (i.e. day 233; Table 2.1) and the presence of freshwater dominated during the winter (days 347 and 387; Fig. 2.1). However, both lower salinities and warmer water were responsible for the lower density water observed on day 541 (Fig. 2.1).

Figure 2.1. Contour plots of (a) temperature, (b) salinity, and (c) density (σ_t) for days 191 to 597 at a site in the Oregon upwelling zone. Sampling times and depths are denoted by black dots on the plots. The duration of the upwelling and non–upwelling seasons are shown as bars across the top of the plot.

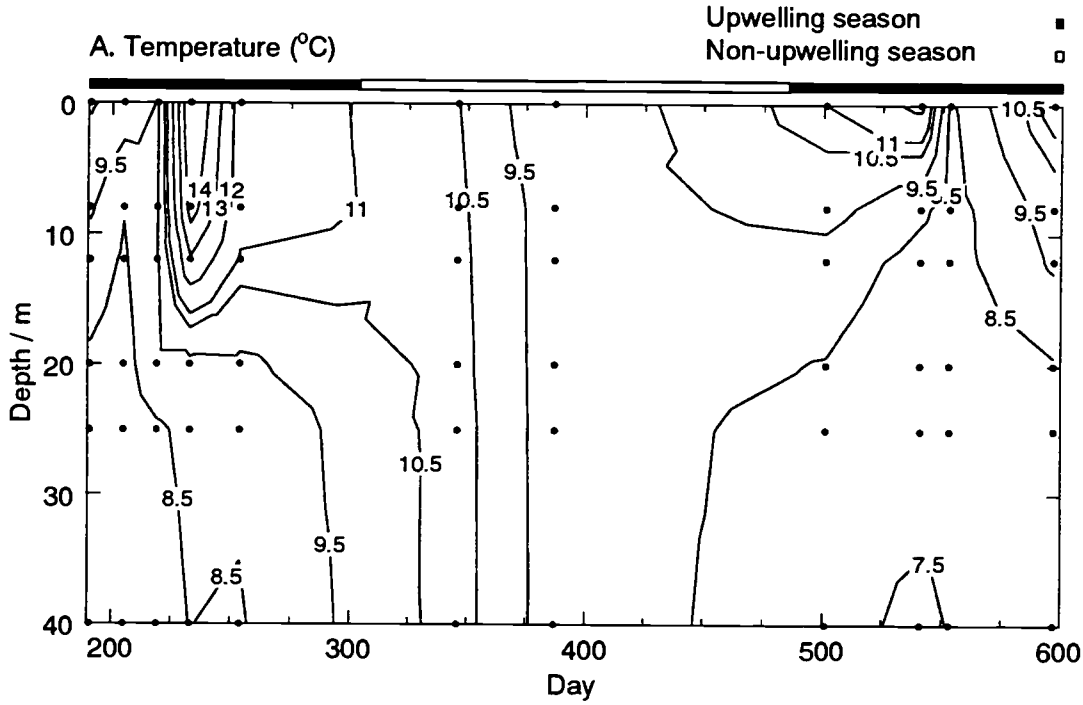
A. Temperature (°C)
Upwelling season
Non-upwelling season
Depth / m
Day
0
10
20
30
40
200
300
400
500
600
9.5
14
12
13
11
10.5
9.5
11
10.5
9.5
9.5
10.5
8.5
10.5
8.5
9.5
8.5
7.5

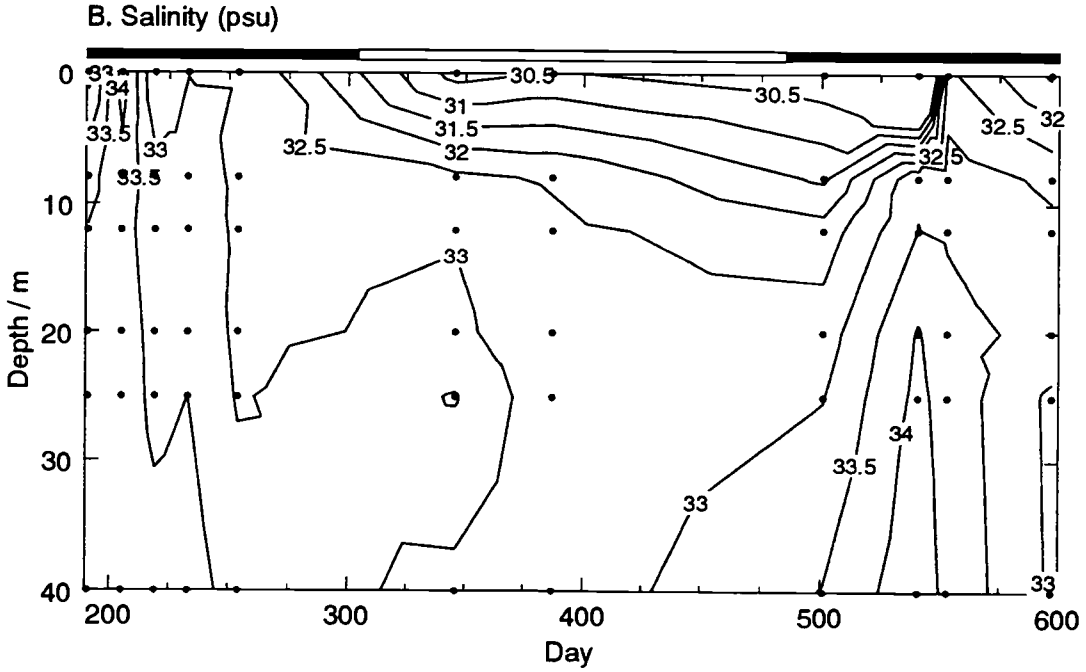
B. Salinity (psu)
Depth / m
Day
0
10
20
30
40
200
300
400
500
600
34
33.5
33
33.5
32.5
30.5
31
31.5
32
30.5
32.5
32
32.5
33
33
34
33.5
33
33

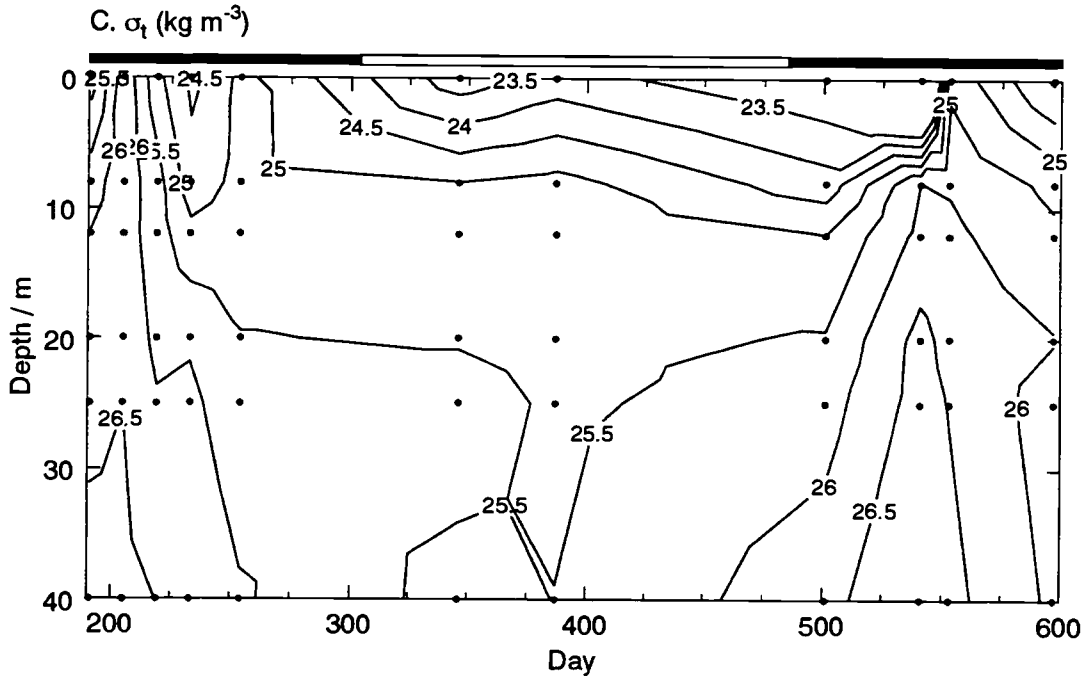
C. σ_t (kg m^{-3})
Depth / m
Day
0
10
20
30
40
200
300
400
500
600
25.5
24.5
23.5
24
25
26
26.5

Nitrate and Biomass Concentrations

A wide range of NO_3^-, Chl *a* and PN concentrations were observed at the study site (Fig. 2.2a–c). Nitrate concentrations in the upper 8 m of the water column varied over two orders of magnitude, from 0.2 to 30 μM, during the upwelling season (Fig. 2.2a). Highest [NO_3^-] indicated recently upwelled water, while lower concentrations were indicative of bloom and post–bloom conditions (Table 2.1). During the winter, surface [NO_3^-] were between 5.8 and 8.8 μM and showed little variation with depth. Maximum Chl *a* concentrations were almost always found at either 0 or 8 m and decreased with depth. Surface Chl *a* concentrations ranged from 1 to 57 μg liter^{-1} during the upwelling season (Fig. 2.2b, Table 2.2). Lowest Chl *a* concentrations were observed during upwelling events, and Chl *a* concentrations of >10 μg liter^{-1} were used as the criterion to designate bloom conditions (Table 2.1). Wintertime concentrations were between 0.5 and 3.0 μg Chl*a* liter^{-1}. The distribution of PN concentrations (Fig. 2.2c) was similar to that for Chl *a*, although high PN concentrations were sometimes found at 12 m. These patches coincided with post–bloom conditions. The highest and lowest PN concentrations were also measured in the summer. During upwelling events PN was between 1 and 4 μM, while during phytoplankton blooms PN concentrations were as high as 17 μM (Table 2.2). Wintertime PN concentrations were between 5 and 9 μM.

Relatively high Chl *a* and PN concentrations observed in the upper 8 m on day 387 suggest the occurrence of a winter bloom, possibly a result of the increased water column stability due to the presence of low salinity water (Fig. 2.1c).

Table 2.2. Observed range of nitrate and biomass concentrations and nitrate uptake rates at 0 meters during the upwelling cycle and winter.

	Active Upwelling	Upwelling Bloom	Post–Bloom	Winter
$[NO_3^-]$ (μM)	21 – 25	0.2 – 14	0.2 – 0.3	6 – 9
Chl *a* (μg liter^{-1})	1 – 4	11 – 57	2 – 9	0.5 – 3
PN (μM)	1 – 3	8 – 17	2 – 6	2 – 9
$V_{NO_3}^{PN}/10^{-3}$ (h^{-1})	9 – 83	34 – 74	7 – 34	5 – 9
ρ_{NO_3} (nM h^{-1})	24 – 96	253 – 1292	40 – 78	10 – 83
$V_{NO_3}^{Chl}$ (μmol μg^{-1} h^{-1})	24	8 – 34	8 – 22	21 – 26
n	2	5	4	2

Figure 2.2. Same as Figure 2.1, except for (a) nitrate, (b) chlorophyll *a*, and (c) particulate nitrogen concentrations.

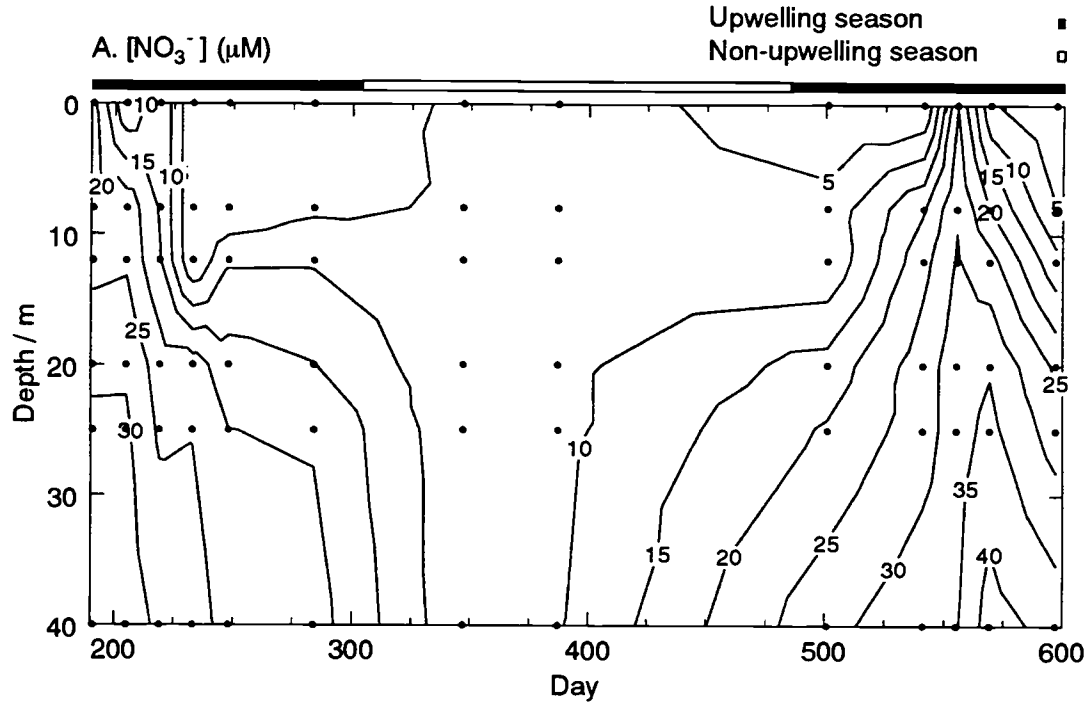
A. [NO3-] (μM)
Upwelling season
Non-upwelling season
Depth / m
Day
0
10
20
30
40
200
300
400
500
600

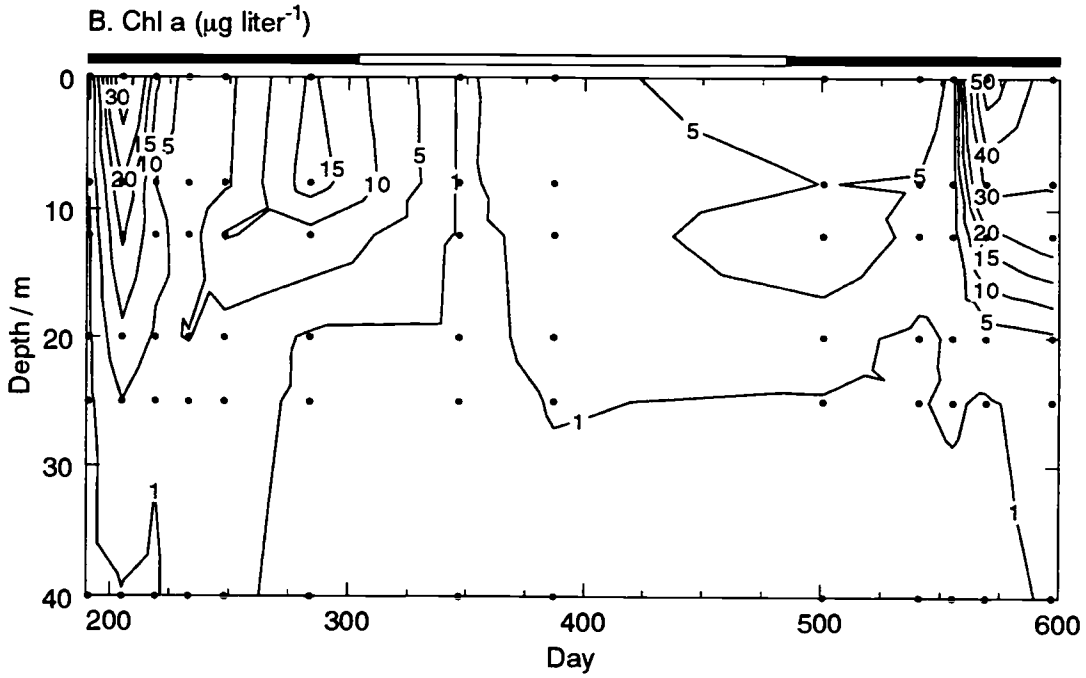
B. Chl a (μg liter-1)
Depth / m
Day
0
10
20
30
40
200
300
400
500
600

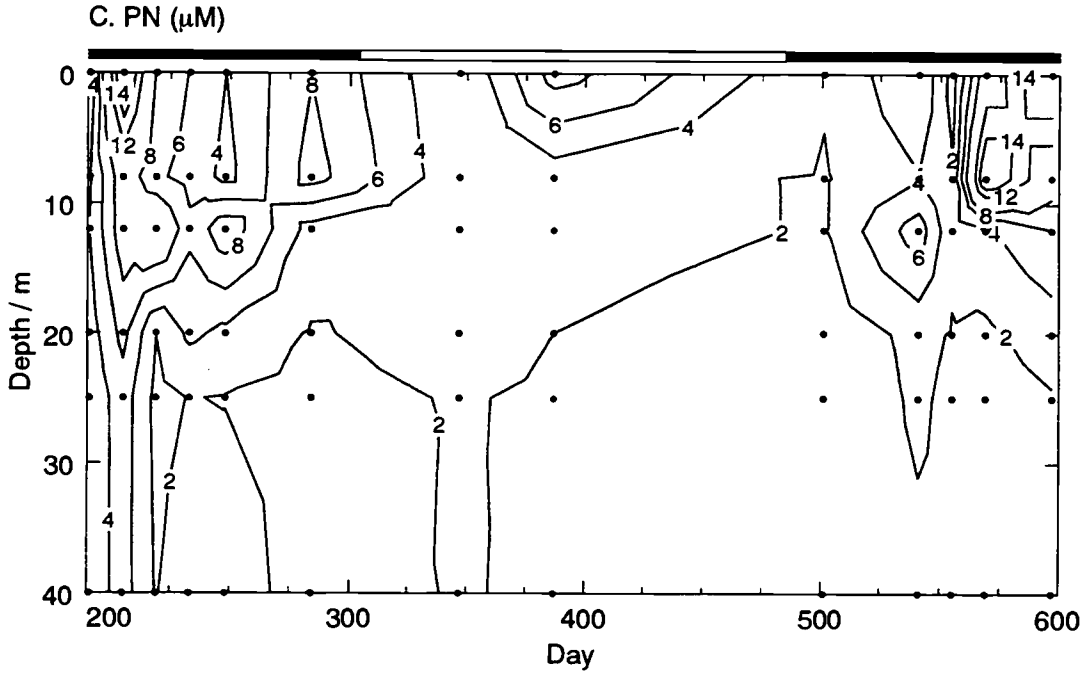
C. PN (μM)
Depth / m
0
10
20
30
40
200
300
400
500
600
Day
14
12
8
6
4
2

The percentage of phytoplankton nitrogen in the PN pool (Fig. 2.3) was estimated to assess the effect of changes in the composition of the planktonic assemblage (i.e. autotrophic vs. heterotrophic) on nitrate uptake rates. During the upwelling season phytoplankton nitrogen made up between 20 and 80% of the PN pool. The lowest amounts of phytoplankton nitrogen (i.e. 20 to 40%) in the upper 12 m of the water column were associated with the onset of an upwelling event (day 191) and under post–bloom conditions (day 233). During upwelling–induced blooms, phytoplankton nitrogen made up $\geq$50% of the PN pool. The lowest amounts of phytoplankton nitrogen ($\sim$10–20%) were usually found from 25 to 40 m depth, however, at the end of a bloom it was not uncommon for phytoplankton to make up 50% of the PN pool at those deeper depths. In the early part of the winter on day 347, phytoplankton nitrogen made up approximately 20% of the PN pool throughout the water column. At a later date (i.e. day 387) the percentage of phytoplankton nitrogen in the upper 12 m increased to be 60–85% of the PN pool. This event coincided with increases in Chl *a* and PN concentrations.

Comparison of Nitrate Uptake Rates

Generally, PN–specific ($V_{NO_3}^{PN}$), absolute (ρ_{NO_3}) and Chl *a*–specific ($V_{NO_3}^{Chl}$) nitrate uptake rates were highest in the surface layer (0–8 m) and decreased with depth due to lower irradiances (Fig. 2.4). The vertical and

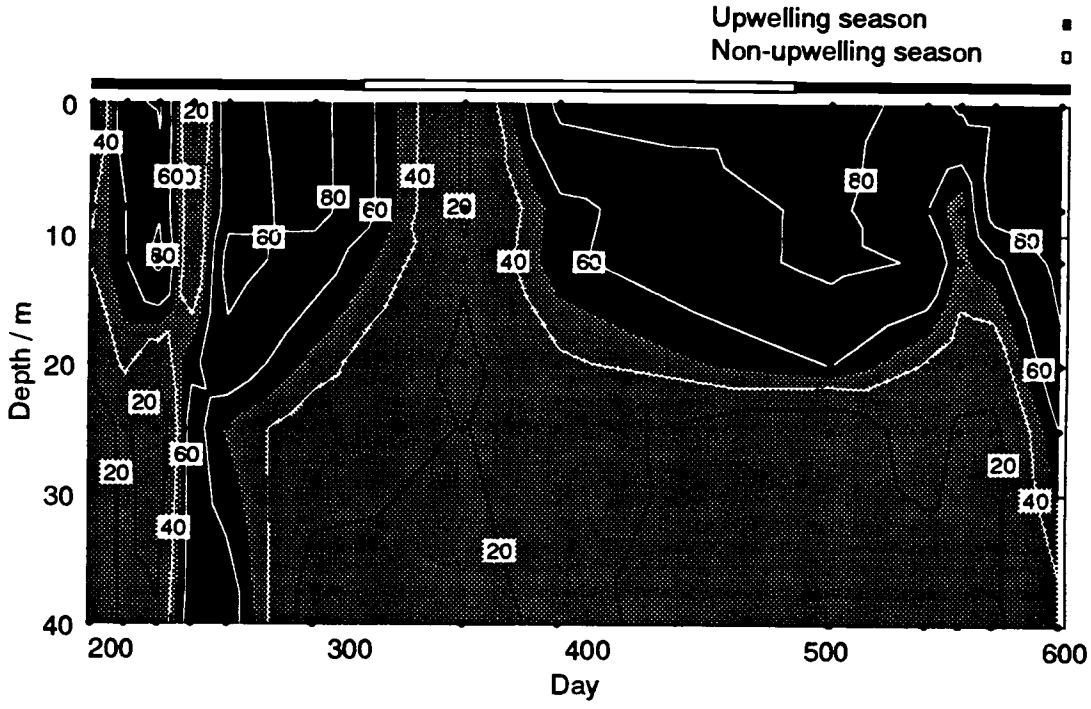

Figure 2.3. Same as Figure 2.1, except for the percentage of phytoplankton nitrogen in the particulate nitrogen pool. The areas shaded grey indicate where the percentage of phytoplankton nitrogen was $\leq$50% of the PN pool, while in the blackened areas it was >50%.

temporal distribution of ρ_{NO_3} values in the water column were similar to $V^{PN}_{NO_3}$ values (Fig. 2.4a, b). This was to be expected, since ρ_{NO_3} values are calculated by multiplying each $V^{PN}_{NO_3}$ value by its PN concentration (Dugdale and Goering 1967). Relatively high $V^{PN}_{NO_3}$ and ρ_{NO_3} uptake rates were measured either at 0 or 8 m on days 205, 284, 541, 555, 569 and 597. High PN– and Chl *a*–specific nitrate uptake rates were found during upwelling events, blooms and post–bloom periods (Table 2.2). Generally the highest absolute uptake rates were measured in the upwelling season during phytoplankton blooms and lower rates coincided with upwelling events and post–bloom periods.

Overall patterns in $V^{PN}_{NO_3}$ and ρ_{NO_3} values appeared to be related to the distribution of Chl *a* and the proportion of phytoplankton nitrogen, not the ambient $[NO_3^-]$. The highest uptake rates in the upper water column were found when the percentage of phytoplankton nitrogen in the PN pool was $\geq$50%. Subsurface maxima were observed in $V^{Chl}_{NO_3}$ values in post–bloom periods when NO_3^- had been depleted from the surface water (days 233 and 541), as well as during periods of strong upwelling (day 555).

$V^{Chl}_{NO_3}$ values did not appear to be as severely affected as $V^{PN}_{NO_3}$ and ρ_{NO_3} by reduced irradiances at depth. Elevated $V^{Chl}_{NO_3}$ uptake rates were occasionally measured at depth on days 191, 205, 219 and 284 at 40 m and day 541 from 20 to 40 m (Fig. 2.4c). Some of these high rates were also apparent in the 40 m $V^{PN}_{NO_3}$ (days 191, 205, and 541) and ρ_{NO_3} (day 191 and

Figure 2.4. Same as Figure 2.1, except for (a) PN–specific, (b) absolute, and (c) Chl *a*–specific nitrate uptake rates.

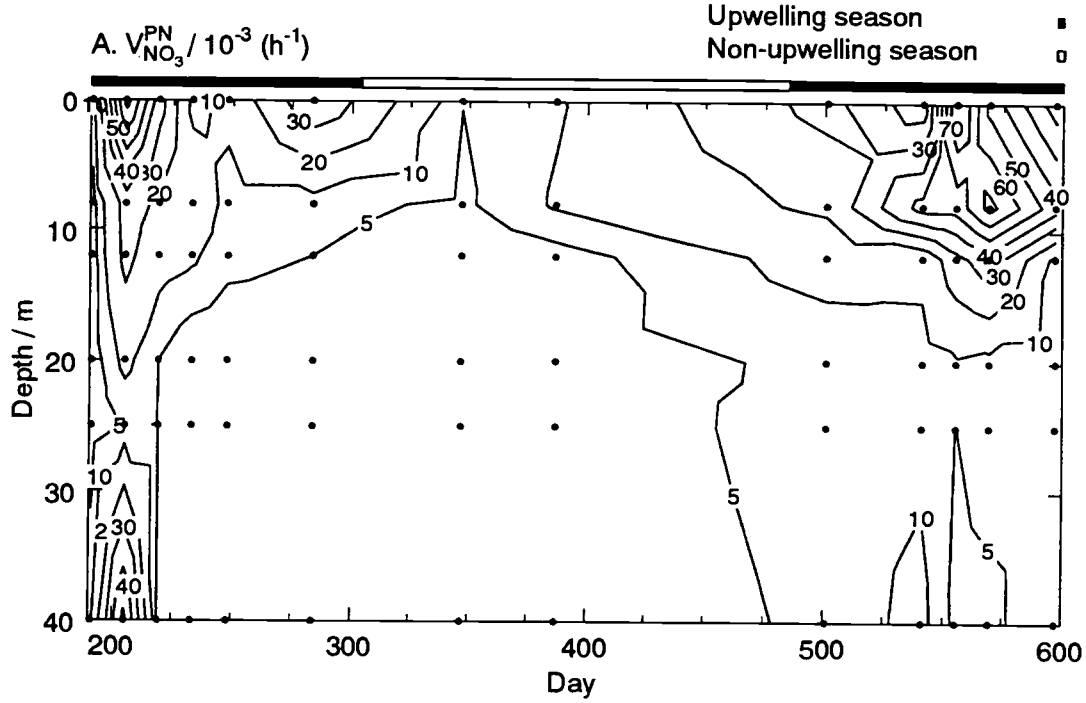
A. $V_{NO_3}^{PN}$ / 10^{-3} (h^{-1})
Upwelling season
Non-upwelling season
Depth / m
Day
0
10
20
30
40
200
300
400
500
600

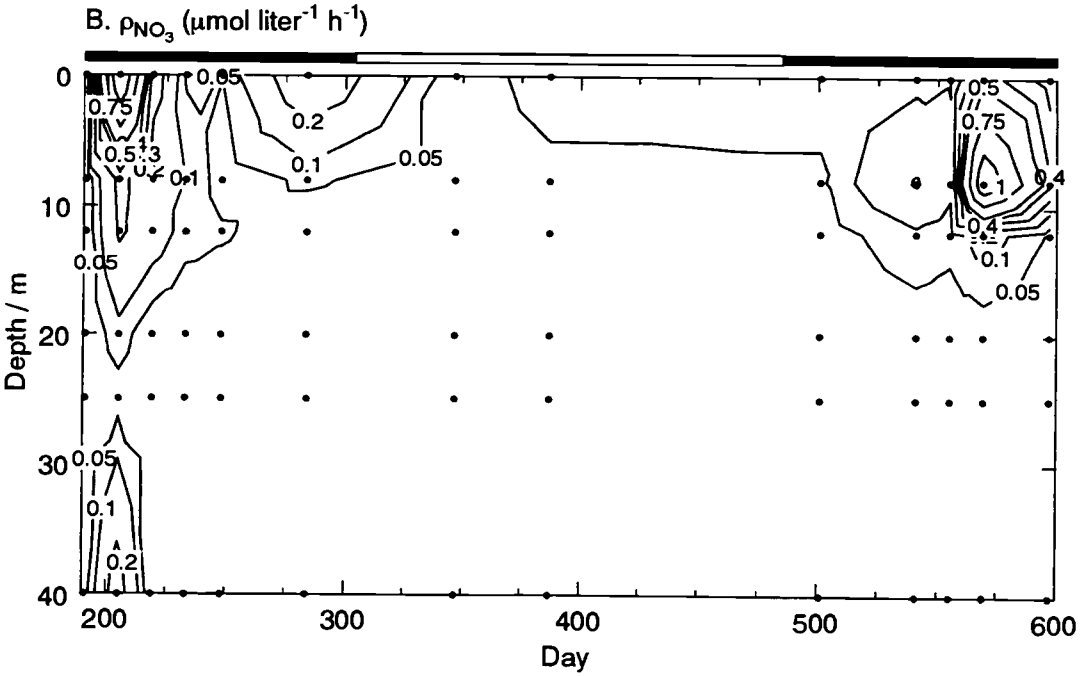
B. ρ_{NO_3} (μmol liter^{-1} h^{-1})
Depth / m
Day
0
10
20
30
40
200
300
400
500
600

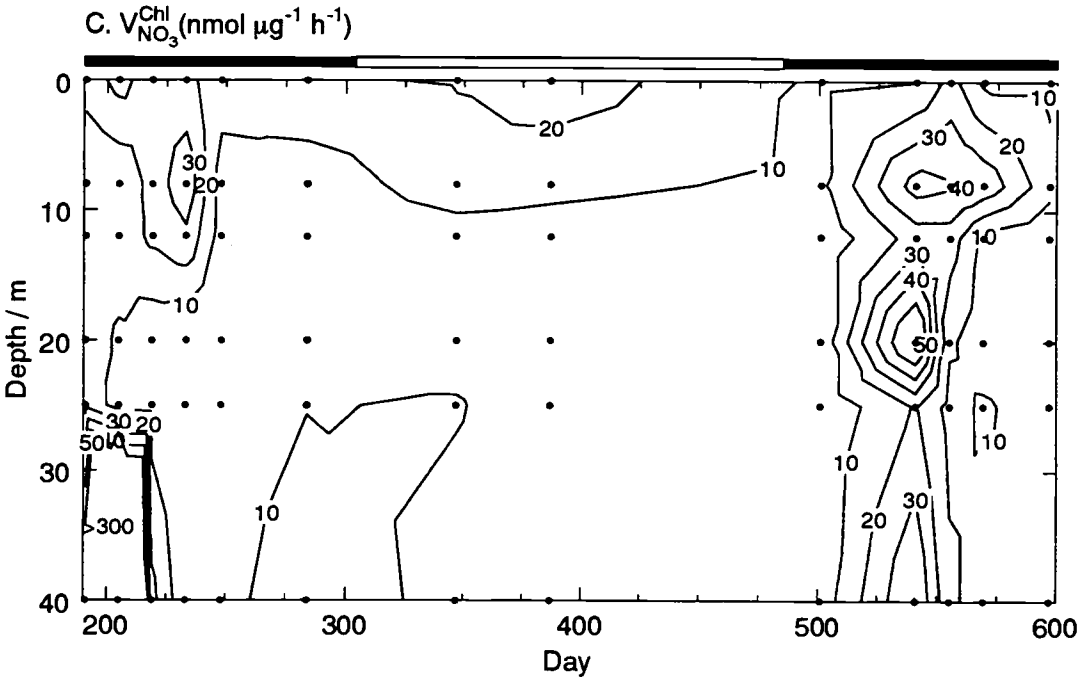
C. $V_{NO_3}^{Chl}$ (nmol μg^{-1} h^{-1})
Depth / m
Day
0
10
20
30
40
200
300
400
500
600
10
20
30
40
50
>300

205) data. These events were found throughout the upwelling cycle and were associated with upwelling, phytoplankton blooms in the surface layer (Fig. 2.4a–c) and post–bloom conditions which resulted in significant amounts of autotrophic biomass sinking out of the surface layer to deeper parts of the water column (Figs. 2.2b and 2.3).

The relationship between $V_{NO_3}^{PN}$ and Chl *a* in 0 m water is shown in Fig. 2.5a. A dashed line shows that for a majority of the samplings, uptake rates were a function of the Chl *a* concentration. Three points that deviated from the relationship are labeled on the plot and their significance will be addressed below. A linear relationship was also found between ρ_{NO_3} and the Chl *a* concentration for a majority of the samplings (Fig. 2.5b).

No relationship was found between $V_{NO_3}^{PN}$ and ρ_{NO_3} and the ambient $[NO_3^-]$ (Fig. 2.6a, b). A clearer relationship was found between uptake rates and ambient $[NO_3^-]$, when those uptake rates were normalized to the Chl *a* concentration (Fig. 2.6c). When $V_{NO_3}^{Chl}$ values were plotted as a function of the $[NO_3^-]$, a Michaelis–Menten relationship emerged. The hyperbolic curve in Fig. 2.6c was drawn using the Michaelis–Menten equation with coefficients (V_{max}=26.04 nmol μg^{-1} h^{-1} and K_s=1.26 μM) determined from a non–linear least squares fit of the data (Press et al. 1989). The goodness of fit was highly significant (X^2=155.5, 10 df, P<0.005). The K_s value determined in this study is similar to others reported from studies of neritic diatoms in culture (Eppley et al. 1969) and the field (MacIsaac and Dugdale 1969).

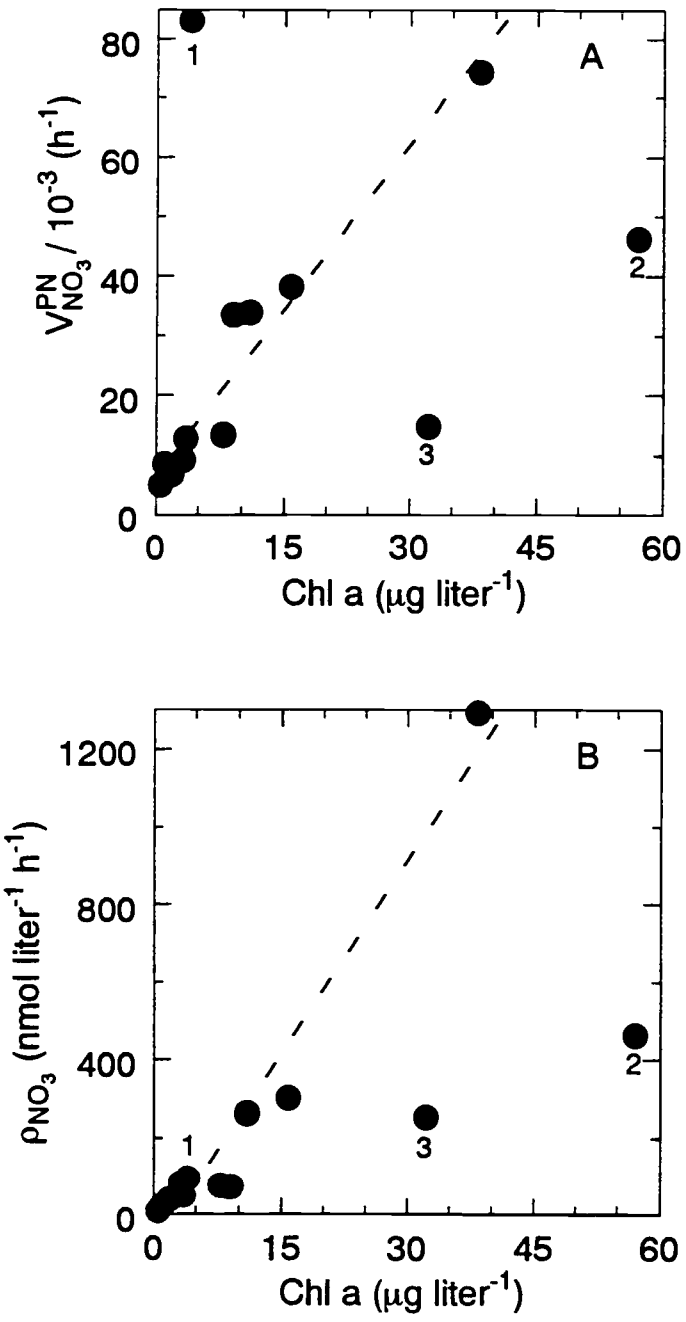

Figure 2.5. PN–specific and absolute nitrate uptake rates as a function of the Chl *a* concentration at 0 meters. (a) $V^{PN}_{NO_3}$, and (b) ρ_{NO_3}. In (a) and (b) r^2=0.94 for the dashed line, omitting the points labelled 1 to 3.

Figure 2.6. Nitrate uptake rates as a function of the ambient nitrate concentration. (a) $V_{NO_3}^{PN}$, (b) ρ_{NO_3}, and (c) $V_{NO_3}^{Chl}$. The hyperbolic curve in (c) was drawn using the Michaelis–Menten equation with coefficients determined from a non–linear least squares fit of the data. The two outliers at $\sim$7 μM NO_3^- were omitted from the analysis.

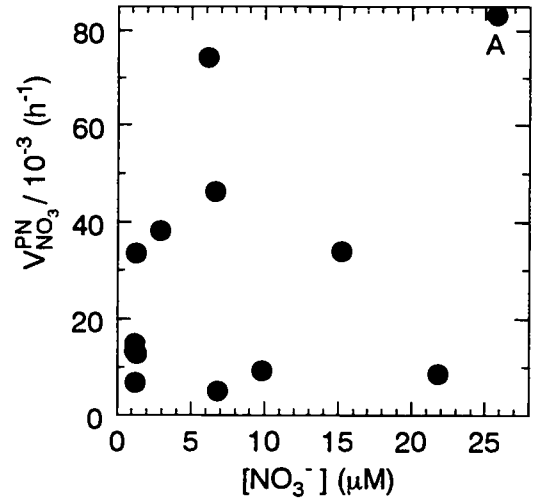
A
80
60
40
20
0
0
5
10
15
20
25
$V^{PN}_{NO_3}$ / 10^{-3} (h^{-1})
[NO_3^-] (μM)

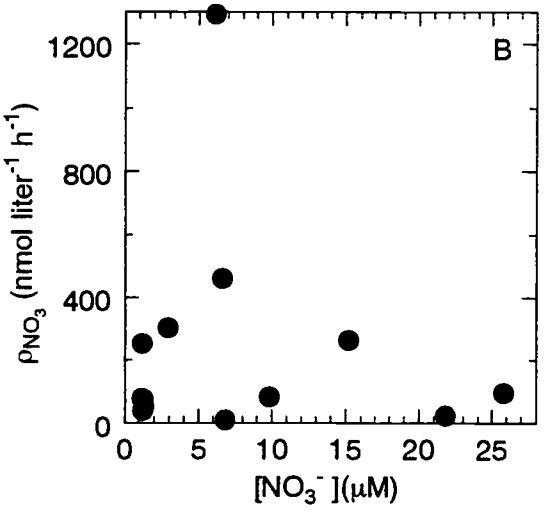
B
1200
800
400
0
0
5
10
15
20
25
ρ_{NO_3} (nmol $liter^{-1}$ h^{-1})
[NO_3^-](μM)

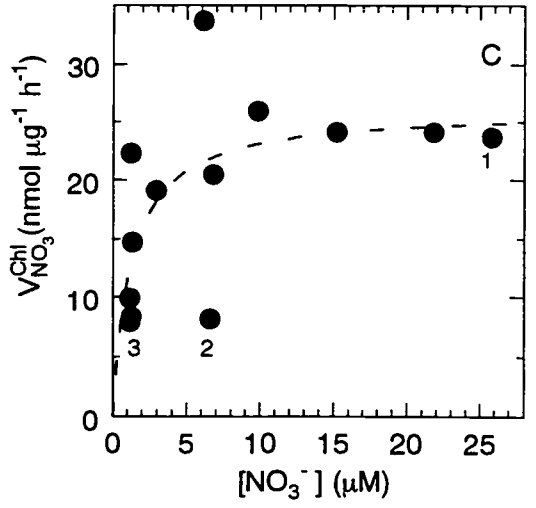
C
30
20
10
0
0
5
10
15
20
25
1
2
3
$V^{Chl}_{NO_3}$(nmol μg^{-1} h^{-1})
[NO_3^-] (μM)

Deviations from the relationships shown in Figs. 2.5 and 2.6 are instructive in showing how ambient NO_3^- and Chl *a* concentrations interacted in regulating nitrate uptake rates. The highest $V_{NO_3}^{PN}$ value measured over the course of our study came from a parcel of freshly upwelled water on day 555; #1, Chl *a*=4 μg liter^{-1}, [NO_3^-]=24.7 μM. Once the $V_{NO_3}^{PN}$ value of point #1 was converted to ρ_{NO_3}, its uptake rate was consistent with that of other samples with a low Chl *a* concentration. Our data indicated that higher and nearly constant $V_{NO_3}^{Chl}$ values characterized uptake rates when [NO_3^-] were $\geq$5 μM, even in parcels of recently upwelled water. Conversely, lower uptake rates were either found in water with large accumulations of biomass or low [NO_3^-]. Shading of the phytoplankton probably reduced uptake rates on day 569 (#2), even though NO_3^- was abundant; Chl *a*=57 μg liter^{-1} and [NO_3^-]=5.6 μM. Low uptake rates were also found in water (#3 on day 597) with a fairly high biomass (Chl *a*=32.2 μg liter^{-1}) but having an extremely low [NO_3^-] (=0.2 μM). For comparison with this last point, it is interesting to note that a relatively high uptake rate was attained for a sample with a Chl *a* concentration of 38 μg liter^{-1} when NO_3^- was abundant (=5 μM).

A quantitative comparison of PN–specific and Chl *a*–specific nitrate uptake rates is possible by converting the Chl *a*–specific rates to phytoplankton–N specific rates using the mean Chl *a*:cell N for phytoplankton in these coastal waters (Table 2.3). We expected phytoplankton–N specific rates to exceed PN–specific rates when Chl *a* was low and phytoplankton contributed <50%

to the PN pool. Indeed, we found that phytoplankton–specific rates were five–fold greater than PN–specific rates when Chl *a* was <4 μg liter^{-1} (Table 2.3). Conversely, we expected the two rates to be similar when phytoplankton dominated the plankton, and we found no significant difference between phytoplankton–specific and PN–specific rates when Chl *a* was $\geq$4 μg liter^{-1} (Table 2.3). These results clearly show that PN–specific uptake rates cannot be interpreted as phytoplankton–specific rates unless the dominance of the PN pool by phytoplankton is also verified.

Table 2.3. A comparison of phytoplankton N–specific and PN–specific nitrate uptake rates at 0 meters. The mean Chl *a*:PN ratio of 2.19 μg Chl *a* μmol N^{-1} was used to convert Chl *a*–specific rates into phytoplankton N–specific rates. Mean ± SE.

Chl *a* (μg liter^{-1})	Phyto. N–specific NO_3 uptake rate × 10^{-3} (h^{-1})	PN–specific NO_3 uptake rate × 10^{-3} (h^{-1})	n
< 4	47.0 ± 2.8	8.5 ± 1.3	5
≥4	37.0 ± 7.4	42.0 ± 8.8	8

An interannual and interseasonal comparison of $V_{NO_3}^{PN}$, ρ_{NO_3} and $V_{NO_3}^{Chl}$ uptake rates in the surface layer (0 and 8 m) is presented in Table 2.4.

Average $V_{NO_3}^{PN}$ uptake rates during the 1991 upwelling season were two times larger than those in 1990 and significantly different at the 95% level. Comparison of mean $V_{NO_3}^{PN}$ values in the 1990 and 1991 upwelling seasons with the winter revealed significant differences at the 80 and 99% levels, respectively. The two–fold change in mean annual $V_{NO_3}^{PN}$ values between upwelling seasons appeared to reflect differences in the amount of phytoplankton biomass. The average Chl *a* concentration from 0 to 8 m during the 1991 upwelling season was almost two times higher than that found in 1990; 18.6 vs 10.2 μg liter^{-1}. The mean wintertime Chl *a* concentration was 1.7 μg liter^{-1}. $V_{NO_3}^{Chl}$ values were practically the same for each season and mean values of ρ_{NO_3} were not statistically different between upwelling seasons or the winter (Table 2.4). One advantage of normalizing uptake rates to Chl *a* was a reduction in the amount of variability around the mean. The coefficient of variation (CV) associated with $V_{NO_3}^{Chl}$ values was 44%, versus 88% for $V_{NO_3}^{PN}$ and 148% for ρ_{NO_3}. The CV's of $V_{NO_3}^{PN}$ and $V_{NO_3}^{Chl}$ were significantly different from that of ρ_{NO_3} at the 95 and 99.9% levels, respectively, whereas the CV's of $V_{NO_3}^{PN}$ and $V_{NO_3}^{Chl}$ were different from each other at the >98% significance level (p. 190, Sokal and Rohlf 1981).

Table 2.4. An interannual and interseasonal comparison of nitrate uptake rates at 0 and 8 meters.

$^{15}NO_3^-$ uptake rates	1990 Upwelling season			1991 Upwelling season			Winter		
	Mean ± SE	Range	n	Mean ± SE	Range	n	Mean ± SE	Range	n
$V_{NO_3}^{PN}/10^{-3}$ (h^{-1})	21.0 ± 5.8	3.1 – 74.3	12	43.8 ± 7.4	13.4 – 83.2	10	7.3 ± 1.6	4.0 – 10.7	4
$V_{NO_3}^{Chl}$ (nmol μg^{-1} h^{-1})	19.2 ± 3.0	3.4 – 37.7	12	20.2 ± 4.8	7.9 – 44.5	10	18.6 ± 2.9	12.6 – 25.9	4
ρ_{NO_3} (nmol $liter^{-1}$ h^{-1})	209.3 ± 102.6	12 – 1292	12	296.6 ± 112.3	74 – 1217	10	33.3 ± 17.2	10 – 83	4

Comparison of Coastal and Oceanic Upwelling Regions

We compared $V_{NO_3}^{Chl}$ values for other coastal upwelling regions with our data from Oregon to see if the same relationships existed in other NO_3^-–rich waters (Table 2.5). $V_{NO_3}^{Chl}$ values from various coastal upwelling systems were similar to those off Oregon and ranged from 30.0 to 36.5 nmol μg^{-1} h^{-1}. In addition, we compared NO_3^- uptake rates obtained off Oregon to those from oceanic HNLC (High Nutrient Low Chlorophyll) regions characterized by high surface water $[NO_3^-]$. Mean ρ_{NO_3} values ranged from 3 to 5 nmol $liter^{-1}$ h^{-1} in HNLC regions, while in Oregon the range was from 10 to 1292 nmol $liter^{-1}$ h^{-1} (Table 2.6). The large difference between coastal upwelling and HNLC uptake rates were diminished when the data were normalized to the Chl *a* concentration. $V_{NO_3}^{Chl}$ values for the HNLC regions were similar to the minimum seen off Oregon. We find about a two–fold difference between Chl *a* normalized NO_3^- uptake rates between those ecosystems, but not the order of magnitude difference reported by Dugdale and Wilkerson (1991). Consideration of both NH_4^+ and NO_3^- uptake, however, indicates identical average Chl *a*–specific nitrogen uptake rates (V_{Sum}^{Chl}) of 33 nmol μg^{-1} h^{-1} for these waters (Table 2.6).

Table 2.5. A comparison of Chl *a*–specific nitrate uptake rates (mean ± SE), Chl *a* and nitrate concentrations in various coastal upwelling regimes.

Upwelling Region	$V_{NO_3}^{Chl}$ (nmol μg^{-1} h^{-1})	Chl *a* (μg liter^{-1})	$[NO_3^-]$ (μM)
Oregon[1]	34.1 ± 9.4	0.2 – 57	0.1 – 30
California[2]	30.0 ± 4.7	0.4 – 6	0.0 – 22
Peru[3]	36.5 ± 1.8	0.9 – 18	9.0 – 25
Benguela[4]	33.6 ± 3.0	2.0 – 7	1.0 – 7

[1]Kokkinakis and Wheeler (1987) and this study
[2]Wilkerson and Dugdale (1987)
[3]Dugdale and Wilkerson (1986)
[4]Probyn (1985)

Table 2.6. A comparison of the mean biomass concentrations, absolute nitrate uptake rates (ρ_{NO_3}), chlorophyll *a*–specific nitrate uptake rates ($V_{NO_3}^{Chl}$) and chlorophyll *a*–specific nitrogen uptake rates (V_{Sum}^{Chl}) in three HNLC regions and the Oregon upwelling zone.

Location	PN (μM)	Chl *a* (μg liter^{-1})	ρ_{NO_3} (nmol liter^{-1} h^{-1})	$V_{NO_3}^{Chl}$ (nmol μg^{-1} h^{-1})	V_{Sum}^{Chl} (nmol μg^{-1} h^{-1})
Antarctic[1]	1.34	0.40	5.3	9	24
Equatorial Pacific[2]	0.71	0.27	4.0	8	53
Subarctic Pacific[3]	1.40	0.38	3.4	10	21
Mean	1.15	0.35	4.2	9	33
Oregon[4]					
Mean	6.31	8.83	233.0	19	33
Minimum	1	0.50	10.2	8	11
Maximum	17	57	1292.1	33	95

[1] Olson (1980), Glibert et al. (1982a), Rönner et al. (1983)
[2] Murray et al. (1989), Price et al. (1991), Wilkerson and Dugdale (1992)
[3] Wheeler and Kokkinakis (1990)
[4] This study

Discussion

The major difficulty in calculating phytoplankton–specific nitrogen uptake rates lies in not being able to directly measure phytoplankton nitrogen concentrations (Banse 1977). Phytoplankton nitrogen concentrations can be estimated either by using Chl *a*:cell N ratios from the literature or by estimating the amount of non–phytoplankton nitrogen by regression analysis of measured PN and Chl *a* concentrations. Neither approach is without problems. For instance, the use of Chl *a* as an estimator of phytoplankton biomass has been critized due to changes in the amount of Chl *a* per cell that can take place in response to changes in the local light field (Cullen 1982). Chl *a* concentrations per cell and Chl *a*:cell N values can vary between taxonomic groups (Eppley et al. 1977) and can be affected by changes in irradiance (Cullen and Lewis 1988) and possibly nutrition. However, since diatoms photoadapt to local light fields in a matter of hours (Riper et al. 1979), it is unlikely that changes in the amount of Chl *a* per cell affected our results. Until methods to accurately measure phytoplankton nitrogen concentrations become available, normalizing uptake rates to the Chl *a* concentration is the simplest way to estimate phytoplankton–specific uptake rates. To avoid interpretive problems due to the light–dependence of nitrate uptake rates (MacIsaac and Dugdale 1972), we restricted our data

set to the surface water when we examined relationships between the various uptake rates and biomass/nutrient concentrations.

Phytoplankton standing stocks have been found to vary significantly over small temporal and spatial scales. A comprehensive study of the distribution of planktonic biomass in the English Channel by Holligan et al. (1984) found phytoplankton carbon accounted for 4 to 77% of the total particulate organic carbon pool. When phytoplankton carbon was low, the proportion of organic carbon in the form of bacteria, protozoa, microzooplankton and mesozooplankton was significantly higher. At our study site off Oregon, we estimated that phytoplankton nitrogen at times accounted for between <10–95% of the total PN pool. Kokkinakis and Wheeler (1987) reported similar results (9–76%) for a series of stations on the Oregon/Washington shelf. In our study, $V_{NO_3}^{PN}$ values were a function of Chl *a* and phytoplankton nitrogen concentrations. Comparison of $V_{NO_3}^{PN}$ and $V_{NO_3}^{Chl}$ measurements with Chl *a* concentrations (Table 2.3) found that the data fell into two distinct and separate groups. The largest difference between the two rate measurements occurred when Chl *a* concentrations were low and phytoplankton nitrogen was a minor constituent of the PN pool. Conversely, PN–specific and Chl *a*–specific NO_3^- uptake rates were similar when Chl *a* concentrations were ≥ 4 μg liter^{-1} and phytoplankton nitrogen made up at least 70% of the PN pool.

Results reported by Dugdale and Wilkerson (1991) for a variety of coastal upwelling regimes suggested that $V_{NO_3}^{PN}$ values increase linearly as a function of the $[NO_3^-]$ (their Fig. 2). In contrast to these results, our data showed that there was no relationship between either $V_{NO_3}^{PN}$ or ρ_{NO_3} and the ambient $[NO_3^-]$. Instead, our NO_3^- uptake rates were related to the Chl *a* concentration. Chl *a*–specific nitrate uptake rates were only a function of the $[NO_3^-]$ when ambient concentrations were below 5 μM. LeBouteiller (1986) also found that NO_3^- uptake rates were strongly related to the Chl *a* concentration in the equatorial Atlantic, although the $[NO_3^-]$ at which uptake rates were saturated was only 0.2 μM, compared to 5 μM at our coastal site.

Dugdale and Wilkerson (1991) also noted the presence of an intercept at 6 μM when $V_{NO_3}^{PN}$ values were plotted against $[NO_3^-]$ (their Fig. 2), and refer to this as the "critical nitrate point". They suggest that this is the minimum $[NO_3^-]$ required for a phytoplankton bloom to develop. From the analysis of our data, we suggest that the "critical nitrate point" is in fact the $[NO_3^-]$ at which uptake rates become saturated in coastal upwelling ecosystems. Based on our $V_{NO_3}^{Chl}$ results (Fig. 2.6c) and the similarity of $V_{NO_3}^{Chl}$ values in various upwelling systems (Table 2.5), we suspect that if Dugdale and Wilkerson's $V_{NO_3}^{PN}$ data were normalized to Chl *a* and plotted against $[NO_3^-]$ a hyperbolic relationship would also be found, although they did not have uptake rate data when $[NO_3^-]$ was less than $\sim$7 μM.

The results of this field study suggest that temporal changes in $V_{NO_3}^{PN}$ values can be explained by changes in phytoplankton biomass (Garside 1991) and ambient nitrate concentration rather than physiological adjustments by the phytoplankton assemblage. The Michaelis–Menten relationship found between $V_{NO_3}^{Chl}$ values and $[NO_3^-]$ is not entirely consistent with the Shift–Up hypothesis (Wilkerson and Dugdale 1987). If the Shift–Up hypothesis were valid for our data set we would have expected a bell–shaped curve describing the relationship between $V_{NO_3}^{Chl}$ and $[NO_3^-]$. $V_{NO_3}^{Chl}$ values should have been low when the $[NO_3^-]$ was highest (>15 μM) due to the inability of the phytoplankton to take up nitrate quickly when subjected to higher irradiances in the surface water. Likewise, the highest $V_{NO_3}^{Chl}$ values should have been observed at intermediate $[NO_3^-]$ (i.e. 5 to 15 μM), since the phytoplankton would have had time to adapt to surface water irradiances and saturating $[NO_3^-]$. In neither case did we observe the pattern predicted by the Shift–Up hypothesis. At both high and intermediate $[NO_3^-]$, $V_{NO_3}^{Chl}$ values were saturated. Low $V_{NO_3}^{Chl}$ values were observed to coincide with low ambient $[NO_3^-]$, as the Shift–Up hypothesis predicts, and also when the phytoplankton biomass reached extremely high concentrations. However, it is unlikely that the phytoplankton "shifted–down" their metabolism on such occasions.

The phytoplankton assemblage appeared to be adapted to local conditions even during upwelling events. The highest ambient $[NO_3^-]$ measured

in the surface water, 22 and 25 μM, were consistent with concentrations reported by Small and Menzies (1981) at the same site under active upwelling conditions. Our intermediate and high [NO_3^-] were similar to those used by Wilkerson and Dugdale (1987) and Dugdale and Wilkerson (1991) to characterize intermediate and strong upwelling conditions and to simulate newly upwelled conditions. Thus we believe that our uptake results for samples at the highest [NO_3^-] were representative of newly upwelled phytoplankton. Unless the phytoplankton were able to physiologically adapt over the short incubation period (4–6 h), no evidence was found to suggest the presence of a lag period prior to the onset of maximum uptake rates.

High nitrate uptake rates were occasionally measured at depth between 25 and 40 m. Several lines of evidence suggest that bacteria, and not phytoplankton, may have been responsible. Low Chl *a*:PN values (Kokkinakis and Wheeler 1987, Dortch and Packard 1989) and percentages of phytoplankton nitrogen indicate that a heterotrophic community dominated at depth. Extremely low ^{14}C assimilation rates were routinely measured from 25 to 40 m (Dickson, Fessenden and Neuer unpubl. data) and unrealistically high phytoplankton growth rates calculated for those depths suggest that there may have been bacterial utilization of NO_3^-. Although work to date has shown that heterotrophic bacteria primarily use NH_4^+ as a nitrogen source (Wheeler and Kirchman 1986), NO_3^- assimilation by bacteria has been demonstrated (Kirchman et al. 1990) and inferred (Cochlan et al. 1991).

The mechanisms or processes that may have been responsible for triggering such high assimilation rates of nitrate at depth are unknown.

Similar $V_{NO_3}^{Chl}$ values were found for a variety of coastal upwelling regimes, over a broad range of Chl *a* and NO_3^- concentrations. New production rates in these ecosystems appeared to be a function of the phytoplankton biomass and the ambient NO_3^- concentration when the latter were below saturating levels. Hayward and Venrick (1982) found a linear relationship between integrated Chl *a* concentrations and integrated total primary production, while LeBouteiller (1986) found that integrated new production was a function of the integrated phytoplankton biomass. If similar relationships exist in other coastal upwelling regimes, we may eventually be able to estimate new production by accurately knowing Chl *a* concentrations (LeBouteiller 1986) and $[NO_3^-]$ determined from remotely sensed sea surface temperature data (Sathyendranath et al. 1991).

Comparison of Chl *a*–specific nitrogen uptake rates in coastal and HNLC oceanic waters indicated that the major difference between them was the form of nitrogen used (i.e. nitrate vs. ammonium), rather than phytoplankton–specific nitrogen uptake rates. High nitrogen uptake rates in both coastal and HNLC waters implies high growth rates. Measurements of photosynthetic activity, pigment–specific rates of labeling and dilution experiments suggest that phytoplankton growth rates are high in HNLC regions. Growth rates have been estimated to be about one biomass doubling

per day in the equatorial Pacific (Chavez et al. 1991, Cullen et al. 1992) and the subarctic Pacific (Miller et al. 1991). This is comparable to growth rates off Oregon (Kokkinakis and Wheeler 1987, Dickson 1994). High growth rates in coastal upwelling regimes are primarily supported by nitrate assimilation during upwelling–induced phytoplankton blooms. Conversely, high growth rates are also maintained by ammonium utilization between upwelling events and during the winter months (see Chapter 3) and at all times in HNLC regions (Wheeler and Kokkinakis 1990, Peña et al. 1992). These findings indicate that healthy phytoplankton assemblages can be supported by nitrogen recycling and point to our need to understand how interactions between phytoplankton and their grazers affect nitrogen utilization.

Recent determinations of phytoplankton biomass (Dickson and Wheeler 1993), primary production and estimated phytoplankton growth rates (Laws et al. 1987, Booth et al. 1988) indicate very little variation between oligotrophic subtropical and nutrient–rich subarctic waters in the Pacific despite a six–fold gradient in inorganic nutrients (Martin et al. 1987). This information and the results of this study lead us to question the validity of the generalization that nitrogen uptake rates are related to the distribution of macronutrients in the ocean and to wonder if Chl *a*–specific nitrogen uptake rates are also similar over basin–wide scales.

CHAPTER 3

NITROGEN DYNAMICS

Abstract

Nitrate, ammonium and urea concentrations and uptake rates were measured repeatedly at a site in the Oregon upwelling zone over two upwelling seasons and one winter. During upwelling blooms the highest NO_3^- uptake rates occurred in the upper 8 m of the water column. On those occasions NO_3^- turnover times were estimated to be on the order of one day. The highest NH_4^+ uptake rates were measured between 0 and 12 m during and after phytoplankton blooms. On three occasions NH_4^+ plumes having concentrations of between 2 and 4 μM were observed. Two of the three plumes had cores centered at 20 m. The presence of these plumes coincided with the end of blooms and may have been the result of increased fecal pellet production by grazers. Urea uptake rates were highest in the surface water and decreased with depth. Compared to NO_3^- and NH_4^+, urea concentrations and uptake rates were relatively low. Elevated urea concentrations were also associated with the demise of an upwelling bloom and coincided with an NH_4^+ plume. The total nitrogenous production at this site was estimated to be 257 g N m^{-2} y^{-1}. Annual new production was estimated to be 137 g N m^{-2} y^{-1} and regenerated production was 119 g N m^{-2} y^{-1}. Of the annual regenerated production, NH_4^+ utilization accounted for 92 g N m^{-2} y^{-1}, while urea assimilation comprised 27 g N m^{-2} y^{-1}.

Introduction

Wind–driven coastal upwelling ecosystems offer a unique opportunity to study the biotic and abiotic factors regulating primary production rates in general and nitrogen utilization patterns in particular, due to the broad range of hydrographic conditions encountered. Wide fluctuations in biomass and nutrient concentrations occur in response to physical forcing. For example, during upwelling events the introduction of nutrient–rich water from depth into the euphotic zone stimulates phytoplankton blooms and results in high levels of primary production, while relaxation of upwelling ultimately results in the decay of the bloom (Wroblewski 1977, Small and Menzies 1981). Although the waters off Oregon are perhaps the best known example of such an ecosystem, relatively little is known about the specific temporal patterns of nutrient utilization and the rates at which they take place.

Wind–driven coastal upwelling ecosystems are among the most productive in the ocean (Ryther 1969); however, very little information is available on annual primary production rates, and even less is known about rates of new and regenerated production (Dugdale and Goering 1967). Eppley and Peterson (1979) estimated that approximately 50% of the total primary production in these regions can be attributed to new production (i.e. the utilization of new sources of nitrogen, such as nitrate). Nevertheless, our knowledge of the factors regulating nitrate utilization in the coastal ocean is rudimentary; light and low ambient nitrate concentrations limit the amount of new production (MacIsaac and Dugdale 1972). In addition, the availability of silicate has been suggested to control new production rates in some coastal regions (MacIsaac et al. 1974). High ambient ammonium concentrations

may also affect the rate at which nitrate is assimilated by phytoplankton (Wheeler and Kokkinakis 1990), however the occurrence and extent of this phenomenom has not been well established (Dortch 1990). As for the factors regulating the ammonium use, even less is known.

The most comprehensive field study of the biological response to upwelling was carried out by Small and Menzies (1981). They noted, for example, that strong upwelling conditions early in the upwelling season resulted in a single band of high phytoplankton biomass and production that ran parallel to the bathymetry. Later in the season, when a two–cell circulation pattern had been established, similar wind conditions caused two bands of biomass. Weak upwelling conditions produced biomass bands further inshore that were twice as productive as when strong upwelling conditions prevailed. Results of previous nitrogen studies on the Oregon and Washington shelf have been presented by Kokkinakis (1987), Kokkinakis and Wheeler (1987, 1988) and Dortch and Postel (1989), although none of these entailed a seasonal study. To date probably the most complete picture of the nitrogen dynamics in this region during the development of a phytoplankton plume has come from the coupling of a numerical model of the upwelling circulation with a model of primary production (Wroblewski 1977).

In this study we examined the seasonal nitrogen dynamics in the Oregon upwelling zone under a variety of hydrographic conditions. A site located on the Newport hydrographic line, which has a fairly large biological (e.g. Curl and Small, Small and Menzies 1981, Peterson et al. 1979) and physical oceanographic (e.g. Huyer 1976, 1977, Halpern 1976) database, was selected and sampled repeatedly over two upwelling seasons and one winter. Ambient biomass and nutrient concentrations were measured, as well as nitrate,

ammonium and urea uptake rates using ^{15}N–labelled substrates. In addition to identifying temporal and vertical patterns in nitrogen utilization, we were also able to estimate annual new and regenerated production rates. These results indicate that the coastal waters off Oregon are much more productive than previously thought.

Materials and Methods

Sampling Protocol

A site 8 km off the Oregon coast (44° 40'N, 124° 40'W) was sampled from July 7, 1990 until August 20, 1991 (days 191 to 597, where day 1 was January 1, 1990). During the upwelling season (May through October) sampling was carried out approximately every two weeks. Winter sampling was conducted on a monthly basis when weather permitted. The water depth at our sampling site was 70 m. Water was collected between 0800 and 0900 hrs from 6 depths (0, 8, 12, 20, 25, 40 m) with 5 liter Niskin bottles. It was immediately placed in acid–washed polypropylene carboys, which in turn were immediately placed inside large containers filled with surface seawater to maintain ambient temperature. The containers were transported the Hatfield Marine Science Center, Oregon State University, Newport, Oregon. Once on shore, the water was mixed by gently inverting the carboys a number of times, before samples were drawn for experimental work.

Biomass and Nutrient Concentrations

Ammonium concentrations were measured manually in triplicate within two hours of collection using the phenolhypochlorite method (Solórzano 1969). Initial and final seawater samples were taken from the experimental bottles used in uptake experiments and this water was frozen until analyzed later for $[NO_2^- + NO_3^-]$ and $[NO_2^-]$ concentrations using a Technicon II

AutoAnalyzer (Whitledge et al. 1986). Urea concentrations were also determined on initial and final samples that were frozen. The diacetyl monoxime thiosemicarbizide protocol of Price and Harrison (1987) was used to measure urea concentrations in triplicate. Samples were not filtered prior to storage and analysis.

Total chlorophyll *a* concentrations were determined by filtering duplicate 100 ml aliquots of seawater onto combusted 25 mm Whatman GF/F filters. The amount of Chl *a* in the <20 μm fraction was determined by first putting the water through a 20 μm Nitex mesh. Filters were extracted in 90% acetone at 4°C in the dark for 24 h and measured using a Turner Designs 10 fluorometer (Strickland and Parsons 1972). The fluorometer was calibrated with a primary standard of pure Chl *a* and with daily working standards of coproporphyrin I. Standards were purchased from Sigma Chemical Co.. The instrument was zeroed with extracted filter blanks and 90% acetone blanks (Venrick 1987).

Particulate organic nitrogen (PN) concentrations were determined by filtering 500–1000 ml of seawater onto a combusted 25 mm Whatman GF/F filter, freezing the filter and then drying it at 60°C for 24 h. A persulfate digestion converted the particulate organic nitrogen to NO_3^-, which was then measured with a Technicon II AutoAnalyzer (Grasshoff et al. 1983).

^{15}N Uptake Experiments

Trace amounts (~10% of the ambient NO_3^- concentration) of $Na^{15}NO_3$ (98.9 atom%) or 0.1 μM (final concentration) of $(^{15}NH_4)_2SO_4$ (99.0 atom%) or $CO(^{15}NH_2)_2$ (95.1 atom%) were added to 1 liter subsamples in Nalgene

polycarbonate bottles. All ^{15}N isotopes were purchased from MSD Isotopes. Once spiked with label, the bottles were placed in an environmental chamber simulating ambient seawater temperatures (~8–10°C) and saturating light conditions (~500 μE m^{-2} s^{-1}). Bottles from the lower 5 depths were placed in bags made of neutral density screening to simulate light levels of 50, 30, 15, 5 and 1% of saturated irradiance. Incubations lasted from 4 to 6 h. At the end of the incubations, samples were filtered under low vacuum pressure (<180 mm of Hg) onto combusted 47 mm Whatman GF/F filters. The filters were frozen and then dried at 60°C for 24 h. Dried filters were prepared for emission spectrometry following the micro–Dumas dry combustion method of LaRoche (1983), and were analyzed for ^{15}N incorporation into particulate matter with a Jasco N–150 emission spectrometer (Fiedler and Proksch 1975). Ammonium uptake rates were corrected for isotope dilution using the methods described in Wheeler et al. (1989). The equations of Dugdale and Goering (1967) were used to calculate PN–specific (V) and absolute (ρ) hourly uptake rates for each nitrogen species. Daily nitrate uptake rates were calculated by multiplying the hourly uptake rate data by each day's photoperiod. Dark nitrate uptake rates were assumed to be negligible. Light ammonium and urea uptake rates were calculated in the same way as for nitrate. Dark ammonium uptake rates were assumed to be 52% of light uptake rates, while dark urea uptake rates were 27% of those in the light (Price et al. 1985). Daily ammonium and urea rates were calculated by adding together the estimated light and dark uptake rates.

Annual ammonium, nitrate and urea production rates were estimated by taking the mean depth–integrated production rates (calculated using the trapezoid rule method) for the upwelling season and the winter and

multiplying each mean production rate by the number of days in the season (upwelling season=183 days, winter=182 days). The production rates estimated for the upwelling season and winter were summed to give an annual rate. The variability associated with these estimates was calculated using the propagation of error method (Press et al. 1989).

Phytoplankton Growth Rates, the Percentage of Phytoplankton Nitrogen and the Relative Preference Index

Phytoplankton–specific growth rates, μ (doublings d^{-1}), were calculated using:

$$\mu = 3.32\log_{10}[(P_{PN} + \rho_N)/P_{PN}]$$

where P_{PN} was the estimated phytoplankton nitrogen concentration in μM and ρ_N was the calculated daily uptake rate in μM. The percentage of phytoplankton nitrogen in the PN pool was estimated either from regressions of the PN concentration on the Chl *a* concentration or by assuming a Chl *a*:cell N of 2.25 μg Chl *a* μmol N^{-1} (Chan 1980, Darley 1980), as described in Chapter 2.

The relative preference index (RPI) of McCarthy et al. (1977) was used to determine whether phytoplankton were using ammonium, nitrate or urea preferentially relative to their availability. The RPI for each substrate was calculated using:

$$RPI_N = \left[\frac{(\rho_N/\Sigma\rho_N)}{([N]/\Sigma[N])}\right]$$

where, ρ_N and [N] were the daily uptake rate of substrate N and its concentration, while $\Sigma\rho_N$ and $\Sigma[N]$ were the sums of the daily uptake

rates of all the nitrogenous substrates measured and their concentrations. An $RPI_N=1$ indicates when the uptake was equivalent to the availability of substrate N, an $RPI_N>1$ indicates a preference for substrate N, and an $RPI_N<1$ indicates a rejection of substrate N.

Criteria Used to Characterize the Upwelling State

Neuer (1992) used the mean weekly wind data collected at Newport, OR to calculate the Bakun upwelling index (Bakun et al. 1974) for the physical characterization of the upwelling conditions during this sampling. Upwelling–favorable winds were present during six of the 11 sample days during the upwelling season (see Table 2.1). However, the Bakun index is a broadscale, slow responding parameter for the assessment of upwelling status (Small and Menzies 1981). Consequently, we used the surface nitrate and Chl *a* concentrations for a more accurate biological characterization of the upwelling status (see Table 2.1). High nitrate and low Chl *a* on days 191 and 555 indicated active upwelling conditions. Moderate nitrate and high Chl *a* indicated the occurrence of phytoplankton blooms on days 205, 219, 284, and 569. On day 597, high Chl *a* and low nitrate suggests that a phytoplankton bloom had recently depleted surface nitrate. The remaining four days during the upwelling period were characterized by very low nitrate (<1 μM) and low Chl *a* concentrations and these days are designated as post–bloom conditions.

Results and Discussion

Nutrient and Biomass Concentrations

Contour plots of NO_3^-, NH_4^+ and urea concentrations are shown in Figure 3.1. During the spring and summer, NO_3^- concentrations in the upper 8 m of the water column varied between 0.1 and 30 μM, depending on the time since an upwelling event (Fig. 3.1a). After an upwelling event a strong nitracline often developed either at 8 or 12 m, separating water with lower NO_3^- concentrations in the surface layer from water with higher concentrations below. Nitrate concentrations at 40 m were between 22 and 42 μM during the upwelling season. During the winter months, NO_3^- concentrations in the water column ranged from 6 to 10 μM and were evenly distributed. The lowest NO_3^- concentrations at depth were measured during the winter.

Generally, the highest NH_4^+ concentrations were found between 12 and 25 m. On two occasions plumes of water with high NH_4^+ concentrations were observed from 20 to 40 m (Fig. 3.1b), with the highest NH_4^+ concentrations (4.2 and 3.5 μM) located at 20 m. High NH_4^+ concentrations were also observed once in the upper part of the water column (0 to 20 m) shortly after an upwelling event (day 191), when the surface water NO_3^- concentration was quite large ($\sim$21 μM). At that time the subsurface NH_4^+ maximum was located at 12 m. The presence of high NH_4^+ concentrations close to shore has also been reported by Codispoti and Friederich (1978) off northwest Africa.

Figure 3.1. Contour plots of nutrient distributions. (a) nitrate, (b) ammonium, and (c) urea for days 191 to 597. Sampling times and depths are denoted by black dots on the plots. The upwelling season is shown by a filled bar at the top of each plot, while the wintertime is shown by an open bar. Urea measurements were begun on day 284.

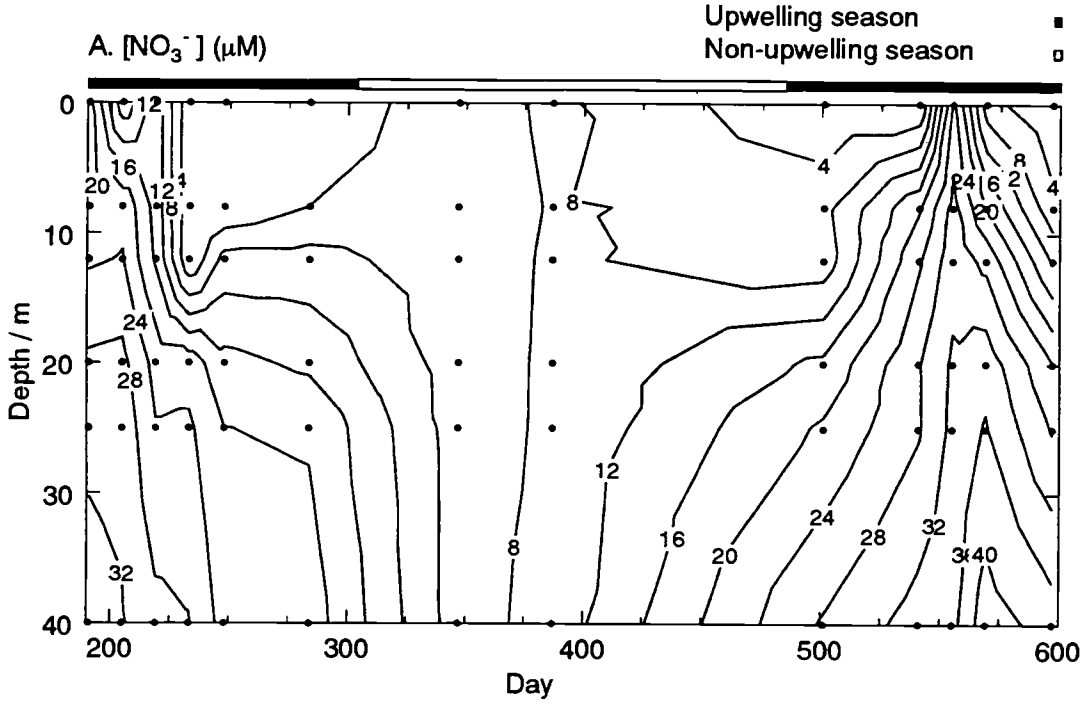
A. [NO3-] (μM)
Upwelling season
Non-upwelling season
Depth / m
Day
0
10
20
30
40
200
300
400
500
600
4
8
12
16
20
24
28
32
40

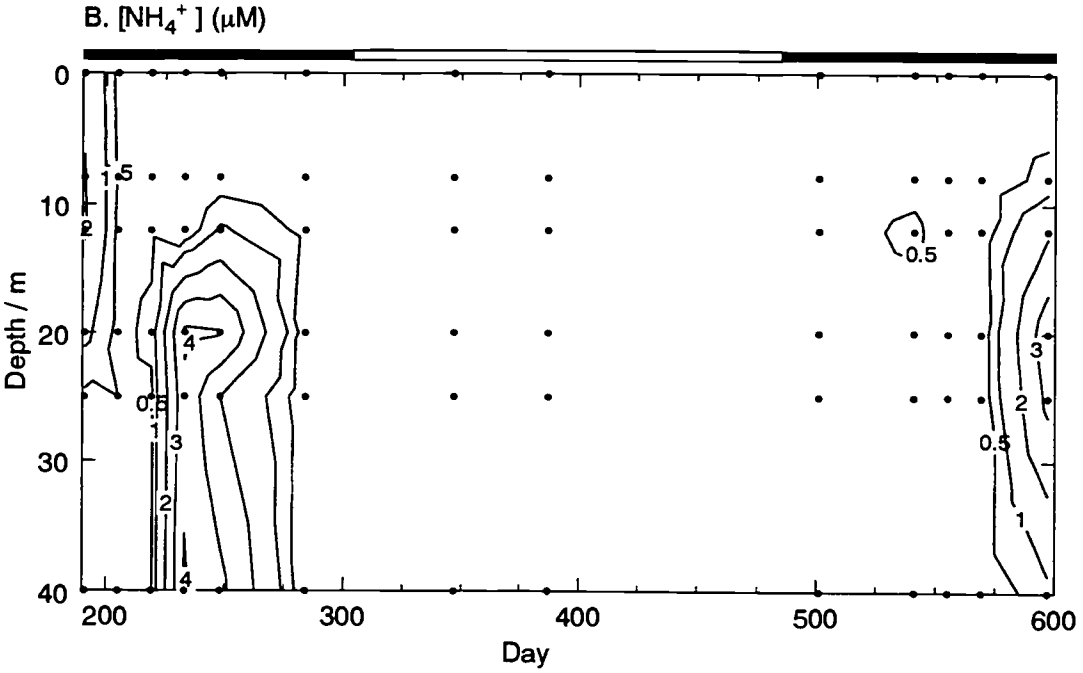
B. [NH4+] (μM)
Depth / m
Day
0
10
20
30
40
200
300
400
500
600
0.5
1
2
3
4
5

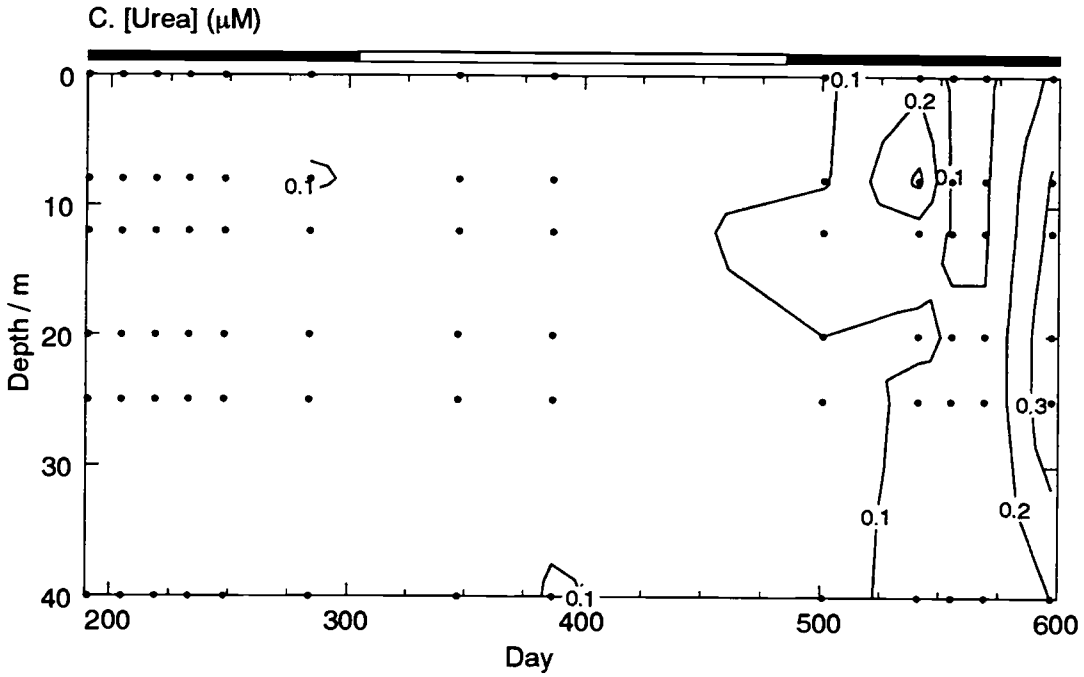
C. [Urea] (μM)
Depth / m
Day
0
10
20
30
40
200
300
400
500
600
0.1
0.2
0.1
0.1
0.3
0.1
0.2
0.1

They found that high NH_4^+ concentrations in the surface waters were related to the cross–shelf circulation. During upwelling events, when there is surface outflow and deeper inflow, the NH_4^+–laden water is transported close to the surface. Under relaxed upwelling conditions, characterized by wind reversals and weak wind speeds, the inflow of surface water and outflow of deep water maintains the plumes at depth within the water column.

It is interesting to note that Wroblewski's (1977) model for the Oregon upwelling zone predicts the occurrence of a NH_4^+ plume after a phytoplankton bloom. At that time, no data were available to corroborate his prediction. The NH_4^+ plumes predicted by Wroblewski's model originated from the dissolution of zooplankton fecal pellets. Barber and Smith (1981) have suggested that as material is advected offshore in the Ekman layer and sinks, it is remineralized by bacteria and zooplankton. The resultant NH_4^+ and urea is then returned to the nearshore zone by onshore flow at depth. Results from a recent model (Hermann et al. 1989) support this idea and suggest that net regeneration of NH_4^+ at 20 m is a widespread feature extending from the mid– to outer continental shelf off the northwest USA.

In our study, the cores of the two subsurface NH_4^+ plumes generally coincided with times when approximately 60 to 80% of the Chl *a* was in the $\geq$20 μm fraction (i.e. diatoms) (Fig. 3.2) and phytoplankton nitrogen comprised 50 and 70% of the PN pool (see Chapter 2). At other times, diatoms usually made up <50% of phytoplankton assemblage and

phytoplankton nitrogen made up only 10 to 20% of the particulate nitrogen at depths greater than 20 m. The highest PN concentrations were routinely measured in the upper 8 m of the water column. However, when the NH_4^+ plumes were present, the highest PN concentrations were deeper (between 12 and 20 m). It is not known whether these NH_4^+ plumes were associated with high concentrations of detritus, as the model predicts (Wroblewski 1977).

Observations on the meridional and zonal extent of these NH_4^+ plumes are lacking. Small and Menzies (1981) found that bands of high phytoplankton biomass and productivity run parallel to the coast. We might expect a similar alongshore distribution of discrete plumes at mid–depth when onshore flow is low, such as during upwelling relaxation. The occurrence of an NH_4^+ plume in the upper part of the water column (i.e. on day 191 in Fig. 3.1) suggests that upwelling events may also be important in distributing regenerated nitrogen to autotrophs in the surface layer.

The amount of time between productivity events in the surface layer and the formation of NH_4^+ plumes deeper in the water column was about 2 weeks. In Wroblewski's (1977) model, subsurface NH_4^+ plumes were found 10 days after a strong upwelling event. According to this model, it is unlikely that the strong upwelling event on day 555 would have produced the subsurface plume observed on day 597. An unsampled upwelling bloom probably took place sometime between those dates. Although these NH_4^+ plumes appear

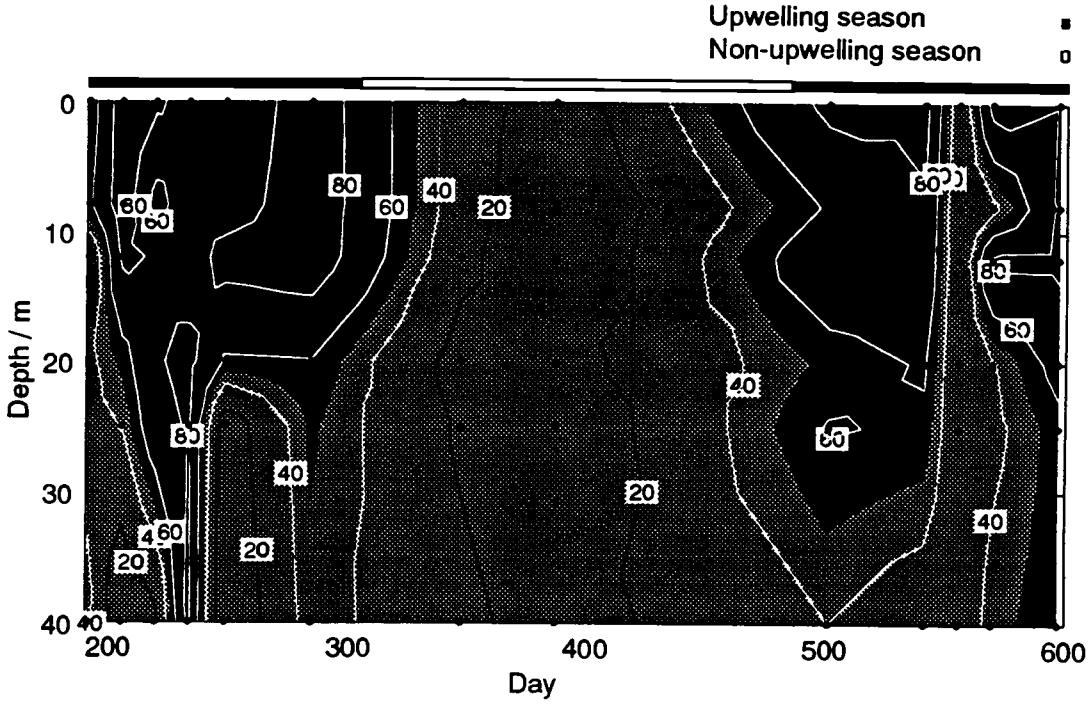

Figure 3.2. Same as in Figure 3.1, but for the fraction of Chl a $\geq$20 μm. Grey areas represent $\leq$50%, while blackened regions had >50%.

to be ephemeral features, it should be noted that the core of one plume was coherent over a 2 week period (day 233 to 248) between upwelling events.

Of the three nitrogenous nutrients, urea concentrations were the lowest measured (Fig. 3.1c). Urea concentrations were approximately an order of magnitude lower than those of NH_4^+ and ranged from <0.10 to 0.35 μM. Most of the time, urea concentrations were low and evenly distributed throughout the water column. The concentrations we measured are similar to those in the subarctic Pacific (0.17 to 0.40 μM; Mitamura and Saijo 1980) and those previously reported for the Washington/Oregon coast (0.03 to 0.35 μM; Kokkinakis and Wheeler 1988) but quite a bit lower than reported for Peru (1.7 to 7.0 μM; Remsen 1971). The large difference between urea concentrations off Peru and Oregon may reflect differences in the presence of various groups of organisms required for the regeneration of urea. Whitledge (1981) showed that off Peru, nekton rather than zooplankton were the major source of urea. On one occasion (day 597), a subsurface maximum in urea concentrations was observed extending from 8 to 25 m. Some of the highest concentrations measured (~0.35 μM) coincided with the NH_4^+ plume observed on day 597. High urea concentrations may have resulted from increased regeneration rates and reduced uptake rates. Low uptake rates at depth may have resulted from either low irradiance levels or the inhibition of urea assimilation by phytoplankton due to high ambient NH_4^+ concentrations

(1–2 μM). Similar NH_4^+ concentrations have been found to inhibit urea uptake by natural phytoplankton populations (Kristiansen 1983).

Nitrate, NH_4^+, Chl *a* and PN concentrations integrated from 0 to 40 m are shown in Figure 3.3 and summarized with respect to the upwelling cycle and winter in Table 3.1. Integrated NO_3^- concentrations were lowest during the winter months (237 to 351 mmol m^{-2}), intermediate during relaxed upwelling (541 to 968 mmol m^{-2}) and highest during upwelling events (1100 to 1260 mmol m^{-2}). Integrated NH_4^+ concentrations were lowest during the winter (4–11 mmol m^{-2}), but reached extremely high concentrations (up to 78 and 96 mmol m^{-2}) during blooms and relaxation events, in addition to upwelling events (up to 47 mmol m^{-2}). Low integrated urea concentrations were found during the winter (0.22 to 2.16 mmol m^{-2}) and active upwelling events (4 mmol m^{-2}). During the 1991 upwelling season the mean integrated concentration was 6.1 mmol m^{-2}, with the highest concentration (12.5 mmol m^{-2}) being measured on day 597 at the end of a bloom.

Integrated Chl *a* concentrations were highest during blooms (158 and 558 mg Chl *a* m^{-2}), and lowest during the winter (21 to 60 mg Chl *a* m^{-2}) and at the onset of upwelling (23 to 74 mg Chl *a* m^{-2}) (Fig. 3.3c, Table 3.1). During relaxation events integrated concentrations were between 95 and 229 mg Chl *a* m^{-2}. Particulate nitrogen concentrations followed the same pattern as Chl *a* (Fig 3.3d, Table 3.1). The highest concentrations

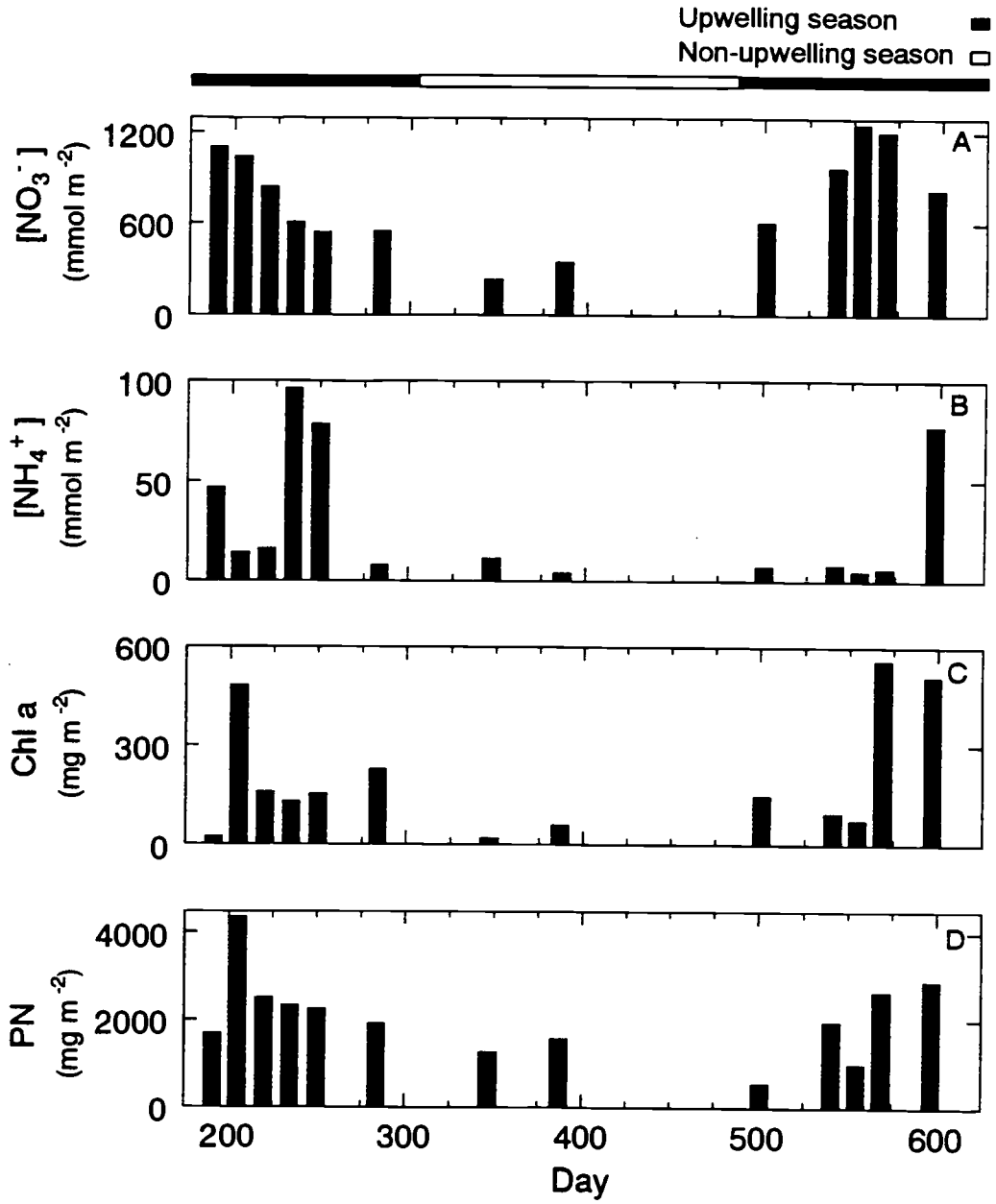

Figure 3.3. Depth–integrated nutrient and biomass concentrations. (a) nitrate, (b) ammonium, (c) chlorophyll *a*, and (d) particulate nitrogen.

Table 3.1. Integrated biomass, nutrients and uptake rates from 0 to 40 meters during the upwelling cycle and winter.

	Active Upwelling	Upwelling Bloom	Relaxed Upwelling	Winter
Chl *a* (mg m^{-2})	23–74	158–558	95–229	21–60
PN (mg m^{-2})	1000–1700	2500–4400	560–2300	1300–1600
$[NO_3^-]$ (mmol m^{-2})	1100–1300	800–1200	500–1000	200–350
$[NH_4^+]$ (mmol m^{-2})	6–47	14–78	7–96	4–11
[urea] (mmol m^{-2})	4	4–13	1–7	<1–2
ρ_{NO_3} (mmol m^{-2} d^{-1})	7–26	100–200	20–100	2–6
ρ_{NH_4} (mmol m^{-2} d^{-1})	9–14	15–60	6–90	4–8
ρ_{urea} (mmol m^{-2} d^{-1})	4	8–18	1–9	1–6

were found during phytoplankton blooms (2652 to 4385 mg N m^{-2}), they were intermediate during relaxation events (~2300 mg N m^{-2}) and lowest in the winter and recently upwelled water (1300 to 1700 mg N m^{-2}).

Absolute Nitrogen Uptake Rates

The initiation of two distinct blooms was apparent from the NO_3^- uptake rates on day 205 and 569 during the 1990 and 1991 upwelling seasons (Fig. 3.4a). The possible remnants of two smaller blooms were observed on day 284 and 541. Unfortunately, we are not able to ascertain whether these smaller blooms occurred at our site prior to sampling or were advected to the site from an older upwelling center situated further to the north. Generally, the highest NO_3^- uptake rates were measured in the surface water (0 m) after high concentrations of NO_3^- had been transported to the surface layer (Fig. 3.1a). After NO_3^- concentrations in the surface water were depleted to submicromolar concentrations, uptake rates there were reduced and higher uptake rates were observed in the NO_3^-–replete water at 8 m. During these periods of high uptake rates, 19 μM NO_3^- could potentially be removed from the surface layer per day. At that rate, NO_3^- turnover times were estimated to be on the order of a day. Low uptake rates were routinely measured at depths deeper than 8 m, reflecting the light–dependence of NO_3^- uptake (MacIsaac and Dugdale 1972) and occasionally at the surface between upwelling events.

Figure 3.4. Same as in Figure 3.1, but for daily absolute uptake rates. (a) nitrate, (b) ammonium, and (c) urea.

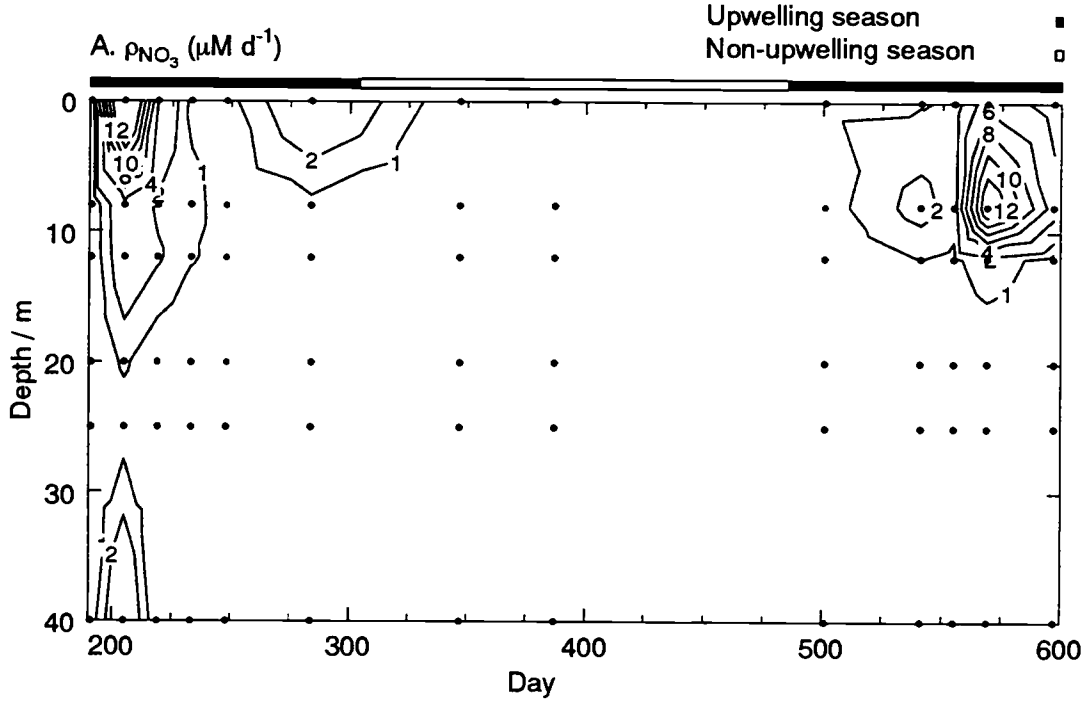
A. ρ_{NO_3} (μM d^{-1})
Upwelling season
Non-upwelling season
Depth / m
Day
0
10
20
30
40
200
300
400
500
600
12
10
4
1
2
1
6
8
10
12
2
4
1
2

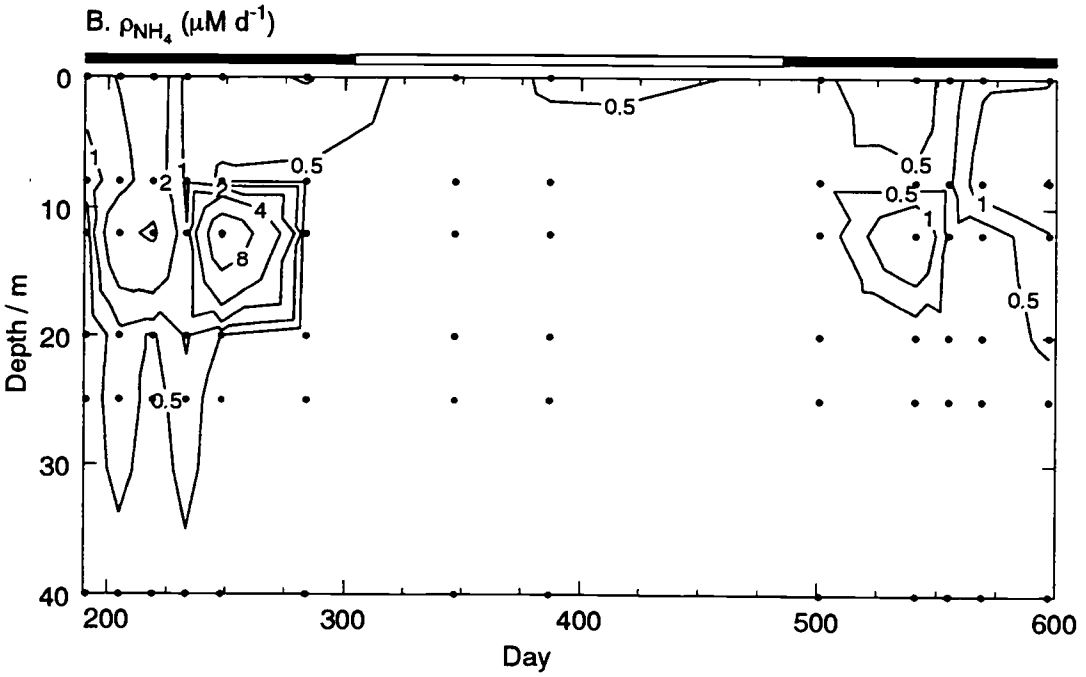
B. ρ_{NH_4} (μM d^{-1})
Depth / m
Day
0
10
20
30
40
200
300
400
500
600
0.5
1
2
1
0.5
2
4
8
0.5
0.5
0.5
1
1
0.5

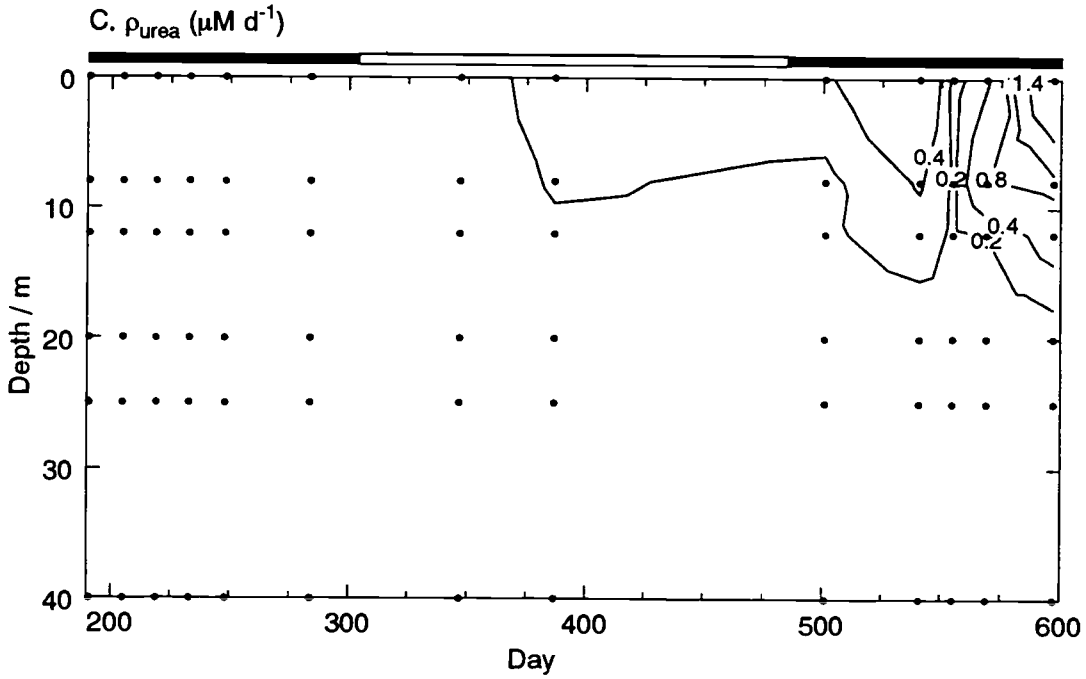
C. ρurea (μM d-1)
0
10
20
30
40
Depth / m
200
300
400
500
600
Day
1.4
0.4
0.2
0.8
0.4
0.2

Relatively high NH_4^+ uptake rates (>1 μM d^{-1}) usually occurred after a bloom event, although sometimes they coincided with high NO_3^- uptake rates (Fig. 3.4b). Ammonium uptake rates after a bloom were similar to NO_3^- uptake rates during the bloom; ρ_{NO_3} = 18–19 μM d^{-1} versus ρ_{NH_4} = 13 μM d^{-1}. The highest NH_4^+ uptake rate was measured at 12 m (Fig. 3.4b), deeper in the water column than the high NO_3^- uptake rates (Fig. 3.4a) and offset in time. Low NH_4^+ concentrations were observed at 12 m on day 205 (Fig. 3.1b), likely due to the rapid uptake rate there. Conversely, the deeper NH_4^+ concentrations were higher during this time, and able to exist for an extended period, because of the low NH_4^+ assimilation rates. Similar results found off northwest Africa indicate that high NH_4^+ concentrations result from reduced primary production and enhanced community catabolism, leading to the production of NH_4^+ faster than it can be consumed (Codispoti and Friederich 1978).

Daily urea uptake rates never reached the highest rates observed for NO_3^- and NH_4^+ (Fig. 3.4c). The highest rates (to 2.1 μM d^{-1}) were found in the surface water after the last upwelling event on day 597, and decreased with depth.

Nitrate supplied almost half ($\bar{X}$=49%, SE=3.0, n=78) of the nitrogen utilized at this site (Fig. 3.5a). Comparison of NH_4^+ and urea daily uptake rates revealed that, on average, NH_4^+ utilization accounted for 69% (SE=2.0, n=48) of the regenerated nitrogen used (Fig. 3.5b). The rule of thumb

of multiplying NH_4^+ uptake rates by 1.5 to account for the contribution of other regenerated forms of nitrogen, such as urea, appears to be appropriate (1/0.69=1.45), although urea uptake rates were not corrected for isotope dilution. Urea utilization was only occasionally greater than NH_4^+ use (Fig. 3.5b). This occurred once during the winter (day 387 at 8 and 25 m) and twice during the 1991 upwelling season (day 541 at 25 m and day 597 at 0 m). On average, urea uptake accounted for 15% (SE=1.8, n=48) of the total nitrogen assimilated. However, urea was a more important component of the nitrogenous nutrition of the phytoplankton during the non–upwelling season. In winter, 24% (SE=4.8, n=12) of the nitrogen assimilated was in the form of urea, while during the upwelling season urea only accounted for 12% (SE=1.5, n=36). Work on arctic phytoplankton by Harrison et al. (1985) found that urea accounted for, on average, 32% of the nitrogen used, while Kristiansen (1983) reported a value of 19% for a coastal site.

The highest f–ratios (the proportion of "new nitrogen" (i.e. NO_3^-), utilized relative to the total amount of nitrogen (i.e. $NO_3^- + NH_4^+ +$ urea) assimilated) were calculated for active upwelling events (i.e. day 555) and upwelling blooms (i.e. day 205). At those times surface water f–ratios were between 0.80 and 0.90, reached a minimum between 12 and 20 m (0.3–0.4) and increased again at 40 m (0.65–0.95) (Fig. 3.6). Low f–ratios (<0.5) were encountered in the upper 20 m during an active upwelling event on day 191, due to the assimilation of NH_4^+ in water that was upwelled from depth.

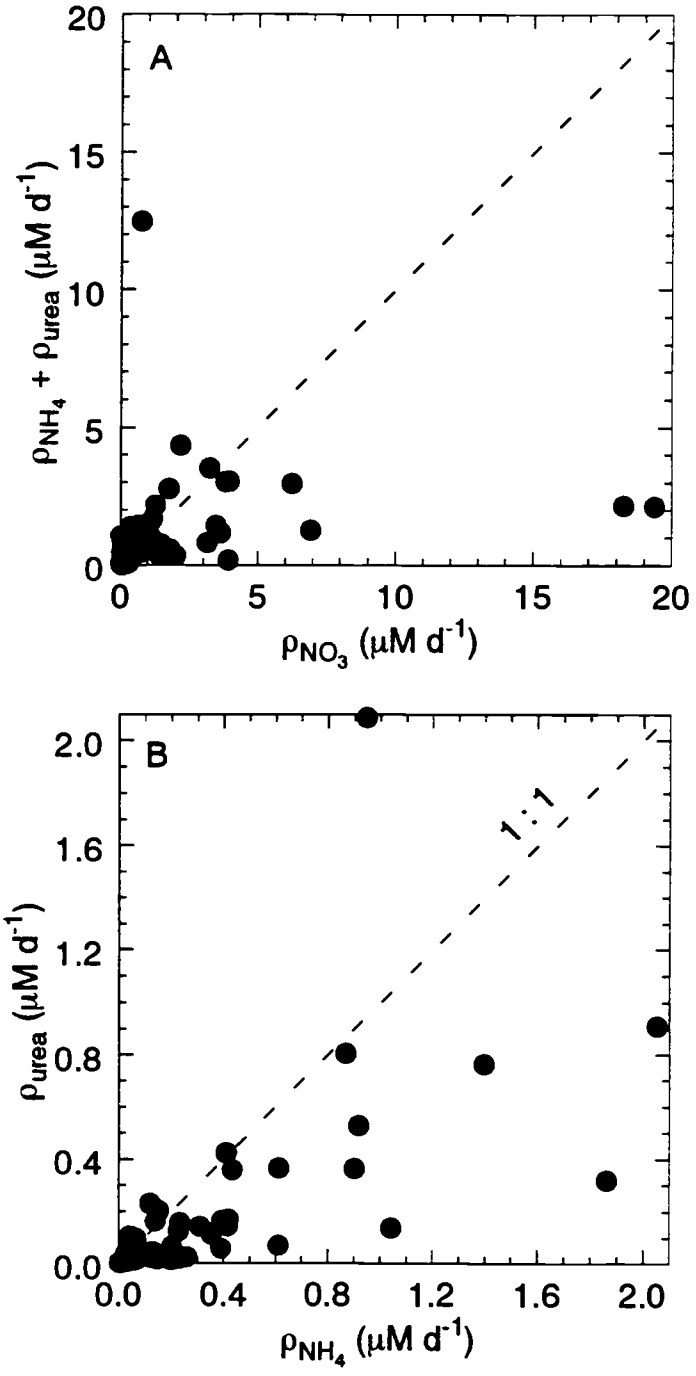

Figure 3.5. Comparison of daily (a) regenerated nitrogen uptake rates with new production rates, and (b) absolute urea uptake rates with absolute ammonium uptake rates.

During the winter, low f–ratios (<0.4) were observed throughout most of the water column. Low f–ratios during the upwelling season (<0.5) also coincided with the same depths and times as the NH_4^+ plumes (Fig. 3.1b). This finding is consistent with Eppley's (1981) notion that at such times, a large fraction of the sinking particles are in the form of fecal pellets and with Wroblewski's (1977) model results that dissolving fecal pellets result in the formation of NH_4^+ plumes. Since the NH_4^+ plumes were only detected after major phytoplankton blooms, one potential source of the NH_4^+ may have been grazing zooplankton, such as *Pseudocalanus* sp., found by Peterson et al. (1979) to be the dominant macrozooplankter between 10 and 20 m at our site. It has been suggested that these animals undergo long periods without feeding between upwelling events and depend mainly on primary production sinking out of the surface layers during upwelling relaxation (Peterson et al. 1979).

Chl *a*–Specific Nitrogen Uptake Rates

During this study, nutrients (Fig. 3.1) and biomass (Fig. 3.2) underwent large fluctuations. To take those changes into account when comparing our uptake data, we normalized rates to Chl *a*. Daily Chl *a*–specific NO_3^- ($V_{NO_3}^{Chl}$), NH_4^+ ($V_{NH_4}^{Chl}$), and urea (V_{urea}^{Chl}) uptake rates are presented in Figure 3.7. The distribution of $V_{NO_3}^{Chl}$ values (Fig. 3.7a) was quite different from that

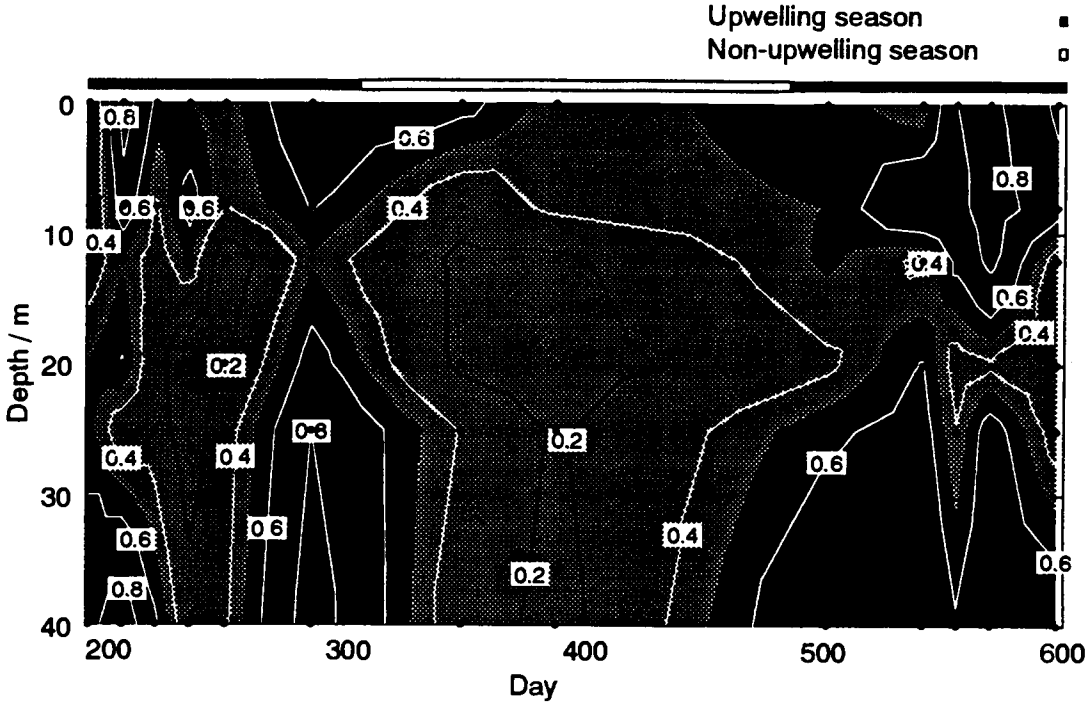

Figure 3.6. Contour plot of the f–ratio with respect to depth and time. Grey areas represent where the f–ratio was ≤ 0.5, while in the blackened regions the f–ratio was >0.5.

of ρ_{NO_3} (Fig. 3.4a). With the exception of high specific uptake rates between 25 and 40 m on day 205, (which may indicate bacterial utilization of nitrate), the rates were relatively low and similar for the first bloom period and during the winter. The highest near–surface $V_{NO_3}^{Chl}$ values (up to 2.5 μmol μg^{-1} d^{-1}) were found on day 541, when ρ_{NO_3} (Fig. 3.7a) was not that impressive (2 μM d^{-1}). The presence of a smaller secondary peak at 20 m was apparent for $V_{NO_3}^{Chl}$ but not for ρ_{NO_3}, and a small $V_{NO_3}^{Chl}$ peak also appeared at 40 m at this time. We believe that the complex vertical pattern in $V_{NO_3}^{Chl}$ values observed during the 1991 upwelling season may reflect differences in the phytoplankton assemblage, particularly in the upper 20 m. During both upwelling seasons, diatoms dominated the phytoplankton assemblage most of the time (Fig. 3.2). However, on days 541 and 555, at the end of a bloom and during an active upwelling event (Fig. 3.1a), small phytoplankton cells were predominant throughout the water column (Fig. 3.2). This cell population, characterized by a small biomass and a small amount of Chl *a*, nevertheless had a relatively high affinity for nutrients and thus could immediately exploit the freshly upwelled NO_3^-.

Differences between the absolute and Chl *a*–specific NH_4^+ uptake rates (Fig. 3.4b and 3.7b) were not as dramatic as those for NO_3^-. Chl *a*–specific NH_4^+ uptake rates tended to be higher after the occurrence of the first upwelling bloom, up to 1 μmol μg^{-1} d^{-1} at 12 m depth. However, high

Figure 3.7. Same as Figure 3.1, but for daily Chl *a*–specific uptake rates. (a) nitrate, (b) ammonium, and (c) urea.

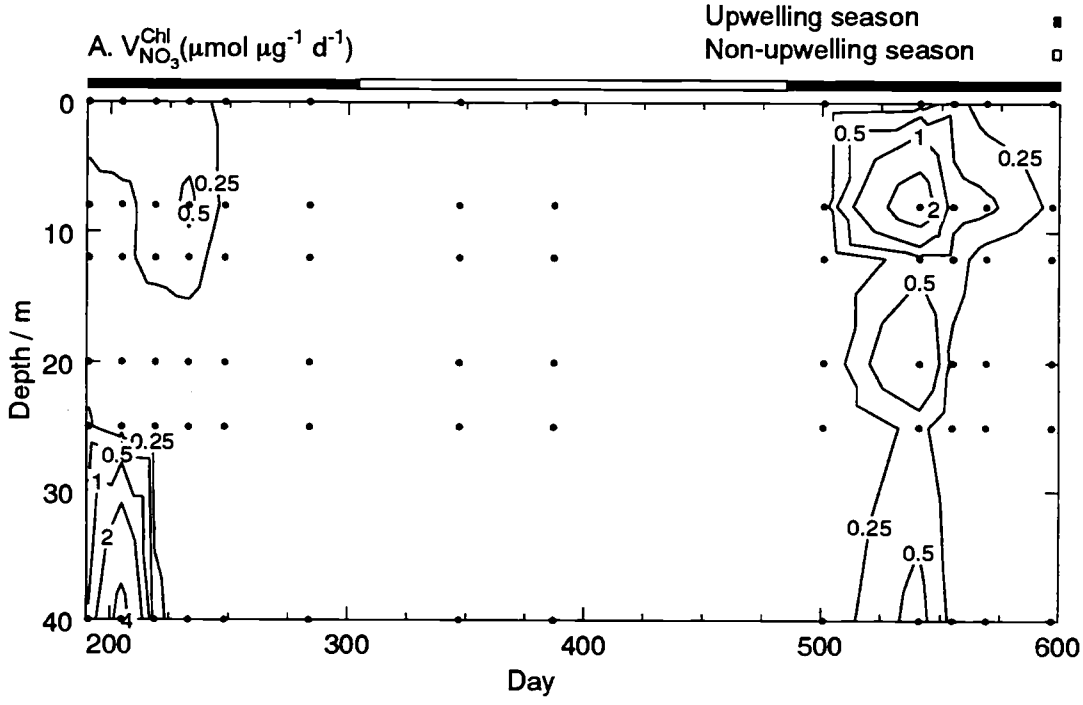
A. $V_{NO_3}^{Chl}$(μmol μg^{-1} d^{-1})
Upwelling season
Non-upwelling season
Depth / m
Day
0
10
20
30
40
200
300
400
500
600
0.25
0.5
1
2
4

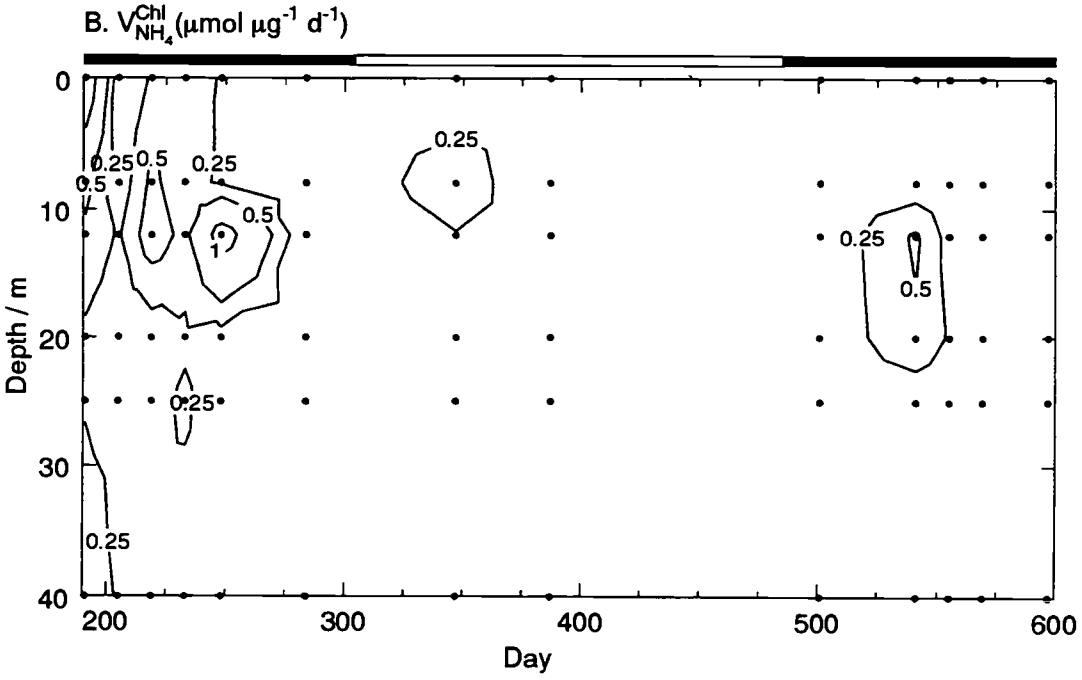
B. $V_{NH_4}^{Chl}$(μmol μg^{-1} d^{-1})
Depth / m
Day
0
10
20
30
40
200
300
400
500
600
0.25
0.5
1

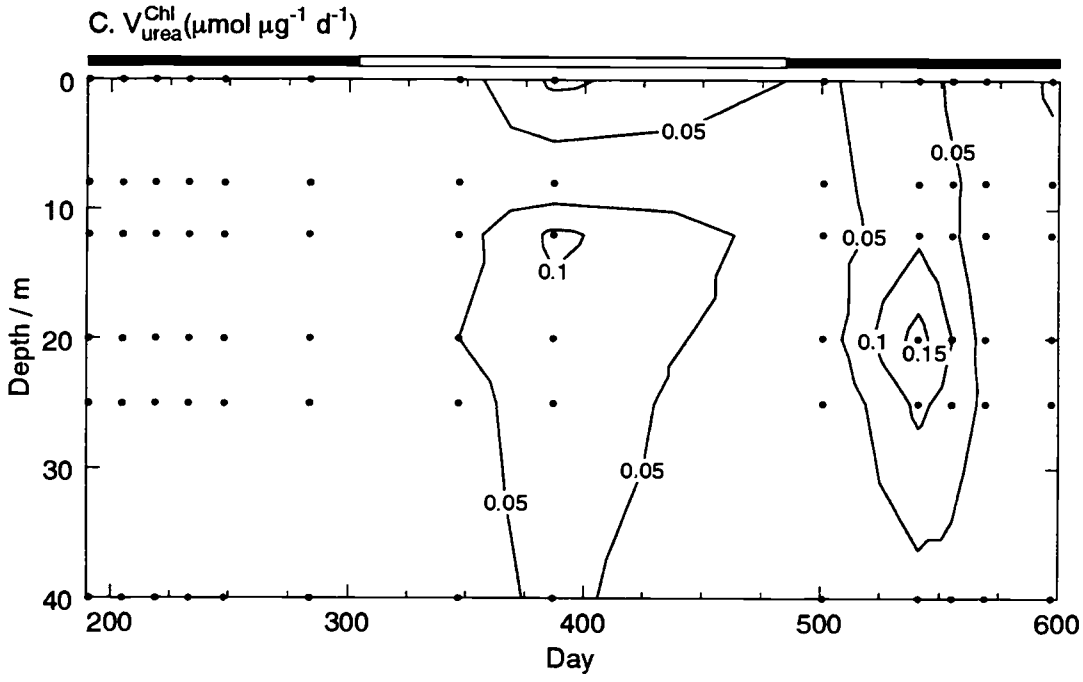
C. V_{urea}^{Chl}(μmol μg^{-1} d^{-1})
0
10
20
30
40
Depth / m
200
300
400
500
600
Day
0.05
0.05
0.05
0.1
0.05
0.1
0.15
0.05

normalized uptake rates also occurred on day 191 in the surface layer (0–8 m). These rates coincided with a recent upwelling event and the presence of an NH_4^+ plume within the surface layer (Fig. 3.1b). No comparable rates occurred during the second upwelling period, although rates exceeding 0.25 μmol μg^{-1} d^{-1} did appear from 12–20 m on day 541 (Fig. 3.5b), prior to the maximal upwelling on day 555.

Chl *a*–specific urea uptake rates were about an order of magnitude lower (Fig. 3.7c) than those of NH_4^+ and NO_3^-. The highest rates were found in the winter (day 387) in the surface water and at 12 m, and on day 541 throughout most of the water column. The highest V_{urea}^{Chl} value of 0.15 μmol μg^{-1} d^{-1} occurred at 20 m on day 541 and coincided with observed peaks in NO_3^- and NH_4^+ uptake rates.

Vertical profiles of absolute and Chl *a*–specific uptake rates of NO_3^-, NH_4^+ and urea averaged over the entire sampling period show the utilization of these nutrients as a function of depth (Fig. 3.8). Vertical profiles of nutrient concentrations are also given. Absolute NO_3^- uptake rates were highest in the near–surface water and decreased with depth, although elevated rates sometimes occurred at 40 m due to presumed bacterial uptake. However, Chl *a*–specific NO_3^- uptake rates were actually highest at 8 m (excluding 40 m data). Absolute NH_4^+ uptake rates were also highest in the near–surface water, with the highest rate at 12 m (Fig. 3.8b). The highest Chl *a*–specific NH_4^+ uptake rate was also at 12 m. Although the absolute

NH_4^+ uptake rates were lower than those for NO_3^- in the upper 12 m, Chl *a*–specific rates were similar. Absolute urea uptake rates were the lowest of the three nutrients at each depth (Fig. 3.8c) and had a vertical profile similar to NO_3^-. Chl *a*–specific urea uptake rates were low and reasonably similar throughout the water column.

The distribution of absolute and Chl *a*–specific NO_3^- uptake rates in the water column were not correlated with the NO_3^- distribution (Fig. 3.8). Absolute NO_3^- uptake rates decreased with depth while NO_3^- concentrations increased, showing that light–dependent uptake kinetics were more important overall than the NO_3^- distribution. Ammonium uptake rates and concentrations also appeared to be inversely related. The lowest NH_4^+ concentrations (0.29–0.59 μM) were found in the upper 12 m and corresponded to the locations of the highest uptake rates. However, there was no direct correspondence between the depth of the highest uptake rate and lowest ambient concentration, and vice versa. Absolute urea uptake rates, like NO_3^-, also suggested that light–dependent processes were more important than the ambient urea concentration. These data indicate a depth partitioning of the highest Chl *a*–specific uptake rates: 8 m for NO_3^-, 12 m for NH_4^+ and 20 m for urea.

Figure 3.8. Vertical profiles of mean (± SE) absolute (μM d^{-1}) and Chl *a*–specific (μmol μg^{-1} d^{-1}) uptake rates. (a) nitrate, (b) ammonium, and (c) urea. Profiles of mean ambient nutrient concentrations are shown below the appropriate uptake rate profile. For the nitrate and ammonium data n=13 and for the urea data n=8.

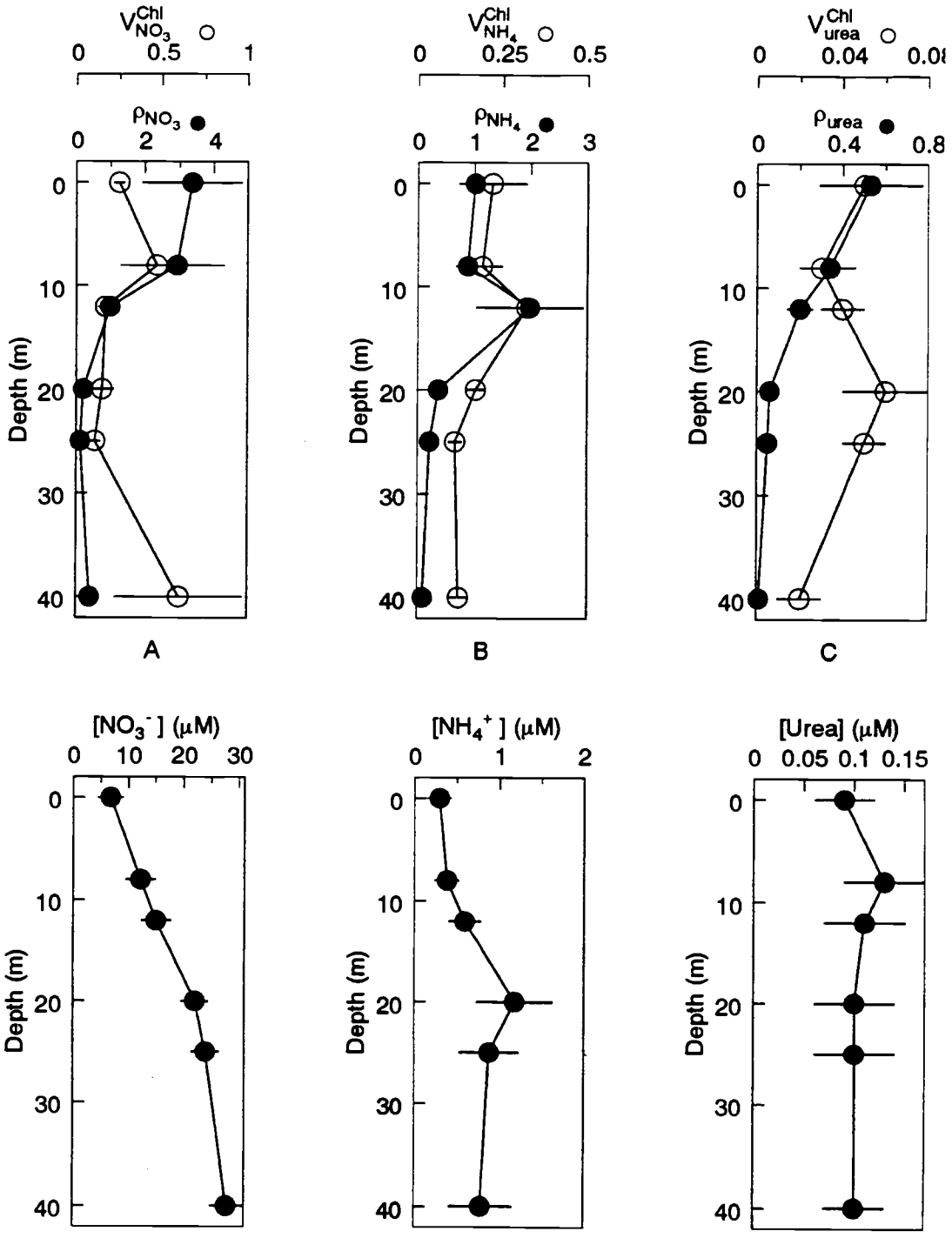
$V^{Chl}_{NO_3}$
0 0.5 1
ρ_{NO_3}
0 2 4
$V^{Chl}_{NH_4}$
0 0.25 0.5
ρ_{NH_4}
0 1 2 3
V^{Chl}_{urea}
0 0.04 0.08
ρ_{urea}
0 0.4 0.8
Depth (m)
0 10 20 30 40
A
B
C
$[NO_3^-]$ (μM)
0 10 20 30
$[NH_4^+]$ (μM)
0 1 2
[Urea] (μM)
0 0.05 0.1 0.15

Daily, Seasonal and Annual Nitrogen Production Rates

Integrated ρ_{NO_3} during the upwelling season ranged from 2 to 159 mmol N m^{-2} d^{-1} (Fig. 3.9a). The highest NO_3^- production rates measured in each upwelling season were similar; 159 mmol N m^{-2} d^{-1} in 1990 versus 152 mmol N m^{-2} d^{-1} in 1991. Production rates measured on days 284 and 541 were also similar (21 and 38 mmol N m^{-2} d^{-1}, respectively). The lowest amount of new production occurred during the winter (2 and 6 mmol N m^{-2} d^{-1}) and at the onset of upwelling (7 to 26 mmol m^{-2} d^{-1}). After an upwelling bloom new production rates steadily decreased. For instance from day 205 to 248, water column new production decreased 93%, from 159 to 11 mmol N m^{-2} d^{-1}.

Integrated ρ_{NH_4} were higher during the 1990 upwelling season than 1991 (Fig. 3.9b). This corresponded to our sampling of a bloom and a prolonged relaxation period (day 219–248). High NH_4^+ uptake rates in 1990 (31 to 86 mmol N m^{-2} d^{-1}) coincided with the peak in new production on day 205 and continued for 28 days afterwards. Lower NH_4^+ uptake rates were observed during the 1991 upwelling season, although if the data from 1990 are any indication, high rates probably occurred after day 597. Ammonium uptake rates at other times were low and similar to those for NO_3^-; 4 to 19 mmol N m^{-2} d^{-1}. These lower values are similar to NH_4^+ utilization rates determined by Whitledge (1981) off northwest Africa (8 mg–at m^{-2} d^{-1}),

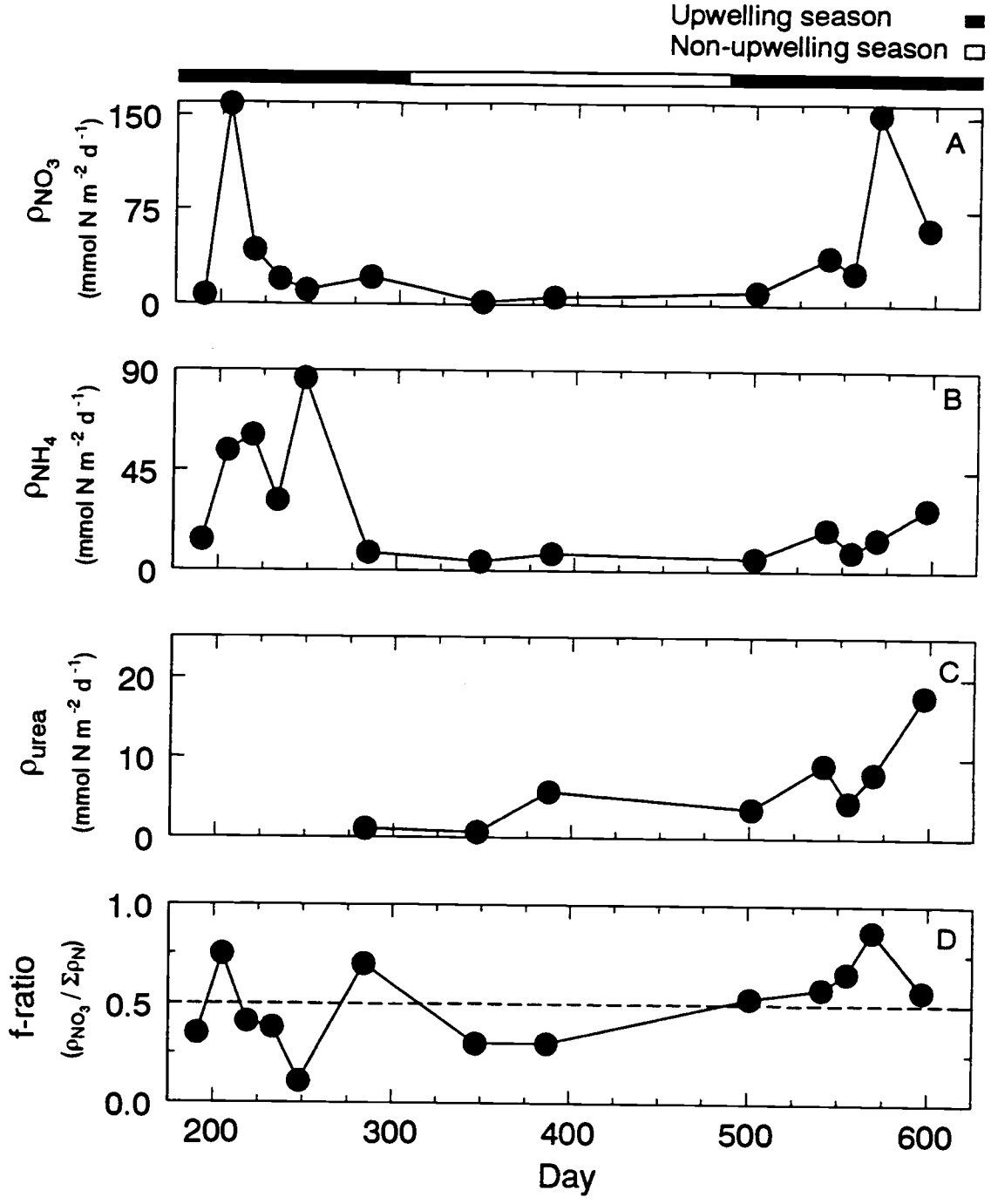

Figure 3.9. Depth–integrated daily absolute uptake rates. (a) nitrate, (b) ammonium, and (c) urea. Changes in the depth–integrated f–ratio with time is shown in (d).

Peru (15 mg–at m^{-2} d^{-1}) and Baja California (22 mg–at m^{-2} d^{-1}) during the upwelling season. These results suggest that in absolute terms, NH_4^+ utilization off Oregon is higher than in other upwelling regimes, although the percentage that NH_4^+ contributes to the overall nitrogen production may not be different.

Urea uptake rates were low most of the time (1 to 9 mmol N m^{-2} d^{-1}) (Fig. 3.9c). The highest integrated urea uptake rate was measured on day 597 (18 mmol N m^{-2} d^{-1}) when most of the uptake took place in the surface layer.

Using our estimates of integrated new and total production, f–ratios were calculated for each sampling date (Fig. 3.9d). Low f–ratios were commonplace during the 1990 upwelling season (0.11 to 0.41) and the winter months (0.30). Higher f–ratios, between 0.53 and 0.87, characterized the 1991 upwelling season. The highest f–ratios were measured on days 205, 284 and 569 (0.75, 0.70, and 0.87, respectively) after upwelling events and during blooms.

Total nitrogen production rates ranged from 7 (winter) to 213 mmol N m^{-2} d^{-1} (upwelling bloom on day 205; Table 3.2). Average depth–integrated nitrogen production rates were similar for both upwelling seasons; 86 mmol N m^{-2} d^{-1} in 1990 compared to 81 mmol N m^{-2} d^{-1} for the 1991 upwelling season (Table 3.3), but the proportion of new and regenerated production were different for each season. Nitrogen assimilation rates in the

Table 3.2. Estimates of daily new, regenerated and total primary production.

	Daily Production (mmol N m^{-2} d^{-1})		
Day	New	Regenerated	Total
191	7.2	13.6	20.8
205	158.8	53.9	212.7
219	42.4	60.7	103.2
233	19.6	31.4	50.9
248	10.9	86.4	97.3
284	21.2	9.0	30.2
347	2.0	4.8	6.9
387	5.8	13.4	19.2
501	10.3	9.2	19.5
541	37.9	27.9	65.8
555	25.8	13.3	39.1
569	152.0	22.6	174.6
597	60.9	45.9	106.9

winter were lower (13 mmol N m^{-2} d^{-1}) than those measured during either upwelling season. Regenerated production was equivalent to new production during the 1990 upwelling season, 42 compared to 43 mmol N m^{-2} d^{-1}. Conversely, during the 1991 upwelling season new production was almost two and one–half times greater than regenerated production, while the reverse was true for the winter. Our estimates of integrated daily production during the upwelling seasons when converted to carbon (5.7 g C m^{-2} d^{-1} assuming a C/N ratio by weight of 5.7) were similar to those reported for the Peruvian

upwelling system by Barber and Smith (1981); 4.3 and 6.3 g C m^{-2} d^{-1}, and the maximum measured by Harrison et al. (1981) of 7 g C m^{-2} d^{-1}.

Table 3.3. Seasonal comparison of daily new, regenerated and total primary production. Mean ± SE.

Year / Season	Daily Production (mmol N m^{-2} d^{-1})			n
	New	Regenerated	Total	
1990 upwelling	43.4 ± 16.1	42.3 ± 12.3	85.8 ± 28.9	6
1990 / 1991 winter	3.9 ± 1.9	9.1 ± 4.3	13.0 ± 6.2	2
1991 upwelling	57.4 ± 25.1	23.8 ± 6.5	81.2 ± 27.6	5

At our site, the total annual nitrogenous production was estimated to be 256.7 ± 164.2 g N m^{-2} y^{-1}. Of the total production, 137.4 ± 140.1 g N m^{-2} y^{-1} was attributable to NO_3^- and 119.3 ± 65.9 g N m^{-2} y^{-1} was due to regenerated nitrogen sources. Assimilation of NH_4^+ accounted for 91.9 ± 67.4 g N m^{-2} y^{-1}, while urea made up 26.9 ± 17.6 g N m^{-2} y^{-1}. The large errors associated with our annual production estimates reflect the episodic nature of upwelling events at our study site. Based on our annual

estimates of new and total nitrogen production, the overall f–ratio was 0.55. Thus, regenerated production accounted for 45% of the total annual production in this system. This is similar to other upwelling ecosystems in which regenerated production was found to make up from 28 to 58% of the total primary production (Whitledge 1981). Converting the total nitrogen production to carbon (by assuming a C/N ratio of 5.7 by weight) represents an annual primary production rate of 1412 g C m^{-2} y^{-1}. This estimate of primary production is similar to that determined from ^{14}C measurements also made during this study; 1938 g C m^{-2} y^{-1} (Dickson, Fessenden and Neuer, unpublished data). However, both these primary production rates are higher than either Ryther's (1969) estimate of 300 g C m^{-2} y^{-1} for coastal upwelling regimes or that made by Perry et al. (1989) on the Washington shelf. On the basis of ^{14}C incubations and the application of pigment–productivity algorithms to pigment concentration data obtained from the Coastal Zone Color Scanner, Perry et al. (1989) estimated an annual primary production rate of 646 g C m^{-2} y^{-1}.

Substrate Turnover Times

To assess the time scales over which biological processes could potentially utilize nutrients, turnover times were calculated for NO_3^-, NH_4^+ and urea. In the surface layer (0–8 m) NO_3^- turnover times were longest during

upwelling events (17 to 121 days) and the winter (12 to 58 days), but were usually less than a day under relaxed upwelling conditions. When all the data were taken into consideration, NO_3^- turnover times were fastest in the upper 8 m (11.7 to 20.5 days) and increased steadily with depth (Table 3.4). The longest turnover time was estimated to be just over a year at 40 m, where high ambient concentrations and low uptake rates were found. The relatively fast NO_3^- turnover time in the surface water (11.7 days) corresponded to the maximum turnover times for NH_4^+ (10.8 days) and urea (13.8 days) at depth. Turnover times for NH_4^+ in the upper 12 m were on the order of a day, with the fastest turnover occurring at 8 m. Slow NH_4^+ turnover times were associated with the plumes. Due to high NH_4^+ concentrations and low uptake rates in the plumes, turnover times at 20 and 25 m were on the order of 18 days. Nitrate and NH_4^+ turnover times between 0 and 8 m measured in this study are similar to those in the the euphotic zone of the Middle Atlantic Bight (Harrison et al. 1983), even though concentrations (and hence uptake rates) were about an order of magnitude higher in Oregon waters.

Urea was turned over faster than either NO_3^- or NH_4^+, taking about half a day in the upper 12 m. Like NO_3^-, the fastest urea turnover times occurred in the surface water. Generally, urea was turned over almost twice as fast as NH_4^+. Inter– and intra–seasonal differences were not apparent in urea turnover times. Kristiansen (1983) also estimated urea turnover times of

Table 3.4. Turnover times (τ) for nitrate, ammonium, and urea. Where, τ = [concentration/uptake rate]. For the nitrate and ammonium data n=13, and for the urea data n=6 at 12 and 20 meters and n=7 at 0, 8, 25 and 40 meters. Mean ± SE.

Depth (m)	τ (days)		
	NO_3^-	NH_4^+	urea
0	11.7 ± 5.9	0.8 ± 0.6	0.3 ± 0.1
8	20.5 ± 9.4	0.6 ± 0.2	0.6 ± 0.2
12	50.4 ±18.0	1.2 ± 0.5	0.5 ± 0.1
20	247.0 ± 75.2	3.7 ± 1.1	2.0 ± 0.8
25	308.7 ± 66.4	7.7 ± 2.3	4.3 ± 1.9
40	371.6 ±101.2	10.8 ± 2.6	13.8 ± 3.0

less than a day, but found that uptake rates and turnover times were fastest in the summer.

Phytoplankton Growth Rates

Phytoplankton–specific growth rates, based on the total daily nitrogen uptake rate, averaged 1.02 doublings d^{-1} (± 0.11 SE, n = 78) across all sampling periods and depths. Nitrate and regenerated nitrogen sources, (NH_4^+

plus urea), contributed equally to the overall growth of the phytoplankton. The growth rate based on NO_3^- utilization was 0.53 $\pm$ 0.06 doublings d^{-1}, while for NH_4^+ and urea assimilation it was 0.41 $\pm$ 0.06 and 0.12 $\pm$ 0.01 doublings d^{-1}, respectively.

The highest growth rates in the upper water column (above 20 m) ranged from 1.0 to 2.9 doublings d^{-1} (Fig. 3.10), and these rates occurred during upwelling blooms and relaxation periods. Lower growth rates characterized the entire water column in the winter. Extremely high growth rates (5.2 and 6.4 doublings d^{-1}) were estimated on day 191 at 40 m and on day 219 at 25 m. On both occasions the uptake of NO_3^- and NH_4^+ contributed almost equally to the growth. Extrapolating Eppley's (1972) relationship between growth rate and temperature, we estimate a maximum growth rate of 1.4 doublings d^{-1} at the in situ temperature. It is likely that heterotrophic, and not autotrophic, utilization of NO_3^- and NH_4^+ was responsible for our measured growth rates of $>$ 2 doublings d^{-1}. In their analysis of phytoplankton growth rate data, Kokkinakis and Wheeler (1989) also suggest there are times when significant heterotrophic utilization of nitrogen occurs in upwelling regimes.

During the upwelling seasons phytoplankton grew at a rate of about a doubling per day, whether the ambient NO_3^- concentration was high ($\geq$5 μM) or low ($<$5 μM) (Table 3.5). Previous results from this site showed that phytoplankton uptake rates are saturated when NO_3^- concentrations are $\geq$5 μM (see Chapter 2). The percentage that NO_3^-, NH_4^+ and urea

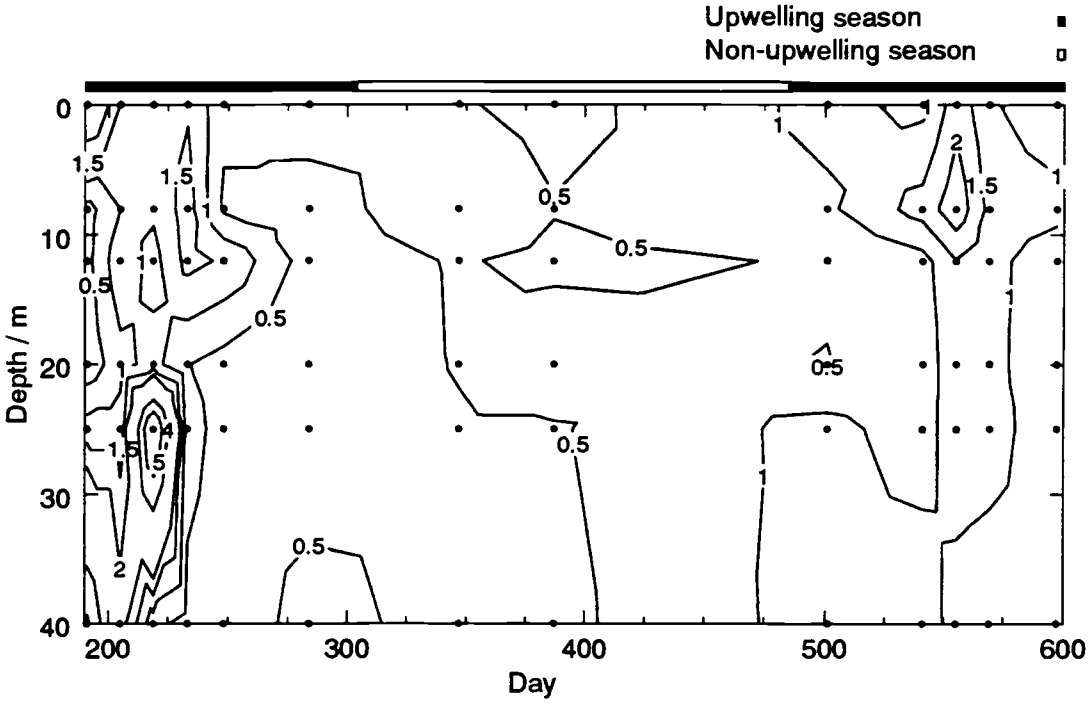

Figure 3.10. Contour plot of phytoplankton nitrogen–supported growth rates between days 191 and 597.

contributed to the overall nitrogen–supported growth rate was essentially the same, regardless of the nutrient concentration. Under low ambient NO_3^- concentrations, NO_3^-–supported growth accounted for 54% of the total nitrogen–supported growth rate compared to 56% when the NO_3^- concentration was $\geq$5 μM. Similarly, for NH_4^+ these values were 39% versus 41% and for urea, 15% compared to 13%. In the winter, nitrogen–supported growth rates in the upper 12 m were about half that calculated for the upwelling season, 0.55 $\pm$ 0.10 (SE, n=6). Of this nitrogen–supported growth, 65% was due to the utilization of NH_4^+ and urea.

Table 3.5. A comparison of nitrate–, ammonium–, urea– and nitrogen–supported phytoplankton–specific growth rates from 0 to 12 meters at high and low ambient nitrate concentrations during the upwelling season. Mean $\pm$ SE.

μ (doublings d^{-1})	$[NO_3^-]$ (μM)			
	< 5	n	≥ 5	n
NO_3^-–supported	0.51 $\pm$ 0.10	10	0.67 $\pm$ 0.09	23
NH_4^+–supported	0.37 $\pm$ 0.09	10	0.49 $\pm$ 0.10	23
urea–supported	0.14 $\pm$ 0.05	5	0.16 $\pm$ 0.03	13
N–supported	0.95 $\pm$ 0.17	10	1.19 $\pm$ 0.13	23

Nitrogen–supported (1.4–4.8 doublings d^{-1}), NO_3^-–supported (1.0–2.0 doublings d^{-1}) and NH_4^+–supported (0.3–3.0 doublings d^{-1}) growth rates reported by Kokkinakis and Wheeler (1987) for a variety of stations on the Oregon/Washington shelf are similar to those estimated during this study. We compared our data to the phytoplankton growth rates measured at 8 m by Neuer (1992) in a series of dilution experiments undertaken at the same site. Average growth rates (n=8) obtained with the dilution method (0.75 d^{-1}) were identical to those estimated using ^{15}N uptake rate and PN concentration data (0.76 d^{-1}=1.09 doublings d^{-1} x 0.693).

Community Composition and Nitrogen Utilization

Examination of the contour plot of the relative preference index (RPI; McCarthy et al. 1977) for NO_3^- (Fig. 3.11a) showed that during both upwelling and non–upwelling seasons, phytoplankton had a strong preference for NH_4^+, relative to its ambient concentration. Nitrate was only used in proportion to its concentration on one occasion. That occurred towards the end of a bloom on day 597 when the surface water had an RPI_{NO_3} of 1.67, the ambient NO_3^- concentration was low, and the f–ratio was 0.31. Dortch and Postel (1989) noted, and were also unable to explain, a similar

situation of a RPI_{NO_3} ~1 coinciding with high NH_4^+ and urea uptake rates. Generally RPI_{NO_3} values reached a minimum between 12 and 25 m and then increased again at 40 m. There was no relationship between the ambient NO_3^- concentration and the RPI_{NO_3} for 0 and 8 m data (Fig. 3.12a). The preference for NO_3^- was a function of the composition of the phytoplankton assemblage (Fig. 3.12b). When the phytoplankton community was composed primarily of small cells (during the onset of upwelling and during the winter, for example), RPI_{NO_3} values were lowest and hence the rejection of NO_3^- relative to its availability was the greatest. As the proportion of diatoms $\leq$20 μm increased, so did the relative preference index. The highest RPI_{NO_3} values were obtained when diatoms made up ~80% of the phytoplankton assemblage. Similar results were obtained for the f–ratio (data not shown). There was no relationship between the f–ratio and the NO_3^- concentration. The f–ratio increased as the percentage of diatoms in the phytoplankton assemblage increased. These latter results agree with Malone's (1980) contention that netplankton depend mainly on NO_3^- while smaller cells rely on reduced nitrogen sources, such as NH_4^+.

A strong preference for NH_4^+ ($RPI_{NH_4} >> 1$) and urea ($RPI_{urea} >> 1$) was always observed at this site (Fig. 3.11b and c). The largest RPI_{NH_4} values were associated with the lowest phytoplankton biomass; e.g., during the winter, and during the onset of upwelling around day 555, when small cells dominated the phytoplankton assemblages (Figs. 3.2 and 3.11b).

Figure 3.11. Contour plots of the relative preference index (RPI) for (a) nitrate, (b) ammonium, and (c) urea.

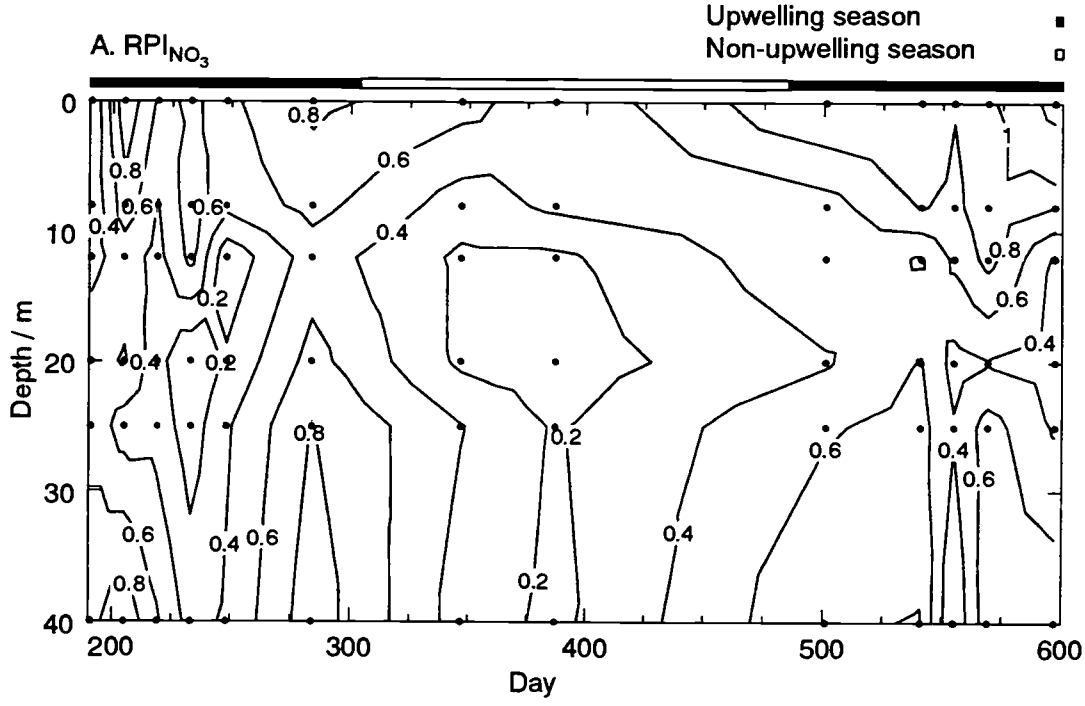
A. RPI$_{NO_3}$
Upwelling season
Non-upwelling season
Depth / m
Day
0
10
20
30
40
200
300
400
500
600
0.8
0.6
0.4
0.2
1

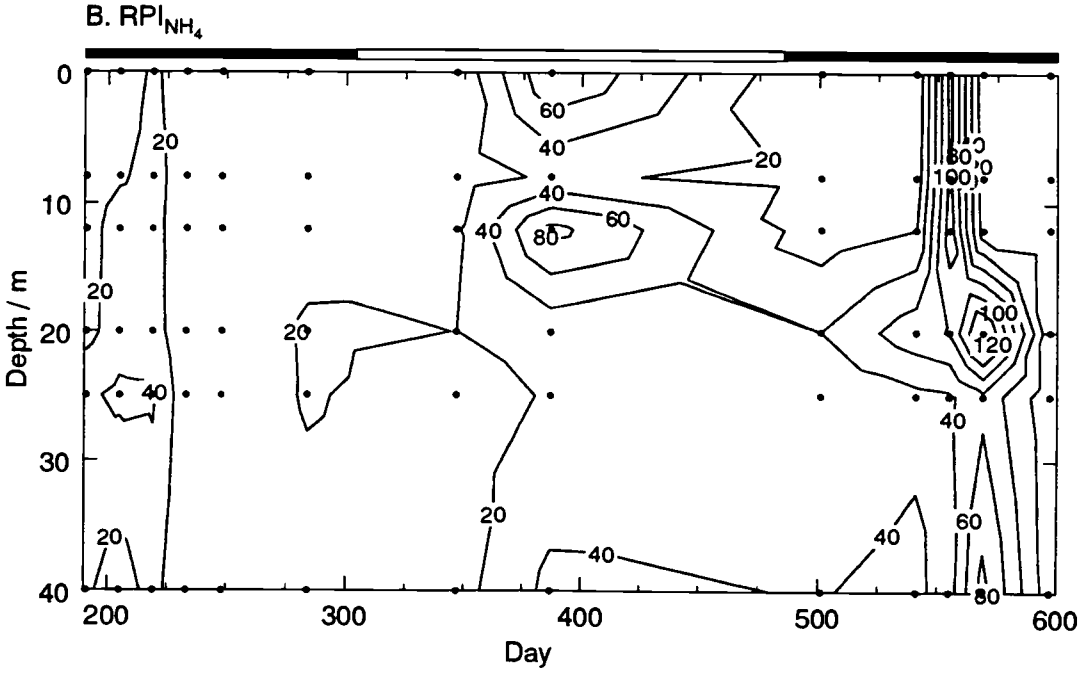
B. RPI$_{NH_4}$
Depth / m
Day
0
10
20
30
40
200
300
400
500
600
20
40
60
80
100
120

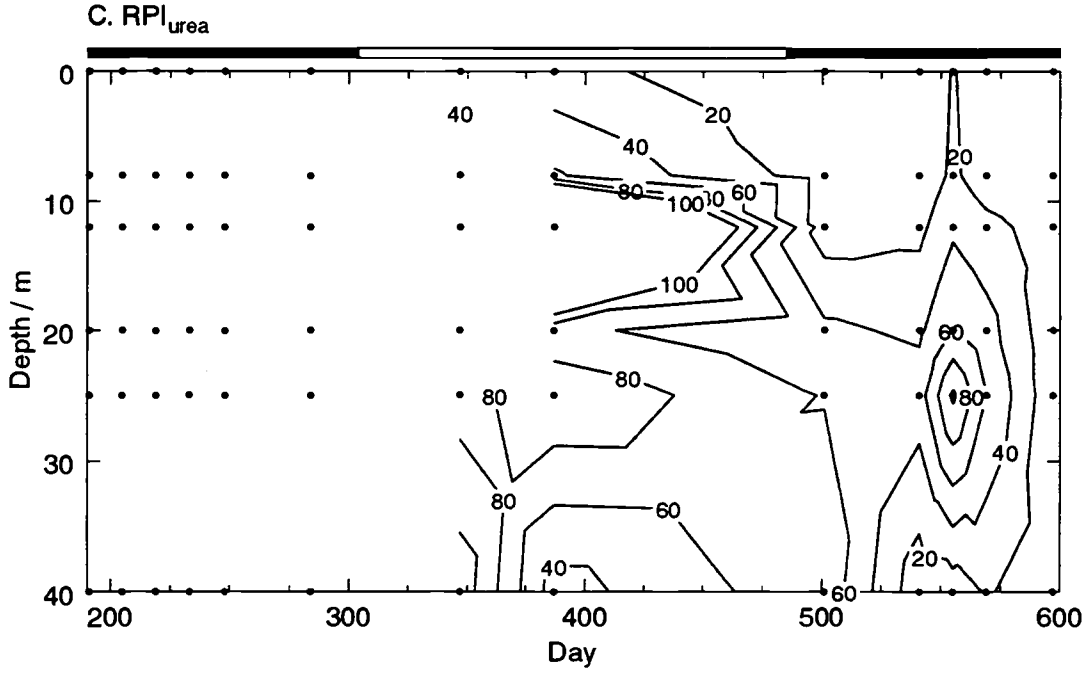
C. RPI urea
Depth / m
Day
0
10
20
30
40
200
300
400
500
600
40
20
40
80
100
10
60
100
60
80
80
180
40
80
60
40
20
60

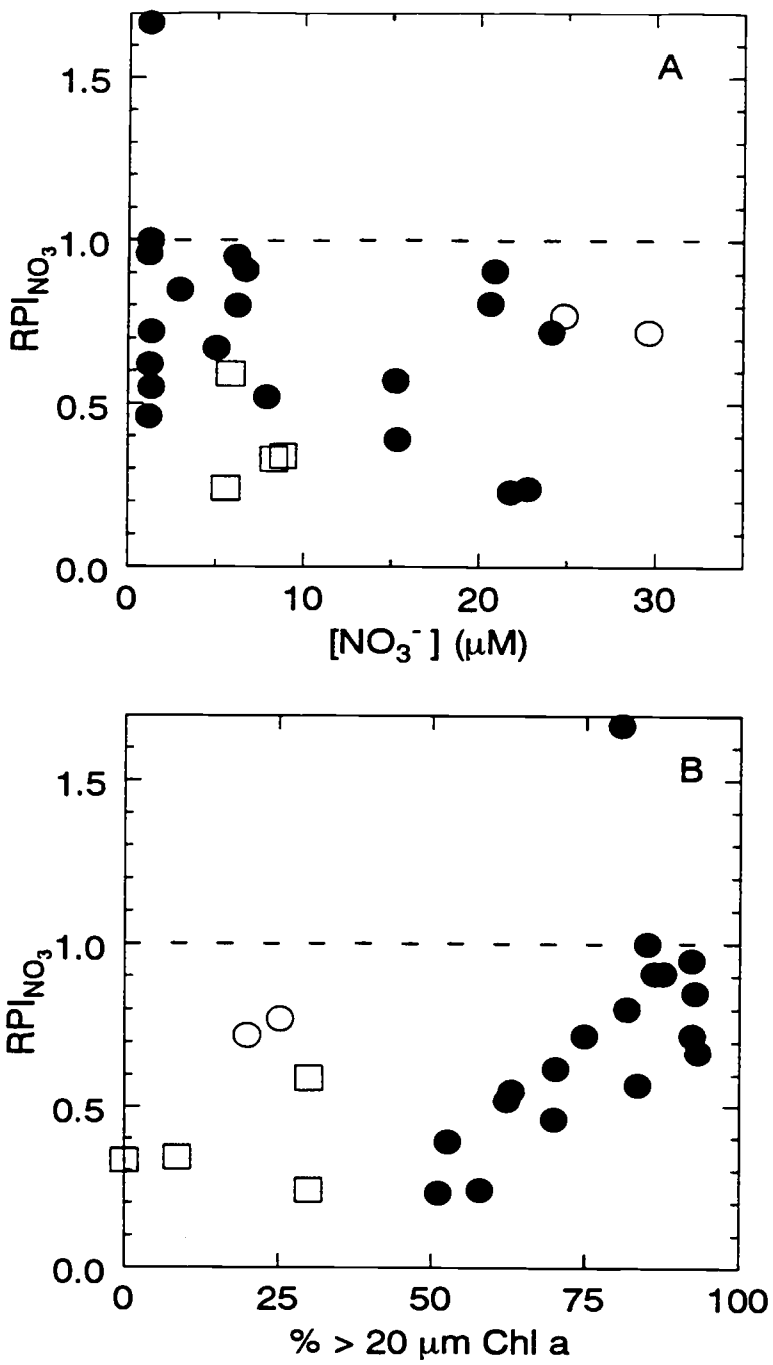

Figure 3.12. Relationship in 0 and 8 meter water between the relative preference of phytoplankton for nitrate (RPI_{NO_3}) with (a) the ambient nitrate concentration, and (b) the percentage of Chl *a* in the $\geq$20 μm fraction. Open circles represent data for the active upwelling event on day 555, while the open boxes are for winter data.

Similar results were obtained for urea (Fig. 3.11c). The highest RPI_{urea} values were found during the winter at mid–depth and during upwelling on day 555 at 25 m, just below where high RPI_{NH_4} values were located.

Most studies to date have also concluded that phytoplankton prefer NH_4^+ to NO_3^- and urea (Harrison et al. 1985, Cochlan 1986, Dortch and Postel 1989). The relationship between size class and nitrogen preference is not a clear one. Unlike this study, Probyn (1985) could not find any evidence for a relationship between phytoplankton size and the RPI's of NO_3^-, NH_4^+, or urea. Similarly, Kokkinakis and Wheeler (1988) found that both net– and nanoplankton prefer NH_4^+ over urea in high and low NO_3^- waters off Oregon.

Not all of our data support the generally accepted model of phytoplankton succession in an upwelling system. Large phytoplankters usually make up most of the phytoplankton community following the onset of upwelling, and then are replaced by smaller cells after the bloom (Margalef 1967), when NH_4^+ becomes abundant (Malone 1980). Although diatoms were the dominant members of the phytoplankton community after upwelling events at our site (Fig. 3.2), smaller cells never made up a significant fraction of the Chl *a* during upwelling relaxation or at the end of blooms (days 233–248, 501–541, 597). Small cells only dominated the upper water column during the winter and in the most recently upwelled water (day 555). At those times they made up between 70 and 100% of the Chl *a*. This suggests that the abundance of small phytoplankton cells may be controlled by the grazing of

microzooplankton. At our site, rates of herbivory by microzooplankton were highest during upwelling blooms/relaxation periods and lowest during the winter and when active upwelling was taking place (Neuer 1992). Whether higher grazing rates distinguish the Oregon upwelling front from other coastal upwelling systems, cannot be addressed since no other micrograzing studies are available for comparison. It has been suggested that macrozooplankton grazing pressure may be more intense close to the coast and decrease seaward (Peterson et al. 1979), allowing the succession of smaller cells further offshore. Our findings suggest that different–sized zooplankton might play an important role in structuring phytoplankton communities, and ultimately may affect the the utilization of nitrogen by autotrophs (Walsh 1976).

The ratio of regenerated primary production to total primary production, which can be written as [1−(f–ratio)], can be used to estimate the amount of production recycled by heterotrophs in an ecosystem (Eppley 1981). Further analysis of the data presented in Figure 3.6 showed that during upwelling blooms (days 205, 219, 284, 569, and 597) heterotrophs, on average, removed about 34% of the primary production. Conversely, at the end of blooms/relaxation events (day 233, 248, 501, and 541) about 60% of the water column production was recycled via heterotrophs. Multiplying the daily integrated nitrogen production rates by the corresponding [1−(f–ratio)] values translated into mean removal rates of approximately 537±304 and 543±467 mg N m^{-2} d^{-1} for the upwelling blooms and non–upwelling

season/relaxation events, respectively. Even though the proportion of production that was recycled differed during various phases of the upwelling cycle and seasonally, the actual amount of organic matter remineralized was not different. Our values are comparable to estimates off the Washington coast by Perry et al. (1989) based on changes in Chl *a* concentrations determined from satellite imagery and shipboard observations. They estimated that for a 2 day period about 50–100 mg C m^{-3} d^{-1} was removed from coastal waters. Converting our values to carbon we estimate a mean removal rate of 89 mg C m^{-3} d^{-1} in the Oregon upwelling zone.

By looking at the ratio of the daily NH_4^+ and NO_3^- uptake rates, the number of times an atom of nitrogen will be recycled before sinking out the euphotic zone as particulate matter can be estimated (Eppley 1981). In nutrient–rich ecosystems nitrogen is recycled on the order of one to three times before leaving the euphotic zone (Cochlan 1986). Conversely, in oligotrophic waters each nitrogen atom may be recycled approximately 20 times before leaving the euphotic zone (Eppley 1981). Analysis of the data collected during this study suggested that the number of recycling times in the upper 8 m was usually ≤ 1 (Fig. 13.13), regardless of the season. In other upwelling ecosystems similar results have been found (Probyn 1985, Kokkinakis and Wheeler 1988). However, during the upwelling season, the number of times recycling occurs increases as the upwelled water ages. The highest number of recycling events in this study occurred below 8 m

(Table 3.6) and coincided with the demise of upwelling blooms (Fig. 13.13). Recycling events also increased below 8 m in winter. The number of recycling events below 8 m were similar to those reported for aged upwelled waters in other regions (6 to 18 times; Probyn 1990) and at times were similar to values reported for oceanic waters (6 to 80 times; Probyn 1985).

Table 3.6. Mean (± SE) number of times an atom of nitrogen was recycled in the water column before settling out as particulate matter. The recycling parameter was calculated as $(\rho_{NH_4}/\rho_{NO_3})$ using daily uptake rate data. For each depth n=13.

Depth (m)	$(\rho_{NH_4}/\rho_{NO_3})$
0	0.79 ± 0.27
8	0.96 ± 0.29
12	2.77 ± 1.23
20	5.97 ± 3.77
25	2.00 ± 0.88
40	0.93 ± 0.30

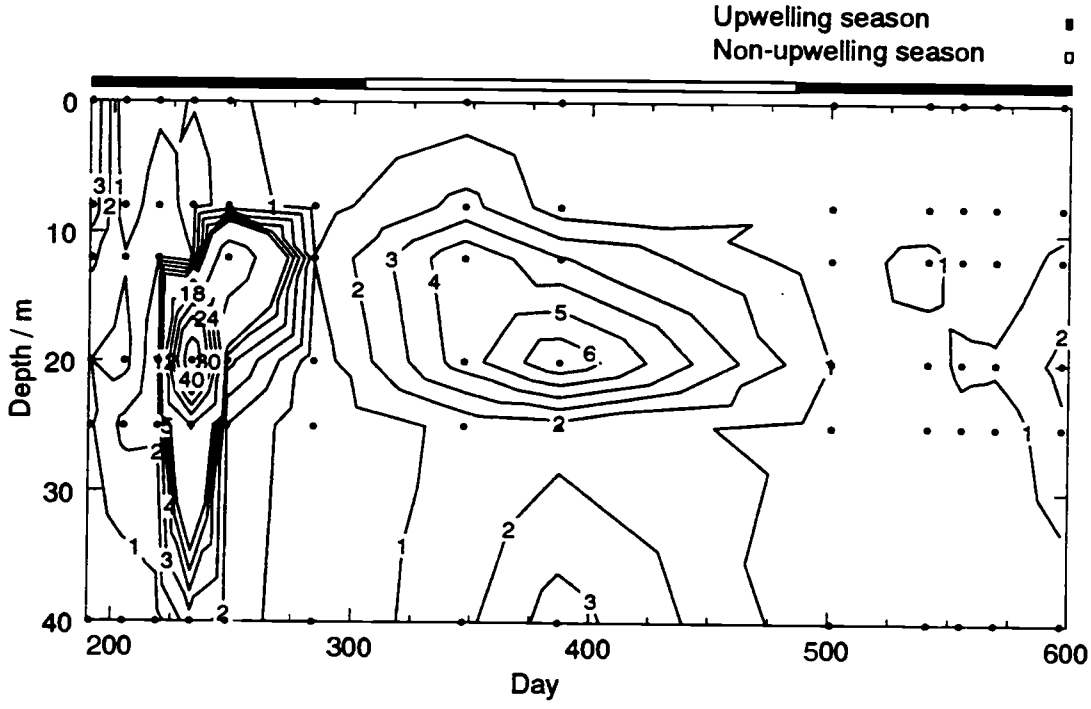

Figure 3.13. Contour plot of the estimated number of times nitrogen was recycled in the water column before sinking out of the euphotic zone as particulate matter.

Conclusions

The results of this study have shown that in the nearshore Oregon upwelling region regenerated sources of nitrogen, i.e. NH_4^+ and urea, were as important to the nitrogenous nutrition and growth of the phytoplankton as NO_3^-. Estimates of annual new and regenerated production were similar; 137 versus 119 g N m^{-2} y^{-1}. Of the three nitrogen sources, NO_3^- accounted for 55% of the primary production, compared to 35% contributed by NH_4^+ and 10% by urea. Very high levels of new primary production (f–ratio ~0.8) followed the upwelling of NO_3^-–rich waters from depth, and were restricted to the upper 8 m of the water column. The highest amounts of regenerated production were measured at 12 m during and after upwelling blooms ([1–(f–ratio)] ~0.8). Plumes of water characterized by extremely high NH_4^+ concentrations (2 to 4 μM) occurred below 8 m after major upwelling–induced phytoplankton blooms. Usually the core of the NH_4^+ plumes was centered at 20 m. High concentrations of NH_4^+ occurred on one occasion (day 191) in the upper water column, as this plume appeared to result from the transport of NH_4^+–laden water from depth via upwelling. Other parameters indicated that most of the recycling of particulate matter took place between 12 and 25 m after phytoplankton blooms and during the winter. The rate of occurrence of these blooms and the amount of recycling in the water column, along with the local circulation patterns, will ultimately determine

the amount of organic matter retained on the continental shelf or transported to deeper waters over the slope.

CHAPTER 4

AMMONIUM UPTAKE AND REGENERATION RATES

Abstract

Time course measurements of ammonium assimilation and regeneration rates off Oregon were made during two upwelling seasons and one winter. The production of ammonium was significant and if not taken into account would have resulted in uptake rates being underestimated by two to five–fold. Uptake and regeneration rates remained essentially constant for 10 to 18 h. However, for long incubations, 55% of the uptake data and 60% of the regeneration data violated key assumptions of the method and could not be used. Mass balance calculations indicated that approximately 36% of the added $^{15}NH_4$ that was removed from the dissolved pool was not recovered in the particulate fraction. Uptake and regeneration rates were fastest in the upper 12 m of the water column and decreased with depth. Ammonium uptake rates were either greater than or equal to regeneration rates at 0, 12 and 20 m, while at 8 and 25 m net regeneration occurred. Regeneration by the microbial community supplied all the ammonium utilized by the phytoplankton and accounted for 27% of all the assimilated nitrogen. Mean daily regeneration rates were not different between upwelling seasons (18–20 mmol N m^{-2} d^{-1}), but were slightly faster than the mean ammonium uptake rate (11–17 mmol N m^{-2} d^{-1}). The regeneration rate during the winter was three times greater than the uptake rate, 11 versus 3 mmol N m^{-2} d^{-1}, but these rates were not statistically different.

Introduction

Early investigations of upwelling systems concentrated on the utilization of nitrate by phytoplankton, even though there was evidence of high levels of grazing activity (Menzel 1967). Recognizing that phytoplankton assimilated different nitrogen sources, Dugdale and Goering (1967) proposed the concept of "new" and "regenerated" primary production. They defined new production as primary production dependent on nitrogen sources introduced from outside the euphotic zone and made available to the phytoplankton via the advection or diffusion of water from depth or from atmospheric and terrestrial inputs. Regenerated production is based on the assimilation of ammonium and/or urea produced within the water column as a result of grazing by micro– and macrozooplankton or the remineralization of organic matter by bacteria. Eppley and Peterson (1979) refined the idea of new and regenerated primary production by defining the f–ratio (i.e. the ratio of new to total primary production). They were able to show that regenerated nitrogen sources were an important component of autotrophic production in oceanic, *as well as*, coastal ecosystems.

Since regenerated production can be a significant fraction of the total primary production, the key to supporting this production is the recycling of nutrients. This is especially important when one considers that ambient ammonium and urea concentrations usually only contribute a few percent to the dissolved nitrogen pool. Thus, in order for reduced nitrogen to be available to the phytoplankton, it is implicit that it is turned over rapidly. Ammonium and urea turnover times are typically less than a day, and often times have been measured to be on the order of hours (Paasche and

Kristiansen 1982, Harrison et al. 1983 and 1985, Glibert 1982, Kokkinakis and Wheeler 1988).

Early efforts to quantify ammonium regeneration rates often stressed the importance of larger organisms in nutrient recycling due to methodological limitations (Harris 1959), even though the role of smaller organisms was the subject of speculation (Johannes 1964). With the development of isotope dilution methods (Harrison 1978, Caperon et al. 1979) and our new concept of marine trophodynamics (i.e. the microbial loop; Azam et al. 1983) the importance of the microbial community as a source of nutrients was realized. It is now generally accepted that most ammonium regeneration is carried out by organisms less than 100 μm in size (Harrison 1980, 1992). Size–fractionation studies by Glibert (1982) and later by Probyn (1987) clearly demonstrated that by far most (i.e. >95%) ammonium is produced by the <15 μm size class. Although bacteria and nanoflagellates dominate that particular size class, it is not yet clear whether bacteria are mainly producers (Harrison et al. 1983) or consumers (Wheeler and Kirchman 1986) of ammonium, or what conditions favor one role over the other (Goldman et al. 1987).

Coastal upwelling systems are much more productive as a result of nutrient recycling than they would be if only new production were to take place (Barber and Smith 1981). Approximately 50% of the primary production in these ecosystems is derived from ammonium and/or urea (Eppley and Peterson 1979). Whitledge (1981) found that regenerated production accounted for 28 to 58% of the total primary production in a variety of upwelling regions. Off Oregon ammonium and urea utilization contribute about 45% to the overall productivity of the ecosystem; in terms of

carbon, regenerated production is substantial, amounting to approximately 630 g C m^{-2} y^{-1} (see Chapter 3). Ammonium regeneration in these environments is fast, compared to offshore waters (Harrison 1978), due to high concentrations of biomass and high levels of primary production. However, uncovering the abiotic and biotic factors that regulate regenerative processes and the appropriate time scales over which they operate have proven fairly elusive.

The site chosen for this study was situated on the Newport hydrographic line in the Oregon upwelling zone. The local hydrography and upwelling circulation of this area has been extensively studied (e.g. Huyer 1976, Halpern 1976) and, to a lesser extent, the biological response to upwelling events (e.g. Wroblewski 1977, Peterson et al. 1979, Small and Menzies 1981). The results presented in this paper represent one aspect of a larger study undertaken to quantify the nitrogen dynamics of this ecosystem. Since very little information is available regarding seasonal regeneration rates, the objective of this study was to measure ammonium uptake and regeneration rates over a broad range of biological, chemical and physical conditions in order to assess their contribution to phytoplankton nutrition.

Materials and Methods

Sampling

A site 8 km off the Oregon coast (44° 40'N, 124° 40'W) was sampled from July 21, 1990 until August 20, 1991 (day 205 to 597) encompassing 12 experiments. The water depth at this location was 70 m. During the upwelling season (May through October) sampling was carried out every two weeks. Winter sampling was conducted on a monthly basis when weather permitted. Water was collected between 0800 and 0900 h from 3 depths (0, 8 m and either 12, 20, or 25 m) with 5 liter Niskin bottles. It was immediately placed in acid–washed polypropylene carboys and transported to shore in containers filled with surface seawater to keep the samples close to ambient temperatures. All experimental work was carried out at the Hatfield Marine Science Center, Oregon State University, Newport, Oregon. Once on shore, the water was mixed by gently inverting the carboys a number of times before samples were drawn.

Biomass and Nutrient Concentrations

Initial and final seawater samples were taken from the uptake experiments and stored frozen until analyzed for $[NO_2^- + NO_3^-]$ and $[NO_2^-]$ using a Technicon II AutoAnalyzer (Whitledge et al. 1986). Samples were not filtered prior to storage and analysis. Ammonium concentrations were measured manually in triplicate using the phenolhypochlorite method

(Solórzano 1969). Concentrations were measured initially for each depth and then at each time point in triplicate.

Particulate organic nitrogen (PN) concentrations were determined by filtering 500–1000 ml of seawater onto a combusted 25 mm Whatman GF/F filter, freezing the filter and then drying it at 60°C for 24 h. A persulfate digestion converted the particulate organic nitrogen to NO_3^-, which was then measured with a Technicon II AutoAnalyzer (Grasshoff et al. 1983).

Ammonium Uptake and Regeneration Experiments

The water used in the uptake and regeneration experiments was not screened to remove large grazers. A 0.1 μM (final concentration) addition, or at times one that was ~10% of the ambient concentration, of $(^{15}NH_4)_2SO_4$ (99.0 atom%, MSD Isotopes) was added to water from each depth in 5 liter Nalgene polycarbonate bottles. Once spiked with label, the bottles were placed in an environmental chamber simulating ambient seawater temperatures (~8–10°C) and saturating light conditions (~500 $\mu E\ m^{-2}\ s^{-1}$). Bottles from the lower 2 depths were placed in bags made of neutral density screening to simulate ambient light levels. Uptake and regeneration time course experiments were run simultaneously on water from three depths (0 and 8 m for all 12 experiments from day 205 to 597, 12 m from day 205 to 233 for 3 experiments, 20 m on day 248, and 25 m from day 284 to 597 for 8 experiments) and consisted of four time points (0.1, 1–3, 4–8, and 10–18 h). At the end of the incubations samples were filtered under low vacuum pressure (<180 mm of Hg) onto combusted 47 mm Whatman GF/F filters. The filters were frozen and then dried at 60°C for 24 h.

The protocol of Selmer and Sörrensen (1986) was used to measure the dilution of $^{15}NH_4^+$ with $^{14}NH_4^+$. A brief description of the solid phase extraction method for aqueous $^{15}NH_4^+$ follows. Approximately 1 liter of filtrate was collected from each of the three depths at each time point. Nine hundred milliliters of filtrate were dispensed into one liter Nalgene polyethylene bottles that had been acid washed and thoroughly rinsed with distilled/deionized water and a portion of the filtrate. Into the filtrate were added 6.3 ml of phenol reagent (10 g phenol dissolved in 100 ml 95% EtOH), 6.3 ml of sodium aquopentacyanoferrate (AqF) reagent (0.03 g AqF dissolved in 250 ml of deionized/distilled water) and 31.5 ml of oxidizing reagent (1.6 ml 5.5% sodium hypochlorite solution in 50 ml of 0.25 M NaOH). An addition of 100 μl of 5.0 atom% $^{15}NH_4^+$ carrier from a 0.5 μg NH_4^+–N/μl solution was added to each bottle of filtrate plus reagents. Samples were placed in the dark for 15 to 25 h to allow complete indophenol formation. In addition, a carrier blank was processed for each depth. Once colour development was complete, samples were acidified to a pH of 6.30 with 1.0 M H_3PO_4 and split into duplicates. The indophenol red (containing the aqueous $^{15}NH_4$) was collected on 6 ml C_{18} extraction columns (J.T. Baker) that were conditioned with rinses of HPLC grade methanol and deionized/distilled water. Impurities were removed from the indophenol red on the sorbent with a 2.5% methanol rinse (the rinse solution had its pH adjusted to 10.0 with a 0.25 M NaOH solution). The indophenol red was removed from the sorbent with 2 ml of HPLC grade acetone and collected in glass vials. The volume of the solution in the vials was reduced to ~200 μl by heating in a vacuum oven set at 55–60°C. At this point the solution was a two phase mixture. After the desired volume was obtained, 200 μl of HPLC grade acetone was added to

remove any dried material from the wall of the vial and to transform the two phase mixture into a homogeneous solution. The red indophenol extract was pipetted onto a precombusted 47 mm Whatman GF/F glass fiber filter and dried in a vacuum oven set at 80°C for at least 12 h. This method of extracting aqueous $^{15}NH_4^+$ has a recovery rate of 75 ± 16% (Wheeler and Kokkinakis 1990).

Dried filters from the uptake experiments and the solid phase extractions were prepared for emission spectrometry following the micro–Dumas dry combustion method of LaRoche (1983) and analyzed for ^{15}N with a Jasco N–150 emission spectrometer (Fielder and Proksch 1975).

Calculations

The equations of Dugdale and Goering (1967) were used to calculate PN–specific (V) and absolute (ρ) hourly uptake rates. Ammonium uptake rates (ρ) were corrected for isotope dilution. Daily ammonium uptake rates were calculated by adding together estimated light and dark uptake rates. Light ammonium uptake rates were calculated by multiplying the mean hourly uptake rate data (obtained from the time course experiments) by that particular day's photoperiod. Dark ammonium uptake rates were assumed to be 52% of the uptake in the light (Price et al. 1985).

Ammonium regeneration rates were calculated using either the equations of Blackburn (1979) and Caperon et al. (1979) or Glibert et al. (1982b). The Blackburn/Caperon method involves calculating the ammonium regeneration rate using the rate of change in the ammonium concentration and the relative abundance of $^{15}NH_4^+$. Conversely, the Glibert et al. equations

use the change in the ^{15}N content of the NH_4^+ to calculate regeneration rates and were used when no change was observed in the ammonium concentration. Mean hourly regeneration rates obtained from the time course experiments were multiplied by 24 h to calculate daily regeneration rates.

Mass balance calculations were done to compare the amount of $^{15}NH_4^+$ removed from the dissolved pool with the amount of ^{15}N measured in the PN fraction (Laws 1984). It was possible to calculate the amount of ^{15}N in the dissolved ammonium pool at each time point by multiplying the measured isotopic enrichment of the ammonium by its concentration. Similarly, the ^{15}N content of the PN fraction was estimated by multiplying the PN concentration by its measured atom% ^{15}N excess. The difference between the amount of labelled ammonium removed from the dissolved pool with that measured in the PN fraction was considered to be "missing ^{15}N". The "missing ^{15}N" was then divided by the initial amount of added label and the percentage of label that could not be accounted for was estimated.

Annual ammonium uptake and regeneration rates were estimated by integrating the daily rates with respect to depth (integration was by the trapezoid rule method) and then averaged for the upwelling season and the winter. Average production and regeneration rates for the upwelling and winter season were multiplied by the number of days in each season (i.e. upwelling season=183 days, winter=182 days) and summed to give an annual rate. The variability associated with the annual ammonium assimilation and regeneration rates were calculated from the standard deviations of the mean upwelling and winter data using the propagation of error method.

Results

Time Course Experiments

Changes observed in the isotopic composition of the PN and the dissolved NH_4^+ pool during a typical time course experiment are shown in Fig. 4.1. These results were fairly representative of those obtained from the other experiments. Over the time course the PN became increasingly labelled with ^{15}N while the specific activity of the ammonium pool decreased (Fig. 4.1). Ammonium concentrations in the incubation bottles usually decreased, often reaching the analytical limit of detection (i.e. 0.03 μM) some 10 to 18 h after the start of an experiment.

The incorporation of ^{15}N into the PN was linear for incubations of 12 h or less, with most of the labelling (i.e. 50 to 65%) occurring during the first 3 h of an experiment (Fig. 4.2a, b). Overall, the maximum amount of label incorporated into the PN was 40% of the initial addition. When incubations lasted 12 to 18 h a decrease in the ^{15}N content of the PN, indicating a loss of label, was observed 32% (11 of 34) of the time.

To evaluate whether ammonium uptake and regeneration rates changed over time, regressions were done for each experiment. Regression slopes represent the change in the uptake or regeneration rate as a function of time. The mean rate of change for 24 uptake experiments was -0.52 nmol liter^{-1} h^{-2}, while for 12 regeneration experiments it was 0.14 nmol liter^{-1} h^{-2} (Fig. 4.3). In general there was no significant change

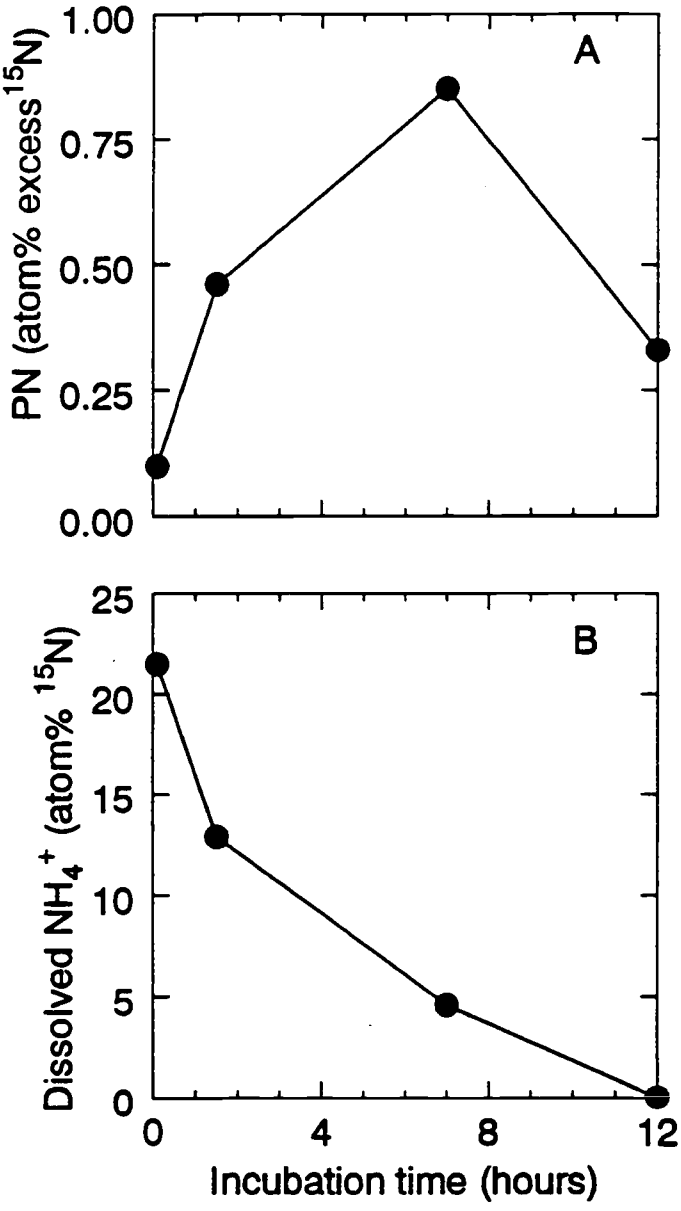

Figure 4.1. Time course experiment showing the isotopic composition of (a) the particulate nitrogen fraction and (b) dissolved ammonium pool throughout the incubation period on day 219 at 12 meters.

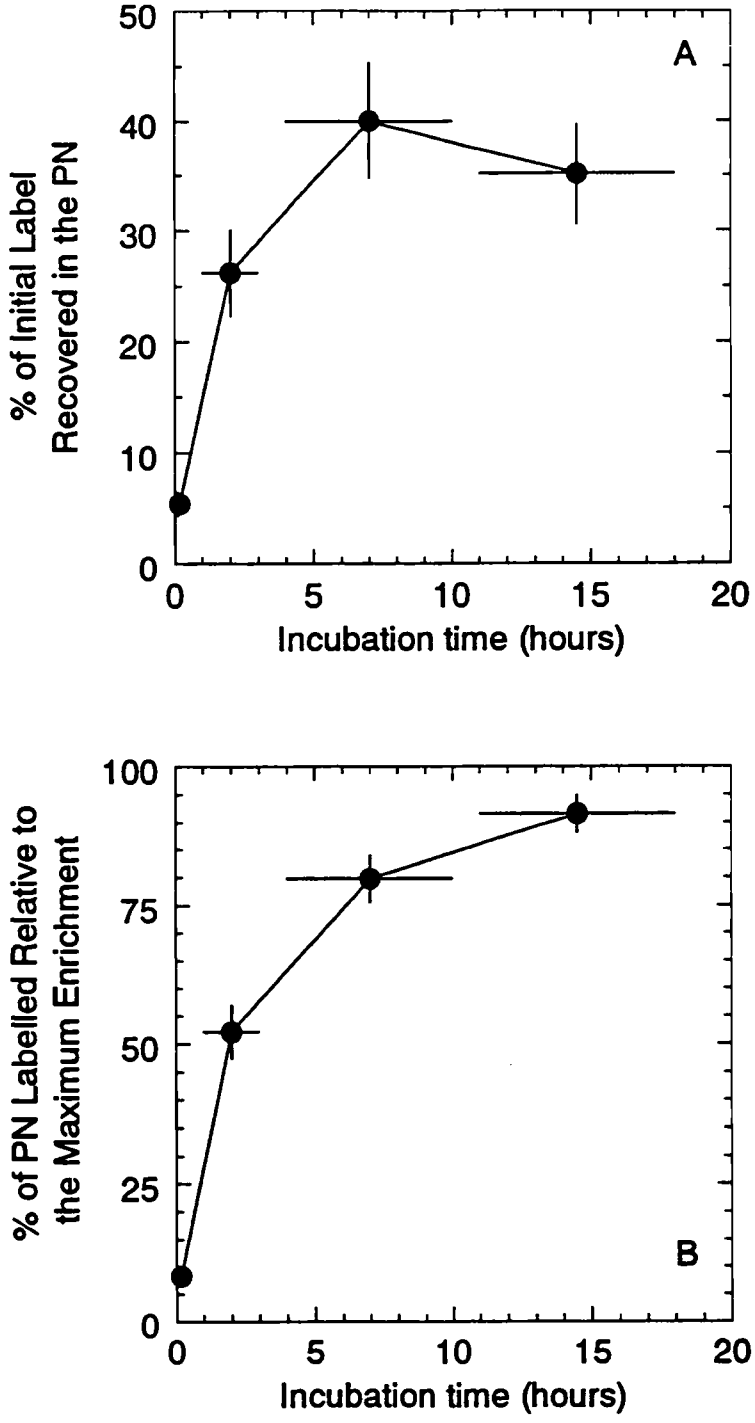

Figure 4.2. The percentage of particulate nitrogen labelled with ^{15}N during the time course experiments. (a) Percentage of initial label recovered in the PN, and (b) percentage of PN labelled relative to the maximum enrichment attained during an experiment. Horizontal lines indicate the range in incubation times, while the vertical lines are the standard error calculated for each average. The sample number at each time point was; $T_0 = 30$, $T_1 = 27$, $T_2 = 32$ and $T_3 = 28$.

in either uptake or regeneration rates with time. The calculated rates of change were small compared to the average uptake and regeneration rates (36 nmol liter^{-1} h^{-1} and 38 nmol liter^{-1} h^{-1}, respectively). It is important to realize though, that as the duration of the time course experiments increased the amount of usable data decreased due to violations of the assumptions inherent in the ^{15}N method (e.g. substrate depletion, loss of label in the PN fraction, etc.). To illustrate this point, the percentage of usable data in the uptake and regeneration rate experiments was plotted as a function of time (Fig. 4.4). In the uptake experiments, 90% of the data from the 1–3 h incubations but only 45% of the data from the 10–18 h incubations met the required assumptions for the ^{15}N method. In the regeneration experiments, the percentage of usable data decreased from 57% to 43% for the 1–3 h and 10–18 h incubations.

Isotope dilution of the dissolved ammonium pool was significant over the duration of the time course experiments. P/ρ values increased as a function of the incubation time, from a minimum of 1 (by definition) at the start of an experiment, a maximum value of 5.5 at the 10 to 18 h time point (Fig. 4.5). Only when incubations were kept very short, between 1 and 3 h, was the potential for underestimation slight (only 15%). P/ρ values reported by Harrison and Harris (1986) for a variety of coastal sites were between 1.5 and 3.2 for 12 to 24 h incubations. Those data agree with our 1 to 8 h values but indicate that ammonium uptake rates would have been more seriously

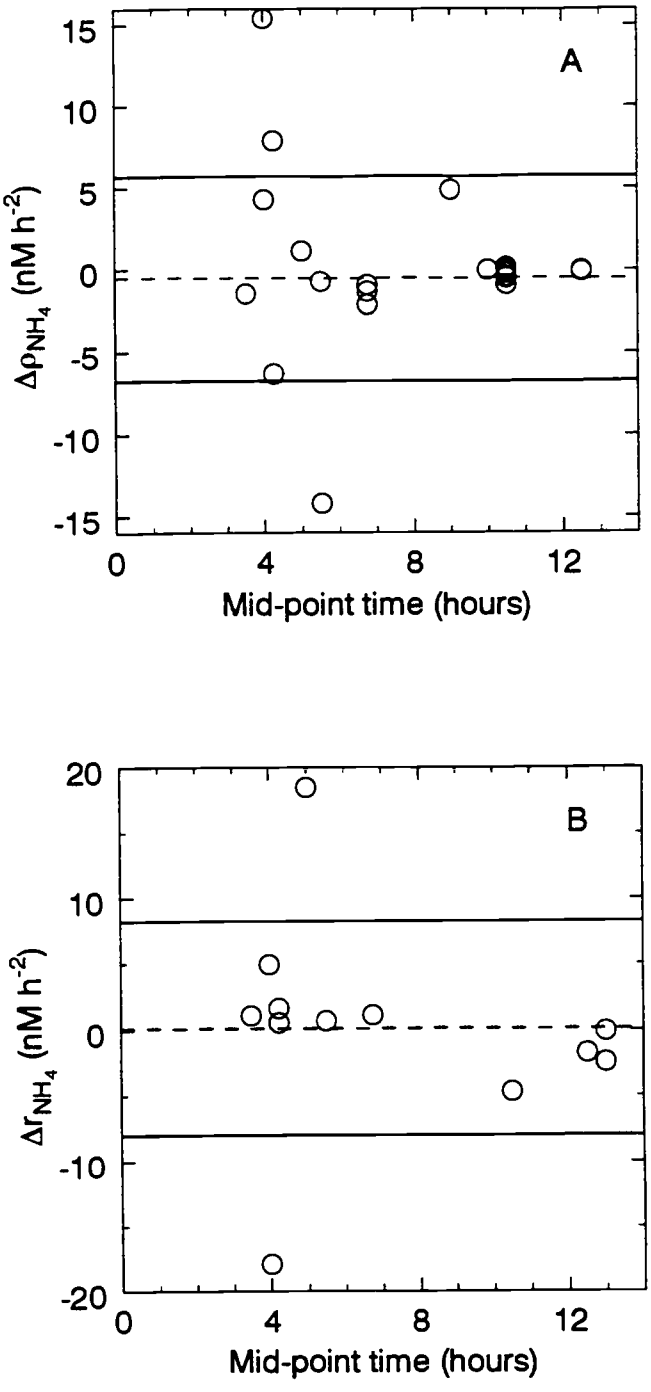

Figure 4.3. Regression slopes from (a) ammonium uptake and (b) regeneration time course experiments plotted against the mid–point incubation time for each experiment. The dashed horizontal lines indicate the mean rate of change, while the solid horizontal lines are $\pm$ 1σ. Mean $\Delta\rho_{NH_4}$=-0.52 $\pm$ 6.21 nmol liter^{-1} h^{-2}, n=24 and mean Δr_{NH_4}=0.14 $\pm$ 8.11 nmol liter^{-1} h^{-2}, n=12.

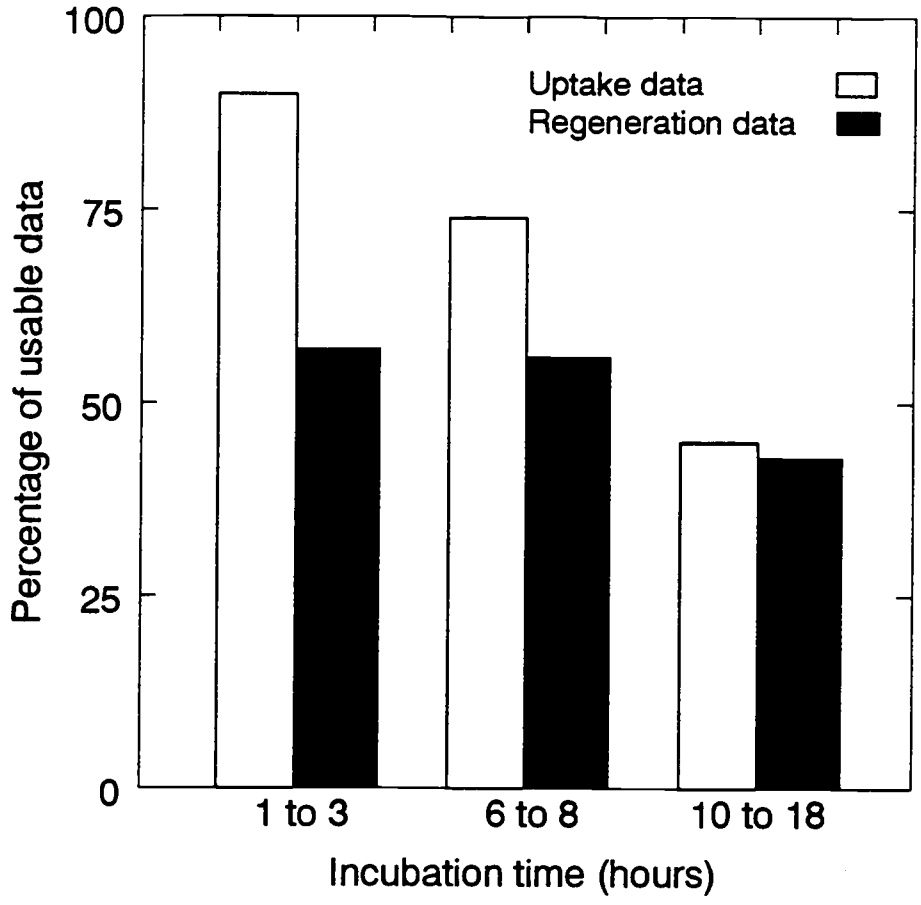

Figure 4.4. The percentage of usable data as a function of incubation time for ammonium uptake and regeneration experiments.

underestimated if ammonium regeneration had not been taken into account for the longer incubation times. We did not carry out any 24 h incubations and can only speculate that over those times isotope dilution becomes even more problematic than previously thought.

Mass balance calculations showed that, overall, 36% of the $^{15}NH_4^+$ removed from the dissolved pool was not recovered in the PN fraction (Table 4.1). The percentage of missing ^{15}N increased slightly with time, from 31% for 1 to 3 h incubations to 43% for 10 to 18 h incubations. Far more dramatic was the variation in missing ^{15}N with depth. The percentages of missing $^{15}NH_4$ at 0, 8 and 12 m were not significantly different from one another ($P>0.5$). Approximately twice as much ^{15}N could not be accounted for in the upper 8 m of the water column than at 25 m, ~47% compared to ~22%. These differences were statistically significant ($P<0.05$). At 20 m virtually all of the added $^{15}NH_4$ was accounted for in either the dissolved or particulate pools. Since only one sample was available, it is impossible to conclude anything for that depth.

Depth–Dependent Ammonium Uptake and Regeneration Rates

The highest daily ammonium uptake and regeneration rates generally occurred in the upper 12 m of the water column, although elevated

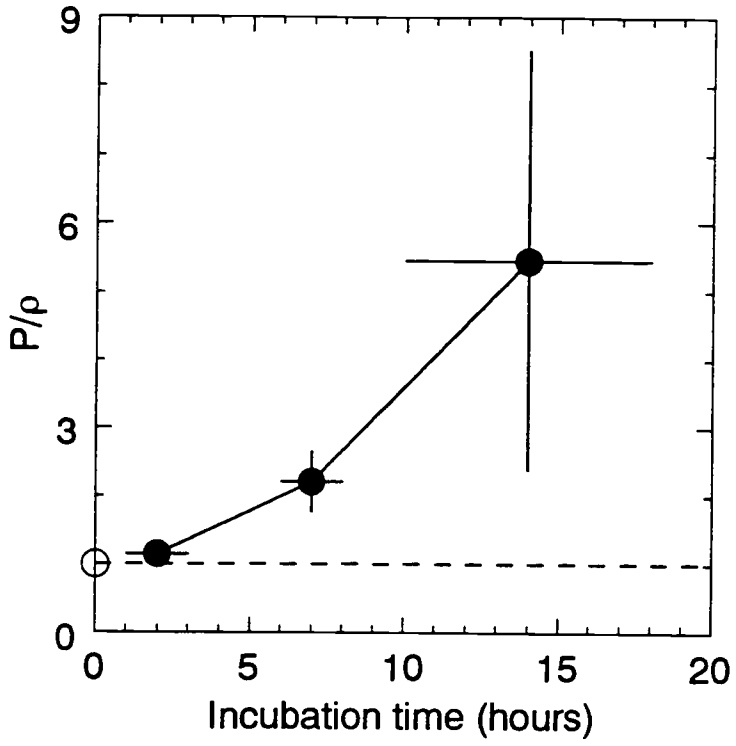

Figure 4.5. Ammonium uptake rates corrected (P) and uncorrected (ρ) for isotope dilution as a function of the incubation time. Horizontal lines indicate the range in incubation times, while the vertical lines are $\pm$ 1 SE. $P/\rho =$ 1 along the dashed line. The open symbol at 0 h has a P/ρ value of 1 by definition. Sample numbers were; $T_1 = 17$, $T_2 = 17$ and $T_3 = 11$.

Table 4.1. The percentage of $^{15}NH_4^+$ not recovered in the uptake and regeneration experiments for all time points at each depth. Mean ± SE.

Depth (m)	% of Missing $^{15}NH_4^+$	n
0	43.8 ± 8.9	9
8	50.8 ± 11.2	8
12	33.9 ± 26.8	2
20	1.8	1
25	21.7 ± 7.1	8
$\bar{X}$ ± SE	35.8 ± 5.5	28

regeneration rates were apparent periodically at 25 m (Fig. 4.6). Between 0 and 12 m, peaks in ammonium uptake rates usually coincided with peaks in regeneration rates, especially during relaxed upwelling conditions, such as on day 219. In contrast, uptake rates at 25 m (day 284 to 597) were always uniformly low, regardless of the upwelling state, and did not correspond to changes observed in the regeneration rate. Relatively low uptake and regeneration rates coincided with the onset of an upwelling event on day 555. Ammonium regeneration rates in the winter were variable, ranging from being extremely low (<0.01 to 0.04 μmol liter^{-1} d^{-1} on day 387) to

being similar to rates measured during the upwelling season (0.8 to 1.4 μmol liter^{-1} d^{-1} on day 347).

A comparison of mean uptake and regeneration rates with depth is given in Table 4.2. The fastest ammonium uptake rates (0.8 to 2.3 μmol liter^{-1} d^{-1}) took place in the upper 12 m of the water column and decreased with depth. The lowest uptake rates ($\sim$0.1 μM d^{-1}) were consistently measured at 25 m. Regeneration rates in the upper 12 m were between 0.9 and 1.1 μmol liter^{-1} d^{-1} and decreased slightly with depth. Depth–dependent differences in uptake and regeneration rates were reflected in r:ρ ratios (i.e. regeneration:uptake) calculated from the daily rate data (Table 4.2). At 0 and 12 m uptake rates were greater than regeneration rates (r:ρ<1), while at 20 m the two rates were essentially equal (r:$\rho\sim$1). Regeneration rates at 25 m were slightly lower than those measured at shallower depths, however the r:ρ value increased dramatically due to extremely low uptake rates. Net ammonium production (r:ρ>1) occurred at 8 and 25 m. In 0 m water r:ρ values were lowest during upwelling events (0.16) and were between 0.9 and 1.0 during phytoplankton blooms and at the end those blooms. Conversely, r:ρ values at 8 m were relatively low during blooms (0.9), highest at the end of blooms (2.6) and intermediate for upwelling events (1.5). At 25 m r:ρ >>1 regardless of the state of the

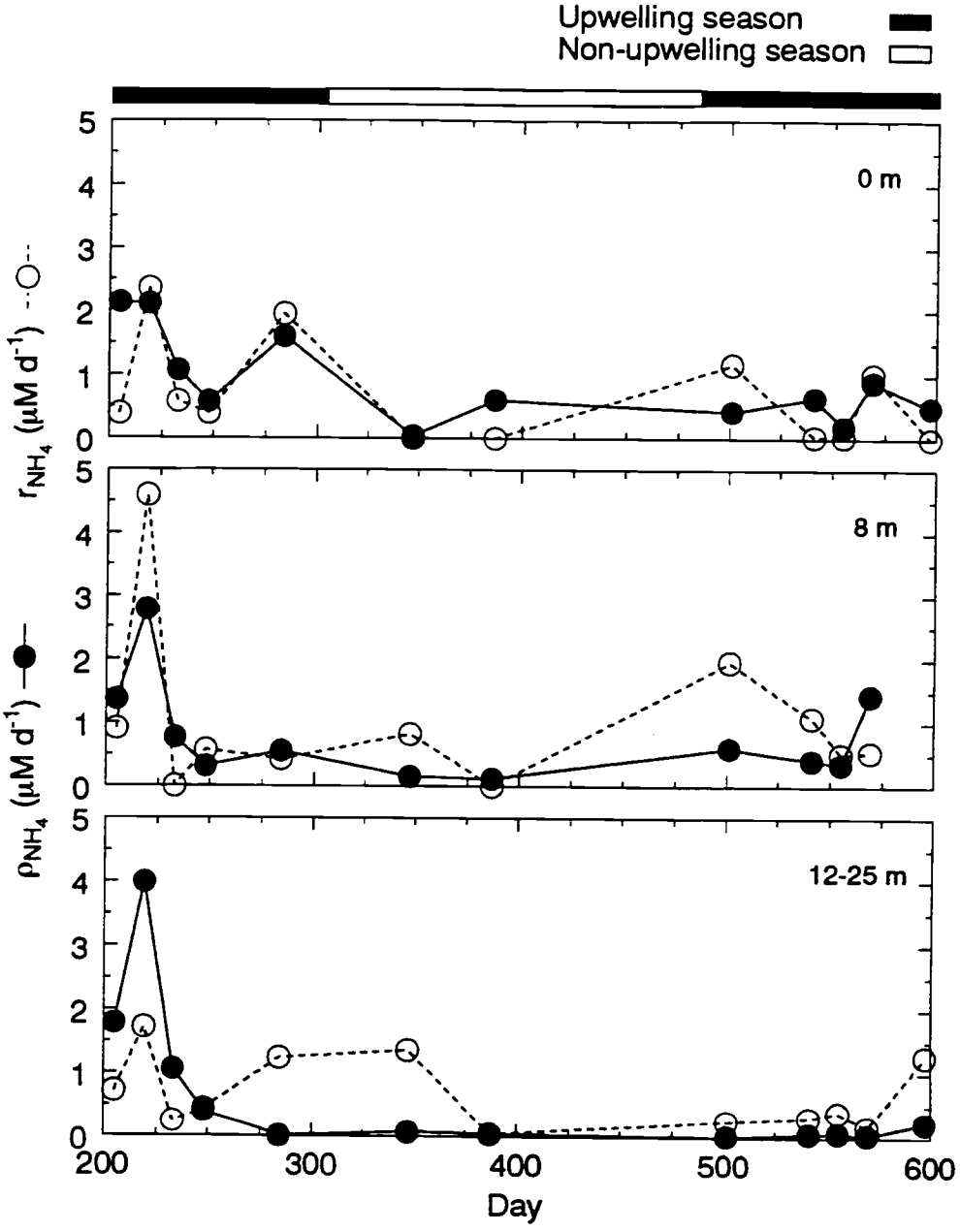

Figure 4.6. Daily ammonium uptake (•) and regeneration (o) rates at 0, 8 and 12 to 25 meters.

Table 4.2. A comparison of daily ammonium uptake (ρ) rates, regeneration (r) rates, and regeneration:uptake (r:ρ) ratios with depth. Sample numbers are in parentheses. Mean ± SE.

Depth (m)	ρ_{NH_4} (μM d^{-1})	r_{NH_4} (μM d^{-1})	r:ρ
0	0.90 ± 0.20 (12)	0.88 ± 0.27 (9)	0.86 ± 0.28 (9)
8	0.80 ± 0.24 (11)	1.14 ± 0.42 (10)	1.82 ± 0.52 (10)
12	2.28 ± 0.88 (8)	0.89 ± 0.43 (3)	0.35 ± 0.06 (3)
20	0.40 (1)	0.43 (1)	1.08 (1)
25	0.06 ± 0.02 (8)	0.62 ± 0.20 (8)	24.00 ± 14.60 (8)

upwelling cycle.

Daily and Seasonal Ammonium Uptake and Regeneration Rates

Ammonium regeneration rates were greater than uptake rates most of the time, both when considering daily (Fig. 4.7a) and depth–integrated rates (Fig. 4.7b). The highest uptake (4.0 μmol liter^{-1} d^{-1}) and regeneration rates (4.6 μmol liter^{-1} d^{-1}) were measured on the same day (day 219) but at different depths (12 and 8 m, respectively). Such high uptake

and regeneration rates, however, were the exception rather than a common occurrence. For the majority of uptake and regeneration data, rates were ≤ 1 μmol liter^{-1} d^{-1} (Fig. 4.8a, b).

A seasonal comparison of uptake and regeneration rates during the two upwelling seasons and winter is given in Table 4.3. Uptake rates during the two upwelling seasons and the winter ranged from 3 to 17 mmol N m^{-2} d^{-1} and were not significantly different ($0.1<P<0.2$) from each other. Regeneration rates (11–20 mmol m^{-2} d^{-1}) were also not different from each other ($0.4<P<0.5$) or from the uptake rates ($0.1<P<0.5$).

Table 4.3. A seasonal comparison of integrated ammonium uptake (ρ_{NH_4}) and regeneration (r_{NH_4}) rates. Mean $\pm$ SE.

Year/Season	ρ_{NH_4} (mmol N m^{-2} d^{-1})	r_{NH_4} (mmol N m^{-2} d^{-1})	n
1990 Upwelling	17.2 $\pm$ 4.5	20.0 $\pm$ 8.9	5
1990/91 Winter	3.4 $\pm$ 0.9	11.1 $\pm$ 10.7	2
1991 Upwelling	10.8 $\pm$ 2.8	17.8 $\pm$ 3.9	5

Overall the average ammonium uptake and regeneration rates were similar, 12.2 versus 17.6 mmol N m^{-2} d^{-1} (Table 4.4). Ammonium regeneration

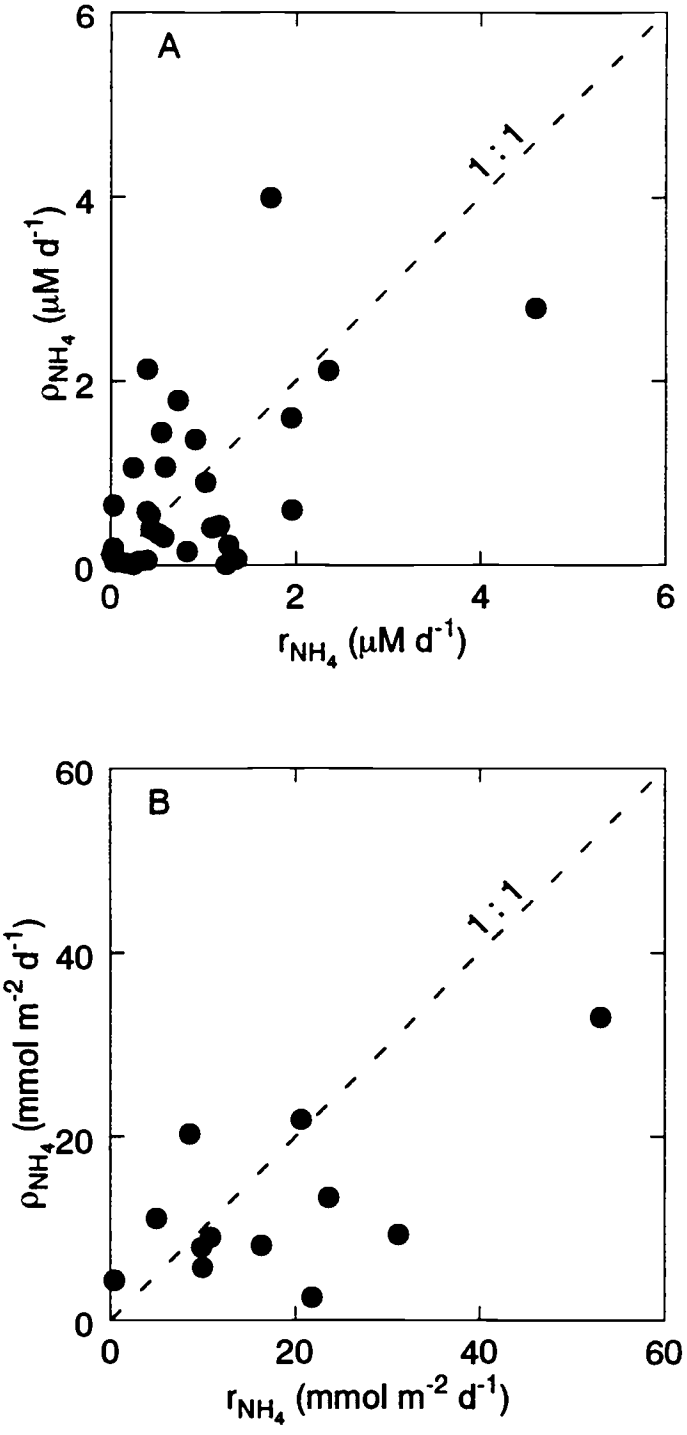

Figure 4.7. Relationships between (a) daily and (b) depth-integrated ammonium uptake and regeneration rates.

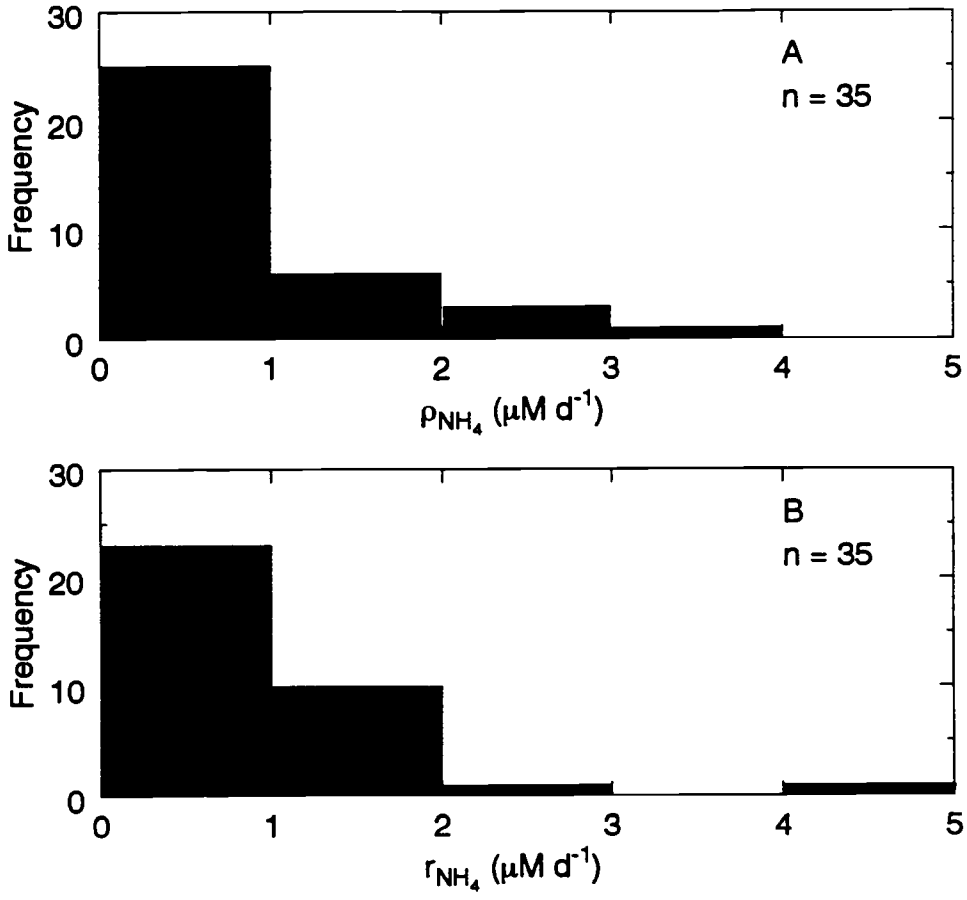

Figure 4.8. Frequency histograms for daily (a) ammonium uptake and (b) regeneration rates.

supplied 144% of the ammonium assimilated by the phytoplankton and accounted for 27.3% of all the nitrogen taken up. Using depth–integrated rates the annual ammonium uptake and regeneration rate were estimated to be 44.6 ± 29.0 g N m^{-2} y^{-1} and 76.7 ± 49.4 g N m^{-2} y^{-1}, respectively. Correcting the uptake rate data by 36% (to account for the missing $^{15}NH_4$) results in an annual rate of 60.7 g N m^{-2} y^{-1}.

Table 4.4. The contribution of ammonium regeneration (r_{NH_4}) to ammonium uptake (ρ_{NH_4}) and total nitrogen utilization ($\rho_{\Sigma N}$)*.

Day	ρ_{NH_4} (mmol N m^{-2} d^{-1})	r_{NH_4} (mmol N m^{-2} d^{-1})	$\rho_{\Sigma N}$ (mmol N m^{-2} d^{-1})
205	20.8	8.5	125.0
219	33.1	53.1	63.7
233	11.1	4.9	24.5
248	10.3	9.8	14.2
284	13.3	23.6	37.2
347	2.5	21.8	4.6
387	4.3	0.4	11.0
501	9.3	31.2	20.7
541	8.1	16.3	54.5
555	5.7	9.9	34.8
569	21.9	20.6	279.0
597	9.0	10.8	103.5
$\bar{X}$ ± SE	12.2 ± 2.5	17.6 ± 4.1	64.4 ± 22.3

* $\rho_{\Sigma N} = \rho_{NH_4} + \rho_{NO_3}$

Discussion

The time–dependent nature of ammonium uptake and regeneration rates has been reported by Glibert et al. (1982b) and Harrison and Harris (1986) for oceanic and coastal waters. In both studies the fastest ammonium uptake and regeneration rates coincided with the shortest incubation times and then decreased over the course of an experiment. Glibert et al. (1982b) suggested, but did not demonstrate, that initially fast rates were a reflection of the community being perturbed due to being placed and confined in an incubation bottle. Harrison and Harris (1986) used the same argument to explain their results and speculated that handling and subsequent confinement of the community probably led to a loss of physiological vigor and increased levels of mortality. In this study the rate data were screened to remove any data that were compromised due to substrate depletion or decreases in the ^{15}N enrichment of the PN. From the analysis of the ammonium uptake and regeneration time course results we found no evidence of time–dependence. Uptake and regeneration rates remained essentially constant for 10 to 18 h. It is important to bear in mind, however, that as the length of the incubations increased the amount of usable data decreased significantly.

Mass balance calculations indicated that more ^{15}N was removed from the dissolved ammonium pool than was measured in the particulate fraction.

Our calculations estimated that approximately 36% of the added ^{15}N was not recovered. This value is close to that of Kokkinakis (1987) for the Oregon/Washington coast (43%) and the 40% calculated by Laws (1984) for data collected in the Chesapeake Bay and Sargasso Sea by Glibert et al. (1982b). Finding no explanation for such a discrepancy in either measurements of ambient $[NH_4^+]$ or isotope ratios, Laws (1984) suggested losses might have arisen due to nitrification, adsorption of ammonium onto clay particles or the walls of the incubation bottles and/or the transformation of labelled ammonium and subsequent release as dissolved organic nitrogen (DON). Assuming that bacteria primarily utilize DON and that bacterial production should be equivalent to DON production, Kokkinakis (1987) was able to show the rate at which ammonium was lost during incubations compared favourably with bacterial production rates measured by Wheeler and Kirchman (1986) (i.e. 92 nmol N liter^{-1} h^{-1} versus 0.2 to 178 nmol N liter^{-1} h^{-1}). More recently, Bronk et al. (1994) have reported that 21 to 35% of the ammonium and nitrate taken up by phytoplankton is released as DON. Their values agree with our estimate that 22 to 51% of the labelled ammonium could not be accounted for at various depths in the water column.

Ammonium uptake (0.01 to 4.0 μM d^{-1}) and regeneration rates ($\sim$0.0 to 4.6 μM d^{-1}) measured during this study were not unlike those reported for a variety of other coastal locations. Studies off Oregon by Kokkinakis

and Wheeler (1988) measured ammonium uptake rates between ~0.0 and 3.0 μM d^{-1}. Regeneration rates on the Scotian Shelf ranged from 0.23 to 0.33 μM d^{-1} (Cochlan 1986), while in Bedford Basin, Nova Scotia they reached 1.6 μM d^{-1} (LaRoche 1983) in the summer. Similar rates have been measured in Oslofjord (~0 to 1.5 μM d^{-1}; Paasche and Kristiansen 1982), the Benguela upwelling system (~0 to 2.4 μM d^{-1}; Probyn 1987) and off the Oregon/Washington coast (~0 to 4.8 μM d^{-1}; Kokkinakis 1987).

The fastest ammonium uptake rates occurred in the upper part of the water column and decreased with depth. At 0, 12 and 20 m uptake rates were either greater than or balanced regeneration rates. Conversely, at 8 and 25 m uptake rates were extremely low and net regeneration occurred. Similar depth–dependent relationships have been reported by Harrison (1978) and Probyn (1987). It is not surprising that the highest ammonium uptake rates took place in the surface layer, as that was where the highest Chl *a* concentrations were located (Neuer 1992, see Chapter 2) and ammonium uptake rates are proportional to the Chl *a* concentration (Probyn 1987). On the other hand, ammonium regeneration rates have been found to increase in response to changes in primary and new production rates (Harrison 1978, LaRoche 1983, Cochlan 1986) particulate nitrogen concentrations (Probyn 1987), and the heterotrophic standing stock (Paasche and Kristiansen 1982). At our site primary and new production rates and PN concentrations were highest in the upper 12 m of the water column and decreased with depth

(see Chapters 2 and 3). However, we could not find a robust relationship between those variables and regeneration rates.

The majority of studies in coastal environments have found that microplankton regeneration supplies all or most of the ammonium consumed by phytoplankton (e.g. Harrison 1978, Harrison et al. 1983, Cochlan 1986, Probyn 1987, Probyn and Lucas 1987). In this study, we also found that ammonium regeneration by the microplankton assemblage could potentially provide all of the ammonium utilized by the phytoplankton and made up 27% of all the nitrogen used. This latter value agrees with estimates made by Herbland et al. (1973) and Smith and Whitledge (1977). They calculated that ammonium excretion supplied approximately 28 and 25%, respectively, of the total phytoplankton nitrogen demand off northwest Africa, whereas Whitledge (1978) estimated it was 20% in the Peruvian system. Even though the dominant grazers that characterize these ecosystems may be taxonomically distinct, their contributions are remarkably similar.

The dominance of various protist taxa and their grazing rates change seasonally at this site; nanoflagellates are numerically abundant during the upwelling season and cilates are more common in the winter (Neuer 1992). Wintertime grazing rates are between 0.00 and 0.16 d^{-1}, compared to 0.18 and 0.50 d^{-1} during the upwelling season. The regeneration data (Table 4.3) indicates that when the entire water column was considered, the rate at which organic nitrogen (i.e. particulate and/or dissolved) was tranformed

into ammonium either by grazing and/or bacterial remineralization was the same, regardless of the season. This suggests the total heterotrophic activity may have been similar for each season and raises questions about the partitioning of activities by the heterotrophic community. For instance, since wintertime microzooplankton grazing rates are only a fraction of those during the upwelling season, are bacteria or some other assemblage more important in producing ammonium at that time of year?

In this study we did not determine whether depth–dependent differences in heterotrophic activity occurred. Evidence from other studies suggests that micrograzers may be responsible for more of the ammonium regenerated in the upper part of the water column than at depth. At the same site, Neuer (1992) estimated that 26 to 50% of primary production in the upper water column is grazed by phagotrophic protists. In the Benguela upwelling system, Probyn (1987) was able to attribute 87% of the ammonium regenerated in the surface water to microplankton excretion (primarily by nanoflagellates), compared to 55% at depth. Deeper in the water column 33% of the ammonium was regenerated by bacteria, versus 11% in the surface water. Similarly, LaRoche (1983) estimated that bacteria only contributed 16% to the ammonium regeneration in the surface water of Bedford Basin. It is possible that a similar scenario occurs in Oregon coastal waters; most of the ammonium regenerated in the highly productive surface layer is a by–product

of the grazing activity of microzooplankton while bacterial decomposition of organic matter releases ammonium at depth.

Macrozooplankton excretion rarely accounts for more than 30% of phytoplankton ammonium requirements (Seki 1974, Bidigare 1983). A mass balance study of the ammonium budget for the Middle Atlantic Bight found that zooplankton were responsible for 30% of ammonium regeneration, compared to 63% by microplankton (Harrison et al. 1983). On average, 74% of the regeneration associated with the microplankton was by organisms less than 1 μm in size. On the Oregon/Washington shelf, macrozooplankton (i.e. copepod) excretion has been reported to contribute <10% to phytoplankton ammonium requirements (Jawed 1973), although the data set was extremely limited. Although our regeneration data indicated that the microbial community alone was able to meet phytoplankton ammonium requirements, there may be times when macrozooplankton excretion is enhanced. The presence of ammonium–laden water having concentrations of 2 to 4 μM was found to coincide with the end of phytoplankton blooms when relaxed upwelling conditions prevailed (see Chapter 3) and depths where the greatest abundance of *Pseudocalanus* sp. occurs (Peterson et al. 1979, see Fig. 1.8b). Results of a numerical model simulation of phytoplankton plume formation off Oregon predicts the occurrence of high ambient ammonium concentrations after bloom events due to the leaching of macrozooplankton fecal pellets (Wroblewski 1977). From the net change in the uptake and

regeneration rate data we estimate that it would have taken between 2 and 32 days to form the ammonium plumes. Thus it seems unlikely that microplankton were the sole source of the ammonium. Alternatively the ammonium might have been derived from the benthos, however the highest ammonium concentrations were usually centered at 20 m while the sediment was at 70 m. Cochlan (1986) estimated that the benthos contributed only 1.4% to the ammonium production of the Scotian Shelf, while Harrison et al. (1983) calculated 7% for the Middle Atlantic Bight. At this point neither the benthos or macrograzers can be ruled out as potentially significant sources of ammonium.

CHAPTER 5

CONCLUSIONS

The objective of this thesis was to measure the assimilation and regeneration rates of various nitrogen sources and to identify some of the environmental factors important in affecting these rates. Prior to this study, very little information was available about the nitrogen dynamics in the waters off Oregon. The major conclusions to come out of this study are summarized below.

The second chapter of this thesis compared PN–specific, absolute and Chl *a*–specific nitrate uptake rates in order to determine if temporal changes observed in the uptake rates were due to the phytoplankton metabollically adapting to the upwelling environment or whether such changes reflected variations in phytoplankton biomass. The major conclusions reached were:

1. Our results indicated that observed temporal changes in PN–specific nitrate uptake rates reflected variations in phytoplankton biomass rather than a physiological adaptation by the phytoplankton to upwelling conditions.

2. Chl *a*–specific nitrate uptake rates were found to be similar for a variety of wind–driven coastal upwelling ecosystems over a broad range of nutrient and biomass concentrations. Chl *a*–specific *nitrogen* uptake rates were similar in coastal upwelling ecosystems and oceanic high nutrient, low chlorophyll waters. The major difference between these two ecosystems was the form of nitrogen used (nitrate versus ammonium) rather than the rate at which they were used.

The third chapter of this thesis examined the seasonal and intra-seasonal patterns in the nitrogen dynamics of this ecosystem under various hydrographic conditions. Of interest was the biological response to episodic physical forcing during the upwelling season. Observations on the physical structure of the water column were combined with measurements of the ambient nutrient and biomass concentrations and nitrogen uptake rates. The major conclusions reached were:

1. Nitrate uptake rates were highest during the spring and summer months after upwelling events injected high concentrations of nitrate into the euphotic zone. The highest new production rates were restricted to the upper 8 m of the water column and decreased with depth due to light-dependent uptake kinetics. High ammonium uptake rates coincided with the upwelling blooms and with the demise of those blooms when upwelling had ceased. The highest uptake rates were usually found at 8 and 12 m. Generally, ambient urea concentrations and uptake rates were the lowest of the three nitrogenous nutrients studied. Urea uptake rates were highest during the demise of an upwelling bloom and exhibited light-dependent uptake kinetics like nitrate.

2. Overall, nitrate uptake contributed 55% to the total nitrogen assimilation in this ecosystem. Ammonium made up 35% and urea the remaining 10% of all the nitrogen used. Annual new production was estimated to be 137 ± 140 g N m^{-2} y^{-1}, compared to regenerated production of 119 g N m^{-2} y^{-1}. Of this regenerated production, ammonium uptake accounted for 92 ± 67 g N m^{-2} y^{-1} while the annual uptake of urea was estimated to be 27 ± 18 g N m^{-2} y^{-1}.

3. From the above values, annual primary production was estimated to be 256.7 ± 164.2 g N m^{-2} y^{-1}. This value converted to carbon (1407 g C m^{-2}

y^{-1}) was similar to an estimate of primary production derived independently from measurements of ^{14}C incorporation; 1938 g C m^{-2} y^{-1}. Previous estimates of primary production in these ecosystems are three to six–fold lower than what we measured.

4. An unexpected, but exciting, finding was the presence of ammonium–laden water with concentrations from 2 to 4 μM at 20 m. These plumes were only found after the demise of an upwelling bloom and may have resulted from the grazing activity of macrozooplankton, such as *Pseudocalanus* sp..

5. Phytoplankton growth rates were estimated to be one to two doublings d^{-1}. Analysis of this data indicated no differences in phytoplankton growth rates when nitrate concentrations were at saturating or limiting levels. High growth rates were maintained by the phytoplankton when nitrate concentrations were low due to the utilization of ammonium and urea. Thus, it is unlikely that phytoplankton growth is ever nitrogen–limited in this ecosystem.

The fourth chapter of this thesis evaluated the time course experiments used to measure ammonium uptake and regeneration rates and the role that ammonium played in the nitrogenous nutrition of the phytoplankton. The major conclusions reached were:

1. Mass balance calculations showed that approximately 36% of the labelled ammonium removed from the dissolved pool was not recovered in the particulate fraction. The percentage of missing ^{15}N was not time–dependent, remaining essentially constant over the course of the incubations. However, it was depth–dependent. Twice as much ^{15}N was missing from the upper 8 m (47%), as at 25 m (22%).

2. Ammonium uptake and regeneration rates were highest in the upper 12 m of the water column and decreased with depth. The net difference between uptake and regeneration rates and regeneration to uptake ratios indicated that ammonium uptake rates were either greater than or balanced regeneration rates at 0, 12 and 20 m while net regeneration occurred at 8 and 25 m.

3. Mean daily ammonium uptake rates were highest during the upwelling seasons (11 to 17 mmol N m^{-2} d^{-1}) and lowest during the winter (3 mmol N m^{-2} d^{-1}). Regeneration rates were always higher than uptake rates and were similar within and between seasons (11 to 20 mmol N m^{-2} d^{-1}). Ammonium regeneration by the microbial community was able to supply all of the ammonium used by the phytoplankton and provided 27% of the nitrogen used in this ecosystem.

We now have a better understanding of the nitrogen dynamics in this particular ecosystem. Not unexpectantly, this work has raised more questions than it has answered. Future studies employing high temporal and spatial resolution of the nutrient, biomass and production fields along and across the shelf are needed to evaluate the degreee of variability in these systems. Also of importance are studies that follow discrete parcels of upwelled water as they are transported across/along the shelf. Such projects would go far in addressing how changes in the planktonic community and nutrients affect rate processes as the upwelled water ages. New research initiatives should also focus on measuring processes during non–upwelling periods, such as during relaxed upwelling conditions and the winter, for which very little data exists.

We know that once an upwelling circulation has been established the biological response evolves quickly. Previously it was assumed that the high nitrate concentrations of the upwelled water fueled high levels of new production. However, another level of complexity, in the form of high concentrations of ammonium in the same upwelled water, has entered into the picture. This not only changes the way in which we thought the interaction between physics and biology worked (i.e. that physical processes were only important in moving nitrate to the surface waters from depth) but also complicates our ability to predict new production. Recent advances (see Sathyendranath et al. 1991) in using satellite–derived data to estimate new production may not be applicable in coastal upwelling systems. The remote sensing method relies on using sea surface temperature to infer nitrate concentrations and ocean color data to estimate Chl *a* concentrations. From the estimated nitrate concentration an *f*–ratio is obtained and from the Chl *a* data the total primary production (P_t) is estimated. New production is then calculated as the product of P_t and the *f*–ratio. The difficulty in applying such a method to the waters off Oregon results from the upwelling of cold, nitrate–rich water to the surface along with extremely high concentrations of ammonium. When this occurs the phytoplankton preferentially use the ammonium first, negating the usual relationship between the *f*–ratio and ambient nitrate concentrations often found in coastal waters (see Harrison et al. 1987). As a result, the *f*–ratio and P_t obtained from remotely sensed data will be significantly overestimated.

As yet we do not know the source of these high ammonium waters or the frequency at which they are upwelled. Very little information is available on macrozooplankton excretion rates or fecal pellet production rates. A

proper evaluation of the role of these zooplankton in nitrogen recycling and the partitioning of regenerative processes by various size classes of the heterotrophic community is long overdue. The presence of the ammonium plumes may also have significant implications for our understanding of the biogeochemical transformations of nitrogen, if for instance they are sites of enhanced nitrification. Future studies in these waters will surely refine our understanding of nitrogen cycling in pelagic ecosystems.

BIBLIOGRAPHY

Atkins, G.L. 1969. Multicompartment Models for Biological Systems. Methuen, London.

Atlas, E.L., L.I. Gordon, and R.D. Tomlinson. 1977. Chemical characteristics of the Pacific northwestern coastal waters: Nutrients, salinities, seasonal fluctuations, p. 57–79. In: The Marine Plant Biomass of the Pacific Northwest Coast, R.W. Krauss (ed.). Oregon State University Press, Corvallis, OR.

Azam, F., T. Fenchel, J.G. Field, J.S. Gray, L.A. Meyer-Reil, and F. Thingstad. 1983. The ecological role of water–column microbes in the sea. Marine Ecology Progress Series 10: 257–263.

Bakun, A., D.R. McLain, and P.V. Mayo. 1974. The mean annual cycle of coastal upwelling off western North America as observed from surface measurements. Fishery Bulletin 72: 843–844.

Banse, K. 1977. Determining the carbon–to–chlorophyll ratio of natural phytoplankton. Marine Biology 41: 199–212.

Barber, R.T., and R.L. Smith. 1981. Coastal upwelling ecosystems, p. 31–68. In: A.R. Longhurst (ed.), Analysis of Marine Ecosystems. Academic Press, New York, NY.

Bidigare, R.R. 1983. Nitrogen excretion by zooplankton, p. 385–409. In: Nitrogen in the Marine Environment, E.J. Carpenter and D.G. Capone (eds.). Academic Press, New York, NY.

Blackburn, T.H. 1979. Method for measuring rates of NH_4 turnover in anoxic marine sediment, using a ^{15}N–NH_4 dilution technique. Applied Environmental Microbiology 37: 760–765.

Booth, B.C., J. Lewin, and C.J. Lorenzen. 1988. Spring and summer growth rates of subarctic Pacific phytoplankton assemblages determined from carbon uptake and cell volumes estimated using epifluorescence microscopy. Marine Biology 98: 287–298.

Bronk, D., B. Ward, and P.M. Glibert. 1994. Dissolved organic nitrogen release and the underestimation of new production. Eos 75: 39.

Caperon, J., D. Schell, J. Hirota, and E. Laws. 1979. Ammonium excretion rates in Kaneohe Bay, Hawaii, measured by a ^{15}N-isotope dilution technique. Marine Biology 54: 33–40.

Chan, A.T. 1980. Comparative physiological study of marine diatoms and dinoflagellates in relation to irradiance and cell size. II. Relationship between photosynthesis, growth, and carbon/chlorophyll *a* ratio. Journal of Phycology 16: 428–432.

Chavez, F.P., K.R. Buck, K.H. Coale, J.H. Martin, G.R. DiTullio, N.A. Welschmeyer, A.C. Jacobson, and R.T. Barber. 1991. Growth rates, grazing, sinking, and iron limitation of equatorial Pacific phytoplankton. Limnology and Oceanography 36: 1816–1833.

Cochlan, W.P. 1986. Seasonal study of uptake and regeneration of nitrogen on the Scotian Shelf. Continental Shelf Research 5: 555–577.

Cochlan, W.P., P.J. Harrison, and K.L. Denman. 1991. Diel periodicity of nitrogen uptake by marine phytoplankton in nitrate–rich environments. Limnology and Oceanography 36: 1689–1700.

Codispoti, L.A., and G.E. Friederich. 1978. Local and mesoscale influences on nutrient variability in the northwest African upwelling region near Cabo Corbeiro. Deep–Sea Research 25: 751–770.

Cullen, J.J. 1982. The deep chlorophyll maximum: Comparing vertical profiles of chlorophyll *a*. Canadian Journal of Fisheries and Aquatic Sciences 39: 791–803.

Cullen, J.J., and M.R. Lewis. 1988. The kinetics of algal photoadaptation in the context of vertical mixing. Journal of Plankton Research 10: 1039–1063.

Cullen, J.J., M.R. Lewis, C.O. Davis, and R.T. Barber. 1992. Photosynthetic characteristics and estimated growth rates indicate that grazing is the proximate control of primary production in the equatorial Pacific. Journal of Geophysical Research 97: 639–654.

Curl, H., Jr., and L.F. Small. 1965. Variations in photosynthetic assimilation ratios in natural, marine phytoplankton communities. Limnology and Oceanography 10: 67–73.

Darley, M. 1980. The chemical composition of diatoms, p. 198–223. In: The Biology of Diatoms, J.A. Hellebust and J.C. Lewin (eds.). University of California.

Dickson, M.–L., and P.A. Wheeler. 1993. Chlorophyll *a* concentrations in the North Pacific: Does a latitudinal gradient exist? Limnology and Oceanography 38: 1813–1818.

Dortch, Q. 1990. The interaction between ammonium and nitrate uptake in phytoplankton. Marine Ecology Progress Series 61: 183–201.

Dortch, Q., and T.T. Packard. 1989. Differences in biomass structure between oligotrophic and eutrophic marine ecosystems. Deep–Sea Research 36: 223–240.

Dortch, Q., and J.R. Postel. 1989. Phytoplankton–nitrogen interactions, p. 139–173. In: Coastal Oceanography of Washington and Oregon,

M.R. Landry and B.M. Hickey, (eds.). Elsevier Science Publishers, Amsterdam.

Dugdale, R.C. 1967. Nutrient limitation in the sea: Dynamics, identification and significance. Limnology and Oceanography 12: 685–695.

Dugdale, R.C., and J.J. Goering. 1967. Uptake of new and regenerated forms of nitrogen in primary productivity. Limnology and Oceanography 12: 196–206.

Dugdale, R.C., and F.P. Wilkerson. 1986. The use of ^{15}N to measure nitrogen uptake in eutrophic oceans; Experimental considerations. Limnology and Oceanography 31: 673–689.

Dugdale, R.C., and F.P. Wilkerson. 1991. Low specific nitrate uptake rate: A common feature of high–nutrient, low–chlorophyll marine ecosystems. Limnology and Oceanography 36: 1678–1688.

Eppley, R.W. 1972. Temperature and phytoplankton growth in the sea. Fishery Bulletin 70: 1063–1085.

Eppley, R.W. 1981. Autotrophic production of particulate matter, p. 343–361. In: Analysis of Marine Ecosystems, A.R. Longhurst, (ed.). Academic Press, New York, NY.

Eppley, R.W., W.G. Harrison, S.W. Chisholm, and E. Stewart. 1977. Particulate organic matter in surface waters off southern California and its relationship to phytoplankton. Journal of Marine Research 35: 671–696.

Eppley, R.W., and B.J. Peterson. 1979. Particulate organic matter flux and planktonic new production in the deep ocean. Nature 282: 677–680.

Eppley, R.W., J.N. Rogers, and J.J. McCarthy. 1969. Half–saturation constants for uptake of nitrate and ammonium by marine phytoplankton. Limnology and Oceanography 14: 912–920.

Fielder, R., and G. Proksch. 1975. The determination of nitrogen–15 by emission and mass spectrometry in biochemical analysis: A review. Analytica Chimica Acta 78: 1–62.

Garside, C. 1991. Shift–up and the nitrate kinetics of phytoplankton in upwelling ecosystems. Limnology and Oceanography 36: 1239–1244.

Glibert, P. 1982. Regional studies of daily, seasonal and size fraction variability in ammonium remineralization. Marine Biology 70: 209–222.

Glibert, P.M., D.C. Biggs, and J.J. McCarthy. 1982a. Utilization of ammonium and nitrate during austral summer in the Scotia Sea. Deep–Sea Research 29: 837–850.

Glibert, P.M., and D.G. Capone. 1993. Mineralization and assimilation in aquatic, sediment, and wetland systems, p. 243–272. In: Nitrogen Isotope Techniques, R. Knowles and T.H. Blackburn, (eds.). Academic Press, New York, NY.

Glibert, P.M., and J.C. Goldman. 1981. Rapid ammonium uptake by marine phytoplankton. Marine Biology Letters 2: 25–31.

Glibert, P., F. Lipschultz, J.J. McCarthy, and M.A. Altabet. 1982b. Isotope dilution models of uptake and remineralization of ammonium by marine plankton. Limnology and Oceanography 27: 639–650.

Goldman, J.C., D.A. Caron, O.K. Andersen, and M.R. Dennett. 1985. Nutrient cycling in a microflagellate food chain: I. Nitrogen dynamics. Marine Ecology Progress Series 24: 231–242.

Goldman, J.C., D.A. Caron, and M.R. Dennett. 1987. Regulation of gross growth efficiency and ammonium regeneration in bacteria by substrate C:N ratio. Limnology and Oceanography 32: 1239–1252.

Grasshoff, K., M. Ehrhardt, and K. Kremling. 1983. Methods of Seawater Analysis. Verlag Chemie, Weinheim.

Halpern, D. 1976. Structure of an upwelling event observed off Oregon during July 1973. Deep–Sea Research 23: 495–508.

Harris, E. 1959. The nitrogen cycle in Long Island Sound. Bulletin of the Bingham Oceanographic Collection 17: 31–65.

Harrison, W.G. 1978. Experimental measurements of nitrogen remineralization in coastal waters. Limnology and Oceanography 23: 684–694.

Harrison, W.G. 1980. Nutrient regeneration and primary production in the sea, p. 433–460. In: Primary Productivity in the Sea, P.G. Falkowski, (ed.). Plenum Press, New York, NY.

Harrison, W.G. 1983. Use of isotopes, p. 763–807. In: Nitrogen in the Marine Environment, D. Capone and E. Carpenter, (eds.). Academic Press, New York, NY.

Harrison, W.G. 1990. Nitrogen utilization in chlorophyll and primary productivity maximum layers: An analysis based on the f–ratio. Marine Ecology Progress Series 60: 85–90.

Harrison, W.G. 1992. Regeneration of nutrients, p. 385–407. In: Primary Productivity and Biogeochemical Cycles in the Sea, P.G. Falkowski and A.D. Woodhead, (eds.). Plenum Press, New York, NY.

Harrison, W.G., D. Douglas, P. Falkowski, G. Rowe, and J. Vidal. 1983. Summer nutrient dynamics of the Middle Atlantic Bight: Nitrogen uptake and regeneration. Journal of Plankton Research 5: 539–555.

Harrison, W.G., and L.R. Harris. 1986. Isotope–dilution and its effect on measurements of nitrogen and phosphorus uptake by oceanic microplankton. Marine Ecology Progress Series 27: 253–261.

Harrison, W.G., E.J.H. Head, R.J. Conover, A.R. Longhurst, and D.D. Sameoto. 1985. The distribution and metabolism of urea in the eastern Canadian Arctic. Deep–Sea Research 32: 23–42.

Harrison, W.G., and T. Platt. 1980. Variation in assimilation number of coastal marine phytoplankton: Effects of environmental co–variates. Journal of Plankton Research 2: 249–260.

Harrison, W.G., T. Platt, R. Calienes, and N. Ochoa. 1981. Photosynthetic parameters and primary production of phytoplankton populations off the northern coast of Peru, p. 303–311. In: Coastal Upwelling, F.A. Richards, (ed.). American Geophysical Union, Washington, D.C.

Harrison, W.G., T. Platt, and M.R. Lewis. 1987. f–ratio and its relationship to ambient nitrate concentration in coastal waters. Journal of Plankton Research 9: 235–248.

Hayward, T.L., and E.L. Venrick. 1982. Relation between surface chlorophyll, integrated chlorophyll and integrated primary production. Marine Biology 69: 247–252.

Herbland, A., R. LeBorgne, and B. Voituriez. 1973. Production primaire, secondaire et régénération des sels nutrifiifs dans l'upwelling de Mauritanie. Documents scientifiques centre de recherches océanographiques de Côte d'Ivoire 4: 1–75.

Hermann, A.J., B.M. Hickey, M.R. Landry, and D.F. Winter. 1989. Coastal upwelling dynamics, p. 211–253. In: Coastal Oceanography of Washington and Oregon, M.R. Landry and B.M. Hickey, (eds.). Elsevier Science Publishers, Amsterdam.

Holligan, P.M., R.P. Harris, R.C. Newell, D.S. Harbour, R.N. Head, E.A.S. Linley, M.I. Lucas, P.R.G. Tranter, and C.M. Weekley. 1984. Vertical distribution and partitioning of organic carbon in mixed, frontal and stratified waters of the English Channel. Marine Ecology Progress Series 14: 111–127.

Huyer, A. 1976. A comparison of upwelling events in two locations; Oregon and northwest Africa. Journal of Marine Research 34: 531–546.

Huyer, A. 1977. Seasonal variations in temperature, salinity, and density over the continental shelf off Oregon. Limnology and Oceanography 22: 442–453.

Jawed, M. 1973. Ammonia excretion by zooplankton and its significance to primary production during summer. Marine Biology 23: 115–120.

Johannes, R.E. 1964. Phosphorus excretion and body size in marine animals: Microzooplankton and nutrient regeneration. Science 146: 923–924.

Kirchman, D.L., R.G. Keil, and P.A. Wheeler. 1990. Carbon limitation of ammonium uptake by heterotrophic bacteria in the subarctic Pacific. Limnology and Oceanography 35: 1258–1266.

Kokkinakis, S.A. 1987. Utilization of inorganic and organic nitrogen by phytoplankton off the Washington and Oregon coasts. M.S. thesis, Oregon State University, Corvallis, OR. 103 pp.

Kokkinakis, S.A., and P.A. Wheeler. 1987. Nitrogen uptake and phytoplankton growth in coastal upwelling regions. Limnology and Oceanography 32: 1112–1123.

Kokkinakis, S.A., and P.A. Wheeler. 1988. Uptake of ammonium and urea in the northeast Pacific: Comparison between netplankton and nanoplankton. Marine Ecology Progress Series 43: 113–124.

Kristiansen, S. 1983. Urea as a nitrogen source for phytoplankton in Oslofjord. Marine Biology 74: 17–24.

Landry, M.R., and B.M. Hickey. 1989. Coastal Oceanography of Washington and Oregon. Elsevier Oceanography Series, 47. Elsevier, Amsterdam.

LaRoche, J. 1983. Ammonium regeneration: Its contribution to phytoplankton nitrogen requirements in a eutrophic environment. Marine Biology 75: 231–240.

Laws, E. 1984. Isotope dilution models and the mystery of the vanishing ^{15}N. Limnology and Oceanography 29: 379–385.

Laws, E., G.R. DiTullio, and D.G. Redalje. 1987. High phytoplankton growth and production rates in the North Pacific subtropical gyre. Limnology and Oceanography 32: 905–918.

LeBouteiller, A. 1986. Environmental control of nitrate and ammonium uptake by phytoplankton in the equatorial Atlantic Ocean. Marine Ecology Progress Series 30: 167–179.

Lentz, S.J. 1992. The surface boundary layer in coastal upwelling regions. Journal of Physical Oceanography 22: 1517–1539.

MacIsaac, J.J., and R.C. Dugdale. 1969. The kinetics of nitrate and ammonium uptake by natural populations of marine phytoplankton. Deep–Sea Research 16: 415–422.

MacIsaac, J.J., and R.C. Dugdale. 1972. Interactions of light and inorganic nitrogen in controlling nitrogen uptake in the sea. Deep–Sea Research 19: 209–232.

MacIsaac, J.J., R.C. Dugdale, R.T. Barber, D. Blasco, and T.T. Packard. 1985. Primary production cycle in an upwelling center. Deep–Sea Research 32: 503–529.

MacIsaac, J.J., R.C. Dugdale, and G. Slawyk. 1974. Nitrogen uptake in the northwest Africa upwelling area: Results from the Cineca–Charcot II. Tethys 6: 69–75.

Malone, T.C. 1980. Size–fractionated primary production of marine phytoplankton, p. 301–317. In: Primary Productivity in the Sea, P.G. Falkowski, (ed.). Brookhaven Symposium in Biology 31, Plenum Press, New York, NY.

Martin, M., L.D. Talley, and R.A. DeSzoeke. 1987. Physical, chemical and CTD data from the Marathon Expedition, May–June 1984. Oregon State University Data Report 131, Ref. 87–15.

McCarthy, J.J., W.R. Taylor, and J.L. Taft. 1977. Nitrogenous nutrition of the plankton in Chesapeake Bay. 1. Nutrient availability and phytoplankton preferences. Limnology and Oceanography 22: 996–1011.

Menzel, D.W. 1967. Particulate organic carbon in the deep sea. Deep–Sea Research 14: 229–238.

Miller, C.B., B.W. Frost, P.A. Wheeler, M.R. Landry, N. Welschmeyer, and T.M. Powell. 1991. Ecological dynamics in the subarctic Pacific, a possibly iron–limited ecosystem. Limnology and Oceanography 36: 1600–1615.

Mitamura, O., and Y. Saijo. 1980. In situ measurement of the urea decomposition rate and its turnover rate in the Pacific Ocean. Marine Biology 58: 147–152.

Mulvaney, R.L. 1993. Mass spectrometry, p. 11–57. In: Nitrogen Isotope Techniques, R. Knowles and T.H. Blackburn, (eds.). Academic Press, New York, NY.

Murray, J.W., J.N. Downs, S. Strom, C.–L. Wei, and H.W. Jannasch. 1989. Nutrient assimilation, export production and ^{234}Th scavenging in the eastern equatorial Pacific. Deep–Sea Research 36: 1471–1489.

Neshyba, S. 1987. Oceanography: Perspectives on a Fluid Earth. Wiley, New York, NY. 506 pp.

Neuer, S. 1992. Role of protist grazing in the Oregon upwelling system. Ph.D. dissertation, Oregon State University, Corvallis, OR. 172 pp.

Olson, R.J. 1980. Nitrate and ammonium uptake in Antarctic waters. Limnology and Oceanography 25: 1064–1074.

Paasche, E., and S. Kristiansen. 1982. Ammonium regeneration by microzooplankton in the Oslofjord. Marine Biology 69: 55–63.

Peña, M.A., W.G. Harrison, and M.R. Lewis. 1992. New production in the central equatorial Pacific. Marine Ecology Progress Series 80: 265–274.

Perry, M.J., J.P. Bolger, and D.C. English. 1989. Primary production in Washington coastal waters, p. 117–138. In: Coastal Oceanography of Washington and Oregon, M.R. Landry and B.M. Hickey, (eds.). Elsevier Science Publishers, Amsterdam.

Peterson, W.T., C.B. Miller, and A. Hutchinson. 1979. Zonation and maintenance of copepod populations in the Oregon upwelling zone. Deep–Sea Research 26: 467–494.

Press, W.H., B.P. Flannery, S.A. Teukolsky, and W.T. Vetterling. 1989. Numerical recipes, 1st ed. Cambridge University Press. 818 pp.

Preston, C.M. 1993. Optical emission spectrometry, p. 59–88. In: Nitrogen Isotope Techniques, R. Knowles and T.H. Blackburn, (eds.). Academic Press, New York, NY.

Price, N.M., L.F. Andersen, and F.M.M. Morel. 1991. Iron and nitrogen nutrition of equatorial Pacific plankton. Deep–Sea Research 38: 1361–1378.

Price, N.M., W.P. Cochlan, and P.J. Harrison. 1985. Time course of uptake of inorganic and organic nitrogen by phytoplankton in the Strait of Georgia: Comparison of frontal and stratified communities. Marine Ecology Progress Series 22: 39–53.

Price, N.M., and P.J. Harrison. 1987. A comparison of methods for the measurement of dissolved urea concentrations in seawater. Marine Biology 92: 307–319.

Probyn, T.A. 1985. Nitrogen uptake by size–fractionated phytoplankton populations in the southern Benguela upwelling system. Marine Ecology Progress Series 22: 249–258.

Probyn, T.A. 1987. Ammonium regeneration by microplankton in an upwelling environment. Marine Ecology Progress Series 37: 53–64.

Probyn, T.A., and M.I. Lucas. 1987. Ammonium and phosphorus flux through the microplankton community in Agulhas Bank waters. South African Journal of Marine Science 5: 209–221.

Probyn, T.A., H.N. Waldron, and A.G. James. 1990. Size–fractionated measurements of nitrogen uptake in aged upwelled waters: Implications for pelagic food webs. Limnology and Oceanography 35: 202–210.

Remsen, C.C. 1971. The distribution of urea in coastal and oceanic waters. Limnology and Oceanography 16: 732–740.

Riper, D.M., T.G. Owens, and P.G. Falkowski. 1979. Chlorophyll turnover in *Skeletonema costatum*, a marine plankton diatom. Plant Physiology 64: 49–54.

Rönner, U., F. Sörensson, and O. Holm–Hansen. 1983. Nitrogen assimilation by phytoplankton in the Scotia Sea. Polar Biology 2: 137–147.

Ryther, J.H. 1969. Relationship of photosynthesis to fish production in the sea. Science 166: 72–76.

Sathyendranath, S., T. Platt, E.P. Horne, W.G. Harrison, O. Ulloa, R. Outerbridge, and N. Hoepffner. 1991. Estimation of new production in the ocean by compound remote sensing. Nature 353: 129–133.

Seki, H., T. Tsuji, and A. Hattori. 1974. Effect of zooplankton grazing on the formation of the anoxic layer in Tokyo Bay. Estuarine and Coastal Marine Science 2: 145–151.

Selmer, J.–S., and F. Sörensson. 1986. New procedure for extraction of ammonium from natural waters for ^{15}N isotopic ratio determinations. Applied and Environmental Microbiology 52: 577–579.

Sheppard, C.W. 1962. Basic Principles of the Tracer Method. John Wiley and Sons, New York, NY. 282pp.

Small, L.F., and D.W. Menzies. 1981. Patterns of primary productivity and biomass in a coastal upwelling region. Deep–Sea Research 28A: 123–149.

Smith, S.L, and T.E. Whitledge. 1977. The role of zooplankton in the regeneration of nitrogen in a coastal upwelling system off northwest Africa. Deep–Sea Research 24: 49–56.

Solórzano, L. 1969. Determination of ammonia in natural waters by the phenolhypochlorite method. Limnology and Oceanography 14: 799-801.

Steele, J.H. 1974. The Structure of Marine Ecosystems. Harvard University Press, Cambridge, MA. 128 pp.

Strickland, J.D., and T.R. Parsons. 1972. A practical handbook of seawater analysis. Fishiers Research Board of Canada Bulletin 167. 310 pp.

Venrick, E.L. 1987. On fluorometric determinations of filter–retained pigments. Limnology and Oceanography 32: 492–493.

Walsh, J.J. 1976. Herbivory as a factor in patterns of nutrient utilization in the sea. Limnology and Oceanography 21: 1–13.

Wheeler, P.A., P.M. Glibert, and J.J.McCarthy. 1982. Ammonium uptake and incorporation by Chesapeake Bay phytoplankton: Short–term uptake kinetics. Limnology and Oceanography 27: 1113–1128.

Wheeler, P.A., and D.L. Kirchman. 1986. Utilization of inorganic and organic forms of nitrogen by bacteria in marine systems. Limnology and Oceanography 31: 998–1009.

Wheeler, P.A., and S.A. Kokkinakis. 1990. Ammonium recycling limits nitrate use in the oceanic subarctic Pacific. Limnology and Oceanography 35: 1267–1278.

Wheeler, P.A., M.R. Landry, and S.A. Kokkinakis. 1989. Diel periodicity in ammonium uptake and regeneration in the oceanic subarctic Pacific: Implications for interactions in microbial food webs. Limnology and Oceanography 34: 1025–1033.

Whitledge, T.E. 1972. Excretion measurements of nekton and the regeneration of nutrients near Punta San Juan in the Peru upwelling system derived from nekton and zooplankton excretion. Ph.D. dissertation, University of Washington, Seattle, WA. 115 pp.

Whitedge, T.E. 1978. Regeneration of nitrogen by zooplankton and fish in the northwest Africa and Peru upwelling ecosystems, p. 90–100. In: Upwelling Ecosystems, R. Boje and M. Tomczak (eds.). Springer–Verlag, Berlin.

Whitledge, T.E. 1981. Nitrogen recycling and biological populations in upwelling ecosystems, p. 257–273. In: Coastal Upwelling Research, F.A. Richards (ed.). American Geophysical Union, Washington, D.C.

Whitlege, T.E., D.M. Veidt, S.C. Malloy, C.J. Patton, and C.D. Wirick. 1986. Automated nutrient analyses in seawater. Brookhaven National Laboratory Technical Report, BNL 38990. 231 pp.

Wilkerson, F.P., and R.C. Dugdale. 1987. The use of large shipboard barrels and drifters to study the effects of coastal upwelling on phytoplankton nutrient dynamics. Limnology and Oceanography 32: 368–382.

Wilkerson, F.P., and R.C. Dugdale. 1992. Measurements of nitrogen productivity in the equatorial Pacific. Journal of Geophysical Research 97: 669–679.

Wroblewski, J.S. 1977. A model of phytoplankton plume formation during variable Oregon upwelling. Journal of Marine Research 35: 357–394.

Zimmerman, R.C., J.N. Kremer, and R.C. Dugdale. 1987. Acceleration of nutrient uptake by phytoplankton in a coastal upwelling ecosystem: A modeling analysis. Limnology and Oceanography 32: 359–367.

APPENDICES

Appendix A. Pressure, temperature, salinity and density measurements made with an Ocean Sensors 100 CTD.

April, 1990:

Press. (dbar)	Temp. (°C)	Sal. (psu)	σ_t (kg m^{-3})	Press. (dbar)	Temp. (°C)	Sal. (psu)	σ_t (kg m^{-3})
2.523	10.91557	25.73991	19.60201	10.426	9.59771	29.46960	22.74854
3.029	10.88292	25.96255	19.78241	10.835	9.41175	29.67010	22.93556
3.819	10.81860	26.58412	20.27905	11.211	9.29423	29.77108	23.03409
4.090	10.78891	26.81440	20.46395	11.260	9.28467	29.82184	23.07541
4.406	10.72900	26.94118	20.57357	11.264	9.28290	29.82537	23.07846
4.305	10.73585	26.90632	20.54492	11.373	9.23055	29.88706	23.13511
4.386	10.73244	26.87110	20.51848	11.697	9.22364	29.90524	23.15184
4.608	10.72897	26.94228	20.57536	11.936	9.22423	29.96648	23.20068
4.592	10.72902	26.82809	20.48656	12.268	9.17868	30.05252	23.27633
4.155	10.79234	26.74118	20.40682	12.742	9.09053	30.22256	23.42473
4.236	10.76687	26.74195	20.41191	13.191	9.08936	30.27585	23.46861
4.317	10.75246	26.78886	20.45104	13.515	9.08609	30.33248	23.51484
4.576	10.72693	26.82081	20.48116	13.859	9.07788	30.36027	23.53938
4.438	10.73794	26.84822	20.50005	13.815	9.08354	30.38605	23.55847
4.361	10.73230	26.80500	20.46703	14.110	9.07026	30.41934	23.58785
4.458	10.72683	26.87869	20.52561	14.466	9.06634	30.46843	23.62844
4.434	10.72908	26.83466	20.49093	14.713	9.04979	30.55051	23.69624
4.175	10.76883	26.75509	20.42152	15.013	9.02298	30.62877	23.76285
4.232	10.73305	26.79777	20.46071	15.207	9.02125	30.66860	23.79513
4.531	10.73027	26.85067	20.50362	15.608	8.96415	30.74469	23.86510
4.353	10.73109	27.26222	20.82244	15.879	8.95398	30.77107	23.88851
4.341	10.73103	27.28565	20.84060	16.191	8.94499	30.79308	23.90850
4.394	10.73090	27.28484	20.84023	16.483	8.94436	30.83000	23.93881
4.632	10.73037	27.32817	20.87508	16.580	8.94132	30.84414	23.95077
4.879	10.72558	27.41153	20.94176	16.726	8.94446	30.84964	23.95526
5.090	10.71807	27.44032	20.96631	17.098	8.91600	30.89300	23.99517
5.187	10.67173	27.56233	21.06910	17.539	8.91347	30.91976	24.01850
5.685	10.60808	27.68247	21.17507	17.855	8.92104	30.95435	24.04585
5.867	10.56450	27.73416	21.22313	17.997	8.90958	30.97856	24.06717
5.916	10.54883	27.76834	21.25246	18.341	8.89810	31.01338	24.09771
6.292	10.45270	27.94584	21.40770	18.539	8.89444	31.03632	24.11711
6.786	10.30191	28.07260	21.53271	18.956	8.88370	31.07740	24.15277
6.977	10.23505	28.14933	21.60394	19.353	8.88567	31.10252	24.17394
7.236	10.20964	28.12809	21.59262	19.430	8.87746	31.13211	24.19868
7.195	10.21418	28.20608	21.65243	19.438	8.88691	31.12624	24.19269
7.584	10.15667	28.41426	21.82540	19.847	8.87115	31.17881	24.23807
8.126	10.08101	28.59030	21.97694	20.244	8.86675	31.22736	24.27852
8.224	10.07511	28.58793	21.97648	20.588	8.86794	31.27476	24.31700
8.385	10.05227	28.68335	22.05514	20.839	8.86787	31.32450	24.35706
8.839	9.94122	28.86240	22.21422	20.916	8.86799	31.33714	24.36729
9.219	9.87629	28.95301	22.29677	21.462	8.86804	31.39234	24.41296
9.284	9.85247	29.01098	22.34598	21.628	8.86797	31.43386	24.44621
9.471	9.82344	29.12912	22.44347	21.900	8.86731	31.46631	24.47293
9.819	9.75428	29.25712	22.55568	22.183	8.87110	31.50424	24.50332
10.098	9.72011	29.32149	22.61248	22.426	8.93747	31.49138	24.48426

Appendix A. [continued]

April, 1990: [continued]

Press. (dbar)	Temp. (°C)	Sal. (psu)	σ_t (kg m^{-3})	Press. (dbar)	Temp. (°C)	Sal. (psu)	σ_t (kg m^{-3})
22.705	8.95444	31.54258	24.52299	38.357	8.65829	32.82121	25.64045
23.147	8.98624	31.61312	24.57530	38.689	8.65884	32.82069	25.64148
23.426	9.04467	31.59772	24.55554	39.337	8.65766	32.83929	25.65918
23.685	9.06955	31.62963	24.57783	39.673	8.65771	32.85095	25.66984
24.033	9.08097	31.69481	24.62862	39.750	8.65762	32.85598	25.67414
24.442	9.08538	31.71553	24.64600	39.912	8.65762	32.86428	25.68138
24.653	9.08992	31.75367	24.67608	39.859	8.65762	32.86430	25.68116
24.883	9.11161	31.78251	24.69632	39.835	8.65774	32.86755	25.68357
24.908	9.12435	31.79002	24.70032	40.317	8.65762	32.87844	25.69432
25.070	9.13769	31.79467	24.70262	40.669	8.65769	32.89482	25.70874
25.434	9.16649	31.80173	24.70531	40.806	8.65769	32.90194	25.71494
25.806	9.16662	31.83063	24.72958	40.936	8.65766	32.90554	25.71836
26.321	9.21920	31.86566	24.75109	41.474	8.64332	32.92577	25.73885
26.499	9.24685	31.93594	24.80249	42.013	8.58209	32.98765	25.79915
26.750	9.26345	31.96812	24.82617	42.329	8.54656	33.02925	25.83860
27.029	9.29752	32.00445	24.85047	42.701	8.52427	33.06302	25.87015
27.434	9.32009	32.03445	24.87219	42.717	8.52501	33.06088	25.86843
27.738	9.32736	32.05446	24.88806	42.389	8.52625	33.05866	25.86501
27.689	9.32723	32.06772	24.89822	42.487	8.53050	33.04882	25.85710
27.993	9.35882	32.10495	24.92369	42.948	8.51197	33.08260	25.88849
28.365	9.36081	32.13222	24.94637	43.418	8.52007	33.09397	25.89831
28.811	9.40025	32.13171	24.94173	43.908	8.51997	33.11805	25.91943
29.288	9.40794	32.17157	24.97382	44.223	8.51880	33.12727	25.92827
29.260	9.39312	32.19067	24.99097	44.523	8.51940	33.13143	25.93281
29.389	9.38091	32.21201	25.01018	44.928	8.51577	33.14407	25.94511
29.636	9.34455	32.24619	25.04380	45.304	8.51704	33.15228	25.95306
29.831	9.29106	32.25327	25.05871	45.547	8.51813	33.15502	25.95616
29.916	9.22411	32.29514	25.10241	45.681	8.51823	33.16309	25.96307
30.333	9.10084	32.33792	25.15713	45.758	8.51331	33.16999	25.96958
31.021	9.04480	32.35539	25.18269	45.677	8.51816	33.16571	25.96512
31.122	9.03386	32.37498	25.20018	46.256	8.51135	33.16818	25.97073
31.377	9.02645	32.37527	25.20272	46.705	8.51143	33.17738	25.97998
31.944	8.94641	32.40786	25.24325	47.094	8.47963	33.21227	26.01394
32.102	8.92420	32.43525	25.26884	47.487	8.47172	33.22406	26.02618
32.430	8.87430	32.48305	25.31547	47.843	8.46791	33.23009	26.03311
32.389	8.86804	32.49108	25.32253	48.126	8.46746	33.23607	26.03915
32.410	8.86870	32.49280	25.32387	48.272	8.47108	33.23880	26.04140
32.559	8.86804	32.49813	25.32882	48.588	8.46736	33.24697	26.04982
32.750	8.86794	32.50307	25.33357	48.620	8.46801	33.24509	26.04839
33.491	8.85974	32.52808	25.35779	48.920	8.46788	33.25614	26.05844
34.179	8.84983	32.55437	25.38304	49.272	8.46858	33.26481	26.06673
34.256	8.83898	32.56808	25.39580	49.620	8.46798	33.27720	26.07812
34.179	8.84209	32.57013	25.39657	49.887	8.46875	33.28450	26.08494
34.608	8.80692	32.59491	25.42335	50.227	8.46801	33.29129	26.09192
35.126	8.74906	32.65160	25.47899	50.539	8.46796	33.29731	26.09807
35.049	8.75147	32.65437	25.48043	50.928	8.46793	33.30081	26.10260
34.948	8.74896	32.66031	25.48501	51.130	8.46741	33.30584	26.10754

Appendix A. [continued]

April, 1990: [continued]

Press. (dbar)	Temp. (°C)	Sal. (psu)	σ_t (kg m^{-3})	Press. (dbar)	Temp. (°C)	Sal. (psu)	σ_t (kg m^{-3})
35.179	8.74713	32.66180	25.48751	51.171	8.46798	33.30778	26.10916
35.365	8.73456	32.67216	25.49840	51.389	8.46677	33.31239	26.11395
35.989	8.69702	32.71004	25.53667	51.912	8.46612	33.31882	26.12147
36.754	8.68087	32.74947	25.57351	52.235	8.46426	33.32645	26.12921
37.045	8.67384	32.76927	25.59142	52.596	8.46367	33.32920	26.13310
37.349	8.66899	32.78172	25.60329	52.859	8.46479	33.33428	26.13811
37.199	8.67257	32.77880	25.59978	53.013	8.46505	33.33585	26.14001
37.167	8.67199	32.77925	25.60007	53.187	8.46431	33.34152	26.14535
37.232	8.66886	32.78571	25.60590	53.434	8.45676	33.34517	26.15049
37.418	8.66571	32.79218	25.61230	53.867	8.44936	33.35795	26.16361
37.944	8.65699	32.80715	25.62776	54.401	8.44085	33.36909	26.17607

Appendix A. [continued]

May, 1990:

Press. (dbar)	Temp. (°C)	Sal. (psu)	σ_t (kg m^{-3})	Press. (dbar)	Temp. (°C)	Sal. (psu)	σ_t (kg m^{-3})
2.691	9.96468	30.54327	23.49258	17.233	8.84575	32.25286	25.07037
3.112	9.97127	30.51003	23.46752	17.674	8.83191	32.29026	25.10377
3.100	9.93042	30.98713	23.84610	17.989	8.77618	32.34316	25.15515
2.932	9.95995	31.08881	23.91985	18.516	8.77045	32.34954	25.16343
3.096	10.02756	31.13627	23.94660	18.724	8.75933	32.36885	25.18119
3.039	10.03037	31.15200	23.95815	18.855	8.74425	32.38749	25.19869
3.018	10.03557	31.16379	23.96639	19.390	8.74057	32.38927	25.20309
3.014	10.06620	31.14188	23.94428	19.717	8.73487	32.40163	25.21513
3.079	10.02231	31.19244	23.99117	20.060	8.73182	32.40771	25.22192
3.133	10.09602	31.19211	23.97910	20.571	8.72982	32.41670	25.23159
3.696	9.92255	31.22281	24.03390	21.053	8.73232	32.42373	25.23892
3.639	9.90978	31.24006	24.04917	21.396	8.73114	32.42810	25.24409
4.015	9.88477	31.26146	24.07163	21.384	8.73057	32.42734	25.24352
4.444	9.86303	31.30437	24.11058	21.691	8.73117	32.43147	25.24807
4.845	9.82948	31.28710	24.10435	22.124	8.72307	32.46013	25.27372
5.265	9.72258	31.39040	24.20408	22.397	8.72982	32.50177	25.30654
5.543	9.71871	31.41095	24.22201	22.606	8.73439	32.52335	25.32369
5.658	9.72014	31.41754	24.22745	22.839	8.72867	32.53346	25.33354
6.168	9.69771	31.47904	24.28137	23.399	8.73047	32.58063	25.37276
6.512	9.67415	31.50078	24.30369	23.958	8.74605	32.59955	25.38773
6.491	9.66914	31.50714	24.30936	24.375	8.75413	32.66480	25.43948
6.761	9.66377	31.51781	24.31978	24.874	8.77377	32.74024	25.49780
7.300	9.67644	31.55822	24.35175	25.348	8.84014	32.75758	25.50330
7.835	9.66321	31.58386	24.37633	25.425	8.84766	32.78043	25.52038
8.027	9.64543	31.58578	24.38155	25.429	8.85824	32.78751	25.52430
8.428	9.64618	31.60103	24.39516	25.805	8.82944	32.78041	25.52491
8.800	9.64681	31.60037	24.39624	25.511	8.82884	32.79059	25.53163
9.090	9.64571	31.61712	24.41081	25.437	8.85703	32.78971	25.52624
9.384	9.64691	31.66378	24.44839	26.173	8.79054	32.81390	25.55882
9.535	9.64415	31.64084	24.43161	26.459	8.85957	32.82378	25.55718
9.813	9.59148	31.66959	24.46375	26.839	8.84633	32.84072	25.57422
10.520	9.56102	31.68904	24.48703	27.582	8.85776	32.86054	25.59135
11.022	9.56369	31.70962	24.50496	28.293	8.83637	32.87412	25.60854
11.312	9.55653	31.74385	24.53415	28.592	8.77288	32.93803	25.66976
11.357	9.55980	31.73623	24.52789	28.972	8.76922	32.95897	25.68845
11.357	9.56097	31.74009	24.53071	28.927	8.76927	32.96244	25.69096
12.028	9.53576	31.73626	24.53480	29.013	8.76686	32.96207	25.69143
12.506	9.36519	31.88057	24.67679	29.270	8.76609	32.98086	25.70743
12.869	9.30472	31.89929	24.70261	29.797	8.76816	32.98907	25.71594
13.449	9.22279	31.94631	24.75487	30.014	8.77107	32.99624	25.72210
13.878	9.10809	32.03596	24.84483	30.434	8.77175	33.02757	25.74844
13.825	9.10619	32.03652	24.84532	30.847	8.77238	33.04114	25.76085
13.592	9.10359	32.04377	24.85033	31.395	8.77413	33.08250	25.79546
14.201	9.06802	32.06607	24.87608	31.869	8.77430	33.10091	25.81201
14.908	9.04638	32.08658	24.89871	31.979	8.77425	33.10099	25.81258
15.227	9.01420	32.10577	24.92016	32.052	8.77423	33.10939	25.81950
15.509	8.96288	32.14391	24.95922	32.669	8.77040	33.12240	25.83309
16.032	8.88659	32.19141	25.01052	32.992	8.77050	33.13272	25.84262
16.342	8.88465	32.19075	25.01172	33.286	8.76972	33.14196	25.85132
16.587	8.88221	32.20102	25.02125	33.797	8.76361	33.16390	25.87177
16.726	8.86460	32.21932	25.03891	34.210	8.76106	33.18293	25.88896

Appendix A. [continued]

May, 1990: [continued]

Press. (dbar)	Temp. (°C)	Sal. (psu)	σ_t (kg m^{-3})	Press. (dbar)	Temp. (°C)	Sal. (psu)	σ_t (kg m^{-3})
34.708	8.75868	33.20024	25.90515	45.381	8.57107	33.56448	26.26809
34.716	8.75798	33.20462	25.90872	45.601	8.56919	33.57223	26.27545
34.610	8.75618	33.20622	25.90977	45.454	8.56922	33.56742	26.27101
35.211	8.75425	33.21502	25.91970	45.810	8.57239	33.56770	26.27236
35.722	8.75358	33.22388	25.92907	45.879	8.57234	33.57382	26.27748
35.938	8.75235	33.23445	25.93853	46.145	8.56991	33.58193	26.28542
36.175	8.74785	33.24239	25.94652	46.451	8.56738	33.58549	26.29000
36.629	8.73919	33.27166	25.97285	46.884	8.55369	33.60804	26.31175
37.094	8.72670	33.29157	25.99250	47.399	8.54997	33.61014	26.31631
37.429	8.71411	33.30944	26.00997	47.722	8.55245	33.60763	26.31544
37.932	8.70667	33.32211	26.02334	48.032	8.54687	33.61159	26.32081
38.447	8.69678	33.34057	26.04167	48.825	8.53196	33.62912	26.34046
38.884	8.68191	33.36379	26.06415	49.560	8.52708	33.64052	26.35349
38.990	8.67740	33.37188	26.07166	49.291	8.52337	33.64419	26.35571
39.133	8.67793	33.37390	26.07382	48.931	8.52834	33.63836	26.34874
39.105	8.67757	33.37493	26.07455	49.123	8.52587	33.64304	26.35366
39.158	8.67740	33.38379	26.08176	49.507	8.52572	33.64087	26.35373
39.521	8.67546	33.39159	26.08983	50.063	8.51280	33.65520	26.36948
39.950	8.65181	33.40768	26.10804	50.778	8.49311	33.67830	26.39387
40.543	8.61719	33.43971	26.14117	51.146	8.48943	33.68039	26.39775
40.853	8.60326	33.45808	26.15912	51.624	8.48810	33.68525	26.40395
41.372	8.58909	33.47824	26.17947	52.175	8.48812	33.68251	26.40431
42.047	8.59163	33.48625	26.18843	52.592	8.48802	33.68139	26.40535
42.455	8.57852	33.50103	26.20389	53.107	8.48812	33.67966	26.40632
42.149	8.57485	33.50817	26.20865	53.123	8.48498	33.68394	26.41023
41.748	8.58038	33.49719	26.19737	52.756	8.48493	33.68547	26.40977
42.230	8.56912	33.51386	26.21436	52.527	8.48691	33.68224	26.40589
42.708	8.57103	33.51775	26.21929	52.515	8.48814	33.68590	26.40851
42.929	8.56869	33.52438	26.22585	52.604	8.48676	33.68263	26.40657
43.346	8.57778	33.52321	26.22544	53.042	8.48634	33.68366	26.40944
43.767	8.57919	33.52134	26.22568	53.356	8.48266	33.68457	26.41215
44.694	8.57737	33.54178	26.24620				

Appendix A. [continued]

July 7, 1990:

Press. (dbar)	Temp. (°C)	Sal. (psu)	σ_t (kg m^{-3})	Press. (dbar)	Temp. (°C)	Sal. (psu)	σ_t (kg m^{-3})
2.172	10.61296	32.33743	24.78037	16.301	8.80246	33.57910	26.11113
2.258	10.61304	32.33263	24.77700	16.534	8.81162	33.55642	26.09300
2.499	10.60287	32.35854	24.80002	17.380	8.64490	33.59052	26.14944
2.740	10.61039	32.36768	24.80694	17.813	8.59085	33.63810	26.19702
2.438	10.61236	32.56911	24.96213	18.111	8.57350	33.64843	26.20914
3.173	10.56063	32.64700	25.03504	18.406	8.52511	33.66201	26.22856
3.803	10.58117	32.66123	25.04544	18.908	8.46210	33.68331	26.25718
3.484	10.58179	32.67802	25.05697	19.072	8.45840	33.68074	26.25648
3.676	10.59816	33.04931	25.34427	19.014	8.45847	33.68659	26.26079
4.068	10.60064	33.07702	25.36720	19.550	8.36117	33.72271	26.30636
4.105	10.60274	33.08987	25.37702	19.926	8.35375	33.72853	26.31376
4.550	10.56275	33.12687	25.41479	20.473	8.35368	33.71032	26.30199
5.086	10.48733	33.14038	25.44077	20.984	8.35382	33.70845	26.30284
5.229	10.49557	33.13150	25.43308	20.796	8.35135	33.71460	26.30717
5.511	10.45882	33.13647	25.44456	21.168	8.34955	33.71725	26.31122
5.984	10.40272	33.15868	25.47365	21.262	8.35194	33.71749	26.31148
5.870	10.40148	33.18382	25.49295	21.343	8.35395	33.71519	26.30974
6.172	10.33079	33.23556	25.54676	22.026	8.35194	33.72197	26.31848
6.667	10.18256	33.23173	25.57125	22.549	8.35189	33.72550	26.32364
6.937	10.09861	33.28198	25.62587	22.683	8.35373	33.72488	26.32349
7.100	10.09457	33.28340	25.62840	23.059	8.35380	33.73054	26.32963
7.455	9.96583	33.29863	25.66352	23.431	8.35397	33.72866	26.32983
7.893	9.86360	33.31713	25.69701	23.435	8.35130	33.72560	26.32786
8.326	9.84049	33.30698	25.69489	23.656	8.34771	33.72995	26.33282
8.775	9.80900	33.31599	25.70919	24.073	8.35135	33.71910	26.32566
8.791	9.78207	33.33746	25.73050	24.306	8.34391	33.72748	26.33442
9.257	9.66762	33.36034	25.76937	24.853	8.32489	33.74305	26.35201
9.731	9.64411	33.35624	25.77218	25.147	8.33425	33.73359	26.34452
9.972	9.64020	33.35273	25.77117	25.584	8.31576	33.75616	26.36702
10.164	9.57831	33.37632	25.80062	26.091	8.35130	33.72435	26.33900
10.401	9.54271	33.39508	25.82217	25.858	8.31746	33.74379	26.35830
10.949	9.45074	33.41483	25.85507	25.838	8.35142	33.73259	26.34429
11.362	9.42938	33.41937	25.86396	26.434	8.28829	33.76620	26.38292
11.419	9.42558	33.41568	25.86195	26.500	8.29498	33.75984	26.37722
11.541	9.42556	33.40157	25.85148	26.986	8.28746	33.76958	26.38822
11.938	9.27701	33.44593	25.91193	27.550	8.28264	33.77139	26.39294
12.424	9.18878	33.45737	25.93722	27.877	8.28273	33.76731	26.39122
12.775	9.10856	33.50759	25.99089	28.281	8.28207	33.77149	26.39644
12.955	9.10656	33.48583	25.97500	28.310	8.28389	33.76978	26.39496
12.595	9.11612	33.49120	25.97604	27.668	8.28448	33.77563	26.39653
13.045	9.10211	33.48879	25.97843	28.052	8.28195	33.77438	26.39768
13.355	9.09392	33.48789	25.98044	28.690	8.27104	33.77467	26.40247
14.070	9.04817	33.51766	26.01425	29.098	8.27904	33.77398	26.40258
14.336	9.02789	33.51881	26.01957	29.662	8.26005	33.78352	26.41551
14.185	9.04366	33.50772	26.00771	30.259	8.20922	33.81059	26.44713
14.508	9.02977	33.51582	26.01771	30.586	8.15872	33.84925	26.48654
14.994	9.00318	33.53709	26.04078	30.643	8.13678	33.86199	26.50008

Appendix A. [continued]

July 7, 1990: [continued]

Press. (dbar)	Temp. (°C)	Sal. (psu)	σ_t (kg m^{-3})	Press. (dbar)	Temp. (°C)	Sal. (psu)	σ_t (kg m^{-3})
15.370	8.97917	33.54405	26.05173	30.798	8.13568	33.86517	26.50345
15.758	8.89142	33.59119	26.10420	31.166	8.12226	33.86832	26.50961
16.150	8.88142	33.57047	26.09133	31.791	8.08160	33.88784	26.53386
16.657	8.76085	33.55902	26.10350	32.244	8.08108	33.89037	26.53799
32.657	8.07684	33.89305	26.54262	43.730	7.89864	33.95813	26.67076
33.123	8.06898	33.89551	26.54785	43.501	7.89750	33.96042	26.67168
32.910	8.07486	33.88910	26.54097	43.922	7.89695	33.95944	26.67292
32.915	8.06838	33.89009	26.54274	44.502	7.89151	33.95714	26.67457
33.650	8.05917	33.89035	26.54767	44.723	7.88853	33.95988	26.67817
34.255	8.03873	33.90958	26.56857	44.706	7.89038	33.96290	26.68019
34.667	8.03500	33.91440	26.57479	45.082	7.88435	33.96373	26.68345
35.101	8.02341	33.92440	26.58635	46.014	7.88250	33.96150	26.68623
35.190	8.02900	33.91865	26.58142	46.378	7.88128	33.96625	26.69180
35.129	8.02658	33.92103	26.58336	46.500	7.88139	33.96460	26.69105
35.611	8.02291	33.91957	26.58497	46.913	7.87935	33.96320	26.69214
36.057	8.01456	33.92110	26.58945	46.831	7.88010	33.96713	26.69474
36.220	8.01328	33.92485	26.59332	47.068	7.87760	33.96718	26.69623
36.714	8.00293	33.92257	26.59533	47.616	7.87534	33.96760	26.69940
37.323	7.99810	33.92696	26.60228	47.951	7.87393	33.96557	26.69954
37.650	7.99868	33.92141	26.59933	48.457	7.87409	33.96851	26.70414
37.634	7.99819	33.92654	26.60336	48.760	7.87411	33.96829	26.70535
37.401	7.99928	33.92583	26.60157	49.140	7.87113	33.96851	26.70770
37.548	7.99801	33.92714	26.60346	49.540	7.87164	33.96925	26.71003
38.410	7.99389	33.92681	26.60775	49.720	7.86806	33.97014	26.71208
39.052	7.96558	33.94778	26.63135	49.900	7.86808	33.96630	26.70989
39.460	7.95528	33.95401	26.63963	50.439	7.86582	33.97041	26.71591
39.158	7.94385	33.96154	26.64586	50.954	7.86820	33.97035	26.71786
39.280	7.94077	33.96462	26.64929	51.138	7.86820	33.96413	26.71382
40.057	7.92819	33.97511	26.66294	51.550	7.86513	33.96584	26.71750
40.559	7.92814	33.96644	26.65843	51.898	7.86148	33.96932	26.72236
41.033	7.92643	33.96891	26.66279	52.241	7.86266	33.97051	26.72469
41.291	7.92508	33.96548	26.66148	52.490	7.86031	33.97013	26.72588
41.605	7.92520	33.96008	26.65865	52.658	7.85377	33.97504	26.73147
41.957	7.92515	33.96128	26.66121	52.845	7.84406	33.98587	26.74226
42.120	7.92200	33.95843	26.66019	53.283	7.84429	33.98128	26.74062
42.500	7.91856	33.95391	26.65888	53.544	7.83645	33.98643	26.74701
43.223	7.90039	33.95676	26.66711				

Appendix A. [continued]

August 7, 1990:

Press. (dbar)	Temp. (°C)	Sal. (psu)	σ_t (kg m^{-3})	Press. (dbar)	Temp. (°C)	Sal. (psu)	σ_t (kg m^{-3})
2.254	9.46258	32.51821	25.11285	15.917	9.42769	33.22421	25.73239
2.516	9.46403	32.56809	25.15278	16.792	9.42781	33.22816	25.73944
2.446	9.46659	32.60219	25.17870	17.155	9.42791	33.22772	25.74072
2.863	9.46012	32.66301	25.22917	17.286	9.42776	33.22926	25.74255
3.292	9.46137	32.74390	25.29413	17.433	9.42771	33.22815	25.74236
3.002	9.46209	32.77258	25.31511	17.707	9.42196	33.22504	25.74210
3.161	9.46010	32.80258	25.33960	18.160	9.36469	33.26613	25.78553
3.508	9.46395	32.85764	25.38359	18.426	9.35685	33.27472	25.79472
3.897	9.46139	32.92434	25.43790	18.965	9.35121	33.27709	25.79993
4.277	9.46211	32.98445	25.48649	19.018	9.34476	33.28666	25.80869
4.795	9.45816	33.02676	25.52255	18.606	9.34468	33.28823	25.80806
5.016	9.46328	33.03731	25.53098	19.035	9.34275	33.30163	25.82080
5.118	9.46075	33.04303	25.53632	19.178	9.33818	33.30479	25.82466
5.572	9.46209	33.06030	25.55167	19.987	9.31197	33.31091	25.83734
5.935	9.46333	33.06848	25.55951	20.681	9.29796	33.31404	25.84520
6.172	9.46080	33.08003	25.57002	20.444	9.29327	33.31771	25.84774
6.422	9.46251	33.08698	25.57632	20.812	9.28588	33.32152	25.85358
6.867	9.46015	33.09324	25.58362	21.065	9.28508	33.32006	25.85372
7.235	9.45953	33.09595	25.58751	21.376	9.27675	33.32296	25.85874
7.468	9.45431	33.11369	25.60328	21.760	9.27283	33.32658	25.86395
7.819	9.45364	33.11655	25.60722	22.087	9.26894	33.33017	25.86887
8.097	9.45242	33.12094	25.61211	22.353	9.26451	33.33409	25.87385
7.721	9.45165	33.12205	25.61139	22.639	9.25621	33.34639	25.88610
8.162	9.45175	33.12863	25.61853	22.949	9.25677	33.34941	25.88979
8.612	9.45038	33.14394	25.63276	23.284	9.25303	33.34902	25.89160
8.930	9.44656	33.14019	25.63189	23.586	9.24218	33.35780	25.90158
9.188	9.43935	33.14810	25.64042	23.840	9.24210	33.34961	25.89635
9.502	9.44059	33.15278	25.64530	24.101	9.24154	33.34278	25.89228
9.417	9.43759	33.15166	25.64452	24.326	9.23952	33.33056	25.88407
9.523	9.43427	33.15488	25.64806	24.592	9.18539	33.35231	25.91095
10.119	9.43548	33.16656	25.65970	24.302	9.19354	33.35339	25.90917
10.663	9.43359	33.17385	25.66818	24.869	9.16368	33.36306	25.92408
10.822	9.43429	33.17539	25.66999	24.992	9.11074	33.40331	25.96456
11.161	9.43163	32.92740	25.47813	25.564	8.97328	33.36902	25.96208
11.603	9.43034	33.18590	25.68240	26.234	8.73201	33.32809	25.97077
11.934	9.42903	33.18701	25.68499	26.214	8.67645	33.32776	25.97900
12.281	9.42828	33.19244	25.69093	26.328	8.66720	33.31105	25.96786
12.354	9.42848	33.19303	25.69169	26.512	8.52292	33.34782	26.01964
12.669	9.42980	33.19397	25.69364	26.814	8.45865	33.34582	26.02924
12.951	9.42833	33.20024	25.70006	27.247	8.41254	33.35284	26.04371
13.233	9.42784	33.20382	25.70422	27.591	8.35464	33.34370	26.04687
13.421	9.42918	33.20475	25.70559	28.011	8.26522	33.37381	26.08584
13.662	9.42900	33.20631	25.70793	28.240	8.25898	33.36048	26.07737
13.948	9.42841	33.21487	25.71602	28.195	8.25363	33.36651	26.08270
13.686	9.42972	33.21020	25.71097	28.436	8.25003	33.36361	26.08206
13.686	9.43032	33.21209	25.71235	28.665	8.24996	33.36251	26.08226
14.642	9.42776	33.21516	25.71951	29.127	8.25372	33.36580	26.08639

Appendix A. [continued]

August 7, 1990: [continued]

Press. (dbar)	Temp. (°C)	Sal. (psu)	σ_t (kg m^{-3})	Press. (dbar)	Temp. (°C)	Sal. (psu)	σ_t (kg m^{-3})
15.055	9.42846	33.22247	25.72698	29.576	8.25360	33.36957	26.09141
15.067	9.42846	33.22011	25.72519	29.850	8.25170	33.37261	26.09533
15.329	9.42722	33.21988	25.72641	29.834	8.24624	33.37285	26.09626
15.680	9.42789	33.22375	25.73092	30.099	8.21952	33.39058	26.11538
30.345	8.21703	33.39171	26.11776	41.258	8.04978	33.74271	26.46796
30.700	8.21276	33.39318	26.12118	41.605	8.02490	33.76058	26.48720
31.076	8.20483	33.40297	26.13176	42.149	8.01887	33.75754	26.48826
31.709	8.19756	33.42285	26.15133	42.578	8.00937	33.76251	26.49553
31.587	8.16949	33.44975	26.17607	42.655	8.00630	33.76431	26.49775
31.926	8.16710	33.46027	26.18623	42.443	8.00395	33.76531	26.49792
32.134	8.16092	33.47599	26.20043	42.537	8.00274	33.76399	26.49749
32.514	8.15118	33.48753	26.21267	42.672	8.00091	33.76575	26.49976
32.424	8.15671	33.47978	26.20536	43.313	7.99557	33.75941	26.49851
32.416	8.15301	33.47855	26.20491	43.844	7.92073	33.79126	26.53701
32.718	8.14262	33.49571	26.22130	44.375	7.86833	33.81496	26.56576
33.045	8.14012	33.50417	26.22980	44.363	7.83653	33.84212	26.59171
33.482	8.13909	33.50700	26.23417	44.494	7.83233	33.84245	26.59318
34.071	8.13783	33.52018	26.24739	44.661	7.83188	33.84130	26.59311
34.059	8.13768	33.52791	26.25342	44.919	7.82519	33.84785	26.60041
34.255	8.13790	33.52961	26.25562	45.323	7.82754	33.84671	26.60102
34.557	8.13724	33.53870	26.26423	46.006	7.82459	33.85159	26.60840
34.962	8.13598	33.54589	26.27191	45.646	7.82512	33.85139	26.60653
35.293	8.13418	33.56322	26.28729	45.687	7.82272	33.85125	26.60695
35.530	8.13418	33.57041	26.29402	45.969	7.82100	33.85510	26.61152
35.865	8.13481	33.59150	26.31200	46.369	7.82330	33.85287	26.61126
36.204	8.13240	33.60332	26.32318	46.770	7.82224	33.85341	26.61367
36.473	8.12927	33.61369	26.33301	47.244	7.82274	33.85411	26.61632
36.526	8.13114	33.61178	26.33147	47.477	7.82164	33.85611	26.61911
36.657	8.13056	33.61345	26.33347	47.554	7.81858	33.85796	26.62137
36.964	8.12990	33.62254	26.34210	47.828	7.82401	33.85246	26.61750
37.258	8.12696	33.62869	26.34871	48.053	7.82227	33.85149	26.61803
37.536	8.12745	33.63684	26.35630	48.220	7.82037	33.85590	26.62253
37.932	8.12696	33.63689	26.35822	48.543	7.81973	33.85524	26.62358
37.834	8.12815	33.63949	26.35964	48.931	7.82033	33.85816	26.62756
38.014	8.12504	33.63523	26.35758	49.103	7.81740	33.85954	26.62986
38.508	8.12200	33.65860	26.37863	49.303	7.82401	33.85175	26.62369
38.929	8.12261	33.67607	26.39417	49.397	7.82093	33.85858	26.62994
39.117	8.12016	33.68935	26.40581	50.177	7.82152	33.85885	26.63363
39.391	8.11960	33.69453	26.41121	50.186	7.82222	33.85430	26.62999
39.595	8.11605	33.70130	26.41799	50.251	7.82159	33.85737	26.63279
39.861	8.10136	33.71067	26.42875	50.643	7.81874	33.85722	26.63489
40.236	8.09048	33.72208	26.44104	50.933	7.82164	33.85813	26.63650
40.241	8.08798	33.72098	26.44057	51.125	7.82159	33.85818	26.63743
40.273	8.08446	33.72167	26.44178	51.432	7.81915	33.85927	26.64004
40.694	8.07900	33.72795	26.44945	51.804	7.82049	33.85629	26.63921
41.037	8.06502	33.73526	26.45883				

Appendix A. [continued]

August 21, 1990:

Press. (dbar)	Temp. (°C)	Sal. (psu)	σ_t (kg m^{-3})	Press. (dbar)	Temp. (°C)	Sal. (psu)	σ_t (kg m^{-3})
1.760	15.28426	32.98853	24.36840	15.198	12.97676	33.31507	25.16107
1.935	15.28166	32.99586	24.37539	15.341	12.97388	33.31085	25.15902
1.980	15.27994	32.99732	24.37709	15.562	12.91684	33.32979	25.18593
2.262	15.28321	32.99664	24.37710	16.191	12.75834	33.38044	25.25912
2.462	15.28344	33.00019	24.38068	16.853	12.59880	33.38625	25.29769
2.712	15.28240	33.00326	24.38438	17.192	12.53400	33.33968	25.27568
3.030	15.28078	33.00750	24.38941	17.029	12.58241	33.35808	25.27983
3.276	15.27484	33.01039	24.39403	16.971	12.58235	33.37244	25.29071
3.455	15.27578	33.01146	24.39544	17.315	12.49679	33.36613	25.30393
3.848	15.27487	33.02242	24.40583	17.727	12.00830	33.43169	25.44986
4.142	15.26485	33.03679	24.42039	18.144	11.61301	33.49025	25.57099
4.313	15.26313	33.04232	24.42578	18.606	11.36740	33.49175	25.61930
4.783	15.25729	33.04903	24.43431	18.969	11.32731	33.42995	25.58018
5.355	15.14945	33.08455	24.48774	19.112	11.22830	33.47008	25.62999
5.347	15.13681	33.09018	24.49479	19.415	11.03486	33.47318	25.66856
5.641	15.12192	33.09829	24.50558	19.586	11.03061	33.48165	25.67669
5.707	15.07177	33.10662	24.52318	19.783	11.00220	33.46543	25.67003
6.013	15.04587	33.10368	24.52789	19.954	10.98142	33.45476	25.66621
6.336	15.00317	33.08521	24.52435	20.175	10.86386	33.47915	25.70709
6.765	14.95984	33.10527	24.55108	20.449	10.59322	33.45295	25.73550
7.214	14.88270	33.11980	24.58091	21.004	9.86090	33.30339	25.74623
7.251	14.87368	33.11178	24.57684	21.527	9.43466	33.36488	25.86672
7.357	14.83961	33.11598	24.58787	22.062	9.23679	33.41372	25.93925
7.525	14.74552	33.17422	24.65369	21.809	9.29309	33.37545	25.89913
7.664	14.69130	33.18292	24.67262	21.572	9.31478	33.41575	25.92607
7.635	14.69136	33.19320	24.68040	21.997	9.25652	33.41557	25.93723
7.884	14.69152	33.16363	24.65868	22.373	9.20100	33.43646	25.96418
7.848	14.79261	33.17227	24.64354	22.769	9.09963	33.42836	25.97581
8.191	14.77631	33.16294	24.64137	23.170	9.06409	33.42469	25.98040
8.522	14.69411	33.20471	24.69263	23.689	8.87705	33.43135	26.01744
8.714	14.60788	33.19934	24.70774	23.823	8.85302	33.39929	25.99671
8.951	14.57360	33.14818	24.67664	23.631	8.98939	33.39109	25.96801
9.404	14.54743	33.16415	24.69653	23.966	8.76341	33.45131	26.05206
9.637	14.54822	33.16134	24.69523	24.412	8.69361	33.44245	26.05797
9.915	14.48937	33.16791	24.71402	24.792	8.67416	33.41652	26.04240
10.258	14.43178	33.19394	24.74781	25.123	8.67368	33.41774	26.04494
10.316	14.42525	33.19641	24.75135	25.327	8.67481	33.43241	26.05719
10.740	14.11578	33.21231	24.83043	25.491	8.67488	33.43212	26.05770
11.149	14.00321	33.19002	24.83844	25.899	8.68742	33.44272	26.06592
11.656	13.86749	33.21184	24.88559	26.193	8.73712	33.45361	26.06809
11.807	13.81455	33.21731	24.90139	26.565	8.76980	33.47855	26.08424
12.040	13.67993	33.24477	24.95123	27.043	8.73230	33.50178	26.11045
12.130	13.77284	33.14485	24.85540	27.325	8.76349	33.51299	26.11566
12.432	13.58212	33.25286	24.97917	27.252	8.75228	33.54151	26.13941
12.930	13.18513	33.15926	24.98894	27.513	8.82613	33.55178	26.13712
13.376	12.94492	33.22687	25.09091	28.032	8.82631	33.55224	26.13982
13.580	12.93205	33.22829	25.09546	28.159	8.82669	33.55229	26.14038

Appendix A. [continued]

August 21, 1990: [continued]

Press. (dbar)	Temp. (°C)	Sal. (psu)	σ_t (kg m^{-3})	Press. (dbar)	Temp. (°C)	Sal. (psu)	σ_t (kg m^{-3})
13.641	12.95107	33.20499	25.07394	28.682	8.83058	33.55531	26.14451
14.152	12.91696	33.26290	25.12779	28.923	8.83326	33.55592	26.14567
14.614	12.95107	33.28362	25.13918	29.053	8.83992	33.56078	26.14903
14.802	12.97461	33.30290	25.15030	29.282	8.85522	33.56370	26.14996
15.043	12.97253	33.31623	25.16211	29.883	8.86462	33.58683	26.16933
30.218	8.82797	33.58595	26.17591	42.194	8.51035	33.76004	26.41615
30.553	8.80611	33.58958	26.18370	42.684	8.49687	33.77007	26.42831
30.810	8.77040	33.59579	26.19531	42.999	8.49865	33.77077	26.43002
30.855	8.76794	33.58723	26.18919	43.648	8.49440	33.76957	26.43270
31.117	8.71975	33.59937	26.20740	43.848	8.49202	33.77156	26.43553
31.391	8.72038	33.59266	26.20329	43.959	8.49620	33.77141	26.43528
31.954	8.78042	33.63844	26.23236	44.163	8.48874	33.77494	26.44012
32.412	8.82109	33.62729	26.21935	44.706	8.48691	33.77277	26.44118
32.910	8.82681	33.63824	26.22930	45.213	8.48577	33.77826	26.44797
32.902	8.82493	33.64003	26.23096	45.548	8.48448	33.77339	26.44588
32.853	8.82809	33.63580	26.22693	45.536	8.48834	33.76942	26.44212
33.307	8.82372	33.64447	26.23647	45.736	8.48506	33.77285	26.44622
33.752	8.81376	33.64761	26.24251	46.255	8.48320	33.77319	26.44914
34.177	8.78297	33.66841	26.26556	46.619	8.48503	33.76406	26.44336
34.573	8.77796	33.66700	26.26704	47.097	8.48201	33.76659	26.44799
34.831	8.77023	33.67346	26.27448	47.170	8.48142	33.76587	26.44785
35.125	8.77548	33.66307	26.26686	47.481	8.47398	33.76686	26.45119
34.884	8.77796	33.66805	26.26928	47.730	8.47337	33.76491	26.45089
35.448	8.77107	33.66356	26.26941	48.061	8.47330	33.76377	26.45151
35.811	8.76845	33.66971	26.27629	48.531	8.46895	33.76172	26.45271
36.445	8.76489	33.66165	26.27342	48.420	8.47216	33.75967	26.45011
36.625	8.76411	33.66498	26.27697	48.359	8.47082	33.76116	26.45120
36.788	8.75345	33.66190	26.27696	48.711	8.47208	33.75974	26.45150
37.143	8.74597	33.66401	26.28140	49.209	8.46594	33.76294	26.45722
37.242	8.74547	33.66301	26.28114	49.597	8.46724	33.76377	26.45944
37.548	8.72994	33.66305	26.28499	49.887	8.46413	33.75821	26.45688
38.132	8.72374	33.67098	26.29483	50.173	8.46280	33.76075	26.46038
38.549	8.71805	33.68475	26.30840	50.745	8.45991	33.76408	26.46605
38.835	8.68852	33.70831	26.33275	50.982	8.45742	33.75796	26.46271
39.101	8.67361	33.69949	26.32937	50.860	8.45734	33.75460	26.45954
39.566	8.67366	33.70274	26.33403	51.035	8.45661	33.74942	26.45638
39.669	8.67299	33.69862	26.33138	51.485	8.45682	33.75220	26.46058
39.861	8.67366	33.70740	26.33903	51.787	8.45673	33.74751	26.45830
40.012	8.67381	33.70571	26.33837	52.008	8.45668	33.74875	26.46028
40.384	8.61396	33.72674	26.36582	52.208	8.45670	33.74859	26.46107
40.858	8.54935	33.74265	26.39042	52.698	8.45490	33.74637	26.46184
41.303	8.53458	33.75517	26.40454	53.013	8.45483	33.74644	26.46334
41.695	8.52649	33.75077	26.40412	53.136	8.44681	33.75285	26.47016
42.128	8.51223	33.75823	26.41413	53.418	8.44069	33.75486	26.47396
42.324	8.50491	33.76375	26.42048	53.695	8.44084	33.75189	26.47287
41.854	8.52580	33.75150	26.40553				

Appendix A. [continued]

October 11, 1990:

Press. (dbar)	Temp. (°C)	Sal. (psu)	σ_t (kg m^{-3})	Press. (dbar)	Temp. (°C)	Sal. (psu)	σ_t (kg m^{-3})
2.654	11.46414	32.98985	25.13958	19.121	10.15744	32.86065	25.34253
2.961	11.46201	33.13499	25.25417	19.043	10.13556	32.89534	25.37292
3.026	11.45547	33.12092	25.24471	19.264	10.09621	32.88255	25.37057
3.304	11.45691	33.19118	25.30032	19.223	10.09278	32.87083	25.36181
3.958	11.45838	33.25787	25.35484	19.268	10.09417	32.87062	25.36162
3.958	11.45416	33.18092	25.29580	19.668	10.05096	32.86460	25.36599
4.465	11.45204	33.08287	25.22225	20.228	9.78768	32.88465	25.42794
5.208	11.45351	32.99937	25.16043	20.657	9.66393	32.86943	25.43832
5.028	11.45263	33.07667	25.21987	21.315	9.43428	32.85687	25.46878
5.404	11.45351	33.06537	25.21261	21.887	9.36718	32.87840	25.49899
5.948	11.45405	32.99323	25.15890	22.316	9.34227	32.88078	25.50680
6.177	11.45127	32.99777	25.16397	22.222	9.32940	32.89271	25.51776
6.107	11.45343	32.99136	25.15827	22.165	9.33834	32.87635	25.50328
6.769	11.45901	32.95040	25.12841	22.434	9.31335	32.89207	25.52079
7.202	11.45206	32.92259	25.11001	23.341	9.25886	32.88642	25.52920
7.394	11.45326	32.95539	25.13615	23.815	9.20060	32.88572	25.54008
7.950	11.45119	32.93563	25.12368	24.187	9.04535	32.92713	25.59869
7.893	11.45252	32.95252	25.13631	24.265	9.04291	32.90544	25.58246
8.608	11.45269	33.01339	25.18681	24.461	9.02583	32.89856	25.58065
9.176	11.44062	33.03070	25.20502	24.747	8.88746	32.96267	25.65375
9.073	11.44199	33.00160	25.18169	24.886	8.83021	32.94318	25.64802
9.274	11.43276	33.04454	25.21765	25.311	8.77311	32.95558	25.66850
9.641	11.38613	33.02100	25.20948	25.760	8.76255	32.94595	25.66464
10.189	11.37119	32.95239	25.16132	26.418	8.69195	32.96235	25.69135
10.671	11.37119	32.93761	25.15200	26.908	8.67691	32.95353	25.68898
10.491	11.37063	32.89759	25.12018	27.362	8.67317	32.96280	25.69889
10.348	11.37125	32.92863	25.14355	27.231	8.67698	32.96275	25.69767
10.802	11.37128	32.91491	25.13493	26.720	8.67694	32.95594	25.69001
11.129	11.37133	32.89893	25.12398	26.782	8.67698	32.95338	25.68828
11.525	11.36851	32.88782	25.11764	26.794	8.67681	32.95745	25.69155
11.864	11.37122	32.88095	25.11334	27.754	8.67694	32.95786	25.69623
12.309	11.36417	32.86573	25.10479	28.052	8.67322	32.94318	25.68666
12.685	11.35364	32.86812	25.11024	28.498	8.58853	33.01979	25.76167
13.065	11.26923	32.89150	25.14536	29.278	8.53345	33.07800	25.81922
13.400	11.22914	32.90365	25.16353	29.850	8.51239	33.11077	25.85072
13.874	11.19348	32.91496	25.18086	30.410	8.49755	33.12925	25.87001
14.201	11.03870	32.94499	25.23332	30.479	8.50187	33.12877	25.86929
14.136	11.03237	32.96327	25.24838	30.340	8.50187	33.12763	25.86776
14.585	10.91522	32.92681	25.24278	30.349	8.50311	33.13128	25.87048
14.986	10.84077	32.93900	25.26719	30.545	8.49453	33.13911	25.87881
15.509	10.76180	32.94492	25.28801	31.366	8.49686	33.13803	25.88136
15.758	10.74186	32.92530	25.27735	32.563	8.49636	33.14733	25.89419
15.995	10.61409	32.91256	25.29074	33.250	8.49695	33.15252	25.90130
16.207	10.57042	32.92121	25.30600	33.711	8.48759	33.16491	25.91454
16.526	10.52756	32.93930	25.32894	33.507	8.49015	33.16601	25.91408
16.951	10.51482	32.92861	25.32473	32.886	8.49812	33.15655	25.90262
17.049	10.50381	32.91589	25.31716	33.184	8.49885	33.15067	25.89926

Appendix A. [continued]

October 11, 1990: [continued]

Press. (dbar)	Temp. (°C)	Sal. (psu)	σ_t (kg m^{-3})	Press. (dbar)	Temp. (°C)	Sal. (psu)	σ_t (kg m^{-3})
16.955	10.50186	32.92329	25.32284	33.511	8.49581	33.15569	25.90515
17.801	10.46051	32.90077	25.31623	34.144	8.48780	33.16769	25.91866
18.491	10.32495	32.94167	25.37444	34.749	8.48766	33.17265	25.92533
18.839	10.20966	32.91011	25.37100	35.252	8.48706	33.17775	25.93171
19.251	10.13146	32.87489	25.35860	35.750	8.48706	33.18353	25.93851
35.893	8.48768	33.18890	25.94328	45.254	8.25291	33.31824	26.12288
36.289	8.48588	33.18791	25.94459	45.675	8.25408	33.31339	26.12082
36.800	8.48583	33.18782	25.94686	46.230	8.23947	33.31842	26.12950
36.723	8.48333	33.18905	25.94785	46.815	8.24083	33.30929	26.12480
37.049	8.48212	33.18999	25.95026	46.835	8.22312	33.31760	26.13407
37.650	8.47054	33.19431	25.95815	46.664	8.22740	33.32090	26.13523
37.920	8.46923	33.19074	25.95678	46.766	8.21810	33.32510	26.14038
37.830	8.46659	33.19962	25.96373	47.142	8.20092	33.33172	26.14986
38.128	8.46360	33.19729	25.96372	47.710	8.17599	33.34898	26.16972
38.712	8.46056	33.19738	25.96692	48.310	8.14259	33.36574	26.19059
39.121	8.45992	33.19182	25.96452	48.715	8.13765	33.36675	26.19397
39.432	8.44929	33.19715	25.97174	49.021	8.13842	33.36553	26.19430
39.975	8.42115	33.21093	25.98928	48.903	8.13762	33.36430	26.19291
40.441	8.36756	33.22643	26.01166	49.152	8.13830	33.36704	26.19610
40.939	8.35527	33.23176	26.01997	49.393	8.13665	33.36331	26.19452
40.882	8.35581	33.21933	26.00988	49.863	8.12500	33.35127	26.18896
40.527	8.35343	33.22644	26.01420	50.280	8.11519	33.35695	26.19678
40.616	8.35336	33.23386	26.02043	50.704	8.08533	33.37569	26.21786
40.890	8.35517	33.22481	26.01431	51.207	8.08123	33.37299	26.21865
41.315	8.35517	33.27172	26.05303	51.558	8.07936	33.37105	26.21901
41.912	8.40635	33.28195	26.05603	51.305	8.08125	33.37166	26.21805
42.296	8.41566	33.27525	26.05112	51.370	8.08198	33.37070	26.21748
42.798	8.41615	33.27961	26.05675	51.750	8.07698	33.37556	26.22377
43.383	8.39643	33.29320	26.07307	52.028	8.07701	33.37536	26.22488
43.730	8.38893	33.29433	26.07667	52.310	8.07584	33.37746	26.22799
43.910	8.37186	33.30045	26.08487	53.021	8.07638	33.40353	26.25162
43.632	8.37496	33.30001	26.08279	53.626	8.07216	33.41574	26.26459
43.910	8.36321	33.30510	26.08982	54.034	8.08562	33.42924	26.27504
43.946	8.36269	33.30418	26.08935	54.055	8.08314	33.43291	26.27838
44.670	8.35357	33.28932	26.08239	54.227	8.05638	33.43421	26.28417

Appendix A. [continued]

December 13, 1990:

Press. (dbar)	Temp. (°C)	Sal. (psu)	σ_t (kg m^{-3})	Press. (dbar)	Temp. (°C)	Sal. (psu)	σ_t (kg m^{-3})
2.973	10.52392	30.29713	23.21047	18.136	10.74781	33.22910	25.52363
3.108	10.52074	30.99633	23.75594	18.495	10.75259	33.23605	25.52983
3.782	10.52053	31.16123	23.88743	18.806	10.76282	33.27569	25.56031
3.843	10.52390	31.14928	23.87783	19.006	10.75169	33.30768	25.58808
3.958	10.52536	31.15916	23.88580	19.550	10.74776	33.29246	25.57938
4.603	10.52593	31.20061	23.92091	19.435	10.75374	33.30333	25.58627
4.763	10.52865	31.23912	23.95116	19.411	10.75388	33.26994	25.56013
4.885	10.53364	31.26279	23.96931	20.113	10.74573	33.27692	25.57018
5.041	10.53964	31.28161	23.98366	20.477	10.74773	33.33204	25.61440
5.617	10.56942	31.25833	23.96311	20.878	10.74974	33.34038	25.62235
5.829	10.57760	31.28069	23.98010	21.221	10.75660	33.33512	25.61860
6.164	10.58504	31.25612	23.96123	20.943	10.75029	33.23975	25.54418
6.487	10.59146	31.28970	23.98775	21.335	10.75734	33.28073	25.57663
7.002	10.61579	31.87976	24.44536	21.523	10.79570	33.34611	25.62164
6.716	10.61102	31.95227	24.50134	21.560	10.79917	33.31327	25.59562
7.251	10.62387	32.06153	24.58665	21.891	10.79835	33.30499	25.59081
8.269	10.63281	32.17369	24.67706	22.447	10.81077	33.23757	25.53865
7.864	10.62872	32.17406	24.67622	23.145	10.81781	33.11230	25.44303
7.684	10.63751	32.18245	24.68043	23.599	10.82745	33.34114	25.62155
8.632	10.63139	32.28983	24.76939	23.337	10.82459	33.37934	25.65061
9.184	10.64998	32.33890	24.80691	23.141	10.82398	33.28650	25.57755
9.045	10.65741	32.35983	24.82129	23.476	10.81980	33.34716	25.62703
9.625	10.65672	32.38864	24.84648	23.787	10.82591	33.40421	25.67177
10.115	10.65885	32.44788	24.89446	24.191	10.82326	33.31519	25.60476
10.287	10.66077	32.48048	24.92029	24.575	10.83356	33.33073	25.61677
10.937	10.66361	32.53671	24.96653	25.413	10.87631	33.22098	25.52756
10.802	10.67380	32.53119	24.95986	25.556	10.89149	33.45944	25.71115
10.998	10.67047	32.55672	24.98120	25.593	10.88857	33.43166	25.69020
11.006	10.67451	32.59419	25.00972	25.870	10.89351	33.48143	25.72932
11.214	10.67708	32.62851	25.03694	26.206	10.89436	33.43930	25.69789
11.987	10.67719	32.70650	25.10116	26.430	10.89401	33.49127	25.73942
12.162	10.68397	32.76538	25.14663	26.606	10.89351	33.48225	25.73329
12.367	10.69644	32.72537	25.11423	27.088	10.89354	33.48651	25.73877
12.783	10.70321	32.76026	25.14211	27.419	10.89340	33.52424	25.76966
13.315	10.71827	32.82054	25.18884	27.815	10.89420	33.42196	25.69169
13.735	10.71827	32.88641	25.24203	28.293	10.89356	33.53368	25.78093
13.531	10.71624	32.90991	25.25976	28.608	10.89356	33.51535	25.76809
13.899	10.71824	32.92627	25.27382	28.461	10.89417	33.49679	25.75287
13.919	10.71885	32.93610	25.28146	28.191	10.89423	33.37286	25.65516
14.205	10.72164	32.98122	25.31740	28.620	10.89497	33.41850	25.69250
15.182	10.73674	32.96372	25.30555	29.033	10.89492	33.51738	25.77134
15.116	10.74008	33.02578	25.35300	29.331	10.89420	33.50998	25.76706
15.407	10.74428	33.03085	25.35753	29.936	10.89351	33.56495	25.81270
15.774	10.74436	33.02592	25.35534	30.720	10.89356	33.66231	25.89203
16.354	10.74491	33.01857	25.35214	30.590	10.89354	33.39859	25.68615
16.694	10.74710	33.09481	25.41266	30.892	10.89486	33.55537	25.80932
16.093	10.74562	33.06469	25.38675	30.998	10.89417	33.63900	25.87503

Appendix A. [continued]

December 13, 1990: [continued]

Press. (dbar)	Temp. (°C)	Sal. (psu)	σ_t (kg m^{-3})	Press. (dbar)	Temp. (°C)	Sal. (psu)	σ_t (kg m^{-3})
16.363	10.74708	33.11438	25.42641	31.362	10.89417	33.65818	25.89160
17.041	10.74770	33.03957	25.37111	31.583	10.89630	33.71749	25.93839
17.515	10.76208	33.18473	25.48377	31.840	10.89624	33.66062	25.89529
17.568	10.76277	33.19547	25.49225	32.367	10.89895	33.67962	25.91198
17.985	10.75193	33.18098	25.48475	32.772	10.89824	33.76777	25.98256
33.103	10.89624	33.71811	25.94575	44.216	10.90039	32.90184	25.35987
33.401	10.89630	33.78613	26.00003	43.926	10.89975	32.98297	25.42181
33.196	10.89622	33.69765	25.93024	43.967	10.90227	33.26708	25.64264
33.764	10.89685	33.73674	25.96313	44.138	10.89959	33.46359	25.79683
34.091	10.89550	33.70366	25.93909	44.416	10.89895	33.47532	25.80733
34.063	10.89415	33.69006	25.92862	44.952	10.90036	33.51582	25.84103
34.545	10.89627	33.68326	25.92512	45.336	10.90119	33.77174	26.04182
34.749	10.89754	33.66056	25.90814	45.752	10.89967	33.69011	25.98042
35.039	10.89685	33.71228	25.94984	46.324	10.89845	33.60425	25.91639
35.264	10.89622	33.72292	25.95925	46.684	10.89895	33.78144	26.05585
35.677	10.89903	33.66885	25.91852	46.978	10.89909	33.60348	25.91863
36.220	10.89914	33.69564	25.94180	46.741	10.90031	33.75631	26.03630
36.576	10.89909	33.70928	25.95404	45.953	10.90022	33.58281	25.89771
36.739	10.89768	33.69576	25.94450	46.149	10.89970	33.64208	25.94482
36.494	10.89895	33.64822	25.90616	46.647	10.90041	33.74697	26.02859
36.657	10.89903	33.62746	25.89072	46.753	10.90025	33.79628	26.06748
36.960	10.89911	33.70563	25.95293	47.358	10.89967	33.73492	26.02255
37.299	10.89906	33.66807	25.92523	48.090	10.89824	33.64726	25.95787
37.630	10.89898	33.71138	25.96045	48.821	10.89417	33.71766	26.01670
38.308	10.89895	33.63492	25.90399	49.213	10.89425	33.55802	25.89419
38.226	10.89826	33.44455	25.75556	49.168	10.89348	33.55547	25.89214
38.439	10.90177	33.46958	25.77538	49.499	10.89406	33.59023	25.92059
38.819	10.89699	33.68865	25.94847	49.654	10.89335	33.78202	26.07070
39.068	10.89890	33.67340	25.93739	49.552	10.89346	33.78520	26.07269
39.603	10.89972	33.69608	25.95731	49.732	10.89337	33.75005	26.04616
39.603	10.90044	33.66920	25.93626	50.325	10.89335	33.74758	26.04692
39.885	10.89975	33.67313	25.94071	50.749	10.89351	33.76405	26.06162
40.384	10.89829	33.74152	25.99646	50.692	10.89404	33.69557	26.00797
40.706	10.89961	33.72660	25.98607	50.578	10.89125	33.62883	25.95600
41.229	10.90047	33.60017	25.88986	51.248	10.89343	33.73445	26.04085
41.662	10.89967	33.70669	25.97487	51.505	10.89080	33.71263	26.02550
41.948	10.89975	33.62900	25.91567	52.224	10.89348	33.49274	25.85711
41.393	10.89956	33.53534	25.84030	52.600	10.89346	33.54153	25.89678
40.825	10.90028	33.17701	25.55871	52.911	10.89354	33.69247	26.01566
41.409	10.90108	33.50303	25.81495	52.719	10.88716	33.67593	26.00305
41.842	10.90020	33.48008	25.79920	52.572	10.89061	33.47947	25.84886
42.002	10.89900	33.56264	25.86440	52.653	10.88592	33.62453	25.96297
42.900	10.90028	32.94237	25.38548	52.817	10.89337	33.52118	25.88194
43.726	10.90031	32.85464	25.32094				

Appendix A. [continued]

January 22, 1991:

Press. (dbar)	Temp. (°C)	Sal. (psu)	σ_t (kg m^{-3})	Press. (dbar)	Temp. (°C)	Sal. (psu)	σ_t (kg m^{-3})
3.414	8.57527	28.41415	22.04338	16.591	8.98783	32.59666	25.31451
3.190	8.57899	30.55680	23.71853	17.151	8.98662	32.57963	25.30393
3.627	8.58821	30.61535	23.76502	17.200	8.98717	32.59822	25.31861
3.860	8.58550	30.61801	23.76857	17.576	8.98599	32.60612	25.32669
3.884	8.58329	31.20583	24.22922	17.682	8.98601	32.59058	25.31502
4.007	8.58260	31.47110	24.43761	17.895	8.98591	32.60262	25.32542
4.783	8.58140	31.69004	24.61280	18.181	8.98599	32.61415	25.33574
4.481	8.57649	31.85690	24.74283	18.393	8.98604	32.61510	25.33744
4.330	8.58009	31.88622	24.76457	18.720	8.98528	32.62063	25.34337
4.840	8.59257	31.76116	24.66709	19.186	8.98545	32.58316	25.31615
5.204	8.58580	31.79087	24.69304	19.488	8.98594	32.61014	25.33857
5.302	8.58816	31.81402	24.71126	19.954	8.98525	32.62133	25.34955
5.829	8.58068	31.85280	24.74516	20.089	8.98596	32.59794	25.33176
6.234	8.58016	31.82185	24.72285	19.966	8.98535	32.62223	25.35030
6.569	8.57959	31.88543	24.77427	20.399	8.98591	32.61692	25.34803
6.912	8.58133	31.80869	24.71547	20.620	8.98717	32.62041	25.35157
7.243	8.58272	31.86076	24.75756	20.820	8.98601	32.61764	25.35050
7.643	8.59329	31.83787	24.73988	20.922	8.98659	32.62783	25.35884
7.844	8.62546	31.84130	24.73867	21.282	8.98543	32.62499	25.35844
8.252	8.64410	31.84227	24.73850	21.638	8.99148	32.61149	25.34856
8.391	8.62548	31.83025	24.73252	22.152	8.98851	32.61361	25.35303
8.604	8.62618	31.83297	24.73552	22.328	8.98846	32.61841	25.35759
9.167	8.67974	31.78212	24.69024	22.679	8.98976	32.62769	25.36625
9.257	8.68464	31.87078	24.75933	23.019	8.98589	32.63361	25.37304
9.347	8.69651	31.90884	24.78775	23.260	8.98793	32.62660	25.36833
9.793	8.75540	31.98139	24.83768	23.133	8.98963	32.63851	25.37681
9.842	8.75942	31.98796	24.84243	23.411	8.98788	32.62192	25.36537
9.833	8.75884	31.98721	24.84189	23.860	8.98990	32.63505	25.37737
10.140	8.78147	32.05684	24.89436	24.114	8.99107	32.64473	25.38592
10.557	8.88755	32.19116	24.98518	24.293	8.99084	32.64765	25.38906
10.769	8.95000	32.29090	25.05458	24.498	8.99175	32.64740	25.38965
11.035	8.98705	32.44480	25.17048	24.992	8.99289	32.63094	25.37885
11.374	8.98912	32.51001	25.22272	25.421	8.98981	32.62395	25.37582
11.206	8.99426	32.49814	25.21187	25.360	8.99082	32.62945	25.37969
11.423	9.03160	32.47223	25.18678	25.294	8.99036	32.64618	25.39254
11.983	9.02193	32.47995	25.19688	25.723	8.99299	32.64457	25.39283
12.121	9.00182	32.50983	25.22401	26.001	8.98912	32.65288	25.40120
12.281	9.00433	32.49803	25.21512	26.275	8.99542	32.64702	25.39688
12.673	8.99190	32.52066	25.23655	26.581	8.99036	32.65627	25.40631
13.057	8.99416	32.55806	25.26721	26.961	8.99433	32.65451	25.40604
13.727	8.98798	32.54890	25.26406	27.390	8.98798	32.65782	25.41158
13.723	8.99224	32.57735	25.28564	27.582	8.99489	32.64674	25.40271
14.066	8.98798	32.59382	25.30075	27.423	8.99170	32.65808	25.41135
14.213	8.98849	32.59827	25.30483	27.987	8.99360	32.63711	25.39722
14.593	8.98978	32.60398	25.31083	28.195	8.99226	32.64194	25.40216
14.761	8.98669	32.59355	25.30391	28.032	8.98973	32.64315	25.40275
14.626	8.98654	32.61182	25.31762	28.273	8.99598	32.63032	25.39284

Appendix A. [continued]

January 22, 1991: [continued]

Press. (dbar)	Temp. (°C)	Sal. (psu)	σ_t (kg m^{-3})	Press. (dbar)	Temp. (°C)	Sal. (psu)	σ_t (kg m^{-3})
14.994	8.98530	32.59851	25.30907	28.739	8.99165	32.63272	25.39752
15.349	8.98613	32.60789	25.31790	29.004	8.99294	32.63612	25.40118
15.856	8.98720	32.58689	25.30362	29.315	8.99241	32.64458	25.40930
15.966	8.98606	32.58291	25.30118	29.605	9.00170	32.63155	25.39898
16.371	8.98672	32.59513	25.31249	29.936	8.99861	32.64003	25.40761
30.324	8.99421	32.64741	25.41584	42.312	9.02013	32.69888	25.50667
30.561	8.99150	32.65248	25.42131	42.418	9.01747	32.70506	25.51241
30.921	8.99299	32.64579	25.41748	42.410	9.02459	32.69825	25.50593
31.137	8.99476	32.65023	25.42166	42.308	9.03331	32.70005	25.50551
31.321	8.99089	32.64790	25.42128	42.884	9.03026	32.68576	25.49743
31.435	8.99243	32.64237	25.41723	43.268	9.02269	32.69487	25.50749
31.987	8.99160	32.63258	25.41222	43.669	9.00486	32.70652	25.52123
32.187	8.99034	32.64196	25.42067	44.155	9.00374	32.70705	25.52403
32.220	8.98781	32.65257	25.42951	44.302	8.99535	32.71384	25.53133
32.526	8.98910	32.64527	25.42500	44.502	8.99545	32.71704	25.53473
32.821	8.99102	32.64451	25.42545	44.862	8.98654	32.71804	25.53854
33.090	8.99158	32.64046	25.42342	45.001	8.98518	32.71704	25.53861
33.417	8.98788	32.64708	25.43066	45.082	8.98594	32.72201	25.54275
34.046	8.98712	32.64653	25.43322	45.368	8.98523	32.70844	25.53354
34.091	8.98591	32.65703	25.44183	45.777	8.97759	32.70943	25.53738
34.492	8.98596	32.65552	25.44247	46.120	8.97585	32.71772	25.54570
34.598	8.98591	32.65798	25.44489	46.394	8.96673	32.71820	25.54875
34.671	8.98528	32.65734	25.44481	46.480	8.96816	32.71532	25.54667
34.970	8.98462	32.65667	25.44575	46.737	8.96698	32.71023	25.54404
35.211	8.98523	32.65843	25.44813	47.260	8.96569	32.69817	25.53719
35.162	8.98520	32.65852	25.44798	47.170	8.96503	32.70242	25.54021
35.395	8.98513	32.64795	25.44079	47.129	8.95881	32.70678	25.54440
36.110	8.98535	32.65411	25.44883	47.665	8.96453	32.69650	25.53791
35.811	8.98538	32.65774	25.45031	47.840	8.95738	32.71167	25.55169
36.122	8.98516	32.65466	25.44935	48.122	8.96387	32.70999	25.55065
36.567	8.98477	32.66028	25.45583	48.441	8.93547	32.73481	25.57596
37.029	8.98530	32.66808	25.46396	48.645	8.95046	32.72237	25.56481
37.115	8.98589	32.67590	25.47038	48.878	8.94803	32.71720	25.56221
37.429	8.98596	32.68386	25.47802	49.499	8.93973	32.71999	25.56852
37.805	8.98591	32.68739	25.48251	49.797	8.92152	32.73769	25.58657
38.144	8.98851	32.69419	25.48897	49.793	8.89685	32.75943	25.60740
38.480	8.98664	32.68859	25.48641	49.834	8.90320	32.75465	25.60286
38.725	8.98788	32.69451	25.49196	50.259	8.89617	32.75518	25.60631
38.251	8.98895	32.69649	25.49118	50.414	8.90123	32.75753	25.60806
38.966	8.99029	32.68056	25.48177	50.856	8.89385	32.76738	25.61893
39.321	8.99413	32.68983	25.49004	50.901	8.90385	32.75827	25.61045
39.485	8.99457	32.69328	25.49342	50.643	8.89705	32.76682	25.61703
39.632	8.98793	32.70227	25.50216	50.847	8.90322	32.75650	25.60892
39.611	8.99287	32.69679	25.49700	51.436	8.90000	32.74627	25.60410
40.053	8.99153	32.68847	25.49272	51.820	8.90715	32.74741	25.60563
40.433	8.99990	32.68744	25.49233	52.032	8.89305	32.76554	25.62298
40.968	8.99282	32.70106	25.50653	52.331	8.89065	32.75786	25.61871
41.225	9.00418	32.69529	25.50141	52.502	8.89048	32.75709	25.61891
41.634	8.99859	32.70837	25.51439	52.939	8.88912	32.74881	25.61464
41.973	9.01501	32.69316	25.50146				

Appendix A. [continued]

May 16, 1991:

Press. (dbar)	Temp. (°C)	Sal. (psu)	σ_t (kg m^{-3})	Press. (dbar)	Temp. (°C)	Sal. (psu)	σ_t (kg m^{-3})
2.540	11.00200	30.15703	23.01878	17.646	8.77720	32.51679	25.28935
2.900	10.93970	30.13857	23.01671	18.034	8.77086	32.51899	25.29382
3.133	10.90100	30.29246	23.14401	18.344	8.75837	32.53028	25.30599
3.316	10.82500	30.31505	23.17534	18.504	8.74784	32.53730	25.31383
3.774	10.81215	30.40609	23.25041	18.884	8.73341	32.53975	25.31968
3.933	10.58155	30.60638	23.44590	19.378	8.69463	32.56339	25.34637
4.191	10.51766	30.64071	23.48450	19.913	8.67774	32.57639	25.36157
4.612	10.51549	30.54627	23.41326	20.191	8.67600	32.57047	25.35847
4.943	10.51643	30.75117	23.57412	20.224	8.67794	32.56852	25.35680
4.971	10.50346	30.74976	23.57532	20.473	8.59500	32.63690	25.42410
5.245	10.48446	30.69765	23.53918	20.939	8.53985	32.68640	25.47336
5.997	10.46688	30.70871	23.55414	21.237	8.53680	32.69139	25.47909
6.156	10.46680	30.79285	23.62039	21.311	8.53738	32.69212	25.47991
6.238	10.45949	30.79764	23.62571	21.458	8.53550	32.69024	25.47939
6.479	10.40003	30.81945	23.65370	22.181	8.48796	32.74101	25.52965
6.867	10.39784	30.89308	23.71317	22.594	8.45692	32.74714	25.54102
6.990	10.38920	30.87396	23.70028	22.761	8.38923	32.79544	25.58980
7.590	10.38119	30.89404	23.71998	22.945	8.37941	32.79481	25.59162
7.913	10.32851	31.02106	23.82915	23.423	8.36039	32.80142	25.60183
8.007	10.32113	31.04552	23.84986	23.840	8.35184	32.81273	25.61388
8.105	10.32186	31.02880	23.83716	23.893	8.34516	32.81999	25.62081
8.620	10.25990	31.03960	23.85819	24.212	8.28188	32.86836	25.66963
8.984	10.17641	31.15077	23.96027	24.784	8.25920	32.89666	25.69781
8.894	10.17443	31.14101	23.95258	24.894	8.25675	32.89649	25.69855
9.437	10.05522	31.21588	24.03300	24.939	8.25502	32.89911	25.70107
10.017	9.89302	31.38273	24.19221	25.462	8.25490	32.89075	25.69692
10.128	9.88771	31.39889	24.20618	25.703	8.25483	32.90295	25.70760
10.385	9.87114	31.41916	24.22585	25.658	8.25502	32.89757	25.70315
10.593	9.84429	31.44571	24.25187	26.075	8.25487	32.89417	25.70241
10.834	9.83513	31.46045	24.26595	26.757	8.23420	32.91424	25.72434
11.112	9.76285	31.52595	24.33001	26.925	8.24277	32.91213	25.72218
11.345	9.67855	31.61358	24.41305	26.937	8.22933	32.92109	25.73125
11.705	9.65817	31.60954	24.41481	27.676	8.16647	32.98475	25.79388
12.113	9.57231	31.71753	24.51473	28.240	8.13907	33.03094	25.83674
12.089	9.53923	31.74324	24.53998	28.514	8.13853	33.04817	25.85159
12.391	9.46274	31.82277	24.61565	28.469	8.13909	33.05261	25.85479
12.930	9.36816	31.90746	24.69926	28.441	8.13841	33.05704	25.85824
13.212	9.29424	31.99577	24.78123	28.604	8.13795	33.05470	25.85721
13.441	9.26988	32.00338	24.79205	28.951	8.13720	33.06038	25.86336
13.907	9.20653	32.06712	24.85395	29.364	8.13797	33.07855	25.87939
14.034	9.14146	32.11742	24.90404	29.703	8.13911	33.11751	25.91134
14.250	9.11169	32.15096	24.93590	30.365	8.13722	33.15555	25.94448
14.573	9.07843	32.23326	25.00692	30.761	8.13554	33.16153	25.95124
14.920	8.98086	32.32635	25.09648	30.892	8.13542	33.16788	25.95684
15.088	8.98220	32.31900	25.09129	30.941	8.13612	33.17065	25.95913
15.505	8.96524	32.33050	25.10482	31.117	8.13418	33.17751	25.96560
15.893	8.94552	32.36159	25.13397	31.501	8.13495	33.18355	25.97198

Appendix A. [continued]

May 16, 1991: [continued]

Press. (dbar)	Temp. (°C)	Sal. (psu)	σ_t (kg m^{-3})	Press. (dbar)	Temp. (°C)	Sal. (psu)	σ_t (kg m^{-3})
16.289	8.88948	32.41837	25.18886	31.881	8.12820	33.20084	25.98828
16.432	8.88757	32.41416	25.18652	32.032	8.13002	33.20390	25.99110
16.734	8.88384	32.41258	25.18723	32.179	8.12205	33.21516	26.00179
17.119	8.85554	32.43827	25.21345	32.686	8.11236	33.24109	26.02589
17.437	8.82660	32.46945	25.24376	33.319	8.10810	33.26062	26.04473
33.634	8.10689	33.27134	26.05476	42.900	8.00146	33.51741	26.30581
33.924	8.10706	33.27801	26.06130	43.440	7.99963	33.51530	26.30689
34.202	8.10708	33.28632	26.06909	43.938	7.99482	33.52938	26.32093
34.140	8.11359	33.28536	26.06708	44.265	7.99122	33.53141	26.32455
33.969	8.11056	33.28468	26.06622	44.817	7.96773	33.55358	26.34794
34.541	8.10883	33.28829	26.07192	45.050	7.95022	33.57155	26.36569
34.966	8.10869	33.30796	26.08932	45.233	7.93942	33.58663	26.37996
35.231	8.11343	33.31695	26.09688	45.221	7.94716	33.58184	26.37501
35.489	8.11177	33.32171	26.10204	45.376	7.93641	33.59068	26.38424
35.954	8.10808	33.33604	26.11596	45.597	7.94289	33.58585	26.38050
36.322	8.10930	33.33593	26.11737	46.161	7.93330	33.59226	26.38952
36.694	8.10869	33.34363	26.12520	46.651	7.92985	33.59867	26.39730
36.955	8.10803	33.35030	26.13173	47.068	7.92983	33.59977	26.40008
37.131	8.10747	33.35310	26.13481	47.334	7.92973	33.59748	26.39951
37.107	8.10628	33.35540	26.13668	47.419	7.93036	33.59923	26.40118
37.205	8.10696	33.35700	26.13828	47.669	7.93161	33.60026	26.40295
37.613	8.09968	33.36618	26.14843	47.832	7.92788	33.60279	26.40623
38.001	8.09415	33.37749	26.15990	48.286	7.92742	33.60028	26.40640
38.337	8.09230	33.38400	26.16681	48.772	7.92617	33.60502	26.41253
38.757	8.08861	33.39958	26.18151	49.172	7.92008	33.60839	26.41790
39.227	8.08931	33.40945	26.19130	49.569	7.91172	33.61731	26.42795
39.554	8.08936	33.41524	26.19733	49.609	7.90740	33.61436	26.42645
39.673	8.08500	33.42202	26.20384	49.597	7.90008	33.62771	26.43795
39.852	8.06797	33.43949	26.22089	49.626	7.89890	33.62756	26.43814
39.950	8.06376	33.44464	26.22600	49.936	7.88032	33.64277	26.45423
40.326	8.05353	33.45774	26.23952	50.541	7.87131	33.64259	26.45818
40.616	8.05053	33.46286	26.24530	51.072	7.87134	33.64472	26.46227
41.009	8.02146	33.49540	26.27694	51.387	7.83418	33.68153	26.49806
41.515	8.01606	33.50267	26.28576	51.607	7.82040	33.69596	26.51242
41.895	8.00997	33.50964	26.29386	51.750	7.82003	33.69086	26.50912
42.210	8.00625	33.51325	26.29868	51.881	7.81927	33.69064	26.50966
42.377	8.00871	33.51559	26.30092	52.090	7.81620	33.69242	26.51246
42.520	8.00456	33.51692	26.30323	52.805	7.80499	33.69645	26.52054
42.749	8.00274	33.52343	26.30966	53.221	7.79601	33.70615	26.53137
42.802	8.00337	33.51787	26.30544	53.569	7.79177	33.70649	26.53385

Appendix A. [continued]

June 25, 1991:

Press. (dbar)	Temp. (°C)	Sal. (psu)	σ_t (kg m^{-3})	Press. (dbar)	Temp. (°C)	Sal. (psu)	σ_t (kg m^{-3})
2.123	12.24231	27.29417	20.57995	20.861	7.68863	33.55977	26.28386
2.479	12.23197	30.80624	23.30316	21.221	7.71182	33.76732	26.44524
2.748	12.02143	31.15560	23.61404	21.658	7.72560	33.59008	26.30599
3.084	11.61956	31.57124	24.01128	21.715	7.72537	33.61165	26.32323
3.598	11.17504	31.98698	24.41608	22.283	7.72553	34.04271	26.66450
4.080	10.89734	32.14766	24.59203	22.532	7.72553	33.83212	26.50017
4.240	10.75341	32.25055	24.69785	23.386	7.72563	34.18724	26.78311
4.587	10.52821	32.36324	24.82595	23.725	7.80927	34.14201	26.73688
4.934	10.25767	32.53468	25.00709	23.603	7.79359	34.12939	26.72871
5.449	9.96388	32.79636	25.26274	24.036	8.06150	33.95634	26.55520
5.788	9.77362	32.88109	25.36188	24.244	8.08939	33.96215	26.55655
6.038	9.75079	32.85736	25.34823	24.530	8.13814	34.14113	26.69102
6.409	9.59607	32.96861	25.46210	24.927	7.93518	34.17207	26.74742
6.712	9.30912	33.12776	25.63420	25.360	7.89686	34.10718	26.70410
7.267	9.07560	33.29749	25.80663	25.703	7.92932	34.01411	26.62779
7.533	8.98878	33.18012	25.72966	26.107	8.05743	34.25824	26.80226
7.790	8.98063	33.17914	25.73134	26.524	8.15451	34.26574	26.79546
8.219	8.88985	33.38546	25.90902	26.876	8.13500	34.13106	26.69430
8.465	8.88338	33.31061	25.85255	27.211	8.11797	34.13047	26.69793
8.857	8.76971	33.49419	26.01579	27.611	8.03561	34.19945	26.76623
9.265	8.75101	33.16202	25.76038	28.065	7.92689	34.13792	26.73617
9.515	8.73214	33.14751	25.75306	28.465	7.90046	34.08989	26.70419
9.964	8.70176	33.32510	25.89890	28.886	7.82600	34.01392	26.65741
10.238	8.67676	33.45299	26.00420	29.115	7.78234	33.99363	26.64891
10.675	8.67672	33.53213	26.06820	29.405	7.73212	34.03032	26.68639
10.982	8.58161	33.55248	26.10018	29.679	7.72549	33.99988	26.66470
11.210	8.54245	33.54044	26.09778	29.973	7.72567	34.00409	26.66932
11.672	8.49184	33.33504	25.94662	30.557	7.63624	34.42017	27.01201
12.085	8.47761	33.58468	26.14636	31.023	7.60108	34.41795	27.01751
12.383	8.45970	33.50386	26.08709	31.149	7.60838	34.27179	26.90213
12.841	8.38081	33.42053	26.03579	31.317	7.58934	34.41807	27.02065
13.086	8.34020	33.68066	26.24704	31.926	7.55207	34.45710	27.05953
13.417	8.25377	33.51728	26.13342	32.285	7.54550	34.44378	27.05165
13.825	8.17389	33.48400	26.12111	32.514	7.54254	34.30292	26.94238
14.230	8.13931	33.50936	26.14800	32.743	7.53372	34.21608	26.87642
14.520	8.10526	33.53210	26.17223	33.135	7.52364	34.07111	26.76569
15.043	8.05868	33.67255	26.29176	33.634	7.50165	34.38521	27.01810
15.398	7.99136	33.69242	26.31893	34.083	7.45162	34.32520	26.98017
15.762	7.92937	33.61603	26.26973	34.533	7.42640	34.17221	26.86552
16.207	7.92930	33.54144	26.21321	34.778	7.40568	34.19656	26.88875
16.502	7.93180	33.55460	26.22453	35.137	7.32367	34.17270	26.88329
16.600	7.92928	33.58290	26.24756	35.436	7.30550	34.30140	26.98849
17.274	7.92645	33.90186	26.50152	35.811	7.29081	34.24990	26.95177
17.674	7.91507	33.67265	26.32503	35.963	7.29500	34.13837	26.86413
17.854	7.89029	33.58039	26.25704	36.339	7.29745	34.29494	26.98869
18.418	7.85077	33.85700	26.48264	36.682	7.27687	34.14222	26.87301
18.851	7.75784	33.74707	26.41181	37.066	7.27465	34.16267	26.89118

Appendix A. [continued]

June 25, 1991: [continued]

Press. (dbar)	Temp. (°C)	Sal. (psu)	σ_t (kg m^{-3})	Press. (dbar)	Temp. (°C)	Sal. (psu)	σ_t (kg m^{-3})
18.880	7.77498	33.58963	26.28577	37.466	7.26522	34.35401	27.04490
19.264	7.76078	33.86703	26.50752	37.818	7.26288	34.32124	27.02105
19.897	7.72549	33.93444	26.56851	38.234	7.26052	34.20498	26.93181
20.134	7.67077	33.80267	26.47398	38.692	7.25648	34.22736	26.95209
20.489	7.64824	33.71458	26.40962	38.794	7.25230	34.17927	26.91531
39.076	7.23653	34.34201	27.04689	46.149	7.15917	34.36163	27.10565
39.734	7.22205	34.52200	27.19360	46.598	7.16210	34.39721	27.13530
40.142	7.21508	34.36507	27.07295	46.819	7.16275	34.24754	27.01842
40.584	7.20341	34.27661	27.00700	47.272	7.15994	34.33867	27.09262
40.898	7.19288	34.16463	26.92180	47.505	7.15920	34.24963	27.02371
41.086	7.19058	34.11559	26.88439	47.836	7.15987	34.24611	27.02236
41.303	7.18939	34.18287	26.93850	48.208	7.15976	34.25753	27.03307
41.736	7.18953	34.28838	27.02350	48.551	7.15520	34.20919	26.99724
42.124	7.18478	34.33433	27.06211	48.907	7.16094	34.17973	26.97488
42.422	7.18353	34.22819	26.98012	49.258	7.15457	34.21956	27.00873
42.860	7.17492	34.20379	26.96413	49.540	7.14807	34.19987	26.99544
43.186	7.15804	34.28916	27.03519	50.006	7.14135	34.17950	26.98248
43.591	7.16336	34.39099	27.11644	50.349	7.13943	34.17664	26.98207
44.004	7.15795	34.39157	27.11955	50.774	7.13532	34.16560	26.97591
44.457	7.16215	34.29435	27.04452	51.121	7.13019	34.15281	26.96815
44.821	7.15795	34.24989	27.01179	51.415	7.11851	34.15937	26.97630
45.160	7.15567	34.24439	27.00933	51.922	7.11165	34.31087	27.09883
45.564	7.15272	34.21222	26.98628	52.384	7.11221	34.26883	27.06777
45.769	7.15860	34.15241	26.93932	53.005	7.10701	34.43765	27.20424

Appendix A. [continued]

July 7, 1991:

Press. (dbar)	Temp. (°C)	Sal. (psu)	σ_t (kg m^{-3})	Press. (dbar)	Temp. (°C)	Sal. (psu)	σ_t (kg m^{-3})
2.434	8.35614	32.61241	25.35832	22.937	7.88431	33.71222	26.38469
2.761	8.31871	33.03577	25.69734	22.822	7.88494	33.71530	26.38649
3.300	8.25499	33.06893	25.73530	23.068	7.88201	33.72032	26.39199
3.660	8.26167	32.97908	25.66549	23.656	7.85304	33.73483	26.41031
4.064	8.26050	32.89886	25.60459	24.154	7.83150	33.75657	26.43282
4.330	8.25984	33.00227	25.68701	24.285	7.83752	33.75431	26.43076
4.652	8.25483	33.02401	25.70628	24.833	7.83097	33.75661	26.43603
5.175	8.14131	33.23060	25.88756	25.106	7.81949	33.77024	26.44967
5.772	8.13051	33.19045	25.86038	25.650	7.81776	33.77519	26.45629
6.168	8.09538	33.22094	25.89130	25.993	7.80814	33.78690	26.46846
6.483	8.10617	33.14765	25.83364	26.373	7.80344	33.79844	26.47995
6.606	8.09825	33.21713	25.88989	26.823	7.80526	33.79273	26.47726
7.223	8.09764	33.16757	25.85391	27.043	7.80517	33.79414	26.47939
7.435	8.09577	33.25932	25.92716	27.272	7.80576	33.80450	26.48849
8.121	8.09158	33.24950	25.92321	27.909	7.80289	33.80797	26.49455
8.571	8.09459	33.21730	25.89955	28.298	7.80346	33.80605	26.49474
8.452	8.10296	33.21573	25.89654	28.919	7.80224	33.81557	26.50523
8.865	8.10255	33.24838	25.92411	29.164	7.80104	33.82030	26.51024
9.437	8.10429	33.28672	25.95656	29.670	7.79020	33.82212	26.51557
10.234	8.10619	33.29292	25.96479	30.026	7.78898	33.82810	26.52207
10.794	8.11153	33.25985	25.94061	30.406	7.78719	33.82720	26.52337
10.839	8.11527	33.24272	25.92683	30.647	7.78896	33.82910	26.52571
10.675	8.11527	33.26711	25.94521	31.023	7.77939	33.83575	26.53404
11.145	8.10733	33.29641	25.97153	31.460	7.77874	33.82890	26.53076
11.635	8.10986	33.28994	25.96832	31.873	7.77042	33.83791	26.54094
12.228	8.11168	33.31104	25.98732	32.375	7.76444	33.84470	26.54944
13.033	8.08733	33.44836	26.10237	32.874	7.75737	33.84991	26.55685
13.490	8.08192	33.45931	26.11385	33.339	7.75677	33.84658	26.55644
13.601	8.07996	33.46264	26.11726	33.740	7.74958	33.85220	26.56374
13.801	8.08427	33.46436	26.11889	33.801	7.74774	33.86265	26.57250
13.948	8.07947	33.46879	26.12374	34.177	7.74058	33.86205	26.57479
14.352	8.08010	33.46308	26.12102	34.549	7.74361	33.85883	26.57352
14.920	8.07026	33.46397	26.12577	34.925	7.74297	33.86184	26.57770
15.390	8.05707	33.47485	26.13840	35.415	7.73764	33.86545	26.58355
15.930	8.01994	33.50568	26.17055	35.893	7.73296	33.86589	26.58677
16.698	8.01218	33.51866	26.18540	36.351	7.73356	33.86509	26.58815
17.278	8.00497	33.52885	26.19711	36.763	7.72695	33.86895	26.59403
17.294	8.00251	33.53741	26.20427	37.152	7.72640	33.84952	26.58062
16.984	8.00923	33.53097	26.19680	37.503	7.72635	33.85319	26.58512
17.078	8.00369	33.53642	26.20233	37.969	7.72628	33.86056	26.59305
17.658	7.98852	33.54963	26.21758	38.316	7.72626	33.86292	26.59649
18.745	7.96332	33.56812	26.24078	38.667	7.72633	33.86746	26.60165
19.476	7.93629	33.60089	26.27382	39.011	7.72628	33.86497	26.60128
19.827	7.93124	33.61218	26.28503	39.468	7.72635	33.87193	26.60883
19.774	7.93017	33.61539	26.28747	39.828	7.72623	33.87333	26.61160
19.889	7.93015	33.61540	26.28800	40.290	7.70069	33.84977	26.59891
20.436	7.92832	33.61695	26.29199	40.853	7.58591	33.88626	26.64677

Appendix A. [continued]

July 7, 1991: [continued]

Press. (dbar)	Temp. (°C)	Sal. (psu)	σ_t (kg m^{-3})	Press. (dbar)	Temp. (°C)	Sal. (psu)	σ_t (kg m^{-3})
20.841	7.92418	33.62794	26.30308	41.417	7.54101	33.87896	26.65006
21.000	7.92656	33.62317	26.29971	41.446	7.52502	33.86121	26.63854
21.544	7.91390	33.64249	26.31923	41.483	7.51266	33.88305	26.65765
22.320	7.88744	33.67007	26.34831	41.989	7.43662	33.89143	26.67742
22.847	7.88484	33.67516	26.35510	42.476	7.35841	33.86238	26.66791
42.786	7.31038	33.89435	26.70126	48.126	6.83750	33.96458	26.84661
43.158	7.26137	33.87234	26.69256	48.474	6.81121	33.97277	26.85823
43.799	7.18789	33.88937	26.71919	48.866	6.80210	33.96763	26.85722
44.286	7.07296	33.91349	26.75640	49.291	6.78095	33.98212	26.87346
44.666	7.04584	33.91231	26.76097	49.667	6.75748	33.98517	26.88077
44.800	7.02449	33.92072	26.77116	50.255	6.75248	33.98198	26.88163
45.111	7.01576	33.91678	26.77069	50.316	6.74092	33.98366	26.88480
45.556	6.99091	33.93238	26.78844	50.647	6.72964	33.98686	26.89036
45.887	6.95295	33.95322	26.81159	50.835	6.72545	33.99263	26.89634
46.222	6.94248	33.95611	26.81684	51.366	6.73010	33.98883	26.89516
46.668	6.92187	33.95345	26.81962	51.967	6.72729	33.99247	26.90117
47.056	6.86280	33.97889	26.84951	52.204	6.72337	33.99105	26.90167
47.575	6.85076	33.96161	26.83993	52.437	6.72495	33.99346	26.90442
47.947	6.85757	33.95106	26.83240				

Appendix A. [continued]

July 23, 1991:

Press. (dbar)	Temp. (°C)	Sal. (psu)	σ_t (kg m^{-3})	Press. (dbar)	Temp. (°C)	Sal. (psu)	σ_t (kg m^{-3})
2.095	10.04558	34.22760	26.35095	14.867	8.35518	33.68798	26.25865
2.029	10.02884	34.06910	26.22975	15.362	8.32372	33.68552	26.26374
2.569	9.92295	34.31377	26.44118	15.819	8.28938	33.71585	26.29480
2.765	9.88811	34.23439	26.38595	15.680	8.29021	33.71469	26.29313
2.789	9.85642	34.18510	26.35289	16.187	8.28953	33.71889	26.29884
3.153	9.83982	34.21267	26.37886	16.551	8.31158	33.70362	26.28520
3.582	9.67943	34.16896	26.37346	16.690	8.34404	33.68830	26.26891
3.635	9.64548	34.09905	26.32470	16.763	8.35313	33.68464	26.26500
3.766	9.63120	34.10188	26.32987	17.139	8.33103	33.71411	26.29317
4.036	9.42622	33.95029	26.24628	17.298	8.31563	33.72775	26.30692
4.317	9.30531	34.18242	26.44880	17.584	8.31028	33.72755	26.30888
4.554	9.29887	34.16126	26.43436	17.797	8.31026	33.71662	26.30128
4.869	9.24321	34.04815	26.35631	18.132	8.29188	33.73894	26.32310
5.175	9.23986	34.17847	26.46021	18.589	8.28397	33.74502	26.33114
5.453	9.21385	34.17559	26.46342	18.585	8.28830	33.74440	26.32998
5.564	9.19785	34.12437	26.42643	18.614	8.28331	33.74574	26.33192
5.584	9.08964	34.11852	26.43931	19.284	8.25219	33.74726	26.34086
6.283	8.97243	34.07794	26.42941	19.652	8.25217	33.72774	26.32723
6.597	8.88272	34.02671	26.40490	19.211	8.25209	33.73787	26.33318
6.544	8.88465	33.96495	26.35599	19.803	8.25229	33.72731	26.32757
6.810	8.88216	33.96000	26.35371	20.477	8.24361	33.72464	26.32986
7.006	8.84804	33.91031	26.32105	20.559	8.24425	33.72638	26.33150
7.129	8.83000	33.86372	26.28795	20.387	8.24906	33.72319	26.32749
7.782	8.75916	33.93846	26.36056	20.510	8.23807	33.73491	26.33890
7.733	8.74955	33.84251	26.28666	21.258	8.09435	33.76469	26.38719
7.974	8.74595	33.84677	26.29166	21.564	8.10357	33.76395	26.38663
8.277	8.72223	33.89209	26.33224	21.507	8.11148	33.76118	26.38302
8.714	8.69486	33.88789	26.33519	21.674	8.10357	33.76268	26.38614
8.791	8.68167	33.84541	26.30430	21.981	8.09384	33.78415	26.40584
9.004	8.67810	33.80033	26.27051	22.491	8.09631	33.77534	26.40089
9.519	8.67491	33.82851	26.29543	22.708	8.07681	33.78448	26.41195
9.641	8.67486	33.76131	26.24334	22.692	8.07814	33.78907	26.41529
9.690	8.65682	33.77367	26.25604	22.961	8.08292	33.80397	26.42750
10.148	8.54861	33.82670	26.31637	23.272	8.11156	33.80032	26.42178
10.446	8.54437	33.79306	26.29202	23.705	8.11459	33.80937	26.43041
10.875	8.53880	33.80182	26.30169	24.142	8.10423	33.80952	26.43407
10.933	8.54187	33.72657	26.24250	24.179	8.09510	33.81958	26.44350
11.092	8.53877	33.76321	26.27242	24.077	8.10415	33.81708	26.43972
11.394	8.53622	33.72467	26.24398	24.314	8.09556	33.82179	26.44578
11.627	8.53456	33.72336	26.24427	24.731	8.08823	33.81657	26.44468
12.048	8.53213	33.74347	26.26233	25.266	8.07574	33.81571	26.44831
12.477	8.48612	33.71780	26.25121	25.646	8.07872	33.81763	26.45111
12.563	8.48439	33.68660	26.22740	25.519	8.07930	33.81595	26.44913
12.604	8.47391	33.70982	26.24739	25.413	8.07746	33.82027	26.45231
13.114	8.45784	33.68757	26.23473	25.789	8.07993	33.82249	26.45540
13.057	8.45762	33.67254	26.22272	26.504	8.14418	33.86634	26.48348
13.449	8.38998	33.69936	26.25583	26.786	8.16197	33.86699	26.48261

Appendix A. [continued]

July 23, 1991: [continued]

Press. (dbar)	Temp. (°C)	Sal. (psu)	σ_t (kg m^{-3})	Press. (dbar)	Temp. (°C)	Sal. (psu)	σ_t (kg m^{-3})
13.838	8.38068	33.68887	26.25079	26.586	8.14666	33.86989	26.48627
14.034	8.37901	33.68521	26.24907	26.344	8.14180	33.87349	26.48872
14.393	8.37028	33.69847	26.26243	27.178	8.14802	33.87532	26.49303
14.741	8.35936	33.69759	26.26498	28.044	8.25280	33.86879	26.47610
14.667	8.37350	33.67683	26.24622	27.897	8.25287	33.86987	26.47627
27.803	8.25221	33.85364	26.46321	41.029	7.91568	33.90081	26.61089
28.248	8.25214	33.86457	26.47383	41.401	7.91512	33.89985	26.61192
28.391	8.25217	33.86079	26.47151	41.524	7.91515	33.89972	26.61238
29.245	8.20037	33.87249	26.49239	41.622	7.91156	33.90065	26.61409
29.250	8.15881	33.89346	26.51511	41.932	7.90013	33.90548	26.62098
28.906	8.21675	33.86920	26.48580	42.063	7.89884	33.90442	26.62094
29.482	8.15214	33.90340	26.52497	42.541	7.89944	33.90483	26.62336
30.246	8.11569	33.87489	26.51155	42.937	7.89780	33.90344	26.62432
30.381	8.11321	33.88219	26.51826	42.876	7.89768	33.90628	26.62629
30.582	8.10481	33.88272	26.52085	42.974	7.89888	33.90261	26.62368
30.422	8.10660	33.88476	26.52146	43.068	7.89705	33.90929	26.62962
30.385	8.10782	33.88239	26.51925	43.624	7.88862	33.90746	26.63197
30.904	8.06965	33.88116	26.52635	43.889	7.88436	33.90911	26.63511
31.697	8.03155	33.88828	26.54123	44.032	7.87672	33.90633	26.63470
32.183	8.00785	33.88437	26.54391	44.539	7.86882	33.90659	26.63839
32.420	8.00495	33.88927	26.54927	44.682	7.87371	33.90403	26.63631
32.114	8.00785	33.89540	26.55225	44.698	7.86750	33.90436	26.63756
31.873	8.00906	33.89678	26.55205	45.013	7.85988	33.90018	26.63684
32.118	8.00729	33.89584	26.55270	45.299	7.84855	33.90968	26.64727
32.747	7.99874	33.88935	26.55175	45.548	7.83411	33.92125	26.65962
33.740	7.98385	33.89431	26.56239	45.957	7.82145	33.92368	26.66526
34.099	7.92996	33.92734	26.59794	46.222	7.81963	33.92169	26.66517
34.148	7.94037	33.91565	26.58744	46.226	7.81966	33.92408	26.66706
33.630	7.93612	33.92373	26.59205	46.369	7.81968	33.92148	26.66567
33.609	7.96932	33.90123	26.56938	46.574	7.81843	33.92515	26.66968
34.108	7.92757	33.92838	26.59915	46.933	7.81539	33.92680	26.67306
34.917	7.92285	33.91156	26.59034	47.064	7.82083	33.92258	26.66955
35.223	7.92473	33.90945	26.58980	47.387	7.81362	33.92212	26.67172
35.566	7.92413	33.91109	26.59274	47.571	7.81374	33.91677	26.66834
35.301	7.92475	33.91302	26.59296	47.632	7.81381	33.91407	26.66649
35.448	7.92464	33.91330	26.59386	48.167	7.78498	33.91502	26.67391
35.832	7.92413	33.91219	26.59483	48.457	7.75204	33.91758	26.68206
36.077	7.92401	33.90998	26.59423	48.723	7.75452	33.91730	26.68270
36.633	7.92237	33.90852	26.59587	48.939	7.74913	33.92250	26.68856
36.935	7.92422	33.90770	26.59633	48.988	7.75390	33.92029	26.68635
36.931	7.92348	33.90994	26.59818	49.058	7.75087	33.91593	26.68369
36.849	7.92466	33.91133	26.59872	49.679	7.74024	33.91713	26.68902
36.857	7.92281	33.90955	26.59763	49.863	7.74313	33.91811	26.69021
37.389	7.92290	33.90779	26.59867	49.908	7.74366	33.92018	26.69197
38.332	7.92293	33.90849	26.60352	50.292	7.73780	33.92053	26.69485
38.561	7.92355	33.90895	26.60484	50.578	7.74015	33.91698	26.69303
38.349	7.92478	33.91270	26.60663	50.578	7.73420	33.91780	26.69454

Appendix A. [continued]

July 23, 1991: [continued]

Press. (dbar)	Temp. (°C)	Sal. (psu)	σ_t (kg m^{-3})	Press. (dbar)	Temp. (°C)	Sal. (psu)	σ_t (kg m^{-3})
38.345	7.92475	33.90788	26.60283	50.803	7.73055	33.91769	26.69602
38.770	7.92237	33.90750	26.60483	51.366	7.72473	33.91420	26.69670
39.199	7.92355	33.90865	26.60752	51.554	7.72468	33.91056	26.69471
38.937	7.92235	33.91116	26.60847	51.509	7.72456	33.91339	26.69674
39.575	7.92475	33.90730	26.60800	51.971	7.72461	33.91303	26.69856
39.971	7.92170	33.91017	26.61252	52.474	7.72404	33.90592	26.69536
40.053	7.92304	33.91098	26.61333	52.265	7.72468	33.90776	26.69576
39.926	7.92167	33.91516	26.61623	52.269	7.72456	33.91426	26.70090
40.314	7.92056	33.90729	26.61199	52.723	7.72396	33.91093	26.70045
40.719	7.91934	33.90344	26.61100	53.234	7.72406	33.90918	26.70140

Appendix A. [continued]

August 20, 1991:

Press. (dbar)	Temp. (°C)	Sal. (psu)	σ_t (kg m^{-3})	Press. (dbar)	Temp. (°C)	Sal. (psu)	σ_t (kg m^{-3})
2.221	11.46518	31.42981	23.92528	19.738	8.82821	33.36539	25.95542
2.422	11.45755	31.51493	23.99367	20.547	8.75182	33.36510	25.97075
2.757	11.45316	32.22754	24.54960	20.739	8.54692	33.38826	26.02132
3.153	11.45875	32.19251	24.52316	20.735	8.54945	33.37855	26.01330
3.447	11.45605	32.18000	24.51526	21.082	8.52963	33.36465	26.00702
3.431	11.45316	32.67977	24.90408	21.470	8.46045	33.36357	26.01848
3.406	11.47366	32.60253	24.84022	21.670	8.46033	33.34212	26.00260
3.333	11.46886	32.59423	24.83431	22.120	8.41045	33.36130	26.02725
3.468	11.46172	32.63074	24.86459	22.900	8.37300	33.32743	26.00992
3.406	11.45526	32.61536	24.85353	23.256	8.36371	33.32896	26.01414
3.627	11.46237	32.88074	25.05948	23.701	8.36138	33.32590	26.01413
4.309	11.47221	32.73537	24.94779	24.187	8.36690	33.33735	26.02449
4.677	11.47955	32.72050	24.93657	24.334	8.36253	33.32465	26.01587
4.861	11.46578	32.74763	24.96098	24.481	8.35580	33.30915	26.00540
5.314	11.47451	32.75502	24.96718	24.322	8.28640	33.33895	26.03848
5.551	11.47011	32.77580	24.98520	25.262	8.25468	32.97372	25.76110
5.862	11.47928	32.77323	24.98294	26.091	8.21626	32.91611	25.72542
6.516	11.46671	32.80169	25.01029	26.300	8.15708	32.94746	25.75973
6.879	11.44331	32.77086	24.99221	26.602	8.13822	32.93471	25.75389
7.149	11.33038	32.80031	25.03674	26.974	8.13345	32.93639	25.75761
7.439	11.30703	32.81326	25.05232	27.141	8.07382	32.90035	25.73888
7.664	10.89026	32.89224	25.18898	27.427	8.02050	32.92125	25.76439
7.897	10.57095	32.83657	25.20234	27.705	7.99953	32.89787	25.75039
8.281	10.39822	32.88345	25.27029	28.032	7.93608	32.92357	25.78129
9.143	10.25838	32.87162	25.28878	28.412	7.92767	32.91908	25.78073
9.539	10.17874	32.86757	25.30088	29.135	7.89172	32.90596	25.77896
9.887	10.05153	32.88359	25.33633	29.299	7.88261	32.88659	25.76582
10.070	9.92181	32.89837	25.37032	29.519	7.87006	32.85909	25.74706
10.311	9.84476	32.86266	25.35631	29.842	7.81896	32.90121	25.78897
10.597	9.72852	32.91420	25.41699	30.340	7.81357	32.88772	25.78144
11.039	9.64691	32.94316	25.45498	30.671	7.79329	32.87108	25.77281
11.439	9.64621	32.92268	25.44091	31.096	7.74067	32.88751	25.79520
11.770	9.57478	32.96556	25.48755	31.546	7.74129	32.88911	25.79844
12.211	9.56304	32.97976	25.50256	31.713	7.75491	32.89969	25.80556
12.612	9.56361	33.02372	25.53864	32.077	7.78975	32.90548	25.80677
13.102	9.64360	33.02255	25.52691	32.200	7.81594	32.92990	25.82274
13.519	9.64629	33.09462	25.58466	32.784	7.86754	32.91389	25.80539
13.838	9.64608	33.12077	25.60657	33.425	7.80224	32.94089	25.83895
14.152	9.64626	33.11546	25.60382	33.785	7.78680	32.93305	25.83667
14.352	9.64621	33.09211	25.58649	34.038	7.76571	32.93483	25.84225
14.606	9.54340	33.15422	25.65295	34.475	7.76399	32.94713	25.85416
15.088	9.53587	33.10419	25.61728	34.957	7.75981	32.94228	25.85316
15.860	9.31244	33.16870	25.70730	35.366	7.72998	32.94329	25.86011
16.681	9.10885	33.23325	25.79398	35.603	7.72642	32.92934	25.85075
16.665	9.08900	33.21766	25.78485	35.497	7.72633	32.91742	25.84092
16.906	9.07059	33.21337	25.78550	35.762	7.72637	32.86324	25.79958
17.388	8.96293	33.24843	25.83208	36.731	7.62570	32.90042	25.84757

Appendix A. [continued]

August 20, 1991: [continued]

Press. (dbar)	Temp. (°C)	Sal. (psu)	σ_t (kg m^{-3})	Press. (dbar)	Temp. (°C)	Sal. (psu)	σ_t (kg m^{-3})
17.539	8.88739	33.28554	25.87365	37.082	7.62580	32.90489	25.85267
17.919	8.86032	33.28456	25.87884	37.360	7.60913	32.91326	25.86289
18.316	8.86291	33.30567	25.89677	37.593	7.60619	32.94047	25.88576
18.773	8.86963	33.32698	25.91449	38.034	7.60790	32.92895	25.87849
19.354	8.85029	33.34461	25.93396	38.475	7.60555	32.93337	25.88431
38.835	7.60204	32.93275	25.88597	44.833	7.48431	32.90738	25.91018
45.274	7.47857	32.90487	25.91104	45.123	7.48551	32.90482	25.90933
38.974	7.60087	32.93128	25.88562	46.043	7.45728	32.92855	25.93617
39.076	7.60083	32.93875	25.89197	46.406	7.45078	32.92967	25.93962
39.730	7.60327	32.95319	25.90596	47.101	7.45094	32.92637	25.94020
40.057	7.59086	32.94749	25.90474	47.342	7.40073	32.99172	25.99971
40.249	7.58434	32.95358	25.91133	47.546	7.39610	32.99960	26.00749
40.927	7.56295	32.97000	25.93037	47.759	7.38547	33.01341	26.02081
41.356	7.54342	32.94894	25.91856	47.697	7.38144	33.02703	26.03179
41.577	7.54219	32.94394	25.91581	48.347	7.38433	33.01789	26.02719
42.006	7.53933	32.94134	25.91614	48.702	7.38026	33.01778	26.02930
42.304	7.53467	32.93562	25.91367	48.984	7.38092	33.02430	26.03563
41.863	7.53509	32.94439	25.91848	49.417	7.38306	33.02620	26.03881
42.962	7.51325	32.90049	25.89211	49.789	7.38719	33.02204	26.03666
43.370	7.48780	32.91102	25.90584	50.030	7.38362	33.02789	26.04287
43.738	7.47666	32.91879	25.91520	50.361	7.38308	33.02939	26.04564
44.163	7.47616	32.91764	25.91632	50.590	7.38261	33.03197	26.04879
44.359	7.48496	32.90560	25.90652	50.819	7.38374	33.02593	26.04493
44.539	7.48381	32.91273	25.91311	51.093	7.38378	33.02689	26.04693

Appendix B. Nutrient and biomass concentrations.

Date/ Day	Depth (m)	[NO3] (μM)	[NH4] (μM)	[urea] (μM)	Chl *a* (μg L^{-1})	PN (μM)
7–10–90/	0	20.80	1.93		1.0	2.80
191	8	21.80	2.02		1.1	3.83
	12	23.50	2.09		0.7	4.05
	20	28.70	1.18		0.5	3.06
	25	31.30	0.40		0.3	2.49
	40	33.30	0.40		0.3	2.39
7–24–90/	0	5.13	0.30		38.3	17.40
205	8	23.11	0.42		20.2	9.52
	12	24.21	0.37		15.8	9.38
	20	29.23	0.36		8.8	6.64
	25	30.88	0.50		4.9	5.00
	40	32.40	0.15		0.8	4.94
8–7–90/	0	14.22	0.25		10.9	7.76
219	8	14.35	0.30		4.9	6.35
	12	15.33	0.37		6.5	11.19
	20	22.67	0.62		4.4	2.03
	25	24.25	0.40		1.6	1.49
	40	29.18	0.42		0.4	1.90
8–21–90/	0	0.21	0.06		1.8	5.93
233	8	0.30	0.03		2.6	5.32
	12	0.30	0.09		2.6	6.45
	20	22.15	4.20		5.2	4.46
	25	24.73	3.73		2.8	2.06
	40	28.22	4.11		4.1	2.91
9–5–90/	0	0.30	0.07		3.5	4.00
248	8	0.17	0.17		4.1	3.39
	12	9.44	1.09		10.3	9.44
	20	17.17	4.07		3.2	3.55
	25	20.06	2.00		1.9	1.92
	40	22.65	3.29		1.6	3.30
10–11–90/	0	1.92	0.24	0.03	15.8	7.91
284	8	4.02	0.25	0.12	17.6	8.79
	12	9.51	0.36	0.03	8.3	3.22
	20	15.16	0.19	0.03	0.6	1.85
	25	19.49	0.14	0.03	0.5	1.46
	40	22.15	0.12	0.03	0.2	0.92
12–13–90/	0	5.83	0.31	0.04	0.5	2.02
347	8	5.57	0.33	0.03	0.6	2.48
	12	5.67	0.26	0.03	0.6	2.06
	20	5.96	0.22	0.03	0.5	2.78
	25	6.10	0.30	0.04	0.5	2.12
	40	6.13	0.29	0.04	0.4	2.16

Appendix B. [continued]

Date/ Day	Depth (m)	[NO3] (μM)	[NH4] (μM)	[urea] (μM)	Chl *a* (μg L^{-1})	PN (μM)
1–22–91/ 387	0	8.83	0.04	0.07	3.2	8.88
	8	8.31	0.07	0.05	2.4	2.84
	12	8.56	0.05	0.04	1.4	2.92
	20	8.67	0.23	0.03	1.4	2.00
	25	8.66	0.11	0.05	1.1	1.76
	40	9.53	0.11	0.11	0.6	1.64
5–16–91/ 501	0	0.25	0.11	0.08	9.0	2.22
	8	6.88	0.19	0.09	5.1	1.83
	12	5.73	0.14	0.16	9.5	1.83
	20	16.89	0.16	0.10	2.0	0.68
	25	20.61	0.29	0.03	0.9	0.22
	40	28.37	0.13	0.02	0.5	0.30
6–25–91/ 541	0	0.15	0.03	0.17	7.9	5.81
	8	19.62	0.26	0.32	4.7	3.90
	12	23.48	0.66	0.15	3.5	7.06
	20	27.71	0.11	0.08	0.3	2.53
	25	27.56	0.08	0.13	0.9	2.33
	40	33.69	0.12	0.17	0.5	1.52
7–9–91/ 555	0	24.80	0.03	0.08	4.0	1.15
	8	29.60	0.05	0.09	2.9	2.21
	12	30.44	0.07	0.09	2.6	2.47
	20	32.63	0.18	0.11	1.4	1.87
	25	32.97	0.22	0.11	1.2	1.54
	40	34.50	0.12	0.13	0.5	1.55
7–23–91/ 569	0	5.63	0.33	0.08	57.1	9.98
	8	19.87	0.21	0.09	32.7	16.63
	12	27.00	0.21	0.09	18.0	3.70
	20	34.55	0.11	0.11	2.2	1.60
	25	36.40	0.09	0.11	0.8	1.14
	40	42.19	0.11	0.13	0.6	0.76
8–20–91/ 597	0	0.17	0.12	0.22	32.2	17.11
	8	5.18	0.64	0.31	30.8	9.49
	12	11.59	1.87	0.33	23.8	5.84
	20	24.19	3.67	0.38	4.0	2.88
	25	27.71	3.24	0.38	1.7	1.83
	40	38.28	0.79	0.20	1.2	1.11

Appendix C. PN–specific uptake rates.

Date/ Day	Depth (m)	$V^{PN}_{NO_3}$ (h^{-1})	V^{PN}_{NH4} (h^{-1})	V^{PN}_{urea} (h^{-1})
7–10–90/ 191	0	0.0086	0.0253	
	8	0.0031	0.0085	
	12	0.0024	0.0039	
	20	0.0022	0.0017	
	25	0.0021	0.0014	
	40	0.0089	0.0027	
7–24–90/ 205	0	0.0743	0.0062	
	8	0.0242	0.0077	
	12	0.0230	0.0191	
	20	0.0119	0.0057	
	25	0.0055	0.0095	
	40	0.0527	0.0019	
8–7–90/ 219	0	0.0339	0.0199	
	8	0.0184	0.0222	
	12	0.0129	0.0197	
	20	0.0050	0.0109	
	25	0.0049	0.0082	
	40	0.0049	0.0023	
8–21–90/ 233	0	0.0068	0.0055	
	8	0.0184	0.0074	
	12	0.0112	0.0084	
	20	0.0003	0.0121	
	25	0.0023	0.0208	
	40	0.0030	0.0057	
9–5–90/ 248	0	0.0128	0.0109	
	8	0.0066	0.0068	
	12	0.0060	0.0707	
	20	0.0024	0.0074	
	25	0.0023	0.0032	
	40	0.0023	0.0028	
10–11–90/ 284	0	0.0382	0.0072	0.0011
	8	0.0067	0.0024	0.0004
	12	0.0050	0.0034	0.0003
	20	0.0024	0.0006	0.0002
	25	0.0032	0.0004	0.0002
	40	0.0043	0.0002	0.0001
12–13–90/ 347	0	0.0051	0.0011	0.0006
	8	0.0040	0.0053	0.0006
	12	0.0015	0.0041	0.0006
	20	0.0010	0.0026	0.0006
	25	0.0026	0.0019	0.0005
	40	0.0009	0.0009	0.0004

Appendix C. [continued].

Date/ Day	Depth (m)	$V^{PN}_{NO_3}$ (h^{-1})	V^{PN}_{NH4} (h^{-1})	V^{PN}_{urea} (h^{-1})
1–22–91/ 387	0	0.0093	0.0041	0.0032
	8	0.0107	0.0025	0.0062
	12	0.0028	0.0047	0.0041
	20	0.0029	0.0105	0.0043
	25	0.0019	0.0015	0.0040
	40	0.0010	0.0018	0.0017
5–16–91/ 501	0	0.0335	0.0101	0.0097
	8	0.0219	0.0118	0.0048
	12	0.0129	0.0040	0.0053
	20	0.0059	0.0042	0.0034
	25	0.0071	0.0031	0.0008
	40	0.0060	0.0010	0.0003
6–25–91/ 541	0	0.0134	0.0076	0.0080
	8	0.0537	0.0053	0.0062
	12	0.0120	0.0134	0.0026
	20	0.0073	0.0026	0.0011
	25	0.0084	0.0009	0.0026
	40	0.0120	0.0018	0.0005
7–9–91/ 555	0	0.0832	0.0100	0.0062
	8	0.0540	0.0096	0.0044
	12	0.0267	0.0080	0.0038
	20	0.0087	0.0084	0.0044
	25	0.0049	0.0022	0.0035
	40	0.0040	0.0014	0.0005
7–23–91/ 569	0	0.0463	0.0046	0.0021
	8	0.0732	0.0043	0.0026
	12	0.0362	0.0021	0.0031
	20	0.0070	0.0064	0.0023
	25	0.0077	0.0011	0.0017
	40	0.0033	0.0008	0.0003
8–20–91/ 597	0	0.0148	0.0029	0.0070
	8	0.0439	0.0110	0.0055
	12	0.0074	0.0080	0.0052
	20	0.0063	0.0108	0.0014
	25	0.0052	0.0072	0.0008
	40	0.0092	0.0020	0.0005

Appendix D. Primary production measurements of hourly and daily rates of $H_2{}^{14}CO_3$ incorporation. Daily rates were calculated by multiplying the hourly rates by each sampling day's photoperiod.

Date/ Day	Depth (m)	$\rho_{H_2CO_3}$ (mg C m^{-3} h^{-1})	$\rho_{H_2CO_3}$ (mg C m^{-3} d^{-1})
2–90/	0	21.92	219.20
	8	9.84	98.40
	12	5.25	52.50
	20	2.13	21.30
	25	1.16	11.60
	40	0.04	0.41
4–90/	0	7.93	103.09
	8	5.42	70.46
	12	1.11	14.43
	20	0.16	2.08
	25	0.29	3.77
	40	0.01	0.08
5–90/	0	97.69	1367.66
	8	57.20	800.80
	12	3.99	55.86
	20	0.12	1.68
	25	0.05	0.64
	40	0.01	0.11
7–10–90/ 191	0	5.19	77.85
	8	3.21	48.15
	12	1.64	24.60
	20	0.30	4.50
	25	0.15	2.25
	40	0.03	0.38
7–24–90/ 205	0	208.00	3120.00
	8	31.62	474.30
	12	27.86	417.90
	20	6.52	97.80
	25	3.51	52.65
	40	0.19	2.85
8–7–90/ 219	0	65.33	979.95
	8	51.90	778.50
	12	25.97	389.55
	20	6.75	101.25
	25	2.12	31.80
	40	0.03	0.38

Appendix D. [continued].

Date/ Day	Depth (m)	$\rho_{H_2CO_3}$ (mg C m^{-3} h^{-1})	$\rho_{H_2CO_3}$ (mg C m^{-3} d^{-1})
8–21–90/ 233	0	19.26	288.90
	8	21.02	315.30
	12	10.65	159.75
	20	9.89	148.35
	25	3.30	49.50
	40	0.43	6.45
9–5–90/ 248	0	16.61	215.93
	8	15.47	201.11
	12	17.86	232.18
	20	5.20	67.60
	25	1.92	24.96
	40	0.25	3.25
10–11–90/ 284	0	107.07	1284.84
	8	81.52	978.24
	12	20.80	249.60
	20	0.66	7.92
	25	0.33	3.96
	40	0.00	0.00
12–13–90/ 347	0	1.67	16.70
	8	1.40	14.00
	12	1.14	11.40
	20	0.58	5.80
	25	0.29	2.90
	40	0.03	0.27
1–22–91/ 387	0	12.81	115.29
	8	7.51	67.59
	12	3.28	29.52
	20	1.62	14.58
	25	0.64	5.76
	40	0.05	0.44
2–25–91/ 420	0	5.61	56.10
	8	4.33	43.30
	12	2.53	25.30
	20	1.44	14.40
	25	0.81	8.10
	40	0.02	0.19

Appendix D. [continued].

Date/ Day	Depth (m)	$\rho_{H_2CO_3}$ (mg C m^{-3} h^{-1})	$\rho_{H_2CO_3}$ (mg C m^{-3} d^{-1})
4–13-91/	0	12.02	156.26
471	8	8.33	108.29
	12	5.92	76.96
	20	1.25	16.25
	25	0.45	5.85
	40	0.02	0.22
5–16–91/	0	47.23	661.22
501	8	18.15	254.10
	12	10.94	153.16
	20	1.25	17.50
	25	0.32	4.48
	40	0.03	0.38
6–25–91/	0	100.50	1507.50
541	8	28.39	425.85
	12	9.31	139.65
	20	0.78	11.70
	25	1.11	16.65
	40	0.06	0.89
7–9–91/	0	18.67	280.05
555	8	11.00	165.00
	12	5.55	83.25
	20	1.20	18.00
	25	0.54	8.10
	40	0.03	0.38
7–23–91/	0	168.58	2528.70
569	8	76.31	1144.65
	12	30.19	425.85
	20	1.90	28.50
	25	0.54	8.10
	40	0.13	1.95
8–20–91/	0	124.97	1874.55
597	8	69.72	1045.80
	12	27.91	418.65
	20	2.40	36.00
	25	0.58	8.70
	40	0.14	2.10

Appendix E. Ammonium uptake and regeneration rate time course data. Regeneration rates marked with an asterisk indicate samples where the Glibert et al. (1982b) equations were used, otherwise rates were calculated with the Blackburn/Caperon equations. ND= No Data.

Date/ Day	Depth (m)	Incubation Time (hrs.)	$[NH_4^+]$ (μM)	^{15}N–NH_4^+ (atom%)	[PN] (μM)	^{15}N–PN (atom%)	ρ_{NH_4} (nM/h)	r_{NH_4} (nM/h)
7–24–90/ 205	0	0.1	0.21	44.1	17.4	0.407	101.2	
		1.0	0.06	43.5		0.636	108.0	1.6
		6.0	0.03	1.4		0.821	220.2	32.1
		10.0	0.03	30.2		0.888	190.5	-0.3*
	8	0.1	0.30	38.7	9.5	0.419	95.3	
		1.0	0.17	32.7		0.635	73.0	38.8
		6.0	0.21	10.4		1.070	65.7	44.4
		10.0	0.18	5.7		0.823	66.3	30.3
	12	0.1	0.31	32.8	9.4	ND	ND	
		1.0	0.25	29.9		0.942	179.1	26.8
		6.0	0.26	16.8		0.868	36.8	29:8
		10.0	0.20	9.7		1.050	56.4	32.8
8–7–90/ 219	0	0.1	0.40	23.7	7.8	ND	ND	
		1.5	0.20	14.4		0.885	154.8	97.8
		7.0	0.03	14.5		1.074	59.9	-0.15
		12.0	0.03	-34.0		0.698	18.6	0.44*
	8	0.1	0.45	21.8	6.4	0.431	109.6	
		1.5	0.55	10.1		0.823	141.1	261.2
		7.0	0.07	-9.3		1.132	591.8	122.2
		12.0	0.25	-0.72		0.883	1370.5	74.1
	12	0.1	0.41	21.5	11.2	0.465	279.2	
		1.5	0.41	12.9		0.824	220.3	35.7*
		7.0	0.13	4.6		1.217	185.5	47.7
		12.0	0.32	0.6		0.696	1490.2	131.3

Appendix E. [continued].

Date/ Day	Depth (m)	Incubation Time (hrs.)	$[NH_4^+]$ (μM)	^{15}N–NH_4^+ (atom%)	[PN] (μM)	^{15}N–PN (atom%)	ρ_{NH_4} (nM/h)	r_{NH_4} (nM/h)
8–21–90/ 233	0	0.1	0.12	80.0	5.9	0.480	72.6	
		1.5	0.10	59.6		0.928	32.5	21.7
		7.0	0.03	6.1		1.851	75.8	24.8
		12.0	0.30	2.3		1.738	432.8	25.7
	8	0.1	0.10	71.9	5.3	0.469	53.2	
		1.5	0.05	73.0		1.155	39.2	-0.7
		7.0	0.03	-76.7		1.565	9.6	2.0*
		12.0	0.03	37.3		1.430	13.1	-1.0*
	12	0.1	0.12	60.8	6.5	0.549	128.8	
		1.5	0.04	72.7		1.184	53.9	-8.4
		7.0	0.03	80.0		1.430	13.1	-0.6
		12.0	0.04	18.7		1.380	14.8	10.2
9–5–90/ 248	0	0.1	0.22	39.1	4.0	0.395	16.2	
		1.5	0.17	30.5		0.915	43.8	32.4
		7.0	0.03	30.0		1.749	28.0	0.2
		12.0	0.30	-0.7		2.009	21.6	0.3*
	8	0.1	0.33	27.5	3.4	0.410	29.7	
		1.5	0.22	28.9		0.737	23.0	-8.7
		7.0	0.03	80.7		0.969	9.1	-18.0
		12.0	0.15	15.6		1.113	9.6	23.6
	20	0.1	2.61	15.0	3.6	0.406	194.0	
		1.5	2.56	14.9		0.526	26.1	11.9
		7.0	2.43	15.4		0.969	22.0	-15.2
		12.0	2.44	14.7		1.113	16.2	23.6

Appendix E. [continued].

Date/ Day	Depth (m)	Incubation Time (hrs.)	$[NH_4^+]$ (μM)	^{15}N–NH_4^+ (atom%)	[PN] (μM)	^{15}N–PN (atom%)	ρ_{NH_4} (nM/h)	r_{NH_4} (nM/h)
10–11–90/ 284	0	0.1	0.16	82.8	7.9	0.527	164.0	
		2.0	0.25	26.2		1.021	57.1	117.1
		6.0	0.07	7.5		1.463	118.7	45.4
		18.0	0.03	9.0		1.231	57.6	-0.7
	8	0.1	0.17	90.3	8.8	0.660	351.0	
		2.0	0.17	43.7		0.669	21.3	6.9*
		6.0	0.14	22.1		1.144	38.4	26.7
		18.0	0.21	6.5		0.628	49.4	18.2
	25	0.1	0.20	67.9	1.5	0.388	4.0	
		2.0	0.17	88.0		0.435	0.6	-24.0
		6.0	0.27	34.1		0.602	1.0	51.5
		18.0	0.25	58.0		0.628	0.5	-11.6
12–13–90/ 347	0	0.1	0.38	-1.5	2.0	0.448	ND	
		3.0	0.31	-2.4		0.450	ND	ND
		7.0	0.34	-1.6		0.404	ND	ND
		18.0	0.28	-4.1		0.418	ND	ND
	8	0.1	0.57	1.2	2.5	0.467	84.1	
		3.0	0.33	0.2		0.382	13.3	-81.0
		7.0	0.38	3.5		0.433	12.6	-65.3
		18.0	0.28	1.4		0.376	0.6	34.0
	25	0.1	0.30	-0.9	2.1	0.365	0.0	
		3.0	0.23	7.0		0.540	4.0	ND
		7.0	0.30	2.8		0.396	2.2	66.0
		18.0	0.23	0.7		0.394	5.6	47.0

Appendix E. [continued].

Date/ Day	Depth (m)	Incubation Time (hrs.)	$[NH_4^+]$ (μM)	^{15}N–NH_4^+ (atom%)	[PN] (μM)	^{15}N–PN (atom%)	ρ_{NH_4} (nM/h)	r_{NH_4} (nM/h)
1–22–91/	0	0.1	0.10	74.6	8.9	0.383	11.7	
387		7.0	0.04	78.8		2.413	36.4	-0.53
		12.0	0.03	97.6		2.887	22.1	0.05*
		18.0	0.03	-29.4		2.694	21.5	0.88*
	8	0.1	0.09	76.9	2.8	0.391	5.7	
		7.0	0.07	79.8		1.656	7.1	-0.45
		12.0	0.03	97.9		2.219	5.1	0.96*
		18.0	0.03	64.5		2.427	4.2	0.22*
	25	0.1	0.14	92.1	1.8	0.417	10.1	
		7.0	0.11	95.7		1.308	2.7	-0.7
		12.0	0.07	86.4		2.044	2.8	1.7
		18.0	0.10	91.2		2.062	1.9	-0.8
5–16–91/	0	0.1	0.19	59.0	2.2	0.607	156.3	
501		7.0	0.11	14.5		2.254	22.5	48.9
		11.0	0.07	-3.9		2.174	150.1	29.6
		18.0	0.03	-191.0		2.182	448.2	15.8
	8	0.1	0.26	48.9	1.8	0.493	83.0	
		7.0	0.19	10.6		2.046	21.6	81.5
		11.0	0.14	11.1		2.377	41.1	-1.0
		18.0	0.07	-1.6		2.284	51.0	16.1
	25	0.1	0.33	37.9	0.2	0.444	7.2	
		7.0	0.29	32.5		1.091	0.7	11.5
		11.0	0.25	36.5		1.434	0.7	-4.7
		18.0	0.21	28.4		1.541	0.5	8.3

Appendix E. [continued].

Date/ Day	Depth (m)	Incubation Time (hrs.)	$[NH_4^+]$ (μM)	^{15}N–NH_4^+ (atom%)	[PN] (μM)	^{15}N–PN (atom%)	ρ_{NH_4} (nM/h)	ρ_{NH_4} (nM/h)
6–25–91/ 541	0	0.1	0.28	37.9	5.8	0.636	133.5	
		3.0	0.03	35.2		1.170	44.2	2.8
		7.0	0.03	36.5		1.159	19.1	-0.01*
		18.0	0.03	29.9		3.916	35.2	0.03*
	8	0.1	0.46	30.2	3.9	0.543	197.0	
		3.0	0.26	28.1		0.816	20.8	8.6
		7.0	0.20	6.9		ND	ND	82.5
		18.0	0.05	17.2		ND	ND	-9.3
	25	0.1	0.08	-256.3	2.3	0.544	36.9	
		3.0	0.09	69.8		0.649	2.2	23.8
		8.0	0.07	81.1		0.916	2.5	-3.1
		18.0	0.04	67.8		1.563	2.1	0.9
7–9–91/ 555	0	0.1	0.27	43.6	1.2	0.469	43.3	
		3.0	0.03	50.9		1.721	11.5	-5.7
		8.0	0.03	29.8		2.318	8.3	1.4*
		18.0	0.03	-9.6		2.125	5.5	0.2*
	8	0.1	0.32	38.6	2.2	0.413	40.8	
		3.0	0.09	74.4		1.847	21.2	-39.9
		8.0	0.08	24.4		2.718	17.5	21.2
		18.0	0.03	28.7		3.084	14.5	-0.8
	25	0.1	0.37	31.3	1.5	0.404	25.3	
		3.0	0.30	40.5		0.599	3.4	-29.0
		8.0	0.39	27.9		0.877	3.2	28.6
		18.0	0.09	25.0		1.202	2.9	4.0

Appendix E. [continued].

Date/ Day	Depth (m)	Incubation Time (hrs.)	$[NH_4^+]$ (μM)	^{15}N–NH_4^+ (atom%)	[PN] (μM)	^{15}N–PN (atom%)	ρ_{NH_4} (nM/h)	r_{NH_4} (nM/h)
7–23–91/	0	0.1	0.23	47.9	10.0	0.408	144.1	
569		3.0	0.07	18.8		0.767	45.8	42.5
		7.0	0.03	21.0		0.843	33.7	-1.2
		18.0	0.03	21.9		0.956	16.1	0.0*
	8	0.1	0.25	59.0	16.6	0.356	0.0	
		3.0	0.25	26.0		0.855	70.9	22.4*
		7.0	0.14	29.0		1.250	75.5	-4.6
		18.0	0.03	-5.7		1.459	63.5	6.8
	25	0.1	0.19	58.0	1.1	0.367	1.1	
		3.0	0.17	66.1		0.580	1.3	-7.9
		8.0	0.15	54.9		0.902	1.4	6.7
		18.0	0.08	32.3		1.576	1.9	5.7
8–20–91/	0	0.1	0.03	71.4	17.1	0.467	217.7	
597		3.0	0.03	-16.6		1.074	49.5	2.2*
		7.0	0.03	-5.7		1.048	22.9	-0.1*
		18.0	0.03	15.0		1.087	25.3	-0.1*
	8	0.1	0.06	89.6	9.5	0.506	208.8	
		3.0	0.03	-6.1		1.006	104.3	4.4*
		7.0	0.03	-44.4		1.029	335.7	0.5*
		18.0	0.03	-73.4		ND	ND	0.1*
	25	0.1	3.26	6.3	1.8	0.412	306.8	
		3.0	3.21	5.7		0.482	13.2	105.4
		7.0	3.20	5.5		0.612	13.6	32.3
		18.0	3.25	5.2		0.634	6.3	20.6